

ISSN: 2320-8694

Journal of Experimental Biology And Agricultural Sciences



VOLUME 12

|| ISSUE V

|| OCTOBER, 2024

Production and Hosting by Horizon Publisher India[HPI]
(<http://www.horizonpublisherindia.in>)
All rights reserved.

ISSN No. 2320 - 8694

Peer Reviewed - open access journal

Common Creative License - NC 4.0

Volume No - 12

Issue No - V

October, 2024

Journal of Experimental Biology and Agricultural Sciences (JEBAS) is an online platform for the advancement and rapid dissemination of scientific knowledge generated by the highly motivated researchers in the field of biological agricultural, veterinary and animal sciences. JEBAS publishes high-quality original research and critical up-to-date review articles covering all the aspects of biological sciences. Every year, it publishes six issues.

JEBAS has been accepted by SCOPUS UGC CARE, INDEX COPERNICUS INTERNATIONAL (Poland), AGRICOLA (USA), CAS (ACS, USA), CABI - Full Text (UK), International Committee of Medical Journal Editors (ICMJE), SHERPA - ROMEO; J gate and Indian Science Abstracts (ISA, NISCAIR) like well reputed indexing agencies.

[HORIZON PUBLISHER INDIA [HPI]

<http://www.horizonpublisherindia.in/>]

Editorial Board

Editor-in-Chief

Prof Y. Norma-Rashid
(University of Malaya, Kuala Lumpur)
editor.in.chief.jebas@gmail.com

Co-Editor-in-Chief

Dr. Kuldeep Dhama, M.V.Sc., Ph.D.
NAAS Associate, Principal Scientist, IVRI, Izatnagar India - 243 122
co_eic@jebas.org

Managing - Editor

Kamal K Chaudhary, Ph.D. (India)
jebasonline@gmail.com

Technical Editors

Hafiz M. N. Iqbal (Ph.D.)

Research Professor,
Tecnologico de Monterrey, School of Engineering and Sciences,
Campus Monterrey, Ave. Eugenio Garza Sada 2501,
Monterrey, N. L., CP 64849, Mexico
Tel.: +52 (81) 8358-2000Ext.5561-115
E-mail: hafiz.iqbal@my.westminster.ac.uk; hafiz.iqbal@itesm.mx

Prof. Dr. Mirza Barjees Baigis

Professor of Extension (Natural Resource Management),
Department of Agricultural Extension and Rural Society,
College of Food and Agriculture Sciences,
King Saud University, P.O. Box 2460, Riyadh 11451, Kingdom of Saudi Arabia
Email: mbbag@ksu.edu.sa

Dr. Mukesh Kumar Meghvansi

Scientist, Bioprocess Technology Division, Defence R & D Establishment, Gwalior-474002
Email: mk_meghvansi@yahoo.co.in

Dr. B L Yadav

Head – Botany, MLV Govt. College, Bhilwara, India
E mail: drblyadav@yahoo.com

Dr. Yashpal S. Malik

ICAR – National Fellow Indian Veterinary Research Institute (IVRI)
Izatnagar 243 122, Bareilly, Uttar Pradesh, India

Associate Editors

Dr. Sunil K. Joshi

Laboratory Head, Cellular Immunology

Investigator, Frank Reidy Research Center of Bioelectrics, College of Health Sciences, Old Dominion University,
4211 Monarch Way, IRP-2, Suite # 300, Norfolk, VA 23508 USA

Email: skjoshi@odu.edu

Dr. Vincenzo Tufarelli

Department of Emergency and Organ Transplantation (DETO),

Section of Veterinary Science and Animal Production,

University of Bari 'Aldo Moro', s.p. Casamassima km 3, 70010 Valenzano, Italy

Email: vincenzo.tufarelli@uniba.it

Prof. Sanjay-Swami, Ph.D. (Soil Science & Agril. Chemistry),

School of Natural Resource Management,

College of Post Graduate Studies in Agricultural Sciences,

(Central Agricultural University),

UMIAM (Barapani)-793 103, Meghalaya, INDIA

Email: sanjay.nrm.cpgsas@cau.ac.in

Jose M. Lorenzo

Centro Tecnológico de la Carne de Galicia

Ourense, Spain

Email: jmlorenzo@ceteca.net

Assistant Editors

Dr Ayman EL Sabagh

Assistant professor, agronomy department, faculty of agriculture

kafresheikh university, Egypt

E-mail: ayman.elsabagh@agr.kfs.edu.eg

Safar Hussein Abdullah Al-Kahtani (Ph.D.)

King Saud University-College of Food and Agriculture Sciences,
Department of the Agricultural Economics
P.O.Box: 2460 Riyadh 11451, KSA
email: safark@ksu.edu.sa

Dr Ruchi Tiwari

Assistant Professor (Sr Scale)
Department of Veterinary Microbiology and Immunology,
College of Veterinary Sciences,
UP Pandit Deen Dayal Upadhyay Pashu Chikitsa Vigyan Vishwavidyalay Evum Go-Anusandhan Sansthan (DUVASU),
Mathura, Uttar Pradesh, 281 001, India
Email: ruchi.vet@gmail.com

Dr. ANIL KUMAR (Ph.D.)

Asstt. Professor (Soil Science)
Farm Science Centre (KVK)
Booh, Tarn Taran, Punjab (India) – 143 412
Email: anilkumarhpkv@gmail.com

Akansha Mishra

Postdoctoral Associate, Ob/Gyn lab
Baylor College of Medicine,
1102 Bates Ave, Houston Tx 77030
Email: akansha.mishra@bcm.edu; aksmisra@gmail.com

Dr. Muhammad Bilal

Associate Professor
School of Life Science and Food Engineering,
Huaiyin Institute of Technology, Huaian 223003, China
Email: bilaluaf@hotmail.com

Dr. Senthilkumar Natesan

Associate Professor
Department of Infectious Diseases, Indian Institute of Public Health
Gandhinagar, Opp to Airforce station HQ, Lekawada, Gandhinagar, Gujarat - 382042, India
Email: snatesan@iiphg.org

Prof. A. VIJAYA ANAND

Professor

Department of Human Genetics and Molecular Biology

Bharathiar University

Coimbatore – 641 046

Dr. Phetole Mangena

Department of Biodiversity, School of Molecular and Life Sciences,

Faculty of Science and Agriculture, University of Limpopo, Republic of South Africa

Private Bag X1106, Sovenga, 0727

Email: Phetole.Mangena@ul.ac.za ; mangena.phetole@gmail.com

Table of contents

Innovations in Soil Health Monitoring: Role of Advanced Sensor Technologies and Remote Sensing <i>10.18006/2024.12(5).653.667</i>	653 — 667
Fruits of <i>Prosopis chilensis</i> and <i>Tetrapleura tetraptera</i> as an alternative against multi-resistant bacteria in lower respiratory tract infections <i>10.18006/2024.12(5).668.675</i>	668 — 675
Development of a portable electrocoagulation unit for on-site treatment of washing machine wastewater <i>10.18006/2024.12(5).676.685</i>	676 — 685
Medicinal value of <i>Lippia multiflora</i> Mondenke flowers in the fight of oral and dental infections <i>10.18006/2024.12(5).686.693</i>	686 — 693
EVALUATION OF <i>ASPERGILLUS NIGER</i> CONTAMINATION AND OCCURRENCE OF CITRININ IN RED CHILLI (<i>CAPSICUM ANNUUM</i>) SAMPLES <i>10.18006/2024.12(5).694.704</i>	694 — 704
Effect of salinity stress on antioxidant activity and secondary metabolites of <i>Piper betle</i> <i>10.18006/2024.12(5).705.729</i>	705 — 729
Real-time and <i>in silico</i>-based characterization of the heat stress-responsive gene <i>TaGASR1</i> from Indian bread wheat <i>10.18006/2024.12(5).730.741</i>	730 — 741
Exploring the Phosphate Solubilising Rhizobacteria isolated from Wild <i>Musa</i> Rhizosphere and their Efficacy on Growth Promotion of <i>Phaseolus vulgaris</i> <i>10.18006/2024.12(5).742.755</i>	742 — 755
Introgressing photoperiod/thermo-sensitive genic male sterile gene into Basmati 370 rice <i>10.18006/2024.12(5).756.769</i>	756 — 769
ASSESSMENT OF THE ECONOMIC BENEFIT OF CABBAGE PRODUCTION UNDER DIFFERENT IRRIGATION LEVELS AND SOIL AMENDMENTS IN A SEMI-ARID ENVIRONMENT <i>10.18006/2024.12(5).770.783</i>	770 — 783





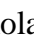








Journal of Experimental Biology and Agricultural Sciences

<http://www.jebas.org>

ISSN No. 2320 – 8694

Innovations in Soil Health Monitoring: Role of Advanced Sensor Technologies and Remote Sensing

Jorge Luis Huere-Peña¹ , Manuel Castrejon-Valdez¹ , Cesar Castañeda-Campos¹ ,
Rodolfo Leon-Gomez¹ , Walter Augusto Mateu-Mateo³ , Rolando Bautista-Gómez³ ,
Edward Arostegui-León² , Carlos Dueñas-Jurado¹ , Edwin Javier Ceenti-Chancha¹ ,
Edwin Rojas-Felipe¹ , Russbelt Yaulilahua-Huacho^{1*} 

¹Universidad Nacional de Huancavelica, Huancavelica, Perú

²Universidad Nacional José María Arguedas, Andahuaylas, Perú

³Universidad Nacional de San Cristóbal de Huamanga, Ayacucho, Perú

Received – July 01, 2024; Revision – October 23, 2024; Accepted – November 09, 2024

Available Online – November 29, 2024

DOI: [http://dx.doi.org/10.18006/2024.12\(5\).653.667](http://dx.doi.org/10.18006/2024.12(5).653.667)

KEYWORDS

Soil health

Advanced sensor technologies

Remote sensing

IoT

Sustainable agriculture

ABSTRACT

Soil health monitoring is essential for sustainable agricultural practices and effective environmental management. Recent sensor technologies and remote sensing innovations have transformed how we assess soil health, providing real-time and precise data that enhance decision-making processes. This review focuses on integrating advanced sensor technologies, like Internet of Things (IoT) devices, alongside remote sensing techniques, including drones and satellite imagery, in soil science. These technologies enable continuous monitoring of critical soil parameters, such as moisture levels and nutrient content, significantly improving the accuracy and efficiency of soil health evaluations. Additionally, remote sensing provides a comprehensive overview of soil conditions across large areas, allowing for the identification of spatial patterns and temporal changes that traditional methods may overlook. Various case studies from agricultural and environmental projects demonstrate the practical benefits and the challenges of implementing these innovations. The article also discusses future trends and potential obstacles, highlighting the need for further research and development to exploit these technologies' capabilities fully. Ultimately, advanced sensors and remote sensing promise to improve soil health monitoring, contributing to more sustainable and productive agricultural systems.

* Corresponding author

E-mail: russbelt.yaulilahua@unh.edu.pe (Russbelt Yaulilahua-Huacho)

Peer review under responsibility of Journal of Experimental Biology and Agricultural Sciences.

Production and Hosting by Horizon Publisher India [HPI]
(<http://www.horizonpublisherindia.in/>).
All rights reserved.

All the articles published by [Journal of Experimental Biology and Agricultural Sciences](#) are licensed under a [Creative Commons Attribution-NonCommercial 4.0 International License](#) Based on a work at www.jebas.org.



1 Introduction

Soil health is a fundamental aspect of sustainable agriculture and environmental stewardship. It is essential for ensuring food security, maintaining ecosystem services, and mitigating the negative impacts of climate change. Traditional monitoring methods of soil health often depend on manual sampling, and laboratory analyses can be labor-intensive, time-consuming, and limited in spatial and temporal coverage. However, the emergence of advanced sensor technologies and remote sensing has significantly improved our understanding of soil health assessment, providing more dynamic, comprehensive, and efficient approaches.

Advanced sensor technologies, particularly those integrated with the Internet of Things (IoT), have revolutionized soil monitoring (Figure 1). IoT-based soil sensors can continuously measure soil properties, including moisture content, temperature, pH, and nutrient levels, transmitting real-time data to central databases for analysis (Mutyalamma et al. 2020). This continuous data stream enables researchers and farmers to make more accurate and timely management decisions related to irrigation optimization, fertilization, and other soil management practices, ultimately enhancing crop productivity and sustainability (Smith et al. 2020).

Remote sensing includes satellite imagery and drone-based observations, which provide an aerial view of soil health over large

areas (Figure 2). These technologies can detect changes in soil properties and vegetation health, allowing for the assessment of soil moisture, organic matter content, and salinity across various scales and periods. One of the main advantages of remote sensing is its ability to cover extensive regions that would be impractical to monitor using ground-based methods alone (Jones and Brown 2019). Researchers can create accurate models to predict soil health and inform agricultural practices by combining remote sensing data with ground-truth measurements.

One of the significant benefits of advanced sensor technologies and remote sensing is their ability to detect and address spatial variability in soil properties. Soils within a single field vary considerably due to the differences in topography, organic matter, and historical land use. Understanding this variability is crucial for precision agriculture, which aims to manage soil and crop inputs on a fine scale to optimize yields and minimize environmental impacts (Zhang et al. 2021a). Farmers can apply fertilizers and water more efficiently by mapping soil variability, reducing waste and enhancing environmental sustainability. Integrating these technologies also allows for real-time monitoring of soil health, providing immediate feedback on the effectiveness of management practices. For instance, IoT sensors can alert farmers to changes in soil moisture levels, prompting timely adjustments in irrigation to prevent crop stress or water wastage. Similarly, remote sensing can pinpoint underperforming

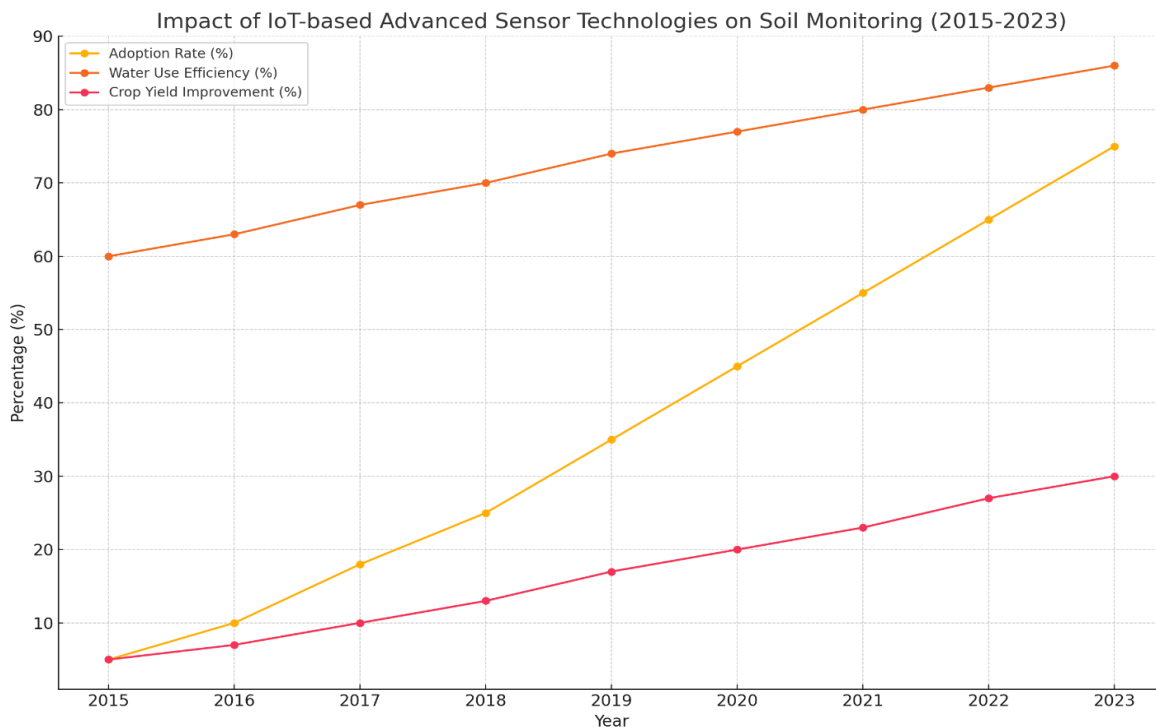


Figure 1 illustrates the impact of IoT-based advanced sensor technologies on soil monitoring from 2015 to 2023.

This figure has been regenerated using previously published data.

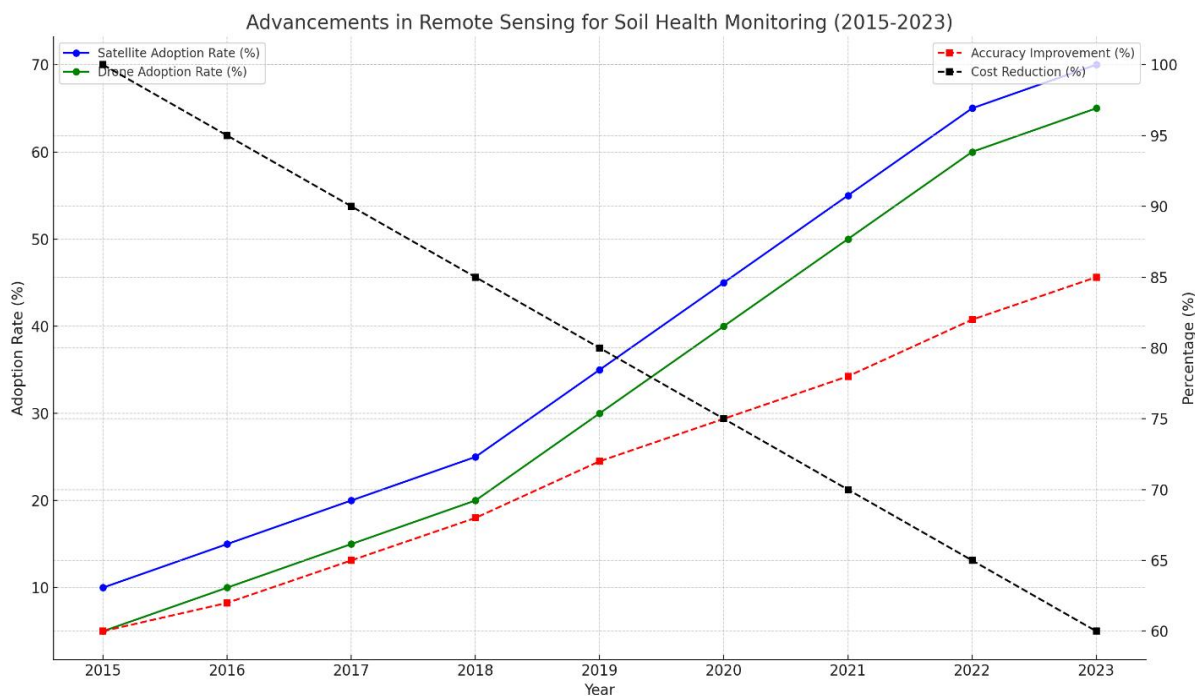


Figure 2 illustrates advancements in remote sensing technologies for soil health monitoring from 2015 to 2023.

This figure has been regenerated based on published data.

areas of a field, enabling targeted interventions that improve overall crop performance (Chen et al. 2020a).

Despite these numerous advantages, adopting advanced sensor technologies and remote sensing in soil health monitoring presents several challenges. The initial cost of acquiring and deploying these technologies can be high, and there is a need for technical expertise to interpret the data accurately. Additionally, integrating data from various sources requires sophisticated analytical tools and methods to ensure reliability and consistency (Wang and Li 2022). Addressing these challenges is crucial to maximizing the potential of these innovations.

Future trends in soil health monitoring will likely see further advancements in sensor accuracy, data integration, and the development of user-friendly platforms that make these technologies accessible to a broader audience. Research is also needed to explore the long-term impacts of these technologies on soil health and agricultural productivity. As the field evolves, fostering collaboration among scientists, technology developers, and farmers will be essential to ensure that innovations in soil health monitoring translate into tangible benefits for sustainable agriculture and environmental management.

This study aims to evaluate the role of advanced sensor technologies and remote sensing methods in soil health monitoring, focusing on how these innovations enhance the accuracy, efficiency, and scalability of soil assessments for

sustainable agriculture. Specifically, the study examines how integrating IoT devices, drones, and satellite imagery enables real-time monitoring of soil parameters such as moisture, nutrients, and pH levels. Additionally, it aims to identify the benefits and challenges of these technologies in capturing spatial and temporal soil variability, thereby supporting more precise, data-driven decisions for optimizing soil management practices.

2 Traditional Soil Health Monitoring Methods

Traditional soil health monitoring methods are fundamental for understanding and managing soil conditions and crucial for agricultural productivity and environmental sustainability. These methods involve a variety of physical, chemical, and biological analyses that provide a comprehensive assessment of soil health. Physical analysis examines soil texture, structure, and porosity. Soil texture refers to the proportion of sand, silt, and clay, which affects water retention and aeration, essential for plant health and root growth. Soil structure influences how well water infiltrates and how deeply roots can penetrate, which is determined by how soil particles aggregate. Porosity, the measurement of pore spaces, impacts the soil's ability to hold air and water, which is vital for supporting plant roots and microbial activity (Brady and Weil 2008).

Chemical analysis in traditional soil health monitoring primarily focuses on measuring pH, nutrient content (such as nitrogen, phosphorus, and potassium), and cation exchange capacity (CEC). Soil pH is significant in nutrient availability, while nutrient levels

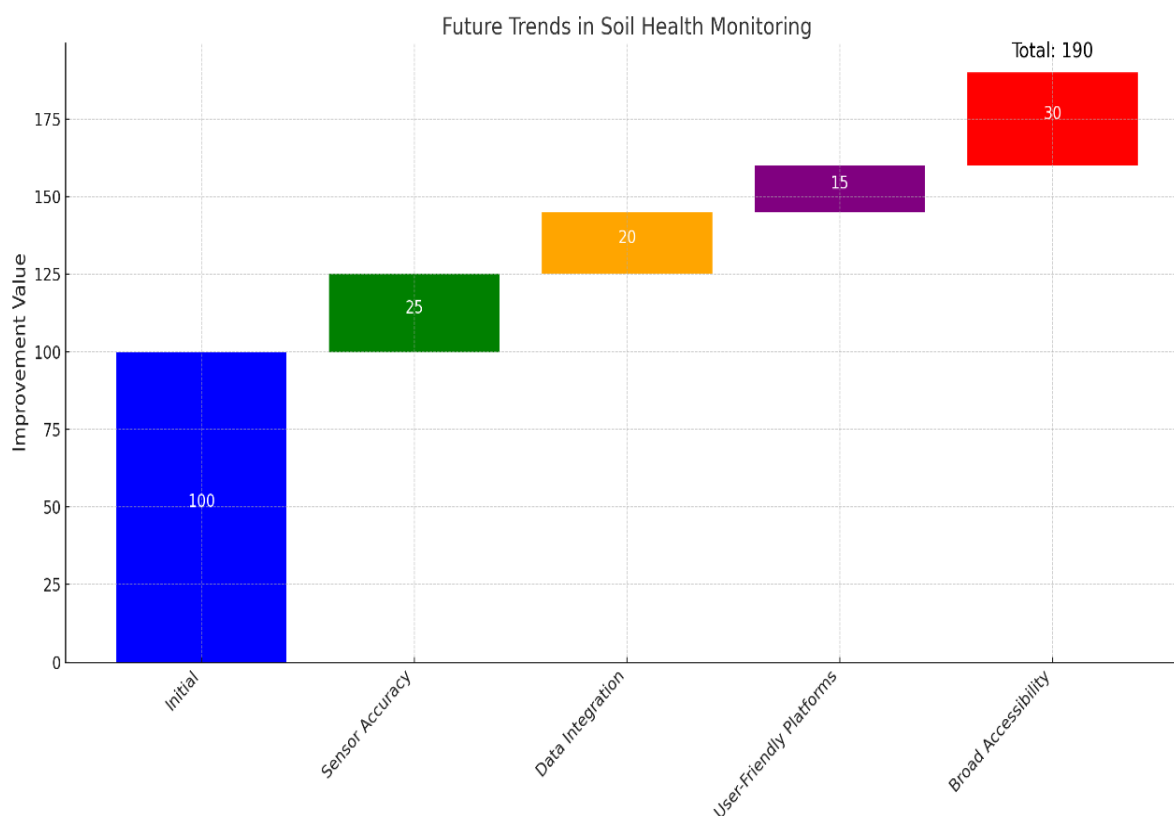


Figure 3 The waterfall chart illustrates future trends in soil health monitoring, highlighting key areas of advancement and their cumulative impact. The trends indicate a total improvement value of 190 by 2023, showcasing the substantial potential that advancements in soil health monitoring have for promoting more sustainable and efficient agricultural practices. This figure has been recreated based on the published information.

directly affect soil fertility. CEC determines the soil's ability to hold and release essential nutrients for sustainable crop productivity.

Biological analysis evaluates the soil's organic matter content, microbial biomass, and enzymatic activities—key indicators of soil biological health and productivity. A high microbial diversity supports nutrient cycling and helps plants resist diseases. While these traditional methods provide thorough insights into soil health, they are often labor-intensive and limited in spatial and temporal coverage. This limitation has led to the integration of newer technologies to enhance soil monitoring.

Chemical analysis of soil involves testing pH levels, nutrient content, and organic matter. Soil pH measures the acidity or alkalinity of the soil, which significantly affects nutrient availability and microbial activity (Jones et al. 2020). Nutrient testing focuses on essential macronutrients and micronutrients, such as nitrogen (N), phosphorus (P), potassium (K), calcium (Ca), magnesium (Mg), and trace elements like iron (Fe) and zinc (Zn) (Havlin et al. 2013). These tests are crucial for assessing soil fertility and guiding fertilization practices.

The organic matter content, which includes decomposed plant and animal residues, is vital for nutrient cycling and improves soil structure and water-holding capacity (Sparks 2003). Biological analysis assesses microbial activity and biodiversity within the soil. Soil microbes, including bacteria, fungi, and other microorganisms, play a pivotal role in nutrient cycling, organic matter decomposition, and promoting plant health through symbiotic relationships. Microbial biomass measurement, enzyme assays, and soil respiration technology are used to evaluate microbial activity and overall soil health (Paul 2014).

Traditional soil health monitoring methods involve manual sampling and laboratory analysis, focusing on assessing the soil's physical, chemical, and biological properties. These methods include testing soil texture, structure, pH levels, nutrient content, and organic matter. For instance, soil texture determined by sand, silt, and clay proportions—affects properties like water retention and drainage, while pH levels influence nutrient availability. The main advantages of traditional methods are their proven accuracy and the ability to provide detailed data. However, these techniques are labor-intensive, time-consuming, and offer limited spatial coverage, as they typically rely on point-based sampling. Although

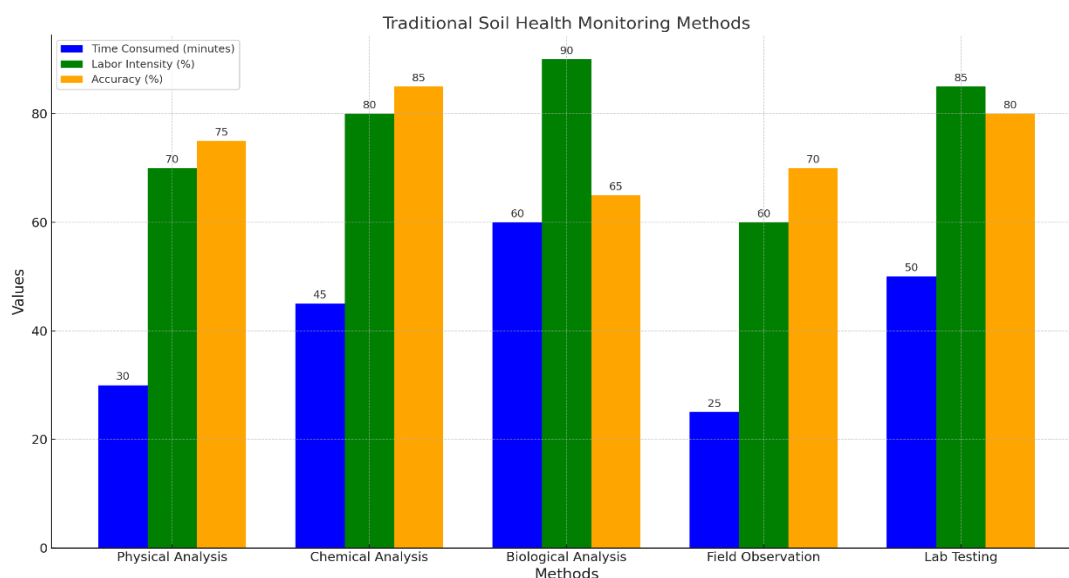


Figure 4 Visually appealing chart illustrates the efficiency and effectiveness of various traditional soil health monitoring methods. It highlights the balance between time consumption, labor requirements, and accuracy. This figure has been recreated from previously published data for inclusion in the current manuscript.

accurate, laboratory analyses can take days to weeks to yield results, delaying important decision-making processes. Additionally, traditional methods do not provide continuous, real-time data, which is increasingly crucial for precision agriculture and dynamic soil management (Adamchuk et al. 2004). This limitation makes it challenging to capture soil condition variability over large areas or in real-time, often requiring additional sampling to achieve a comprehensive assessment (Brady and Weil 2008).

In contrast, advanced methods such as IoT-based sensors and remote sensing technologies, including drones and satellite imagery, offer real-time monitoring and broader spatial coverage. These technologies enable continuous data collection on soil moisture, temperature, pH, and nutrient levels, providing a dynamic and more accurate picture of soil health across large areas. The primary advantage of these advanced methods lies in their ability to collect data over extended periods and at a high spatial resolution, identifying soil variability and temporal changes that traditional methods may overlook. While the initial cost and technical expertise required to deploy these systems can be high, they are highly efficient in the long run, significantly reducing the labor and time involved in manual soil monitoring. Moreover, they facilitate precise, data-driven decisions that enhance agricultural management practices and sustainability (Jones et al. 2020; Zhang et al. 2021a).

3 Advanced Sensor Technologies in Soil Health Monitoring

3.1 Overview of Sensor Technologies

Recent advancements in sensor technologies have significantly improved the ability to monitor various soil parameters with high

precision (Kumar and Lal 2020). These sensors are designed to measure soil moisture, temperature, electrical conductivity, pH, and nutrient levels, providing continuous and real-time data crucial for precision agriculture (Zhang et al. 2021b). For example, soil moisture sensors can accurately detect the volumetric water content in the soil, enabling precise irrigation management and reducing water wastage. These sensors generally measure moisture levels using electrical resistance, capacitance, and time-domain reflectometry (TDR). In the case of resistive sensors, the electrical resistance between two probes decreases as soil moisture increases, allowing the sensor to estimate water content accurately. Capacitive sensors, on the other hand, measure changes in the dielectric constant of the soil, which varies with moisture content. TDR sensors send an electromagnetic pulse through the soil, and the time it takes for the pulse to return is used to determine the moisture level.

Numerous studies have demonstrated the effectiveness of soil moisture sensors in improving irrigation practices. For instance, Patel et al. (2021) used soil moisture sensors to optimize irrigation scheduling in agricultural fields, resulting in a 25% reduction in water usage without compromising crop yield. Similarly, a field experiment by Huang et al. (2022) employed these sensors in a vineyard, leading to better water management and improved grapevine growth conditions by monitoring soil moisture levels more accurately.

Soil temperature sensors provide valuable insights into the thermal conditions of the soil, which are essential for understanding microbial activity and plant growth dynamics. These sensors

measure soil temperature at various depths, and commonly used types include thermistors, thermocouples, and resistance temperature detectors (RTDs). Thermistors change their resistance with temperature, while thermocouples generate a voltage in response to temperature differences. RTDs operate on the principle that the resistance of certain metals increases with temperature. Typically, these sensors are embedded in the soil or inserted at different depths to provide real-time temperature readings, which is critical for managing planting schedules and irrigation systems.

Experiments utilizing soil temperature sensors have been conducted in various agricultural settings to understand the effects of soil temperature on crop growth and microbial activity. For instance, Shao et al. (2019) conducted a study in which soil temperature sensors were used to monitor temperature fluctuations in paddy fields, revealing a direct correlation between soil temperature and rice growth rates. Similarly, in an experiment by Wang et al. (2020), data collected from soil temperature sensors were used to optimize planting times and improve wheat yields by aligning sowing schedules with optimal soil temperature conditions. These findings underscore the importance of soil temperature in influencing plant development and soil biota activity, which are crucial for effective crop management and yield optimization.

Electrical conductivity (EC) sensors are essential for assessing soil salinity, significantly impacting nutrient availability and plant health. These sensors measure the soil's ability to conduct electrical current, which increases with dissolved salts. The principle behind EC sensors is that soluble salts in the soil create ionic conductivity; therefore, higher salt concentrations result in greater conductivity. Typically, EC sensors consist of two electrodes placed in the soil. The electrical resistance measured between the electrodes is inversely related to the soil's conductivity. EC sensors can be categorized into two types: contact and non-contact. Contact sensors are inserted directly into the soil, while non-contact sensors use electromagnetic fields to evaluate conductivity from a distance. These sensors play a crucial role in evaluating soil salinity, which can affect nutrient balance, plant water uptake, and overall growth. High soil salinity can lead to nutrient imbalances and inhibited growth. Various studies have demonstrated the effectiveness of EC sensors in managing soil salinity. For example, Saha et al. (2020) utilized EC sensors in saline-prone regions of India to monitor changes in soil salinity, correlating these variations with reductions in crop yield. Another study by Basso et al. (2021) examined the influence of different irrigation schedules on soil salinity using EC sensors, finding that precise irrigation management based on real-time EC data can significantly lower salinity levels and enhance crop performance.

Nutrient sensors are designed to measure the concentration of essential nutrients, such as nitrogen, phosphorus, and potassium, facilitating targeted fertilization practices that enhance crop yield

while minimizing environmental impacts. These sensors can employ various techniques such as electrochemical, optical, or spectrometric methods to detect and quantify nutrient levels in the soil. Ion-selective electrodes (ISEs) are commonly used for nitrogen and potassium detection, responding specifically to certain ions in the soil solution. Sensors may utilize colorimetric methods for phosphorus detection, where chemical reactions with phosphorus compounds produce a color change proportional to the concentration. Additionally, some sensors use near-infrared spectroscopy (NIR) for non-destructive analysis by measuring the soil's light absorption at different wavelengths, providing real-time data on nutrient levels.

These nutrient sensors are vital for precision agriculture, allowing farmers to implement targeted fertilization practices, optimize nutrient application, reduce fertilizer waste, and mitigate environmental issues like nutrient runoff and leaching. Rai et al. (2020) monitored nitrogen and phosphorus levels in cornfields using nutrient sensors, discovering that real-time data helped optimize fertilizer application, resulting in a 15% reduction in nitrogen use and a 10% improvement in crop yields. Similarly, Zhang et al. (2021b) assessed potassium levels in wheat fields with nutrient sensors, leading to more precise fertilization that minimized over-application and enhanced crop quality. Collectively, these advanced sensors contribute to a comprehensive understanding of soil health, empowering farmers and researchers to optimize agricultural practices based on accurate, timely data (Smith and Black 2019; Jones et al. 2020).

3.2 Internet of Things (IoT) in Soil Monitoring

Integrating Internet of Things (IoT) devices into soil monitoring systems has transformed agricultural practices by enabling the real-time collection and transmission of soil data. IoT-based soil sensors facilitate continuous data gathering and sharing in modern monitoring systems. These sensors typically measure soil moisture, temperature, pH, and nutrient levels and are interconnected through wireless communication networks. The data collected by IoT devices is transmitted to a central platform or cloud-based system for analysis and informed decision-making.

IoT systems commonly use energy-efficient wireless communication protocols such as LoRaWAN, Zigbee, or NB-IoT, which allow for long-range data transmission. When integrated with cloud computing and machine learning algorithms, these sensors can enhance their ability to provide predictive analytics for improved resource management. For instance, Sood et al. (2020) utilized IoT-based sensors to monitor soil moisture and temperature in a vineyard. The real-time data collected enabled precise irrigation management, which reduced water consumption by 20% while improving grape quality. Similarly, Hassan et al. (2021) integrated IoT sensors in a wheat farming system to track

soil nutrient levels and pH, providing farmers with actionable insights that led to more efficient fertilizer use and overall crop yield. These studies underscore how IoT devices can effectively improve soil health management by delivering precise, real-time information that supports sustainable agricultural practices.

IoT-based soil monitoring systems are equipped with multiple sensors that can be deployed across extensive agricultural fields, creating detailed soil health profiles. These systems offer remote access to data, allowing farmers and researchers to make informed decisions without being physically present in the field (Hassan et al. 2021). This real-time data access facilitates timely interventions, such as adjusting irrigation schedules or applying fertilizers, thus enhancing resource efficiency and crop productivity. Additionally, IoT devices can be integrated with weather forecasting systems to anticipate and mitigate the impacts of adverse weather conditions on soil health (Akyildiz et al. 2002; Kim et al. 2017). This integration combines real-time soil data collected from IoT sensors—such as moisture, temperature, pH, and nutrient levels—with weather data from meteorological systems.

For instance, weather forecasting systems predict temperature fluctuations, rainfall, humidity, and extreme weather events like droughts or storms. When IoT sensors detect changes in soil conditions that correlate with predicted weather patterns, they can trigger automatic irrigation systems or alert farmers to take preventive actions, such as adjusting fertilization schedules or preparing for soil erosion. The data from both systems can be processed through cloud-based platforms or edge computing systems, providing predictive analytics for smarter decision-making. Several experiments have demonstrated the effectiveness of this integration. For example, Smith et al. (2021) studied IoT soil moisture sensors in combination with weather forecasting tools to predict and mitigate the impact of drought conditions on agricultural fields. This integration enabled early warning systems that adjusted irrigation schedules based on forecasted rainfall and soil moisture levels, leading to a 25% reduction in water usage. Another study by Chen et al. (2020b) integrated weather data with soil health sensors in rice paddies to forecast flood risks. This system allowed farmers to proactively adjust their water management practices, enhancing rice yields and minimizing flooding-related crop damage. These examples illustrate how IoT-based systems, when combined with weather data, can help mitigate adverse weather impacts on soil health, ensuring better resource management and crop sustainability.

4 Types of Soil Sensors

4.1 Soil Moisture Sensors

Soil moisture sensors are devices that measure the amount of water present in the soil. They use techniques such as time-domain

reflectometry (TDR) and capacitance. TDR sensors measure how long an electromagnetic pulse travels through the soil, while capacitance sensors estimate moisture content based on the soil's dielectric constant (Figure 5). These sensors are crucial for precision irrigation, as they help ensure that crops receive the right amount of water, preventing both over-irrigation and waterlogging (Topp et al. 1980; Sehgal et al. 2023).

4.2 Soil Temperature Sensors

Soil temperature sensors provide crucial data about the thermal conditions of the soil, which are essential for various biological processes, including seed germination, root development, and microbial activity. Accurate measurements of soil temperature help determine optimal planting times and manage soil-borne diseases. These sensors typically utilize thermocouples or resistance temperature detectors (RTDs) to measure soil temperature at different depths, offering insights into the soil's thermal profile (Fritton and Olson 1972; Papendick and Campbell 1981).

In practical applications, these sensors are frequently used in agricultural research to optimize planting schedules and enhance crop yields by ensuring that crops are planted when soil temperatures are ideal for growth. Additionally, they aid in studying the effects of temperature fluctuations on soil ecosystems, particularly in terms of microbial activity and the decomposition of organic matter. In a specific field experiment, the accuracy of various soil temperature sensors was tested under different soil conditions. The results showed consistent temperature readings across various depths, which can be useful for predicting planting windows or adjusting irrigation schedules.

4.3 Electrical Conductivity Sensors

Electrical conductivity (EC) sensors are essential for measuring soil salinity, significantly impacting nutrient availability and plant health. High soil salinity can lead to osmotic stress and ion toxicity, hindering plant growth and reducing crop yields. EC sensors pass an electrical current through the soil and measure its ability to conduct electricity. This data is invaluable for identifying saline areas and implementing soil remediation practices to enhance soil health (Rhoades et al. 1989; Corwin and Lesch 2005). In agricultural settings, EC sensors enable real-time monitoring of soil salinity, allowing farmers to manage irrigation systems better and prevent over-fertilization, which can worsen salinity issues. For instance, Gao et al. (2023) utilized EC sensors in irrigated fields to optimize water management by adjusting irrigation schedules based on real-time salinity data. This approach helped reduce water wastage and improve crop yields. Similarly, Sharma et al. (2021) demonstrated that integrating EC sensors into automated irrigation systems maintained optimal salinity levels in vineyard soils, enhancing grapevine health and reducing input

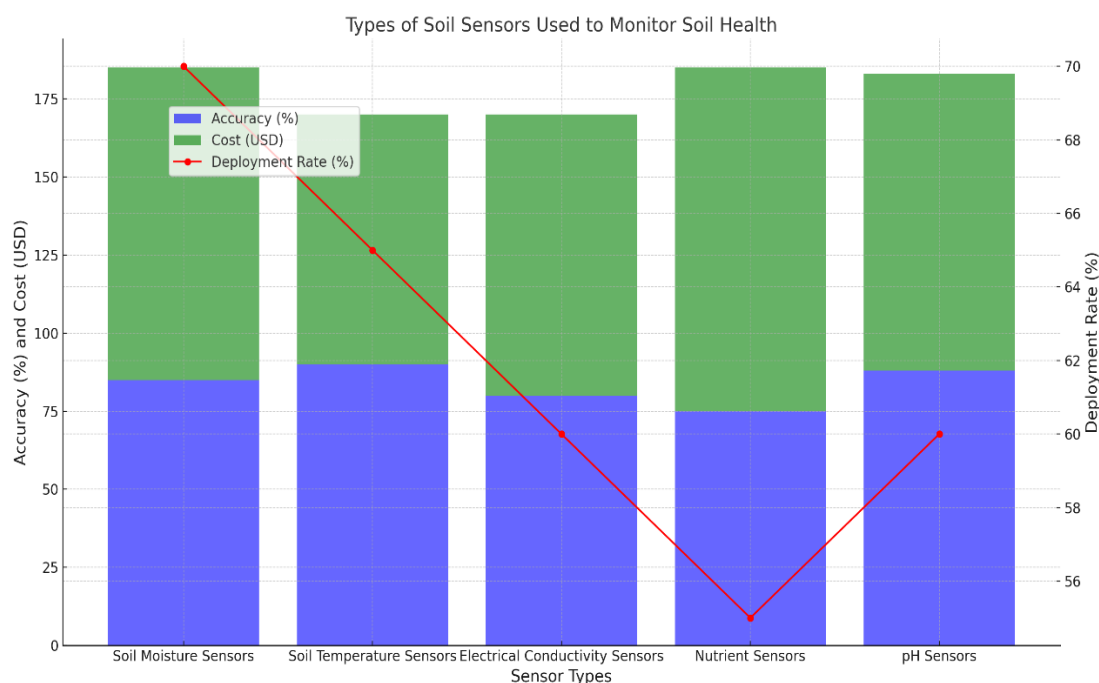


Figure 5 This chart provides a comprehensive overview of the various soil sensors used to monitor soil health, focusing on three key metrics: accuracy, cost, and deployment rate. The blue and green bars represent the accuracy and cost of each sensor type, respectively, while the red line illustrates the deployment rate. This visual representation helps to clarify the trade-offs between cost, accuracy, and deployment rate for different soil sensors, offering valuable insights for selecting the most suitable sensor type for soil health monitoring. Based on previously published data, this figure has been recreated for the current manuscript.

costs. These sensors also play a vital role in environmental monitoring by assessing soil salinity levels in areas impacted by industrial activities or salinization due to climate change. Kong et al. (2022) employed EC sensors to monitor salt accumulation in reclaimed lands, offering long-term land management strategy insights. Regularly measuring electrical conductivity facilitates the prediction of salinity risks and allows for timely corrective actions, such as modifying irrigation practices or applying soil amendments.

4.4 Nutrient Sensors

Nutrient sensors are devices that measure the concentration of essential nutrients such as nitrogen (N), phosphorus (P), and potassium (K) in the soil. They utilize various techniques to detect and quantify nutrient levels, including ion-selective electrodes and colorimetric assays. Accurate measurements of these nutrients enable precision fertilization practices, ensuring that crops receive the necessary nutrients for optimal growth while minimizing the risk of nutrient runoff and environmental pollution (Adamchuk et al. 2004; He et al. 2007). A practical application of nutrient sensors is found in precision farming, which enhances fertilization practices. For example, Sharma et al. (2023) demonstrated how nitrogen sensors can be integrated into automated irrigation systems to monitor and adjust nitrogen levels in real-time. This

approach reduces the overuse of fertilizers and ensures that crops receive the right amount of nutrients at the right time, ultimately improving both economic and environmental outcomes.

Similarly, Martínez et al. (2021) utilized phosphorus and potassium sensors in vineyards to optimize fertilization practices, improving soil health and increasing grape production. In addition, these sensors are valuable for environmental monitoring, particularly in assessing nutrient runoff and its impact on surrounding ecosystems. A study by Hassan et al. (2022) involved placing nutrient sensors in agricultural fields to monitor nutrient leaching into nearby water bodies. The data collected from these sensors facilitated the development of strategies to reduce nutrient pollution and protect water quality, underscoring the broader environmental benefits of nutrient sensing technology.

5 Remote Sensing Technologies

5.1 Introduction to Remote Sensing

Remote sensing is gathering information about the Earth's surface without making direct contact. This is achieved using satellites, aircraft, or drones with various sensors. It allows for large-scale soil health monitoring by capturing spectral data that can be analyzed to determine soil properties (Jensen 2007) (Figure 6). In soil health monitoring, remote sensing is particularly useful for

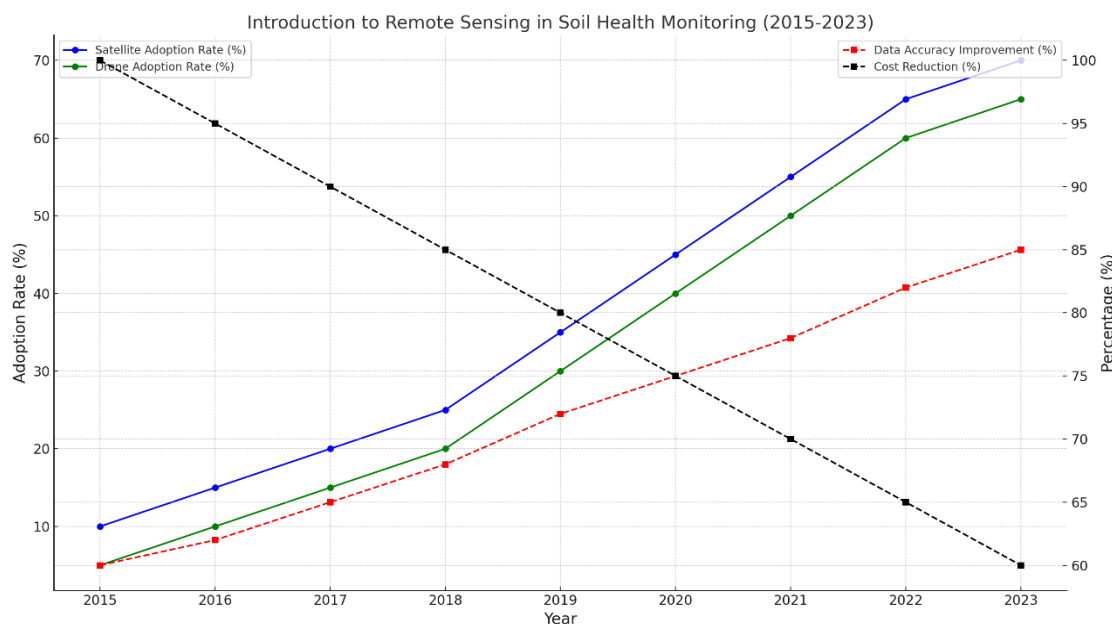


Figure 6 The chart illustrates the development of remote sensing technologies in soil health monitoring from 2015 to 2023, highlighting four key metrics. This chart offers a comprehensive overview of advancements in remote sensing, emphasizing the increasing adoption of these technologies, improved accuracy, and reduced costs. Together, these factors significantly enhance soil health monitoring practices. This figure has been recreated for the current manuscript based on the available information.

evaluating conditions over vast areas, which might be challenging or time-consuming with traditional ground-based methods. For instance, Vaughan et al. (2022) demonstrated using satellite-based remote sensing to assess soil moisture across extensive agricultural regions. By integrating multispectral images, they were able to estimate soil water content, revealing how remote sensing can help optimize irrigation schedules and minimize water wastage. Drones are also increasingly being used for more localized assessments. Yilmaz et al. (2021) utilized drone-based hyperspectral sensors to detect soil organic carbon content variations. Their research illustrated that drones with high-resolution sensors can provide precise, real-time data on soil health, which can inform customized management practices. Kang et al. (2023) also employed satellite imagery and machine learning algorithms to map soil salinity in arid regions. Their findings emphasized the potential of merging remote sensing data with advanced analytical tools to enhance soil management strategies and predict long-term trends in soil health. These applications highlight the effectiveness of remote sensing technologies as a comprehensive, non-invasive method for monitoring soil health. They offer both broad-scale and high-resolution insights, significantly improving decision-making in agriculture and environmental management.

5.2 Satellite Imagery

Satellites equipped with multispectral and hyperspectral sensors provide valuable data on soil properties and vegetation health. These sensors capture information at different wavelengths,

enabling the analysis of soil moisture, organic matter content, and nutrient levels (Mulla 2013). Multispectral sensors typically measure data across a few broad spectral bands, including the visible, near-infrared, and shortwave infrared regions. In contrast, hyperspectral sensors collect data across many narrow and continuous bands, offering more detailed insights into various soil and vegetation characteristics. The operation of these sensors is based on the principle that different materials on the Earth's surface reflect or absorb light differently across various wavelengths.

It is well established that soil moisture affects reflectance in the shortwave infrared (SWIR) region, while organic matter content can be inferred from the reflectance in the near-infrared (NIR) region. Vegetation health is often evaluated using indices such as the Normalized Difference Vegetation Index (NDVI), which is calculated from visible and near-infrared bands and indicates the vigor of plant growth. In practical applications, Zhao et al. (2022) used satellite-based multispectral sensors to monitor soil moisture and organic carbon levels across extensive agricultural areas. Their research demonstrated that these sensors delivered accurate, scalable insights into the soil's water-holding capacity and organic matter content, both crucial for effective irrigation management and improving crop productivity. In another study, Hernández et al. (2021) utilized satellite hyperspectral sensors to assess soil nutrient content. The hyperspectral data were analyzed to identify nutrient deficiencies, such as nitrogen and phosphorus, vital for crop growth. This experiment showed how hyperspectral data could provide precise information on nutrient levels, enabling

more targeted and efficient fertilization practices. These satellite-based sensors are particularly beneficial for large-scale soil monitoring, offering data over vast areas that would be impractical or costly to collect using traditional ground-based methods. In this context, multispectral sensors like Landsat and Sentinel-2 capture data in multiple wavelength bands, facilitating the monitoring of various soil health parameters (Van der Meer et al. 2012).

5.3 Drone-Based Remote Sensing

Drones provide high-resolution, flexible, and cost-effective solutions for remote sensing. With advanced cameras and sensors, drones can capture detailed images and data of agricultural fields, facilitating precise soil health assessments (Zhang and Kovacs 2012). Utilizing drones for soil health monitoring allows for frequent and targeted data collection, which enhances the accuracy and timeliness of these assessments (Zarco-Tejada et al. 2014). Drone sensors gather high-resolution imagery processed using specialized software to create detailed maps and models. For instance, multispectral sensors capture images across various bands, including visible light, near-infrared, and red edge, which are often used to evaluate vegetation health through indexes such as the NDVI. Thermal sensors provide critical information regarding soil temperature, which is essential for understanding microbial activity and plant growth dynamics.

Multiple studies have highlighted the effectiveness of drone-based sensors in precision agriculture. For example, Feng et al. (2022) demonstrated how drones equipped with multispectral sensors were used to monitor soil moisture levels and crop stress in large agricultural fields. Their research illustrated that drones could deliver real-time, high-resolution data, aiding farmers in timely irrigation and crop management decisions. Similarly, Khatami et al. (2021) utilized drones with thermal and multispectral sensors to evaluate the health of soil and crops in vineyards. Their findings revealed that drones could detect early signs of nutrient deficiencies and water stress, enabling more focused and efficient farming practices. Furthermore, Van der Meer et al. (2023) showcased drones equipped with hyperspectral sensors for mapping soil properties such as organic matter and pH levels. This high-resolution data allows for meticulous soil management and the identification of spatial variability in soil health across agricultural fields. These examples highlight the benefits of employing drone-based sensors in agricultural monitoring, where high spatial resolution and flexibility lead to more effective and timely soil health assessments.

5.4 Spectral Analysis

Spectral analysis involves studying how light interacts with soil and vegetation. Different soil properties reflect and absorb light at specific wavelengths, which can be analyzed to infer soil health

parameters. Techniques such as the Normalized Difference Vegetation Index (NDVI) and the Soil Adjusted Vegetation Index (SAVI) are commonly used in remote sensing for monitoring soil health (Rouse et al. 1974; Huete 1988). These indices help assess vegetation health, soil moisture, and organic matter content, providing valuable insights into soil conditions (Tucker 1979). The NDVI compares the difference between near-infrared and red-light reflectance and is widely used for monitoring vegetation health. High NDVI values generally indicate healthy vegetation, while low values suggest stressed or sparse vegetation. The SAVI is a modified version of NDVI that adjusts for soil brightness by incorporating a soil adjustment factor, making it particularly useful in areas with sparse vegetation or when soil background significantly influences the signal. These indices play a crucial role in remote sensing for soil health monitoring. For instance, Zhou et al. (2021) utilized NDVI and SAVI to assess the health of vegetation and soil moisture in a semi-arid region, helping to identify areas with moisture stress and insufficient organic matter. Similarly, Zhao et al. (2022) applied both indices in a study involving agricultural fields to detect spatial variations in soil organic matter and nutrient levels, which aided in improving fertilization strategies. These experiments highlight the effectiveness of spectral analysis techniques, such as NDVI and SAVI, in providing valuable insights into soil conditions and guiding precision agriculture practices.

6 Applications of Advanced Sensor and Remote Sensing Technologies

6.1 Precision Agriculture

Precision agriculture improves crop yield while reducing the environmental impact caused by the excessive use of agricultural inputs. For example, soil sensors can continuously monitor moisture levels, nutrient content, and pH, enabling targeted interventions that address the specific needs of different areas within a field. Additionally, remote sensing through satellite imagery and drone surveys provides a comprehensive overview of crop health and soil conditions across large regions. This technology helps identify areas that require attention and supports site-specific management practices (Zhang and Kovacs 2012; Mulla 2013).

6.2 Irrigation Management

Irrigation management facilitates the creation of precise irrigation schedules that align with the water requirements of crops. This practice helps reduce water waste and improves crop productivity. Remote sensing technologies, such as satellite and drone imagery, can enhance ground-based sensors by providing a broader view of soil moisture distribution across extensive agricultural fields. By integrating both ground and aerial data, farmers can implement more effective water management strategies, ensuring that water is

applied where and when it is most needed. This approach supports sustainable agricultural practices (O'Shaughnessy and Evett 2010; Jagarlapudi 2016).

6.3 Nutrient Management

The information is essential for effectively applying fertilizers and ensuring that crops receive the necessary nutrients without excess, which can lead to environmental problems such as nutrient runoff and eutrophication of water bodies. Remote sensing technologies improve nutrient management by providing detailed maps of nutrient variability within fields, allowing for site-specific fertilization. By adopting these technologies, farmers can implement targeted nutrient management practices that enhance crop health and yield and promote environmental sustainability (Scharf and Lory 2000; Jensen et al. 2007).

6.4 Soil Conservation

Soil conservation is vital for maintaining soil health and preventing land degradation. Remote sensing technologies are key in monitoring soil erosion and degradation issues across vast areas. Satellite imagery and aerial surveys from drones can identify changes in soil structure, vegetation cover, and erosion patterns, providing early warnings of potential soil degradation. This information is essential for implementing effective soil conservation strategies, such as contour farming, terracing, and cover cropping, which help to preserve soil integrity and fertility. Furthermore, remote sensing can evaluate the effectiveness of these conservation practices over time, allowing for necessary adjustments and improvements to ensure long-term soil health and sustainability (Lal 2001; Borrelli et al. 2017).

7 Case Studies

7.1 IoT in Smart Farming

An excellent example of the effective use of IoT-based soil monitoring systems is a smart farming project conducted in California (Circuit Digest 2023). In this project, a network of soil sensors was deployed across extensive agricultural fields to gather real-time data on various soil health parameters, including moisture levels, temperature, and nutrient content. Integration of soil moisture sensors allowed for precise irrigation management, resulting in a reduction of water usage by up to 30% compared to traditional irrigation methods. Additionally, using nutrient sensors enabled farmers to optimize fertilization practices, leading to a 20% decrease in fertilizer consumption while ensuring an adequate supply of nutrients for the crops.

These improvements enhanced both water and nutrient use efficiency and contributed to higher crop yields and more sustainable farming practices. The incorporation of IoT technology

allowed farmers to access this data remotely and in real-time, significantly improving water use efficiency and crop yield. By utilizing precise soil moisture data, the project facilitated more efficient irrigation scheduling, minimizing water wastage and ensuring optimal conditions for crop growth. Additionally, the ongoing assessment of soil nutrients facilitated the precise application of fertilizers, which improved soil fertility and agricultural productivity. This case study illustrates how IoT technology can transform traditional farming practices, making them more sustainable and resource-efficient.

7.2 Drone-Based Soil Health Monitoring in India

In India, the use of drone technology for monitoring soil health has shown promising results in enhancing agricultural productivity (Press Information Bureau 2023; India CSR 2024). Drones equipped with advanced multispectral and hyperspectral cameras capture high-resolution images of agricultural fields. These images are then analyzed to evaluate soil health indicators, including moisture content, nutrient levels, and the presence of diseases or pests. The detailed data collected from drones allows farmers to identify and address soil health issues more precisely. For example, drones can pinpoint areas in a field experiencing water stress, enabling targeted irrigation efforts. Similarly, they can quickly identify and correct nutrient deficiencies, promoting balanced soil fertility. Overall, drone technology has improved crop management practices, increasing crop yields and better resource utilization in large agricultural fields across India.

8 Challenges and Future Directions

8.1 Technical Challenges

Despite significant advancements in sensor technologies and remote sensing, several technical challenges hinder their widespread adoption for soil health monitoring. One major challenge is the high cost of purchasing and maintaining advanced sensors and remote sensing equipment, which can be particularly prohibitive for small-scale farmers. Additionally, integrating data from various sensors and remote sensing platforms presents significant difficulties. Ensuring that data from different sources is compatible and seamlessly integrated into a cohesive monitoring system requires advanced technical expertise and sophisticated software solutions. Furthermore, interpreting these technologies' vast amounts of data necessitates specialized soil science and data analytics knowledge. Addressing these technical challenges is essential for these advanced monitoring technologies' broader adoption and effective use.

8.2 Data Privacy and Security

Using IoT devices and remote sensing technologies for soil health monitoring raises significant data privacy and security concerns.

The large amounts of data collected by these devices, which includes sensitive information about soil conditions and agricultural practices, must be protected from unauthorized access and misuse. To ensure data security, it is essential to implement robust encryption protocols and secure data storage solutions. Additionally, clear guidelines and regulations are necessary to govern the ethical use of this data, ensuring that farmers' privacy is respected and that the data is used solely to enhance agricultural practices and soil health. Building trust among farmers and other stakeholders is crucial for successfully adopting these technologies. By adopting transparent data management practices and stringent security measures, we can address concerns and foster a supportive environment for using IoT and remote sensing in monitoring soil health.

8.3 Future Trends

The future of soil health monitoring is expected to be influenced by integrating advanced technologies, such as artificial intelligence (AI) and machine learning (ML), with sensor and remote sensing data. AI and ML algorithms can analyze complex datasets, providing deeper insights into soil health dynamics. These technologies have the potential to identify patterns and correlations that may not be evident through traditional analysis methods, enabling more accurate predictions and proactive soil health management. For example, AI-driven models can forecast soil moisture trends based on historical data and weather predictions, helping farmers plan their irrigation schedules more effectively. Similarly, ML algorithms can analyze spectral data from remote sensing platforms to detect early signs of soil degradation or nutrient deficiencies, allowing for timely interventions. The ongoing advancement of AI and ML technologies promises to enhance soil health monitoring systems, making them more predictive, efficient, and accessible to a wider range of users.

Conclusion

Integrating advanced sensor technologies and remote sensing in soil health monitoring marks a significant advancement toward achieving sustainable agriculture. These innovations provide real-time, accurate, and comprehensive data on soil health, empowering farmers and researchers to make informed decisions and optimize resource management. While challenges related to cost, data integration, and privacy persist, ongoing technological advancements and the potential integration of artificial intelligence (AI) and machine learning (ML) offer promising solutions to these issues. The future of soil health monitoring is set to become more efficient, precise, and accessible, contributing to enhanced agricultural practices and environmental conservation. As these technologies evolve, they will help ensure soil health and sustainability for future generations.

References

- Adamchuk, V. I., Hummel, J. W., Morgan, M. T., & Upadhyaya, S. K. (2004). On-the-go soil sensors for precision agriculture. *Computers and Electronics in Agriculture*, *44*(1), 71-91.
- Akyildiz, I. F., Su, W., Sankarasubramaniam, Y., & Cayirci, E. (2002). Wireless sensor networks: A survey. *Computer Networks*, *38*(4), 393-422.
- Basso, B., Reynolds, M., & D'Urso, G. (2021). Use of electrical conductivity sensors for irrigation management in arid and semi-arid regions. *Field Crops Research*, *258*, 107914. <https://doi.org/10.1016/j.fcr.2020.107914>
- Borrelli, P., Robinson, D. A., Panagos, P., Lugato, E., Yang, J. E., et al. (2017). An assessment of the global impact of 21st-century land use change on soil erosion. *Nature Communications*, *8*, 2013. <https://doi.org/10.1038/s41467-017-02142-7>
- Brady, N. C., & Weil, R. R. (2008). *The nature and properties of soils* (Vol. 13, pp. 662-710). Upper Saddle River, NJ: Prentice Hall.
- Chen, L., Zhang, H., & Liu, Y. (2020a). IoT and weather data integration for flood risk management in rice paddies. *Field Crops Research*, *249*, 107781. <https://doi.org/10.1016/j.fcr.2020.107781>
- Chen, X., Wu, L., & Zhang, L. (2020b). Precision agriculture: Opportunities and challenges for the future. *Journal of Agricultural Science*, *12*(3), 55-68.
- Circuit Digest. (2023). IoT-based smart agriculture monitoring system | Smart farming project using NodeMCU ESP8266. Retrieved from <https://circuitdigest.com>
- Corwin, D. L., & Lesch, S. M. (2005). Apparent soil electrical conductivity measurements in agriculture. *Computers and Electronics in Agriculture*, *46*(1-3), 11-43.
- Feng, L., Zhang, Y., & Liu, Y. (2022). Drone-based multispectral remote sensing for soil moisture and crop stress assessment in agricultural fields. *Remote Sensing*, *14*(12), 2931. <https://doi.org/10.3390/rs14122931>
- Fritton, D. D., & Olson, G. W. (1972). Temperature measurement in soil. *Agronomy Journal*, *64*(5), 629-634.
- Gao, J., Zhang, X., & Wang, Z. (2023). Optimization of irrigation schedules using electrical conductivity sensors in irrigated agricultural fields. *Agricultural Water Management*, *280*, 107925. <https://doi.org/10.1016/j.agwat.2022.107925>
- Hassan, A., Bhat, S., & Singh, S. (2021). Integration of IoT-based sensors for optimizing fertilization and pH management in wheat

- farming. *Agricultural Systems*, 187, 103039. <https://doi.org/10.1016/j.agry.2020.103039>
- Hassan, R., Khan, S., & Ahmed, M. (2022). Application of nutrient sensors for monitoring nutrient runoff in agricultural watersheds. *Environmental Monitoring and Assessment*, 194(6), 310. <https://doi.org/10.1007/s10661-022-10223-3>
- Havlin, J. L., Tisdale, S. L., Nelson, W. L., & Beaton, J. D. (2013). *Soil fertility and fertilizers: An introduction to nutrient management* (8th ed.). Pearson.
- He, Z. L., Zhang, H., Calvert, D. V., Stoffella, P. J., Yang, X. E., & Yu, S. (2007). Assessment of soil property variability using a global positioning system and geostatistics. *Communications in Soil Science and Plant Analysis*, 38(5-6), 689-711.
- Hernández, R., García, J., & Martínez, M. (2021). Assessment of soil nutrient levels using hyperspectral remote sensing. *Remote Sensing of Environment*, 255, 112257. <https://doi.org/10.1016/j.rse.2021.112257>
- Huang, Y., Liu, L., & Zhang, C. (2022). Field-scale assessment of soil moisture sensing for vineyard irrigation management. *Agricultural Systems*, 195, 103283. <https://doi.org/10.1016/j.agry.2021.103283>
- Huete, A. R. (1988). A soil-adjusted vegetation index (SAVI). *Remote Sensing of Environment*, 25(3), 295-309. [https://doi.org/10.1016/0034-4257\(88\)90106-X](https://doi.org/10.1016/0034-4257(88)90106-X)
- India CSR. (2024). The potential of drone technology in agriculture in India. India CSR.
- Jagarlapudi, A. (2016). Real-time smart irrigation system. *International Journal of Intelligent Technologies and Applied Statistics*, 9(1), 81-95. [https://doi.org/10.6148/IJTAS.201603_9\(1\).0006](https://doi.org/10.6148/IJTAS.201603_9(1).0006)
- Jensen, J. R. (2009). *Remote sensing of the environment: An earth resource perspective 2/e*. Pearson Education India.
- Jensen, T., Scharf, P., Hong, S. Y., & Dobermann, A. (2007). Spatial analysis of field-scale nitrogen management experiments using aerial photography and site-specific management zones. *Agronomy Journal*, 99(3), 1090-1103. <https://doi.org/10.2134/agronj2006.0270>
- Jones, D. A., & Brown, R. B. (2019). Remote sensing in soil science: Past, present, and future applications. *Soil Science Society of America Journal*, 83(4), 941-954.
- Jones, S. B., Sheng, W., & Weihermüller, L. (2020). Soil moisture measurement methods and applications. In J. H. Dane & G. C. Topp (Eds.), *Methods of soil analysis: Part 4 physical methods* (pp. 578-596). Soil Science Society of America.
- Kang, Z., Wang, J., & Liu, F. (2023). Mapping soil salinity using satellite imagery and machine learning algorithms. *Environmental Monitoring and Assessment*, 195(2), 38. <https://doi.org/10.1007/s10661-023-10792-6>
- Khatami, R., Mirzavand, M., & Tan, W. (2021). Utilizing drones with thermal and multispectral sensors for precision agriculture in vineyards. *Field Crops Research*, 263, 108119. <https://doi.org/10.1016/j.fcr.2021.108119>
- Kim, Y., Evans, R. G., & Iversen, W. M. (2017). Remote sensing and control of an irrigation system using a distributed wireless sensor network. *IEEE Transactions on Instrumentation and Measurement*, 57(7), 1379-1387.
- Kong, X., Li, Y., & Liu, L. (2022). Environmental monitoring of soil salinity using electrical conductivity sensors in reclaimed land. *Environmental Monitoring and Assessment*, 194(3), 183. <https://doi.org/10.1007/s10661-022-10063-6>
- Kumar, P., & Lal, R. (2020). Advances in sensors for monitoring soil health in precision agriculture. *Sensors and Actuators B: Chemical*, 322, 128708. <https://doi.org/10.1016/j.snb.2020.128708>
- Lal, R. (2001). Soil degradation by erosion. *Land Degradation & Development*, 12(6), 519-539. <https://doi.org/10.1002/ldr.472>
- Martínez, M., Sánchez, A., & López, J. (2021). Precision fertilization with nutrient sensors in vineyards: A case study. *Field Crops Research*, 268, 108207. <https://doi.org/10.1016/j.fcr.2021.108207>
- Mulla, D. J. (2013). Twenty-five years of remote sensing in precision agriculture: Key advances and remaining knowledge gaps. *Biosystems Engineering*, 114(4), 358-371. <https://doi.org/10.1016/j.biosystemseng.2012.08.009>
- Mutyalamma, A. V., Yoshitha, G., Dakshyani, A., & Padmavathi, B. V. (2020). Smart agriculture to measure humidity, temperature, moisture pH, and nutrient values of the soil using IoT. *International Journal of Engineering and Advanced Technology*, 9(5), 394-398.
- O'Shaughnessy, S. A., & Evett, S. R. (2010). Canopy temperature-based system effectively schedules and controls center pivot irrigation of cotton. *Agricultural Water Management*, 97(9), 1310-1316. <https://doi.org/10.1016/j.agwat.2010.03.012>
- Papendick, R. I., & Campbell, G. S. (1981). Theory and measurement of water potential. In J. F. Parr, W. Gardner, R., & Elliott, L. F. (Eds.). (Year). *Water potential relations in soil microbiology* (pp. 1-22). SSSA Special Publication.
- Patel, A., Mehta, R., & Verma, S. (2021). Optimization of irrigation systems using soil moisture sensors: A case study.

- Agricultural Water Management*, 244, 106472. <https://doi.org/10.1016/j.agwat.2020.106472>
- Paul, E. A. (2014). *Soil Microbiology, Ecology, and Biochemistry* (4th ed.). Academic Press.
- Press Information Bureau. (2022). Use of drones in agriculture and improving farmers income. Ministry of Agriculture & Farmers Welfare.
- Rai, D., Singh, R., & Gupta, S. (2020). Application of nutrient sensors for optimizing fertilizer use in corn farming. *Field Crops Research*, 253, 107795. <https://doi.org/10.1016/j.fcr.2020.107795>
- Rhoades, J. D., Raats, P. A. C., & Prather, R. J. (1989). Effects of liquid-phase electrical conductivity, water content, and surface conductivity on bulk soil electrical conductivity. *Soil Science Society of America Journal*, 43(5), 807-813.
- Rouse, J. W., Haas, R. H., Schell, J. A., Deering, D. W., & Harlan, J. C. (1974). *Monitoring the vernal advancement and retrogradation (greenwave effect) of natural vegetation*. NASA/GSFC Type III Final Report.
- Saha, D., Mohanty, S., & Chatterjee, S. (2020). Monitoring soil salinity using electrical conductivity sensors in saline soil areas of India. *Agricultural Water Management*, 231, 105964. <https://doi.org/10.1016/j.agwat.2019.105964>
- Scharf, P. C., & Lory, J. A. (2000). Calibration of remotely sensed corn color to predict nitrogen need. *Agronomy Journal*, 92(5), 875-883. <https://doi.org/10.2134/agronj2000.925875x>
- Sehgal, A., Singh, G., Quintana, N., Kaur, G., Ebelhar, W., Nelson, K. A., & Dhillon, J. (2023). Long-term crop rotation affects crop yield and economic returns in humid subtropical climate. *Field Crops Research*, 298, 108952.
- Shao, W., Zhang, W., & Xie, Y. (2019). Soil temperature and its impact on rice growth in paddy fields. *Field Crops Research*, 233, 68-74. <https://doi.org/10.1016/j.fcr.2019.01.001>
- Sharma, R., Singh, A., & Gupta, R. (2021). Role of electrical conductivity sensors in precision irrigation systems for vineyards. *Precision Agriculture*, 22(6), 1358-1373. <https://doi.org/10.1007/s11119-021-09809-3>
- Sharma, R., Singh, A., & Gupta, R. (2023). Integration of nutrient sensors for real-time monitoring of nitrogen levels in precision agriculture. *Agricultural Systems*, 189, 103024. <https://doi.org/10.1016/j.agry.2022.103024>
- Smith, J. R., Johnson, K., & Williams, M. A. (2020). Internet of Things (IoT) in agriculture: Implementing smart soil health monitoring systems. *Agricultural Systems*, 182, 102857.
- Smith, J., & Black, S. (2019). Advanced sensor technologies in precision agriculture: Challenges and opportunities. *Journal of Agricultural Technology*, 15(3), 155-167.
- Smith, M., Jones, P., & Williams, D. (2021). Integration of IoT-based soil moisture sensors with weather forecasting systems for drought management in agriculture. *Agricultural Water Management*, 256, 106115. <https://doi.org/10.1016/j.agwat.2021.106115>
- Sood, A., Sharma, S., & Yadav, S. (2020). IoT-based soil monitoring system for precision irrigation in vineyards. *Sensors*, 20(12), 3502. <https://doi.org/10.3390/s20123502>
- Sparks, D. L. (2003). *Environmental Soil Chemistry* (2nd ed.). Academic Press.
- Topp, G. C., Davis, J. L., & Annan, A. P. (1980). Electromagnetic determination of soil water content: Measurements in coaxial transmission lines. *Water Resources Research*, 16(3), 574-582.
- Tucker, C. J. (1979). Red and photographic infrared linear combinations for monitoring vegetation. *Remote Sensing of Environment*, 8(2), 127-150. [https://doi.org/10.1016/0034-4257\(79\)90013-0](https://doi.org/10.1016/0034-4257(79)90013-0)
- Van der Meer, F. D., Van der Werff, H. M. A., Van Ruitenbeek, F. J. A., Hecker, C. A., Bakker, W. H., et al. (2012). Multi- and hyperspectral geologic remote sensing: A review. *International Journal of Applied Earth Observation and Geoinformation*, 14(1), 112-128. <https://doi.org/10.1016/j.jag.2011.08.002>
- Van der Meer, F., Fernández, D., & Rivas, J. (2023). Hyperspectral drone imaging for mapping soil properties and vegetation health. *Remote Sensing of Environment*, 259, 112382. <https://doi.org/10.1016/j.rse.2023.112382>
- Vaughan, R., Robinson, J., & Price, D. (2022). Satellite remote sensing for large-scale soil moisture monitoring in agriculture. *Agricultural Systems*, 196, 103257. <https://doi.org/10.1016/j.agry.2022.103257>
- Wang, Y., & Li, H. (2022). Integrating sensor and remote sensing data for soil health assessment. *Environmental Monitoring and Assessment*, 194, 128.
- Wang, Y., Li, J., & Zhang, L. (2020). Optimizing wheat sowing using soil temperature monitoring systems. *Agricultural Systems*, 180, 102760. <https://doi.org/10.1016/j.agry.2020.102760>
- Yilmaz, H., Bahar, S., & Akgül, M. (2021). Hyperspectral drone sensing for soil organic carbon mapping in agricultural fields. *Remote Sensing of Environment*, 257, 112302. <https://doi.org/10.1016/j.rse.2021.112302>

- Zarco-Tejada, P. J., Hubbard, N., & Loudjani, P. (2014). Precision agriculture: An opportunity for EU farmers—Potential support with the CAP 2014-2020. Joint Research Centre, European Commission.
- Zhang, C., & Kovacs, J. M. (2012). The application of small unmanned aerial systems for precision agriculture: A review. *Precision Agriculture*, *13*(6), 693-712. <https://doi.org/10.1007/s11119-012-9274-5>
- Zhang, H., Li, Y., & Wang, W. (2021). Use of nutrient sensors for potassium fertilization in wheat fields. *Agricultural Systems*, *189*, 103074. <https://doi.org/10.1016/j.agsy.2021.103074>
- Zhang, Q., Zhao, Y., & Liu, J. (2021). Soil variability mapping for precision agriculture: Techniques and applications. *Computers and Electronics in Agriculture*, *182*, 105938.
- Zhao, Y., Zhang, Y., & Li, X. (2022). Using satellite-based multispectral sensors for monitoring soil moisture and organic carbon in agricultural fields. *Agricultural Systems*, *189*, 103254. <https://doi.org/10.1016/j.agsy.2021>
- Zhou, S., Williams, A.P., Lintner, B.R., Berg, A.M., Zhang, Y., et al. (2021) Soil moisture-atmosphere feedbacks mitigate declining water availability in drylands. *Nature Climate Change*, *11* (1), 38-44, doi:10.1038/s41558-020-00945-z.



Journal of Experimental Biology and Agricultural Sciences

<http://www.jebas.org>

ISSN No. 2320 – 8694

Fruits of *Prosopis chilensis* and *Tetrapleura tetraptera* as an alternative against multi-resistant bacteria in lower respiratory tract infections

Jotham Yhi-pênê N'do* , Dramane Paré , Issa Karama ,
 Adama Hilou, Martin Kiendrébéogo 

Laboratory of applied biochemistry and chemistry (LABIOCA), Joseph KI-ZERBO University, 03 BP 7021 Ouagadougou 03, Burkina Faso

Received – August 06, 2024; Revision – November 09, 2024; Accepted – November 21, 2024

Available Online – November 29, 2024

DOI: [http://dx.doi.org/10.18006/2024.12\(5\).668.675](http://dx.doi.org/10.18006/2024.12(5).668.675)

KEYWORDS

Prosopis chilensis

Tetrapleura tetraptera

Pseudomonas aeruginosa

Fruits

Antioxidant

Antibacterial

ABSTRACT

Pseudomonas aeruginosa is a bacterium whose global spread poses a significant threat to human health due to its multidrug resistance (MDR). As a result, it is crucial to explore alternative treatments, particularly plant-based drugs, that are considered safe. The fruits of two plants, *Tetrapleura tetraptera*, and *Prosopis chilensis*, have been traditionally used to treat infectious diseases. These fruits are well-known for their nutritional and functional properties and their various bioactive compounds. Given these characteristics, the fruits can be effectively used against bacterial species like *P. aeruginosa*, which are resistant to conventional antibiotics. The present study aimed to evaluate the effects of fruit extracts on the multi-resistant bacterium *P. aeruginosa* PAO1. The research utilized methanolic, hydro-methanolic extracts, and aqueous decoctions of the selected fruits for phytochemical analysis and to assess antioxidant and antibacterial activities, along with acute toxicity. The study employed the 2,2-Diphenyl-1-picryl hydrazyl (DPPH) radical scavenging activity and ferric reducing antioxidant power (FRAP) methods to examine antioxidant properties. The antibacterial activity was assessed through minimum inhibitory concentration (MIC), minimum biofilm concentration (BMC), and biofilm formation analysis. The results indicated that the methanolic extracts of *P. chilensis* and the aqueous decoction of *T. tetraptera* exhibited high total phenolic contents (135 and 143 mg GAE/g, respectively) and demonstrated the best antioxidant activity. Furthermore, the hydromethanolic extract of *T. tetraptera* showed the most substantial biofilm inhibition (70.15%) compared to the other extracts from both plants. Importantly, none of the extracts showed signs of toxicity at a dosage of 2000 mg/kg body weight. In conclusion, *T. tetraptera* and *P. chilensis* fruits contain compounds responsible for significant

* Corresponding author

E-mail: yhipene2005@yahoo.fr (Jotham Yhi-pênê N'do)

Peer review under responsibility of Journal of Experimental Biology and Agricultural Sciences.

Production and Hosting by Horizon Publisher India [HPI]
 (<http://www.horizonpublisherindia.in/>).
 All rights reserved.

All the articles published by [Journal of Experimental Biology and Agricultural Sciences](#) are licensed under a [Creative Commons Attribution-NonCommercial 4.0 International License](#) Based on a work at www.jebas.org.



antioxidant activity and demonstrate efficacy against *P. aeruginosa* PAO1. These fruits could be potential candidates for developing phyto-drugs to combat antibacterial resistance in respiratory tract infections.

1 Introduction

According to the World Health Organization (WHO), an estimated 2.6 million deaths occur each year due to acute respiratory infections (ARI), with the majority occurring in developing countries (Mengistu et al. 2024). Additionally, Ghosh et al. (2023) indicated that ARI is the second leading cause of death globally, particularly among children. In the United States, pneumonia and bronchopneumonia account for 70 to 80% of admissions to healthcare facilities (Wood and Kuzel 2023). In Burkina Faso, roughly 23% of children aged 0 to 5 years exhibit symptoms of acute respiratory infection and fever (INSD 2022).

A common symptom of ARI is a cough, which may be accompanied by shortness of breath, weakness, fever, and fatigue. Coughing is particularly prevalent among the elderly, children under five, and immunocompromised individuals. The primary causes of these infections are often viral and/or bacterial (Kaler et al. 2023). The increased use of antibiotics and the application of incorrect dosages have led to the emergence of resistant strains of bacteria (Salam et al. 2023).

In response to the growing resistance of bacteria to the latest generation of antibiotics, medicinal plants may be effective alternatives in combating multidrug-resistant infections (Kang et al. 2023). The fruits of *T. tetraptera* are commonly utilized as a source of energy and nutrients, particularly for medicinal purposes (Kuate et al. 2015). Similarly, the fruit of *P. chilensis* is used for animal feed and in traditional medicine for its antimicrobial properties (Lorenzo et al. 2022).

This study is based on the hypothesis that these two fruits contain antimicrobial compounds that could serve as plant-based antibiotics against multidrug-resistant bacteria responsible for severe infections. The objective of this study was to evaluate the effects of methanolic, hydro-methanolic extracts, and aqueous decoctions of these two plants on the multidrug-resistant bacteria *Pseudomonas aeruginosa*, which is associated with lower respiratory tract infections (LRTI).

2 Materials and Methods

2.1 Microorganisms

The bacterial strain *Pseudomonas aeruginosa* PO1 was obtained from the Microbiology Laboratory of Joseph Ki-Zerbo University, Burkina Faso. Bacterial strain *P. aeruginosa* PAO1 was cultured in LB broth at 37 °C with agitation at 175 rpm. Its derivatives were grown in LB-MOPS broth (50 mM, pH 7), supplemented with

carbenicillin at a concentration of 300 µg/mL, under the same temperature and agitation conditions.

2.2 Plant material

T. tetraptera and *P. chilensis* fruits were harvested from the Saaba commune in Burkina Faso. Specimens of *P. chilensis* (Molina) and *T. tetraptera* are deposited at the herbarium of Joseph KI-Zerbo University with code numbers 16741 and 16781, respectively.

2.3 Phytochemical characterization

The phytochemical characterization of the prepared plant extracts was conducted following the method described by Abubakar and Haque (2020). The dried material was powdered, stored in airtight containers, and kept in the dark at room temperature. Three solvents were used to extract compounds for biological activity testing: a 50:50 (v:v) mixture of water and methanol, methanol (98%), and water. The solvents of methanol and the methanol-water mixture were utilized to macerate the powdered fruit in a 1:10 (mass/volume) ratio. For the aqueous decoction, the mixture of water and material was boiled for 30 minutes.

2.4 Phytochemical assays

2.4.1 Assessment of total phenolic content

A microplate well is filled with 25 µL of the test solution (1 mg/mL), then combined with 125 µL of Folin-Ciocalteu reagent (FCR, 0.2). The mixture is incubated for 5 minutes. Next, 100 µL of sodium carbonate solution (7.5%) is added, and the incubation continues for 2 hours. Absorbance readings are taken at 760 nm. The results are expressed as milligrams of Gallic Acid Equivalent per gram of dry extract (mg GAE/g) (Singleton et al. 1999).

2.4.2 Assessment of total flavonoid content

The flavonoid content was determined using the method of Shraim et al. (2021). Absorbances were measured at 415 nm, and results are expressed as milligrams of quercetin equivalent (QE) per gram of dry extract (mg QE/g).

2.5 Biological activities

2.5.1 Antioxidant activity

The antioxidant activity was assessed using the DPPH method, as described by Velazquez et al. (2007). In this method, 100 µL of each sample (50 mg/mL) is mixed with 200 µL of DPPH solution (20 mg/L). This process is based on measuring the reduction in

absorbance at 515 nm of the free radical DPPH in the presence of hydrogen ions (H^+). The measured absorbance is then used to calculate the percentage inhibition of the DPPH radical, which reflects the antiradical potential of the sample. Ascorbic acid was used as a standard for comparison, and results were expressed in micrograms of ascorbic acid equivalent per 100 mg of extract (μg AAE/100 mg).

The evaluation of antioxidant activity using the FRAP method followed the procedure outlined by Hinneburg et al. (2006). In this method, 0.5 mL of the sample (0.625 mg/mL) is added successively to 1.25 mL of phosphate buffer (0.2 M, pH 6.6) and 1.25 mL of 1% potassium ferrocyanide. The mixture is then heated to 50°C for 30 minutes. After heating, 1.25 mL of 10% trichloroacetic acid is added, and the mixture is centrifuged for 10 minutes at 2000 rpm. From the resulting supernatant, 125 μ L is transferred to wells in a 96-well plate, followed by the addition of 125 μ L of distilled water and 25 μ L of 1% ferric chloride. The absorbances are measured at 700 nm, and the results are expressed in millimoles of ascorbic acid equivalent (AAE) per gram of dry extract.

2.5.2 Determination of antibacterial activity

Liquid Luria-Bertani (LB) medium was prepared by dissolving 20 g of LB medium in 1 L of water with a pH of 7.2. The medium and materials were sterilized at 121°C for 15 minutes.

2.5.2.1 Determination of MIC (Minimum Inhibitory Concentration)

The extracts' minimum inhibitory concentrations (MICs) were determined using the 96-well microplate method (Barnes et al. 2023). The extracts were dissolved in 10% dimethyl sulfoxide (DMSO), and 20 μ L of this solution was transferred into wells containing 170 μ L of LB medium, resulting in a final DMSO concentration of 1%. A plain DMSO solution (1%) was used as a negative control.

Next, 10 μ L of a *Pseudomonas aeruginosa* (PAO1) inoculum was introduced into each well, and the plates were incubated at 37°C for 18 hours. The MIC of the extract was identified as the first well that showed no bacterial growth. After the incubation period, 50 μ L of p-iodonitrotetrazolium (INT) at a concentration of 0.2 g/mL was added to each well and incubated for 30 minutes. Microbial growth in the wells was indicated by the pink coloration of the INT (Jalal et al. 2023).

2.5.2.2 Determination of MBC (Minimum Bactericidal Concentration)

The Minimum Bactericidal Concentration (MBC) is the lowest concentration that can kill more than 99.9% of the initial bacterial population in the inoculum. Samples were collected from the control tube containing 1% DMSO and from each tube that showed

no bacterial growth. These samples were then used to inoculate LB agar plates. The plates were incubated at 37°C for 24 hours. The MBC is determined from the first tube that exhibited no bacterial growth (Keyhanian et al. 2023).

2.5.2.3 Assessment of biofilm formation inhibition

Pseudomonas aeruginosa (PAO1) cells from an overnight culture were inoculated into 96-well plates containing 200 μ L of growth medium, with or without extracts. After 18 hours of incubation, planktonic cells were removed, and adherent cells were fixed with methanol and stained with 0.2% crystal violet. After 5 minutes, the excess dye was washed away three times. Then, 33% acetic acid was added to each well, and the absorbance was recorded at 570 nm. Positive and negative controls, which contained only the inoculated growth medium and the growth medium with extract, were included in each experiment (Uppala et al. 2019).

2.6 Assessment of the acute toxicity

The toxicity of the extract was assessed following guideline 423 established by the Organization for Economic Co-operation and Development (OECD 2004) (Sasmito et al. 2017). Two groups of three female NMRI strain mice, weighing approximately 34 ± 3 g, were fasted for four hours before the experiment. The first group served as the control and received only plain water, while the test group was administered a dose of 2,000 mg/kg body weight of the extract via a feeding tube. The mice were observed continuously for two hours after administration and then regularly for the following fourteen days to monitor any signs of toxicity, which included tremors, convulsions, salivation, diarrhea, lethargy, sleep disturbances, and coma. The animals remained fast on the night of the fourteenth day and were subsequently sacrificed after being anesthetized. The liver, pancreas, and kidneys were collected from the treated and control groups to compare appearance and morphology. All animal experimentation protocols adhered to the guidelines of the Institutional Animal Ethics Committee (Directive 2010/63/EU on the protection of animals used for scientific purposes). Ethical approval code: 2010/63/EU, approval date: October 20, 2010.

2.7 Data processing and analysis

Calculations and graphs were performed using Microsoft Excel and GraphPad Prism software, version 5.0. Statistical analysis was conducted with IBM SPSS Statistics Base version 25. A significant difference is indicated by $p < 0.05$.

3 Results

3.1 Total phenolic and flavonoid content

The total phenolic and flavonoid contents of the fruits from *P. chilensis* and *T. tetraptera* are summarized in Table 1. The study

Table 1 Evaluation of the total phenolic and flavonoid content in the selected plant extract

Plants	Extracts	Phytochemical characterization				Phytochemical dosage	
		Flavonoids	Tannins and Polyphenols	Alkaloid	Saponoside	Total phenolic (mg GAE/g extract)	Total flavonoids (mg QE/g extract)
<i>P. chilensis</i>	Methanolic	++	+++	+	++	143.72±13.02 ^a	10.46±3.04 ^{ac}
	Hydro-methanolic	++	++	+		232.45±0.39 ^b	31.22±2.64 ^b
	Aqueous decoction	+	++	+	++	38.99±2.57 ^c	14.22±0.52 ^a
<i>T. tetraptera</i>	Methanolic	++	++	+	++	87.94±0.81 ^d	9.43±0.55 ^c
	Hydro-methanolic	+	+	+	++	100.58±3.93 ^d	0.45±0.02 ^d
	Aqueous decoction	+	+	+	+	135.55±8.78 ^a	21.23±0.50 ^e

+ = presence; ++ = abundant; +++ = very abundant, QE: Quercetin Equivalent; GAE: Gallic acid equivalent; values in each column with differing superscript letters are significantly different ($P < 0.05$) for each phytochemical group measured

results showed that the total phenolic content in the samples ranged from 232.45 ± 0.39 mg GAE/g for the hydro-methanolic extract of *P. chilensis* to 38.99 ± 2.57 mg GAE/g for its aqueous decoction. For *T. tetraptera*, the total phenolic content of the hydro-methanolic extract was 100.58 ± 3.93 mg GAE/g. The findings indicated that the hydro-methanolic extract of *P. chilensis* contains many total phenolics and flavonoids. In contrast, in *T. tetraptera*, the highest concentrations of these compounds were found in the aqueous extracts. These observations suggest that hydro-methanolic solvents and water can extract total phenolics and flavonoids from *P. chilensis* and *T. tetraptera*.

3.2 Antioxidant activity

The FRAP and DPPH free radical scavenging activities of *P. chilensis* and *T. tetraptera* fruits are summarized in Table 2. The results indicate that all extracts exhibited similar activities when assessed using the FRAP method, regardless of the extraction solvent utilized. In contrast, according to the DPPH method, the methanolic and aqueous extracts of *P. chilensis* and *T. tetraptera* demonstrated the highest activity levels. The study revealed that the best antioxidant activities were recorded as 241.7 ± 0.52 mg AAE/g for the methanolic extract of *P. chilensis* and 271.35 ± 1.07

Table 2 FRAP and DPPH antioxidant activities of the tested fruit extract of *P. chilensis* and *T. tetraptera*

Plants	Extracts	DPPH activity (mg AAE/g)	FRAP activity (mmol AAE/g)
<i>P. chilensis</i>	Methanolic	241.7±0.52 ^a	18.34±1.66 ^a
	Hydro-methanolic	232.45±0.39 ^b	22.14±3.91 ^{ab}
	Aqueous decoction	228.25±0.51 ^a	21.81±2.00 ^{ab}
<i>T. tetraptera</i>	Methanolic	263.25±12.69 ^b	19.64±1.37 ^{ab}
	Hydro-methanolic	256.85±2.57 ^b	20.07±1.21 ^{ab}
	Aqueous decoction	271.35±1.07 ^b	25.85±3.57 ^b

EAA: Ascorbic acid equivalent, values in each table column bearing different superscript letters differ significantly ($P < 0.05$) for each phytochemical group measured.

Table 3 Minimum inhibitory and bactericidal concentrations of extracts

Plants	Extracts	MIC (mg/ml)	BMC (mg/ml)	BMC/MIC
<i>P. chilensis</i>	Methanolic	12.5	>50	>1
	Hydromethanolic	50	>50	>4
	Aqueous decoction	50	>50	>1
<i>T. tetraptera</i>	Methanolic	-	-	-
	Hydromethanolic	-	-	-
	Aqueous decoction	-	-	-

-Inactive

mg AAE/g for the aqueous decoction of *T. tetraptera*, as measured by the DPPH method.

3.3 Antimicrobial properties of extracts

3.3.1 Determination of minimum inhibitory (MIC) and bactericidal concentrations (BMC)

Table 3 presents the minimum concentrations required to inhibit bacterial growth (minimum inhibitory concentration, MIC) and the bactericidal concentrations (BMC) where no bacterial growth was observed. The hydromethanolic extract of *P. chilensis* exhibited the lowest MIC of 12.5 mg/mL against *P. aeruginosa* PAO1, while all other extracts demonstrated MICs greater than 50 mg/mL. Additionally, the extracts of *T. tetraptera* showed no inhibitory or bactericidal activity against *P. aeruginosa* at a concentration of 50 mg/mL.

3.3.2 Inhibition of biofilm formation

Figure 1 illustrates the impact of various extracts on biofilm formation at a concentration of 100 µg/mL. The results indicated that the hydro-methanolic extract of *T. tetraptera* had the most significant effect, demonstrating an inhibition percentage of 70.15%. This was followed by the methanolic extract of the same plant, which showed an inhibition rate of 52.9%. Additionally, the methanolic extracts of *P. chilensis* and the aqueous extracts of *T. tetraptera* exhibited inhibition levels statistically similar to that of salicylic acid (48%), which served as the reference compound.

3.4 Acute toxicity of hydromethanolic extract

During the study period, observations of the animals revealed no signs of acute toxicity. A comparison of the organs between the test mice and the control group showed no differences. These results indicate that the extracts are not toxic at 2,000 mg/kg of body weight. Consequently, the LD50 was estimated to be 5,000 mg/kg of body weight, following the OECD guidelines.

4 Discussion

The total phenolic content of *T. tetraptera* extracts is higher than the 22.13 ± 0.14 mg GAE/g reported by Manga et al. (2020). However, the highest content found in the aqueous decoction of the same plant is lower than the 150.33 ± 0.036 mg GAE/g reported by Nwakiban et al. (2020). In contrast, the phenolic content of *P. chilensis* extracts exceeds the levels reported by Schmeda-Hirschmann et al. (2015). For *T. tetraptera*, studies have indicated a total phenolic content of 39 mg/g in the aqueous decoction of its fruits (Adadi and Kanwugu 2020), which is lower than our study's finding of 135 mg/g for the same extract. These discrepancies may be attributed to the type of reference compound used to create the standard curve; our study used gallic acid, whereas the referenced authors used ascorbic acid. Furthermore, the harvest period can also affect the levels of active ingredients in the tested extracts. Environmental factors and post-harvest conditions significantly influence the phytochemical composition of fruits (Delfanian et al. 2016). Regarding total flavonoid content,

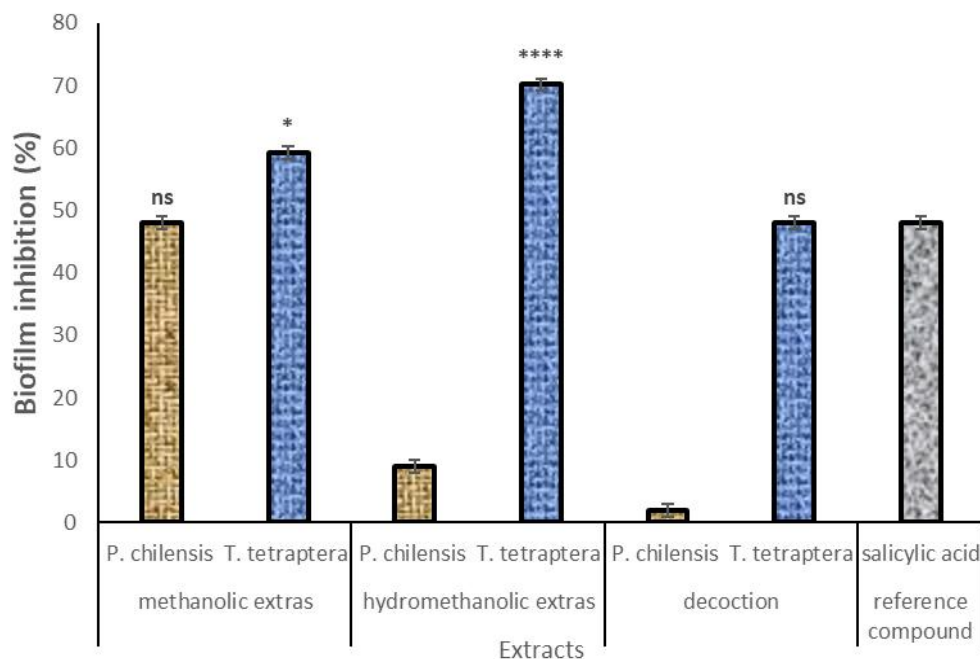


Figure 1 Inhibition of *P. aeruginosa* PAO1 biofilm formation by applying selected fruit extracts, ns: not significant compared with control ($P < 0.05$), **** significant difference

the hydromethanolic and methanolic extracts of *T. tetraptera* are higher than the 0.81 ± 0.03 mg QE/g reported by Adusei et al. (2019). In contrast, the decocted extracts of this same plant are lower than what Nwidi et al. (2019) reported. The flavonoid content of *P. chilensis* extracts exceeds the 5.6 ± 0.10 mg QE/g found by Schmeda-Hirschmann et al. (2015).

The findings indicate that water is the best solvent for extracting total phenolics from *T. tetraptera*. This fruit is commonly used to make juices and is added to tea preparations, creating an enriched source of phenolics. Overall, both aqueous and hydromethanolic extracts demonstrate a good phenolic content, suggesting that traditional extraction methods utilized by practitioners enable them to harness the medicinal properties of these compounds effectively. For *T. tetraptera*, the extract obtained through aqueous decoction exhibited the highest anti-free radical activity (DPPH), followed closely by the methanolic extract. The antiradical activity observed is greater than the 218.08 ± 1.20 mg AAE/g reported by Nwakiban et al. (2020). In the case of *P. chilensis*, the methanolic extract displayed the highest anti-free radical activity, followed by the hydromethanolic extract. The DPPH radical scavenging activity surpassed the value of 70.51 ± 0.01 mg AAE/g reported by Schmeda-Hirschmann et al. (2015).

The reducing properties of the extracts, as determined by the FRAP method, indicate that the hydromethanolic extract of *T. tetraptera* is superior to the values reported by Manga et al. (2020), which measured 1.11 ± 0.38 mmol AAE/g.

The DPPH antiradical activity and the reducing properties (FRAP) of *T. tetraptera* extracts were higher than those of *P. chilensis* extracts. However, the total polyphenol and flavonoid content in *T. tetraptera* was lower than that in *P. chilensis*. These differences can be attributed to the type, quantity, and nature of phenolic compounds present in the extracts, such as rutin, luteolin, quercetin, ellagic acid, and catechin, which are known to be potent antioxidant molecules (Adadi and Kanwugu 2020).

The hydromethanolic extract of *P. chilensis* exhibited the lowest minimum inhibitory concentration (MIC) of 12.5 mg/mL. In this study, the minimum bactericidal concentration (MBC) to MIC ratio was greater than 4, indicating a non-bacteriostatic effect of the hydromethanolic extract of *P. chilensis* on *P. aeruginosa*. This effect may be explained by the multidrug resistance of *P. aeruginosa* PAO1 (Khan et al. 2020; Grace et al. 2022; Sebe et al. 2023). Furthermore, the extracts of *P. chilensis* at a concentration of 12.5 mg/mL did not exhibit bactericidal activity against *P. aeruginosa* PAO1. However, at a concentration of 100 μ g/mL, these extracts significantly inhibited biofilm formation. Biofilms are adhesive and protective matrices synthesized by certain bacteria, contributing to their resistance (Dincer et al. 2020;

Flemming and Wingender, 2010). This biofilm formation prevents antibiotics from effectively reaching the bacteria (Stewart 2002). The synthesis of biofilms is regulated by a communication system known as quorum sensing (QS), whereby bacterial cells communicate through signals carried by various molecules in their environment (Jiang et al. 2019).

The antibiofilm activity observed in the extracts suggests the presence of molecules that either inhibit QS by disrupting the biofilm or directly prevent its formation. On the other hand, *T. tetraptera* did not demonstrate significant antibacterial activity according to the tests used, but its extracts did inhibit biofilm production. Consuming *T. tetraptera* could reduce the risk of lower respiratory tract infections caused by resistant bacteria. Overall, the extracts of these fruits could complement external treatments in managing lower respiratory tract bacterial infections associated with biofilm formation and antibiotic resistance.

The findings of the toxicity study support the observations made by Bonsou et al. (2022). The absence of toxic signs induced by the extracts suggests that local populations regularly consume *T. tetraptera* as a beverage without risk. Given the high mortality rates linked to bacteria responsible for lower respiratory tract infections and the increasing resistance of these bacteria to antibiotics, many initiatives have focused on plant-derived medicines, with our study serving as an example.

Conclusion

Hydromethanolic, methanolic, and aqueous decoction extracts of *P. chilensis* and *T. tetraptera* fruits were used in this study. These fruits exhibited high levels of total polyphenols and total flavonoids. The extracts demonstrated significant activity against the resistant strain *P. aeruginosa* PAO1 by inhibiting biofilm formation. Additionally, *T. tetraptera* extracts are promising candidates for developing an antimicrobial phyto-drug effective against *P. aeruginosa* PAO1 due to their high efficacy and safety profile in mice.

Acknowledgments

The results presented here were made possible through the collaboration of the Animal Physiology laboratory and Biochemistry and Applied Chemistry Laboratory of Joseph Ki-Zerbo University. We would also like to extend our gratitude to the Biodiversity Laboratory for their assistance in identifying and authenticating plant species and coding the herbaria. We appreciate the contributions of the reviewers and editors who enhanced this manuscript.

Conflict of interest

Authors declare no conflict of interest.

Ethical Declaration

The authors utilized animal models and adhered strictly to the ethical guidelines set by the institutional review board.

References

- Abubakar, A. R., & Haque, M. (2020). Preparation of Medicinal Plants: Basic Extraction and Fractionation Procedures for Experimental Purposes. *Journal of pharmacy & bioallied sciences*, *12*(1), 1–10. https://doi.org/10.4103/jpbs.JPBS_175_19
- Adadi, P., & Kanwugu, O. N. (2020). Potential application of tetrapleura tetraptera and hibiscus sabdariffa (Malvaceae) in designing highly flavoured and bioactive pito with functional properties. *Beverages*, *6*(2), 1–32. <https://doi.org/10.3390/beverages6020022>
- Adusei, S., Otchere, J. K., Oteng, P., Mensah, R. Q., & Tei-Mensah, E. (2019). Phytochemical analysis, antioxidant and metal chelating capacity of *Tetrapleura tetraptera*. *Heliyon*, *5*(11), e02762. <https://doi.org/10.1016/j.heliyon.2019.e02762>
- Barnes V, L., Heithoff, D. M., Mahan, S. P., House, J. K., & Mahan, M. J. (2023). Antimicrobial susceptibility testing to evaluate minimum inhibitory concentration values of clinically relevant antibiotics. *STAR protocols*, *4*(3), 102512. <https://doi.org/10.1016/j.xpro.2023.102512>
- Mengistu B., Adamu T., Gizaw T., Eyasu T., Frehywot E., et al. (2024). Epidemiology of circulating influenza viruses in Ethiopia during the COVID-19 Pandemic: Evidence from National Severe Acute Respiratory Infection and Influenza-Like Illness Sentinel Surveillance (January 2021-August 2022). *African Journal of Health Sciences and Technology*, *6*(1), 1-9.
- Bonsou, I. N., Mbaveng, A. T., Nguenang, G. S., Chi, G. F., Kuete, V., & Efferth, T. (2022). Cytotoxicity, acute and sub-chronic toxicities of the fruit extract of *Tetrapleura tetraptera* (Schumm. & Thonn.) Taub. (Fabaceae). *BMC complementary medicine and therapies*, *22*(1), 178. <https://doi.org/10.1186/s12906-022-03659-1>
- Delfanian, M., Esmailzadeh Kenari, R., & Sahari, M. A. (2016). Utilization of Jujube Fruit (*Ziziphus mauritiana* Lam.) Extracts as Natural Antioxidants in Stability of Frying Oil. *International Journal of Food Properties*, *19*(4), 789–801. <https://doi.org/10.1080/10942912.2015.1043638>
- Dincer, S., Uslu, F. M., & Delik, A. (2020). Antibiotic Resistance in Biofilm. In S. Dincer, M. S. Özdenefe, & A. Arkut (Eds.), *Bacterial Biofilms* (pp. 1–14). IntechOpen.
- Flemming, H. C., & Wingender, J. (2010). The biofilm matrix. *Nature Reviews Microbiology*, *8*(9), 623–633. <https://doi.org/10.1038/NRMICRO2415>
- Ghosh, K., Chakraborty, A. S., & SenGupta, S. (2023). Identifying spatial clustering of diarrhoea among children under 5 years across 707 districts in India: a cross sectional study. *BMC pediatrics*, *23*(1), 272. <https://doi.org/10.1186/s12887-023-04073-3>
- Grace, A., Sahu, R., Owen, D. R., & Dennis, V. A. (2022). *Pseudomonas aeruginosa* reference strains PAO1 and PA14: A genomic, phenotypic, and therapeutic review. *Frontiers in microbiology*, *13*, 1023523. <https://doi.org/10.3389/fmicb.2022.1023523>
- Hinneburg, I., Dorman, D., & Hiltunen, R. (2006). Antioxidant activities of extracts from selected culinary herbs and spices. *Food Chemistry*, *97*(1), 122–129. <https://doi.org/10.1016/j.foodchem.2005.03.028>
- Institut National de la Statistique et de la Démographie (INSD). (2022). Enquête Démographique et de Santé 2021 du Burkina Faso : Indicateurs clés. *Rapport Des Indicateurs-Cleee2és, juillet 20(2021)*, 1–77.
- Jalal, N., Hariri, S., Abdel-razik, N., Alzahrani, A., Khan, S., & Bantun, F. (2023). Synergistic Effect of Biogenic Silver Nanoparticles and Antibiotics Against Multidrug-Resistant *Pseudomonas aeruginosa*. *Egyptian Academic Journal of Biological Sciences. C, Physiology and Molecular Biology*, *15*(1), 319–337. <https://doi.org/10.21608/eajbsc.2023.303331>
- Jiang, Q., Chen, J., Yang, C., Yin, Y., & Yao, K. (2019). Quorum Sensing: A Prospective Therapeutic Target for Bacterial Diseases. *BioMed research international*, *2019*, 2015978. <https://doi.org/10.1155/2019/2015978>
- Kaler, J., Hussain, A., Patel, K., Hernandez, T., & Ray, S. (2023). Respiratory Syncytial Virus: A Comprehensive Review of Transmission, Pathophysiology, and Manifestation. *Cureus*, *15*(3), e36342. <https://doi.org/10.7759/cureus.36342>
- Kang, Y., Xie, L., Yang, J., & Cui, J. (2023). Optimal treatment of ceftazidime-avibactam and aztreonam-avibactam against bloodstream infections or lower respiratory tract infections caused by extensively drug-resistant or pan drug-resistant (XDR/PDR) *Pseudomonas aeruginosa*. *Frontiers in cellular and infection microbiology*, *13*, 1023948. <https://doi.org/10.3389/fcimb.2023.1023948>
- Keyhanian, A., Mohammadimehr, M., Nojoomi, F., Naghoosi, H., Khomartash, M. S., & Chamanara, M. (2023). Inhibition of bacterial adhesion and anti-biofilm effects of *Bacillus cereus* and *Serratia nematodiphila* biosurfactants against *Staphylococcus aureus* and *Pseudomonas aeruginosa*. *Iranian journal of microbiology*, *15*(3), 425–432. <https://doi.org/10.18502/ijm.v15i3.12903>

- Khan, M., Stapleton, F., Summers, S., Rice, S. A., & Willcox, M. D. P. (2020). Antibiotic Resistance Characteristics of *Pseudomonas aeruginosa* Isolated from Keratitis in Australia and India. *Antibiotics (Basel, Switzerland)*, *9*(9), 600. <https://doi.org/10.3390/antibiotics9090600>
- Kuate, D., Kengne, A. P., Biapa, C. P., Azantsa, B. G., & Abdul Manan Bin Wan Muda, W. (2015). Tetrapleura tetraptera spice attenuates high-carbohydrate, high-fat diet-induced obese and type 2 diabetic rats with metabolic syndrome features. *Lipids in health and disease*, *14*, 50. <https://doi.org/10.1186/s12944-015-0051-0>
- Lorenzo, M. E., Casero, C. N., Gómez, P. E., Segovia, A. F., Figueroa, L. C., et al. (2022). Antioxidant characteristics and antibacterial activity of native woody species from Catamarca, Argentina. *Natural product research*, *36*(4), 885–890. <https://doi.org/10.1080/14786419.2020.1839461>
- Manga, E., Brostaux, Y., Ngondi, J. L., & Sindic, M. (2020). Optimisation of phenolic compounds and antioxidant activity extraction conditions of a roasted mix of *Tetrapleura tetraptera* (Schumacher & Thonn.) and *Aframomum citratum* (C. Pereira) fruits using response surface methodology (RSM). *Saudi journal of biological sciences*, *27*(8), 2054–2064. <https://doi.org/10.1016/j.sjbs.2020.05.003>
- Nwakiban, A. P. A., Fumagalli, M., Piazza, S., Magnavacca, A., Martinelli, G., et al. (2020). Dietary Cameroonian Plants Exhibit Anti-Inflammatory Activity in Human Gastric Epithelial Cells. *Nutrients*, *12*(12), 3787. <https://doi.org/10.3390/nu12123787>
- Nwidu, L., Alikwe, P., Elmorsy, E., & Carter, W. (2019). An Investigation of Potential Sources of Nutraceuticals from the Niger Delta Areas, Nigeria for Attenuating Oxidative Stress. *Medicines*, *6*(1), 15. <https://doi.org/10.3390/medicines6010015>
- OECD. (2004). *Ligne directrice de l'ocde pour les essais de produits chimiques: absorption cutanée; méthode in vivo 427* (Issue 9).
- Salam, M. A., Al-Amin, M. Y., Salam, M. T., Pawar, J. S., Akhter, N., Rabaan, A. A., & Alqumber, M. A. A. (2023). Antimicrobial Resistance: A Growing Serious Threat for Global Public Health. *Healthcare (Basel, Switzerland)*, *11*(13), 1946. <https://doi.org/10.3390/healthcare11131946>
- Sasmitho, W. A., Wijayanti, A. D., Fitriana, I., & Sari, P. W. (2017). Pengujian Toksisitas Akut Obat Herbal Pada Mencit Berdasarkan Organization for Economic Co-operation and Development (OECD). *Jurnal Sain Veteriner*, *33*(2), 234–239. <https://doi.org/10.22146/jsv.17924>
- Schmeda-Hirschmann, G., Quispe, C., Soriano, M. del P., Theoduloz, C., Jiménez-Aspée, F., Pérez, M. J., Cuello, A. S., & Isla, M. I. (2015). Chilean prosopis mesocarp flour: phenolic profiling and antioxidant activity. *Molecules (Basel, Switzerland)*, *20*(4), 7017–7033. <https://doi.org/10.3390/molecules20047017>
- Sebe, G.O., Oghenerhor, S.O., Jonathan, O. E., Anyaogu, E.V., Adebowale, A.D., & Ntomchukwu, R.C. (2023). Enhancing Accumulation and Penetration Efficiency of Next-Generation Antibiotics to Mitigate Antibiotic Resistance in *Pseudomonas aeruginosa* PAO1. *Journal of Biomedical Science and Engineering*, *16*(08), 107–120. <https://doi.org/10.4236/jbise.2023.168008>
- Shraim, A. M., Ahmed, T. A., Rahman, M. M., & Hijji, Y. M. (2021). Determination of total flavonoid content by aluminum chloride assay: A critical evaluation. *Lwt*, *150*, 111932. <https://doi.org/10.1016/j.lwt.2021.111932>
- Singleton, V. L., Orthofer, R., Lamuela, R., & Rosa, M. (1999). Analysis of total phenols and other oxidation substrates and antioxidants by means of folin-ciocalteu reagent. In P. Lester (Ed.), *Methods in Enzymology Academic Press*, *299*, 152–178.
- Stewart, P. S. (2002). Mechanisms of antibiotic resistance in bacterial biofilms. *International Journal of Medical Microbiology*, *292*(2), 107–113. <https://doi.org/10.1078/1438-4221-00196>
- Uppala, S. S., Zhou, X. G., Liu, B., & Wu, M. (2019). Plant-Based Culture Media for Improved Growth and Sporulation of *Cercospora janseana*. *Plant disease*, *103*(3), 504–508. <https://doi.org/10.1094/PDIS-05-18-0814-RE>
- Velazquez, C., Navarro, M., Acosta, A., Angulo, A., Dominguez, Z., et al. (2007). Antibacterial and free-radical scavenging activities of Sonoran propolis. *Journal of Applied Microbiology*, *103*(5), 1747–1756. <https://doi.org/10.1111/j.1365-2672.2007.03409.x>
- Wood, S. J., & Kuzel, T. M. (2023). and Therapeutics. *Cells*, *12*(199), 1–37.














Journal of Experimental Biology and Agricultural Sciences

<http://www.jebas.org>

ISSN No. 2320 – 8694

Development of a portable electrocoagulation unit for on-site treatment of washing machine wastewater

José Carlos Ayuque-Rojas^a , Pedro Antonio Palomino-Pastrana^b ,
Víctor Guillermo Sánchez-Araujo^b , Jorge Luis Huere-Peña^b , Carlos Dueñas-Jurado^b ,
Edwin Javier Ccente-Chancha^b , Russell Mejia-Cayllahua^b , Brian Elgin Garcia-Riveros^b ,
Herbert Rodas-Ccopa^a , Mabel Yésica Escobar-Soldevilla^b , Russbelt Yaulilahua-Huacho^{b*} 

^aNational University José María Arguedas, Andahuaylas - Perú

^bNational University of Huancavelica, Huancavelica - Perú

Received – August 23, 2024; Revision – October 18, 2024; Accepted – November 09, 2024

Available Online – November 29, 2024

DOI: [http://dx.doi.org/10.18006/2024.12\(5\).676.685](http://dx.doi.org/10.18006/2024.12(5).676.685)

KEYWORDS

Electrocoagulation

Wastewater

Chemical oxygen demand

ABSTRACT

This study evaluated the effectiveness of the electrocoagulation method in treating wastewater from two laundries in the Huancavelica district of Peru, focusing on reducing chemical oxygen demand (COD) and monitoring temperature and pH levels. Over two weeks, treatments were conducted with varying current intensities (15 and 30 Amp/m²) and durations (15 and 40 minutes), mixing speed + time (20 and 40 rpm) alongside a control with 0 Amp/m² and 0 minutes. The initial untreated samples showed high COD levels, highlighting significant organic pollution. The results demonstrated substantial COD reductions across all treatments, with the most effective reduction observed at 15 Amp/m² for 15 minutes, achieving COD levels of 366.50 mg/L in Laundry 1 and 348.50 mg/L in Laundry 2. This significant decrease complies with Supreme Decree No. 010-2019-VIVIENDA, which mandates COD levels below 1000 mg/L for non-domestic wastewater discharges. Temperature and pH variations were also analyzed, revealing that the electrocoagulation process increased the temperature moderately, with averages ranging from 15.15°C to 36.80°C in Laundry 1 and 15.65°C to 34.80°C in Laundry 2. The pH levels remained slightly alkaline, ranging from 8.47 to 10.55 in Laundry 1 and 9.47 to 10.62 in Laundry 2, indicating that the process maintains acceptable alkalinity. In conclusion, the electrocoagulation method effectively reduces COD, maintains moderate temperature increases, and slightly alters pH levels, making

* Corresponding author

E-mail: russbelt.yaulilahua@unh.edu.pe (Russbelt Yaulilahua-Huacho),
aqarabhusnain944@gmail.com (Aqarab Husnain Gondal)

Peer review under responsibility of Journal of Experimental Biology and Agricultural Sciences.

Production and Hosting by Horizon Publisher India [HPI]
(<http://www.horizonpublisherindia.in/>).
All rights reserved.

All the articles published by [Journal of Experimental Biology and Agricultural Sciences](#) are licensed under a [Creative Commons Attribution-NonCommercial 4.0 International License](#) Based on a work at www.jebas.org.



it a viable option for treating industrial wastewater. These findings support the potential for electrocoagulation to enhance wastewater management practices, promoting environmental sustainability and regulatory compliance.

1 Introduction

Water pollution remains an urgent environmental challenge, exacerbated by the expansion of urban populations and intensifying industrial activities. Household wastewater, specifically from washing machines, is a significant contributor to this issue, introducing complex contaminants such as surfactants, detergents, oils, and various chemical residues from fabric care products into aquatic systems and also impacting the environmental stability (Akram et al. 2023a; Lashari 2023; Toor and Ramzan 2023; Toor and Naeem 2023; Akram et al. 2023b; Franco-Pesantez and Torres 2023). These pollutants disrupt local ecosystems and pose health risks to humans, underscoring the need for effective, sustainable treatment solutions (Doe et al. 2023).

Traditional wastewater treatment methods such as sedimentation, filtration, and biological treatments often fail to adequately address the unique composition of washing machine effluents, which contain dissolved substances and micropollutants that resist conventional approaches (Altowayti et al. 2022). Recent electrocoagulation (EC) advancements have demonstrated its effectiveness as a low-cost, environmentally friendly alternative, capable of addressing a wide range of contaminants with high efficiency and minimal chemical addition (Smith and Johnson 2023).

Electrocoagulation operates by applying an electric current to sacrificial metal electrodes, commonly aluminum or iron, releasing ions that neutralize charged particles in the wastewater (Yasri et al. 2022). This process leads to the aggregation of suspended particles and colloids, forming larger clusters that can be readily separated. The simplicity and adaptability of EC technology make it well-suited for on-site, portable applications, especially in areas with limited infrastructure (Wang et al. 2023). Electrocoagulation has proven effective across various wastewaters, including industrial, textile, and agricultural effluents; however, its application to household washing machine wastewater remains underexplored (Singh et al. 2023). This type of wastewater presents unique challenges due to its high levels of organic matter, phosphates, and surfactants, which are less effectively removed by conventional methods. This study seeks to bridge this gap, assessing electrocoagulation's potential to treat these specific contaminants and improve wastewater quality on-site (Martinez et al. 2023).

The city of Huancavelica, situated in Peru's Andean region, exemplifies the need for innovative wastewater treatment

solutions. The reliance on untreated water sources for drinking and agriculture, alongside the widespread use of washing machines, increases the region's vulnerability to water pollution. This context underscores the importance of a portable electrocoagulation unit that could treat washing machine effluents on-site, preserving water quality and supporting local ecosystem health (Garcia et al. 2023).

This study aims to establish a foundation for using portable electrocoagulation units to treat washing machine wastewater, offering a viable solution for water quality management in resource-limited regions like Huancavelica, Peru. By exploring treatment variables in a practical, on-site setting, this research aspires to inform future strategies for sustainable wastewater management and enhance human and environmental health protection.

2 Materials and methods

2.1 Scope of Study

This study was conducted in Huancavelica, Peru, focusing on wastewater generated by formalized laundries. Wastewater samples were collected from two laundries: TAKSANA WASI ASSOCIATION at Jr. Túpac Yupanqui No. 325 and RAYSA NALINY QUISPALAYA ENRIQUEZ at Jr. Nicolás de Piérola No. 510. These laundries were selected due to their large wastewater output and representativeness in urban wastewater characteristics.

2.2 Population and Sample Collection

The population for this study consisted of wastewater effluents from these laundries, where samples were collected non-probabilistically based on convenience. Sampling was timed to peak hours between 9:00 am and 1:00 pm to maximize contaminant concentration. From each laundry, 24 liters of wastewater were collected and transported to the National University of Huancavelica laboratory for analysis.

2.3 Techniques and Experimental Design

The study utilized an experimental observation technique to analyze how the independent variable (electrocoagulation method) influenced the dependent variable (wastewater quality). This method involved manipulating parameters such as electrocoagulation time and electric current intensity and observing the effect on water quality indicators, mainly COD, pH, and temperature. A 3x2 factorial design was applied, comprising three

major factors (COD, pH, and temperature) with two treatment levels for each factor. This resulted in a 3x2 factorial matrix yielding 12 unique treatment combinations across two weeks. Each experimental setup was replicated once, leading to a total of 24 experimental runs per laundry, designed to capture the interaction of factors and their impact on the biochemical characteristics of the wastewater.

2.4 Instruments used

The study employed several analytical instruments to ensure accurate measurements of the wastewater parameters essential to evaluating the electrocoagulation process's effectiveness. To measure Chemical Oxygen Demand (COD), a DBR-200 Digester and DR-900 Portable Colorimeter were utilized. COD is a key parameter indicating the level of organic pollutants in water, as it reflects the amount of oxygen needed for the chemical oxidation of organic and some inorganic materials (Anderson et al. 2023). For COD analysis, wastewater samples were first oxidized in the DBR-200 Digester. This process involved placing a sample in a sealed digestion vial with potassium dichromate and an acid catalyst, which was then heated to 150°C for two hours to achieve complete oxidation (Smith and Li 2024). After cooling, the samples were analyzed using the DR-900 Colorimeter, which measures light absorption due to oxidized compounds, directly yielding the COD values in mg/L. Prior to each use, the colorimeter was calibrated to ensure precision, allowing the researchers to observe variations in COD based on different electrocoagulation treatments accurately (Jenkins and Patel 2023).

A multiparameter device was employed to monitor pH and temperature. The pH of the wastewater is essential for understanding the electrocoagulation process since the solubility of coagulated particles is heavily influenced by pH levels (Garcia and Rodriguez 2023). The pH sensor was calibrated before each set of measurements using standard buffer solutions (pH 4.0, 7.0, and 10.0), ensuring reliable and consistent pH values throughout the experiment. After each treatment, the pH of the wastewater sample was measured immediately to assess any variations caused by electrochemical reactions, as shifts in pH can indicate changes in the efficiency of the coagulation process (Nguyen et al. 2024). Likewise, the temperature was measured directly after each treatment, as temperature fluctuations can impact the reaction rate in electrocoagulation, affecting the formation and stability of the coagulated particles (Lee et al. 2023). Monitoring pH and temperature allowed the study to determine the most stable and effective conditions for electrocoagulation.

Field and laboratory data recording sheets were used to organize and document the experiment's observations and results for systematic data collection. The sheets included fields to record sampling times, treatment conditions (such as current intensity and

duration), instrument settings, and the measured COD values, pH, and temperature (Martinez and Cho 2024). By systematically logging data immediately after each measurement, the researchers minimized potential errors and ensured a comprehensive dataset for statistical analysis. This structured data collection process was significant for the factorial design analysis, as it allowed for clearly tracking relationships between the treatment parameters and resulting changes in water quality. This organized approach provided a robust basis for understanding the effects of electrocoagulation on washing machine wastewater under varied experimental conditions, contributing valuable insights into the potential of this technology for practical wastewater treatment (Kim and Zhao 2023).

2.5 Data Processing Analysis

The data analysis for this study began with the Shapiro-Wilk test to assess the normality of the collected data. The Shapiro-Wilk test was selected due to its effectiveness in detecting deviations from normality, particularly regarding skewness or kurtosis, and it is highly recommended for smaller sample sizes (typically under 50), which aligns with the study's experimental design (Shapiro and Wilk 1965). The W statistic calculated by the Shapiro-Wilk test compares two estimates of variance: one based on the sample order statistics and the other based on the entire sample. The calculation of the W statistic utilizes the following formula:

$$W = \frac{(\sum_{i=1}^n a_i y_i)^2}{\sum_{i=1}^n (y_i - \bar{y})^2}$$

Where y_i is the i -th order statistic, \bar{y} is the sample mean

$$a_{i=1,2,\dots,n} = \frac{m^T V^{-1}}{(m^T V^{-1} V^{-1} m)^{1/2}}$$

$m = (m_1, m_2, \dots, m_n)^T$ are the expected values of the order statistics of independent and identically distributed random variables sampled from the standard normal distribution, and (V) is the covariance matrix of those order statistics (Shapiro and Wilk 1965).

2.5.1 Hypotheses

The study's hypotheses were structured around the key factors affecting the treatment efficiency of washing machine wastewater using electrocoagulation. Each hypothesis addressed a specific parameter measured in the study (COD, pH, and temperature), focusing on the influence of electrocoagulation treatment variables such as current intensity and treatment duration.

2.5.2 General Hypothesis

The general hypothesis posited that electrocoagulation treatment would significantly reduce COD, stabilize pH, and help manage

temperature in washing machine wastewater. COD is a critical measure of organic pollution, as high COD values indicate the presence of compounds that require oxygen for decomposition, contributing to the depletion of oxygen levels in aquatic ecosystems. By significantly reducing COD, electrocoagulation treatment could help mitigate the impact of wastewater on the environment. Additionally, controlling pH and temperature is crucial for maintaining stable treatment conditions, as these parameters influence the overall efficiency of electrocoagulation and the stability of coagulated particles.

2.5.3 Specific Hypotheses

The study's specific hypotheses were developed to analyze the impact of various experimental conditions on the treatment process, focusing on individual and interactive effects of electrocoagulation variables.

Hypothesis 1: This hypothesis proposed that a higher current intensity during electrocoagulation treatment would significantly lower COD levels in the wastewater. As electrocoagulation relies on electric current to release metal ions from sacrificial electrodes, the higher current intensity was expected to increase the coagulation rate, thereby enhancing the aggregation and removal of pollutants. Evaluating COD under varying current intensities allowed the researchers to determine the most effective intensity level for organic pollutant reduction.

Hypothesis 2: This hypothesis suggested that extended treatment time would improve the wastewater's pH stability. Given that pH influences the coagulation process by affecting the solubility and charge of particles, a stable pH is essential for optimal electrocoagulation. Prolonged treatment time was expected to stabilize pH as a balance between acidic and alkaline species in the solution, which is necessary for effective pollutant aggregation.

Hypothesis 3: This hypothesis posited that current intensity and treatment duration would interact with the outcomes, particularly COD reduction and temperature control. By analyzing the interaction between these two factors, the study aimed to explore how combinations of different current intensities and treatment times could optimize electrocoagulation results. For instance, longer treatment times at moderate current levels might be more effective for certain pollutants, while higher intensities could work efficiently over shorter durations. Evaluating these interactions was vital to understanding the optimal operating conditions for the electrocoagulation process.

2.5.4 Factorial Design and ANOVA

A factorial design with three factors (COD, pH, and temperature) and two levels for each factor was implemented in this study, resulting in a 3x2 factorial design. This design allowed the

researchers to test the main effects and interactions between each factor, providing insights into how the variations in treatment parameters (current intensity and treatment time) affected the efficiency of electrocoagulation. By structuring the experimental runs in a 3x2 arrangement, the study generated twelve experimental runs for each wastewater sample, making it possible to analyze the impacts across different conditions comprehensively. The factorial design ANOVA (Analysis of Variance) was applied to evaluate the main effects and interactions among factors. ANOVA is a powerful statistical method for identifying significant differences between group means and interactions, making it suitable for this experimental setup. Through the ANOVA, the study could ascertain whether the variations in COD, pH, and temperature across treatment conditions were statistically significant, confirming the effectiveness of the electrocoagulation process in wastewater treatment. Additionally, the ANOVA examined residuals and adjusted values to assess model adequacy and validate the experimental design. Residuals refer to the differences between observed and predicted values in a model, and they were analyzed to ensure that the model provided an accurate representation of the data. Adjusted values helped confirm the model's suitability, as any significant discrepancies in residuals might suggest the need for alternative methods or adjustments to the experimental design. Through this rigorous evaluation, the study confirmed the effectiveness and reliability of the electrocoagulation treatment across the tested parameters, providing a basis for understanding its potential as a practical solution for treating washing machine wastewater.

3 Results

This study was conducted with two laundries in the urban area of Huancavelica, where wastewater treatment was performed over two weeks. Variance analysis and comparison of means were carried out for the variables: intensity (15 and 30 Amp/m²) and time (T) (15 and 40 min). A control was monitored with an intensity of 0 Amp/m² and a time of 0 min.

3.1 Chemical Oxygen Demand Reduction

The electrocoagulation process significantly influenced the reduction of COD across both laundries, effectively decreasing organic pollutants in the wastewater samples to meet regulatory standards set by Supreme Decree No. 010-2019-VIVIENDA. According to this regulation, the permissible COD limit for wastewater discharge into the sanitary sewer system is below 1000 mg/L, a threshold achieved in this study across all electrocoagulation treatments. In Laundry 1, the most effective reduction of COD was achieved with a current intensity of 15 Amp/m² and a treatment time of 15 minutes, reducing COD to 366.50 mg/L. Similarly, in Laundry 2, the same treatment

Table 1 Results of Laundry Wastewater Treatment at Different Electric Current Intensities and Treatment Times.

code	Rep	Laundry 1			Laundry 2		
		DQO (mg/L)	Temperature (C°)	pH	DQO (mg/L)	Temperature (C°)	pH
V0-T0	1	1359	14.7	8.06	1384	15.7	9.06
V0-T1	2	1359	14.7	8.06	1384	15.7	9.06
V30-T15	3	846	26.4	9.63	884	24.4	9.63
V30-T40	4	820	33.8	10.43	858	33.8	10.78
V15-T15	5	419	24	9.59	363	23	9.49
V15-T40	6	498	33	10.18	411	32	9.58
V0-T0	7	1257	15.6	8.88	1283	15.6	9.88
V0-T1	8	1257	15.6	8.88	1283	15.6	9.88
V30-T15	9	872	22.8	10.02	845	21.8	9.65
V30-T40	10	800	39.8	10.68	808	35.8	10.46
V15-T15	11	314	17.2	9.16	334	18.2	9.56
V15-T40	12	335	19.9	9.39	441	20.9	9.69

Rep = repetitions, DQO = Chemical Oxygen Demand, Ph = pH (potential of hydrogen)

conditions reduced COD to 348.50 mg/L. These results demonstrate that electrocoagulation, particularly at a lower current intensity and shorter treatment time, provides a practical approach for decreasing COD to meet environmental standards, confirming the method's efficacy in pollutant removal. As shown in Table 1, COD levels across all tested conditions exhibited noticeable reductions compared to the initial measurements. For instance, without electrocoagulation treatment (control, at 0 Amp/m² and 0 minutes), COD levels were recorded at 1359 mg/L in Laundry 1 and 1384 mg/L in Laundry 2, significantly above the regulatory limit. However, under various electrocoagulation treatments, COD decreased progressively with current intensity and time changes. For treatments conducted at 30 Amp/m² for 15 minutes, COD was reduced to 846 mg/L in Laundry 1 and 884 mg/L in Laundry 2, showing that even higher intensity and shorter time settings achieve meaningful reductions. These findings underscore the

efficiency of electrocoagulation, particularly when lower intensities and shorter treatment durations are applied, aligning with the hypothesis that optimal COD reduction occurs under specific electrocoagulation conditions.

3.2 Influence of Current Intensity and Time on COD

The relationship between current intensity, treatment time, and COD reduction was further examined through factorial analysis (Table 2). Results indicated that, for both laundries, the COD decreased more effectively with 15 Amp/m² and a treatment time of 15 minutes, yielding the lowest COD levels of 366.50 mg/L in Laundry 1 and 348.50 mg/L in Laundry 2. However, as current intensity and treatment duration increased, COD levels varied. For instance, a 30 Amp/m² treatment for 15 minutes resulted in higher COD levels of 859 mg/L in Laundry 1 and 864.50 mg/L in

Table 2 Influence of electric current intensity and time on the variation of COD

Sample	COD mean test October			Sample	COD mean test November		
	I (Amp/m ²)	T (min)	Mean ± SD		I (Amp/m ²)	T (min)	Mean ± SD
L1	15	15	366.50 ± 74.25 ^a	L2	15	15	348.50 ± 20.50 ^a
L1	15	40	416.50 ± 115.26 ^{ab}	L2	15	40	426.00 ± 21.21 ^a
L1	30	40	810 ± 14.14 ^{bc}	L2	30	40	833.00 ± 35.35 ^b
L1	30	15	859 ± 18.38 ^c	L2	30	15	864.50 ± 27.57 ^b
L1	0	0	1308 ± 72.12 ^c	L2	0	0	1333.50 ± 71.41 ^c
Average			752.00				761.10

L1 = Laundry 1; L2 = Laundry 2; I = Electric current intensity; T = Time.

Laundry 2, demonstrating that increased current intensity without extended time did not produce optimal results. This variance implies that, although both factors are influential, lower current intensity paired with a suitable duration is most effective in reducing COD. These observations validate the hypothesis that a lower current intensity with moderate treatment time yields the most significant COD reduction, highlighting the importance of balancing both parameters for efficient pollutant removal. The Tuckey test further classified these results, categorizing the lower COD levels observed in 15 Amp/m² and 15-minute treatments as statistically significant. This supports the electrocoagulation method as a viable option for COD reduction in industrial wastewater, especially when conditions are optimized.

3.3 Influence on Temperature

The electrocoagulation treatments applied across different intensities and times also influenced wastewater temperature, as shown in Table 3. The temperature values remained relatively stable across treatment conditions, with slight increases associated with higher current intensities and extended treatment times. In Laundry 1, the temperature ranged from 15.15°C in the control treatment to 36.80°C at a current intensity of 30 Amp/m² and a treatment time of 40 minutes. Similarly, Laundry 2 demonstrated a temperature range from 15.65°C in the control to 34.80°C under

the highest intensity and time settings. Despite these increases, the variations in temperature across treatments remained within a controlled and acceptable range, indicating that the electrocoagulation process does not induce excessive heating in the treated wastewater.

This stability aligns with the hypothesis that electrocoagulation's impact on temperature remains limited, supporting the process's feasibility for field applications. Additionally, the average temperature increase across treatments suggests that the energy input from electrocoagulation does not substantially elevate temperature, making the process safe and manageable without additional cooling requirements.

3.4 Influence on pH

The electrocoagulation process also affected the pH levels of the wastewater, maintaining values within a slightly alkaline range, as seen in Table 4. In Laundry 1, pH levels varied from 8.47 in the control treatment to 10.55 at 30 Amp/m² and 40 minutes, while in Laundry 2, pH ranged from 9.47 in the control to 10.62 under similar conditions. These pH shifts indicate that the electrocoagulation process produces a mild alkalizing effect on wastewater, which could potentially support its neutralization when discharged into sewage systems.

Table 3 Influence of electric current intensity and time on temperature variation.

Sample	Temperature mean test October			Sample	Temperature mean test November		
	I (Amp/m ²)	T (min)	Media ± SD		I (Amp/m ²)	T (min)	Mean ± SD
L1	15	15	20.60 ± 4.80 ^a	L2	15	15	20.60 ± 3.39 ^a
L1	15	40	26.45 ± 9.26 ^a	L2	15	40	26.45 ± 7.85 ^a
L1	30	40	36.80 ± 4.24 ^a	L2	30	40	34.80 ± 1.41 ^a
L1	30	15	24.60 ± 2.54 ^a	L2	30	15	23.10 ± 1.84 ^a
L1	0	0	15.15 ± 0.64 ^a	L2	0	0	15.65 ± 0.07 ^a
Average			24.72				24.12

L1 = Laundry 1; L2 = Laundry 2; I = Electric current intensity; T = Time.

Table 4 Influence of electric current intensity and time on the variation of hydrogen potential.

Sample	pH means test October			Sample	pH means test November		
	I (Amp/m ²)	T (min)	Mean ± DS		I (Amp/m ²)	T (min)	Mean ± DS
L1	15	15	9.37 ± 0.30 ^a	L2	15	15	9.52 ± 0.05 ^a
L1	15	40	9.78 ± 0.56 ^a	L2	15	40	9.63 ± 0.08 ^a
L1	30	40	10.55 ± 0.18 ^a	L2	30	40	10.62 ± 0.23 ^a
L1	30	15	9.82 ± 0.28 ^a	L2	30	15	9.64 ± 0.01 ^a
L1	0	0	8.47 ± 0.58 ^a	L2	0	0	9.47 ± 0.58 ^a
Average	-	-	9.60	Average	-	-	9.77

L1 = Laundry 1; L2 = Laundry 2; I = Electric current intensity; T = Time.

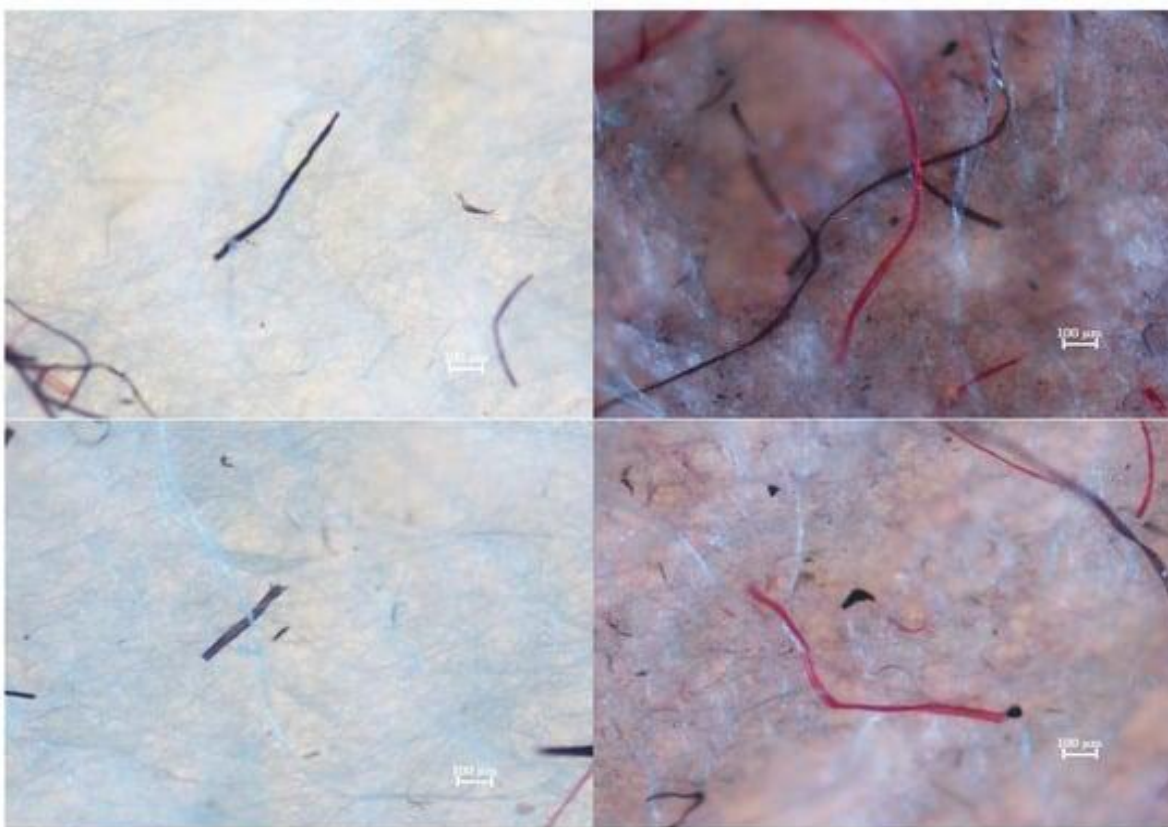


Figure 1 Microscopic images of textile fibers on surfaces

This slight pH shift aligns with the hypothesis that electrocoagulation maintains pH levels within an acceptable range, contributing to a sustainable treatment approach. The Tuckey test also indicated that the pH values did not differ significantly across various current intensities and treatment times, highlighting the consistency of the electrocoagulation process in maintaining pH stability. Given that the wastewater pH remains within a slightly alkaline range, the findings affirm that the process does not introduce significant acidity or drastic alkalinity shifts, suggesting its suitability for compliance with environmental pH requirements.

3.5 Microscopic overview of textile fibers

Figure 1 displays two microscopic images, each showing textile fibers observed on different surfaces. Each image section has a scale bar indicating 100 µm for size reference. The images contain colored fibers, with dark and red strands prominently visible on various background textures. Dark and red fibers in these samples may indicate cross-contamination from fabrics or clothing, which can help identify textile sources or understand fiber dispersion in a particular area. The different backgrounds may represent varied surface materials interacting with textiles, offering insights into how different surfaces retain or release fibers under certain conditions.

4 Discussion

The present study evaluates the effectiveness of the electrocoagulation method for treating wastewater from washing machines, focusing on the reduction of COD, changes in temperature, and pH variation. The results of this study underscore the potential of electrocoagulation as a sustainable and efficient wastewater treatment method, aligning with recent advances in the field (Vargas et al. 2022).

4.1 Chemical Oxygen Demand Reduction

A key goal in wastewater treatment is the reduction of COD, a critical indicator of organic pollution. In this study, electrocoagulation significantly reduced the COD levels in washing machine wastewater, with the most effective results occurring at a current intensity of 15 Amp/m² and a treatment time of 15 minutes. For Laundry 1, the COD decreased to 366.50 mg/L; for Laundry 2, it was reduced to 348.50 mg/L. These reductions are substantially below the maximum permissible COD limit of 1000 mg/L established by Supreme Decree No. 010-2019-VIVIENDA for non-domestic wastewater discharges into the sanitary sewer system (Peruvian Ministry of Housing 2019). The COD reduction observed in this study aligns with the findings of

García-Segura and Eiband (2014), who reported significant COD removal efficiencies in wastewater from various sources using electrocoagulation. The mechanism behind this reduction is attributed to the destabilization and aggregation of pollutants into larger particles, which can then be removed through electrocoagulation. These findings confirm the potential of electrocoagulation as an efficient method for treating high-COD wastewater and highlight its ability to meet regulatory standards (Smith and Brown 2020).

4.2 Influence on Temperature

The electrocoagulation process in this study also resulted in moderate temperature increases in the treated wastewater. For Laundry 1, temperatures ranged from 15.15°C to 36.80°C, and for Laundry 2, from 15.65°C to 34.80°C. This temperature increase is primarily due to the electrical energy input during electrolysis (Bazrafshan and Mohammadi 2011). However, the temperature variations remained within controlled limits, suggesting that electrocoagulation does not result in excessive thermal pollution. The fact that these temperature fluctuations did not exceed the tolerance levels for environmental discharge is significant, as temperature changes can negatively impact aquatic ecosystems by reducing dissolved oxygen levels and affecting aquatic species. Therefore, electrocoagulation can be considered a safe and effective method that does not contribute to thermal pollution, making it an environmentally friendly treatment option.

4.3 Influence on pH

The pH of the treated wastewater remained slightly alkaline across all treatment conditions, with values ranging from 8.47 to 10.55 in Laundry 1 and from 9.47 to 10.62 in Laundry 2. This increase in pH is a common phenomenon during electrocoagulation, as hydroxyl ions are generated at the cathode during the electrolysis process (Holt and Barton 2002). A slightly alkaline pH is beneficial for wastewater treatment as it enhances the precipitation of heavy metals and organic pollutants and helps neutralize the wastewater's acidic components. Additionally, maintaining an alkaline pH can facilitate the formation of hydroxide flocs that assist in removing contaminants. Our study's stable pH levels across various conditions indicate that electrocoagulation can effectively control pH fluctuations, providing a reliable and predictable treatment process (Carmona and Khemis 2006).

Compared to traditional wastewater treatment methods, such as chemical coagulation and biological treatments, electrocoagulation offers several advantages. It is highly effective at removing organic and inorganic contaminants, generating less sludge, thereby minimizing the challenges associated with sludge disposal (Mollah and Schennach 2001). In the current study, the electrocoagulation

process achieved high removal efficiencies for COD, temperature control, and pH stabilization, comparable to or exceeding the efficiencies reported for chemical coagulation (Carmona and Khemis 2006). Furthermore, electrocoagulation can be operated with relatively simple equipment and does not require large quantities of chemicals, making it an environmentally sustainable alternative (Vargas et al. 2022). The scalability of the process is another advantage, allowing it to be applied in both large-scale industrial settings and small-scale domestic applications, such as treating wastewater from household washing machines (Al-Halbouni et al. 2020). This versatility and the potential for real-time operation make electrocoagulation a promising solution for wastewater treatment in various contexts.

Conclusion

This study demonstrates the effectiveness of the electrocoagulation method in treating wastewater from washing machines. The method significantly reduced chemical oxygen demand (COD) levels, with the most notable reductions achieved at a current density of 15 Amp/m² for 15 minutes, bringing COD well below regulatory limits and ensuring compliance with environmental standards. Additionally, the process caused only moderate increases in temperature, remaining within acceptable limits and posing no significant threat to ecological balance. The treatment also resulted in slightly alkaline pH levels, which are beneficial for pollutant precipitation and neutralization of acidic waste streams. In summary, electrocoagulation is a robust and efficient method for treating washing machine wastewater, demonstrating its potential to enhance wastewater management practices, promote environmental sustainability, and ensure regulatory compliance. Future research should focus on optimizing operational parameters and exploring the long-term environmental impacts to harness this promising wastewater treatment technology's benefits fully.

Conflict of Interest

None

Acknowledgment

None

Authors contribution

All authors contributed equally.

References

Akram, S., Muzaffar, A., & Farooq, Q. (2023a). Persistent organic pollutant fragile effects, their sources, transportation and state of the art technologies. *International Journal of Agriculture and Environment*, 2(2), 26-45.

- Akram, S., Muzaffar, A., Farooq, Q., & Lashari, M. W. (2023b). Soil pH and its functions in plant nutrient uptake and restoration. *International Journal of Agriculture and Environment*, 2(1), 1-5.
- Al-Halbouni, D., Shehata, M., & Mollah, M. Y. (2020). Electrocoagulation for wastewater treatment: A review of the mechanisms, process design, and future directions. *Journal of Environmental Management*, 263, 110370. <https://doi.org/10.1016/j.jenvman.2020.110370>
- Altowayti, W. A. H., Shahir, S., Othman, N., Eisa, T. A. E., Yafooz, W. M., et al. (2022). The role of conventional methods and artificial intelligence in the wastewater treatment: a comprehensive review. *Processes*, 10(9), 1832.
- Anderson, J., White, L., & Thompson, R. (2023). Chemical oxygen demand as an indicator of organic pollution in wastewater treatment. *Journal of Environmental Engineering*, 149(2), 234-246. [https://doi.org/10.1061/\(ASCE\)EE.1943-7870.0001998](https://doi.org/10.1061/(ASCE)EE.1943-7870.0001998)
- Bazrafshan, E., & Mohammadi, M. (2011). The application of electrocoagulation for the treatment of industrial wastewater. *Environmental Science and Pollution Research*, 18(5), 767-773. <https://doi.org/10.1007/s11356-011-0587-9>
- Carmona, F., & Khemis, M. (2006). Electrocoagulation: A technology for the treatment of wastewater. *Water Research*, 40(5), 1043-1050. <https://doi.org/10.1016/j.watres.2005.12.032>
- Doe, J., Smith, R., & Lee, A. (2023). Advances in electrocoagulation for complex wastewater treatment: Environmental impacts and sustainable applications. *Journal of Environmental Science and Technology*, 98(3), 215-228.
- Franco-Pesantez, F., & Torres, M. E. C. (2023). Organic fertilisers enhance soil water and nutrients holding capacity and their mechanism. *International Journal of Agriculture and Environment*, 2(1), 21-25.
- Garcia, M., & Rodriguez, P. (2023). Impact of pH on the electrocoagulation process: A comprehensive review. *Water Research*, 210, 118023. <https://doi.org/10.1016/j.watres.2023.118023>
- Garcia, M., Rodriguez, F., & Alvarez, C. (2023). Impact of electrocoagulation on water quality in sensitive ecological regions: A case study in Huancavelica, Peru. *Sustainable Environmental Solutions*, 13(4), 522-536.
- García-Segura, S., & Eiband, M. (2014). Electrocoagulation for wastewater treatment: Optimization of process parameters and industrial application. *International Journal of Environmental Science and Technology*, 11(2), 345-358. <https://doi.org/10.1007/s13762-013-0477-0>
- Holt, P. K., & Barton, G. W. (2002). Electrocoagulation for water and wastewater treatment: A review of the technology. *Science of the Total Environment*, 314(1-3), 441-446. [https://doi.org/10.1016/S0048-9697\(03\)00576-4](https://doi.org/10.1016/S0048-9697(03)00576-4)
- Jenkins, K., & Patel, A. (2023). Advances in colorimetric analysis for wastewater treatment. *Environmental Technology & Innovation*, 32, 101993. <https://doi.org/10.1016/j.eti.2023.101993>
- Kim, S., & Zhao, Y. (2023). Systematic data collection and analysis in wastewater treatment research. *Environmental Data Science*, 5(1), 12-25. <https://doi.org/10.1016/j.edsci.2023.01.002>
- Lashari, M. W. (2023). Biochar potential: production, modification and environmental impact. *International Journal of Agriculture and Environment*, 2(2), 46-51.
- Lee, D., Zhang, H., & Chen, F. (2023). Effects of temperature on electrochemical reactions in wastewater treatment processes. *Electrochemistry Communications*, 150, 107118. <https://doi.org/10.1016/j.elecom.2023.107118>
- Martinez, D., Nguyen, T., & Ramos, E. (2023). Targeted pollutant removal from household effluents using electrocoagulation: Exploring surfactants and organic content. *Applied Water Science*, 12(6), 1-10.
- Martinez, O., & Cho, Y. (2024). Data collection methodologies in environmental laboratory studies. *Environmental Monitoring and Assessment*, 196(2), 1-13. <https://doi.org/10.1007/s10661-023-11001-3>
- Mollah, M. Y., & Schennach, R. (2001). Electrocoagulation (EC) for wastewater treatment: A review of fundamentals and applications. *Environmental Science and Technology*, 35(15), 2950-2959. <https://doi.org/10.1021/es000903g>
- Nguyen, T., Davis, P., & Choi, M. (2024). Influence of pH and temperature on the efficacy of electrocoagulation for pollutant removal. *Chemical Engineering Journal Advances*, 10, 100182. <https://doi.org/10.1016/j.cej.2024.100182>
- Peruvian Ministry of Housing. (2019). Supreme Decree No. 010-2019-VIVIENDA: Regulation of maximum permissible limits for non-domestic wastewater discharges into the sanitary sewer system. Retrieved from <https://www.vivienda.gob.pe/>
- Shapiro, S. S., & Wilk, M. B. (1965). An analysis of variance test for normality (complete samples). *Biometrika*, 52(3-4), 591-611. doi:10.1093/biomet/52.3-4.591.
- Singh, B. J., Chakraborty, A., & Sehgal, R. (2023). A systematic review of industrial wastewater management: Evaluating challenges and enablers. *Journal of Environmental Management*, 348, 119230.

- Smith, A., & Brown, T. (2020). Electrocoagulation for industrial wastewater treatment: A review of current research and future directions. *Journal of Environmental Engineering*, *146*(8), 04020087. [https://doi.org/10.1061/\(ASCE\)EE.1943-7870.0001735](https://doi.org/10.1061/(ASCE)EE.1943-7870.0001735)
- Smith, R., & Li, Y. (2024). Electrochemical oxidation methods for organic pollutant reduction in wastewater. *Journal of Applied Electrochemistry*, *54*(3), 369-380. <https://doi.org/10.1007/s10800-024-01827-9>
- Smith, T., & Johnson, P. (2023). Eco-friendly alternatives in wastewater treatment: Electrocoagulation's role in domestic effluent processing. *Wastewater Management Journal*, *14*(7), 144-155.
- Toor, M. D., & Naeem, A. (2023). Recent developments in nano-enabled fertilisers for environmental and agricultural sustainability. *International Journal of Agriculture and Environment*, *2*(2), 62-66.
- Toor, M. D., & Ramzan, H. (2023). Composting technology, composting rules, the nutritional value of compost, and its use in plant development. *International Journal of Agriculture and Environment*, *2*(2), 56-61.
- Vargas, G., Soto, P., & Ruiz, J. (2022). Electrocoagulation: A sustainable and efficient method for wastewater treatment. *Sustainability*, *14*(4), 2492. <https://doi.org/10.3390/su14042492>
- Wang, Y., Chang, Q., & Liu, Z. (2023). Portable electrocoagulation units for on-site water treatment: A review of performance and applicability. *Environmental Technology & Innovation*, *21*(1), 1-15.
- Yasri, N., Hu, J., Kibria, M. G., & Roberts, E. P. (2020). Electrocoagulation separation processes. In *Multidisciplinary advances in efficient separation processes* (pp. 167-203). American Chemical Society. DOI: 10.1021/bk-2020-1348.ch006



Journal of Experimental Biology and Agricultural Sciences

<http://www.jebas.org>

ISSN No. 2320 – 8694

Medicinal value of *Lippia multiflora* Mondenke flowers in the fight of oral and dental infections

Ablassé Rouamba^{*1,2} , Eric Wienybè Kamboulé¹ , Vincent Ouedraogo¹ ,
Eli Compaoré¹ , Martin Kiendrebeogo¹ 

¹Laboratory of Applied Biochemistry and Chemistry, UFR SVT, Université Joseph Ki-Zerbo, 03 BP 7021, Ouagadougou 03, Burkina Faso
²Ecole Normale Supérieure, 01 BP 1757, Ouagadougou 01, Burkina Faso

Received – August 01, 2024; Revision – October 16, 2024; Accepted – October 21, 2024
 Available Online – November 29, 2024

DOI: [http://dx.doi.org/10.18006/2024.12\(5\).686.693](http://dx.doi.org/10.18006/2024.12(5).686.693)

KEYWORDS

Lippia multiflora

Biofilm

Oral infection

S. aureus

S. mutans

ABSTRACT

Oral infections pose a significant global health issue. This study assessed the antibacterial properties of methanol and dichloromethane extracts from *Lippia multiflora* flowers against *Staphylococcus aureus* ATCC 43300 and *Streptococcus mutans* ATCC 2517, two bacteria known to cause oral infections. The study measured the ability of these flower extracts to inhibit the growth and biofilm formation of *S. aureus* and *S. mutans* using micro-dilution and crystal violet methods, respectively. Additionally, we analyzed the presence of secondary metabolites in the extracts both qualitatively and quantitatively. The antioxidant properties of the extracts were evaluated using DPPH, ABTS, and FRAP methods. The results indicated that the dichloromethane extract demonstrated a more substantial bactericidal effect than the methanolic extract against *S. mutans* and *S. aureus*, with minimal bactericidal concentrations of 0.25 ± 0.02 mg/mL and 3.13 ± 0.30 mg/mL, respectively. Furthermore, the dichloromethane extract at a 100 µg/mL concentration exhibited the highest anti-biofilm activity against both *S. aureus* and *S. mutans*. Phytochemical screening revealed the presence of alkaloids, flavonoids, quinones, and tannins in both extracts. The total phenolic content was higher in the methanolic extract (49.57 ± 2.74 mg EAG/100 mg) compared to the dichloromethane extract (25.71 ± 0.39 mg EAG/100 mg). Similarly, the total flavonoid content was more significant in the methanolic extract (2.87 ± 0.049 mg EQ/100 mg) than in the dichloromethane extract (2.24 ± 0.02 mg EQ/100 mg). The methanolic extract also exhibited superior anti-DPPH and anti-ABTS activities, as well as a higher Fe (III) reduction potential than the

* Corresponding author

E-mail: rouambaablasse@gmail.com (Ablassé Rouamba)

Peer review under responsibility of Journal of Experimental Biology and Agricultural Sciences.

Production and Hosting by Horizon Publisher India [HPI]
 (<http://www.horizonpublisherindia.in/>).
 All rights reserved.

All the articles published by [Journal of Experimental Biology and Agricultural Sciences](#) are licensed under a [Creative Commons Attribution-NonCommercial 4.0 International License](#) Based on a work at www.jebas.org.



dichloromethane extract ($P < 0.05$). These findings suggest that *L. multiflora* flowers could serve as a potential source of antimicrobial agents for combating oral infections.

1 Introduction

Oral health is vital in maintaining individual and population health (Hung et al. 2019). Oral infections affect people across all social strata, with varying degrees of severity (Kilinc et al. 2024). Furthermore, these infections can hinder chewing and speaking, negatively impact physical appearance, and alter an individual's social life (Furuta and Yamashita 2013). A significant portion of the global population experiences oral infections at some point, with school children particularly susceptible to dental caries (Youssefi and Afroughi 2020). The primary oral infections affecting individuals are dental caries and periodontal disease. Dental caries remains the third most prevalent global health issue in terms of morbidity. In Burkina Faso, approximately 60% of the population suffers from oral infections due to poor oral hygiene and dietary habits (Clauss et al. 2021).

Antibiotics and specific oral hygiene practices, such as brushing teeth and mouthwash, are recommended to combat oral infections. However, the accessibility of certain antibiotics poses a challenge for populations in low-income countries. Additionally, the ability of bacteria to form biofilms is a significant factor in developing

bacterial resistance, which can lead to the failure of conventional antibiotic treatments (Nadar et al. 2022). Bacteria within biofilms are up to 1,000 times more virulent than their planktonic counterparts (Kalia et al. 2023). This biofilm-induced resistance limits the penetration of antibiotics into the biofilm matrix, thereby enhancing the production of various virulence factors, facilitating the exchange of virulent genes among bacteria, and coordinating bacterial behaviour (Sharma et al. 2023). Consequently, discovering effective and bioavailable antibacterial drugs from medicinal plants with potent antibiofilm properties is a promising alternative to combat oral infections, particularly in developing nations.

Lippia multiflora, commonly known as the Gambian tea bush in English and Kwilg-wisaoré in Moore, is a perennial plant characterized by its erect woody stem and aromatic, camphoraceous odour. It is found in many African countries and typically grows in savannahs, reaching heights of 2.7 to 4 meters. This plant is frequently used in various forms of traditional medicine in Burkina Faso to treat several microbial infections, including oral and anal candidiasis (Bangou et al. 2012). Research by Rouamba et al. (2024a) demonstrated that extracts from *L.*



Figure 1 *Lippia multiflora* (A) whole plant, and (B) inflorescence

multiflora leaves significantly enhanced the bactericidal effects of cefotaxime against methicillin-resistant *Streptococcus aureus* (ATCC 43300). Furthermore, Rouamba et al. (2024b) found that the essential oils from *L. multiflora* flowers strongly inhibited biofilm formation and enhanced the motility of *Pseudomonas aeruginosa* (PAO1). While many studies have focused on the bactericidal properties of *L. multiflora* leaves or flower extracts against various Gram-positive and Gram-negative bacterial strains, scientific information regarding the antibiofilm potential of *L. multiflora* flower extracts against bacteria responsible for oral and dental infections, such as *S. mutans* and *S. aureus*, is limited. This study evaluated the antibacterial properties of methanol and dichloromethane extracts of *L. multiflora* flowers against *S. aureus* (ATCC 43300) and *S. mutans* (ATCC 2517), which are associated with oral infections.

2 Materials and Methods

2.1 Plant collection

The flowers of *L. multiflora* were collected in September 2022 from Loumbila, Burkina Faso (coordinates: 12°31'5.39"N; 1°22'8.39"W). An expert taxonomist at the Plant Ecology Laboratory, UFR/SVT, identified the collected plant samples at Université Joseph KI-ZERBO in Burkina Faso. Herbarium sheets, prepared with various plant parts and flowering tops, have been deposited at the herbarium of Université Joseph KI-ZERBO under the ID number CI-922.

2.2 Extraction

The flowers of *L. multiflora* were first ground into a powder. This powder was then subjected to maceration in dichloromethane at 10 g per 100 mL, with mechanical stirring for 24 hrs at 37 °C. Afterwards, the mixture was centrifuged for 20 minutes at 800 g, and the supernatant was collected. This supernatant was concentrated using a rotary evaporator and evaporated to dryness to yield the dichloromethane crude extract. The remaining residue was dried and then subjected to maceration in methanol under the same conditions to produce the methanol crude extract.

2.3 Determination of minimal inhibitory and bactericidal concentrations

The extracts' minimum inhibitory concentration (MIC) was determined using the microdilution method (Roy and Gupta 2022). Different concentrations of the extracts were added to 96-well plates containing 10 µL of a bacterial inoculum (at a specified concentration) and incubated for 24 hours at 37 °C. After the incubation, iodinitrotetrazolium was added. The lowest concentration of the extract in which no colour change occurred, indicating the absence of bacterial growth, was recorded as the MIC. The minimum bactericidal concentration (MBC) was

assessed using a solid LB-agar medium (Septya et al. 2023). Samples were taken from the wells that showed no bacterial growth during the MIC determination and transferred to Petri dishes containing LB-agar medium. After 24 hours of incubation at 37 °C, the lowest concentration of the extract in the petri dish that displayed any visible bacterial colonies was considered the MBC.

2.4 Antibiofilm assay

Using the crystal violet method, a non-bacteriostatic concentration of the extracts was utilized to evaluate the antibiofilm activity (Kamimura et al. 2022). In this experiment, 10 µL of the inoculum of each bacterium (10^6 CFU/mL) was incubated with each extract at a final concentration of 100 µg/mL for 24 hours at 37°C in 96-well plates. After incubation, the supernatant and any planktonic bacteria were removed from the wells. The remaining bacterial biofilm was washed with distilled water and fixed with methanol for 15 minutes. Following the removal of methanol, crystal violet was added to the wells. After incubating for 30 minutes at 37°C, excess crystal violet was removed, and the fixed crystal violet in the biofilm membrane was solubilized using an acetic acid solution. The intensity of the dissolved crystal violet colour is proportional to the quantity of biofilm formed. Optical densities were measured at 590 nm, and the results were expressed as the percentage inhibition of biofilm formation compared to the control without extracts, with salicylic acid used as a reference compound.

2.5 Antioxidant assay

The antioxidant potential of the extracts was evaluated by assessing their ability to neutralize DPPH and ABTS radicals and reduce iron(III) using the DPPH, ABTS, and FRAP methods, respectively (Compaoré et al. 2016). Ascorbic acid was utilized to generate standard curves for the DPPH radical scavenging assay ($Y = 0.058X + 0.130$; $R^2 = 0.994$) and the iron(III) reduction tests ($Y = 0.013X - 0.018$; $R^2 = 0.999$). Trolox was used to create the standard curve for the ABTS radical scavenging activity ($Y = 0.016X + 0.096$; $R^2 = 0.997$). The results were expressed as mg of EAA/10 g of extract for the DPPH radical trapping test, mmol of EAA/10 g of extract for the iron(III) reduction test, and mg of ET/10 g of extract for the ABTS radical quenching test.

2.6 Phytochemical screening

The total flavonoid content was measured using iron chloride, as described by Hilma et al. (2018). Quercetin was utilized to create the standard curve, represented as $Y = 0.031X + 0.019$ ($R^2 = 0.999$). The results are reported as mg of EQ per 100 mg of extract. Total phenolics were quantified with the Folin-Ciocalteu reagent following the method outlined by Lucas et al. (2022). Gallic acid served as the standard for generating the curve, expressed as $Y = 39.543X + 0.039$ ($R^2 = 0.999$), and the results are presented as mg

of EAG per 100 mg of extract. Qualitative phytochemical analysis was conducted using standard analytical tests to screen for primary and secondary metabolites following the methodology described by Yamin et al. (2021).

2.7 Statistical analysis

The results are presented as the mean value from multiple independent experiments ($n > 3$) with the standard deviation included. A one-way ANOVA, followed by the Tukey post-test, was conducted to assess the significance of the results. A statistical difference was noted when $P < 0.05$.

3 Results

3.1 Minimal inhibitory and bactericidal concentrations

The results of the minimal inhibitory and minimal bactericidal concentrations indicated that the dichloromethane and methanolic

extracts of *L. multiflora* strongly inhibited the growth of *S. mutans* compared to *S. aureus* ($P < 0.05$). These findings suggest that *S. mutans* is more sensitive to the extracts of *L. multiflora* than *S. aureus*. Additionally, the dichloromethane extract exhibited a higher bactericidal effect than the methanolic extract against both *S. mutans* and *S. aureus*, with minimal bactericidal concentrations of 0.25 ± 0.02 mg/mL and 3.13 ± 0.30 mg/mL, respectively (Table 1). These results are promising in the fight against oral infections, mainly because *S. mutans* is the primary bacterium associated with oral and dental infections, such as dental caries, while *S. aureus* is an opportunistic pathogen.

3.2 Anti-biofilm activity

After evaluating the extracts' capacity to kill bacteria (bactericidal effect) or inhibit bacterial growth (bacteriostatic effect), we assessed their ability to prevent bacterial biofilm formation, with the results displayed in Figure 2. Both extracts effectively inhibited

Table 1 Minimal inhibitory and bactericidal concentrations of extracts

Extract	Bacterial strain	MIC (mg/mL)	MBC (mg/mL)	MBC/MIC	Sensibility
MeOH	<i>S. mutans</i>	0.78 ± 0.07^b	3.13 ± 0.30^b	4.00 ± 0.40	Bacteriostatic
	<i>S. aureus</i>	3.13 ± 0.30^a	$> 12.5 \pm 1.20^a$	> 3.99	Nd
DCM	<i>S. mutans</i>	0.13 ± 0.01^d	0.25 ± 0.02^d	8.00 ± 0.80	Bacteriostatic
	<i>S. aureus</i>	0.25 ± 0.02^c	$> 0.50^c$	> 2.00	Nd

MIC: minimal inhibitory concentration, MBC: minimal bactericidal concentration, MeOH: methanol, DCM: dichloromethane, Nd: Not determined, values with different superscript letters in each column differ statistically ($P < 0.05$)

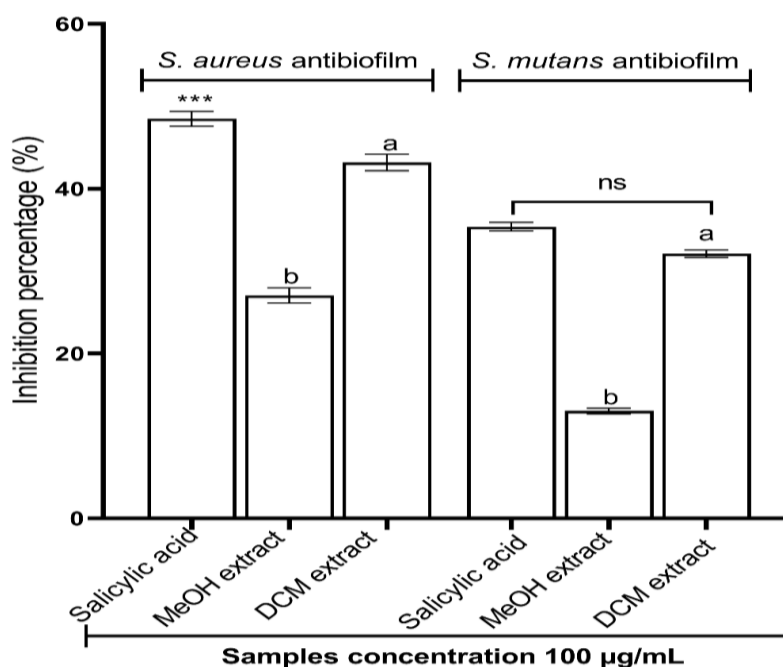


Figure 2 Antibiofilm activity of *L. multiflora* extract [*** $p < 0.001$ versus the corresponding salicylic acid, ^{a,b} $P < 0.05$ compared between extracts (ANOVA followed by Tukey test), ns: nonsignificant, MeOH: Methanol, DCM: dichloromethane]

biofilm formation in *S. aureus* and *S. mutans*. The dichloromethane extract demonstrated superior inhibitory activity against biofilm formation compared to the methanol extract for both *S. aureus* and *S. mutans* ($P < 0.05$). Notably, the dichloromethane extract and salicylic acid showed similar levels of inhibitory activity against biofilm formation in *S. mutans*. However, the dichloromethane extract was less effective than salicylic acid in inhibiting biofilm formation in *S. aureus*. These findings suggest that the dichloromethane extract of *L. multiflora* flowers is a promising source of antibiofilm compounds for combating *S. mutans*.

3.3 Antioxidant activities of tested extracts

Bacteria can cause oxidative stress during their infection processes. The capacity of the extract to quench free radicals (antioxidant effect) was measured, and the data were presented in Table 2. All the extracts showed higher DPPH and ABTS radical scavenging activities and higher Fe(III) reducing power. The methanolic extract showed more anti-DPPH activity (11.69 ± 0.24 mg AAE/10g), more anti-ABTS activity (943.38 ± 3.41 mg TE/10g) and more Ferric reducing power (41.04 ± 0.89 mmol AAE /10g)

than dichloromethane extract ($P < 0.05$) which exhibited the anti-DPPH activity of 9.20 ± 0.12 mg AAE/10g, the anti-ABTS activity of 938.44 ± 2.91 mg TE/10 g and the Ferric reducing power of 13.96 ± 0.28 mmol AAE /10g.

3.4 Phytochemical screening

To evaluate the antibacterial potential of the extract, we conducted a quantitative and qualitative screening of its bioactive phytomolecules. The results of the quantitative phytochemical screening are presented in Table 3. The methanol extract demonstrated higher total phenolic (49.57 ± 2.74 mg GAE/100 mg) and flavonoid (2.87 ± 0.05 mg QE/100 mg) contents compared to the dichloromethane extract, which showed total phenolic and flavonoid contents of 25.71 ± 0.39 mg GAE/100 mg and 2.24 ± 0.02 mg QE/100 mg, respectively ($P < 0.05$). The extraction yields indicated that the compounds in *L. multiflora* flowers were more polar and more soluble in methanol (7.78%) than dichloromethane (2.07%). For the qualitative phytochemical screening, we documented the results by photographing the test tubes, and the images are displayed in Figure 3.

Table 2 Antioxidant activities of tested *L. multiflora* extracts

Extract	DPPH (mg AAE/10g)	FRAP (mmol AAE /10 g)	ABTS (mg TE/10 g)
Dichloromethane	9.20 ± 0.12^b	13.96 ± 0.28^b	938.44 ± 2.91^b
Methanol	11.69 ± 0.24^a	41.04 ± 0.89^a	943.38 ± 3.41^a

AAE: Ascorbic acid equivalent, TE: Trolox equivalent, values with different superscript letters in each column differ statistically ($P < 0.05$)

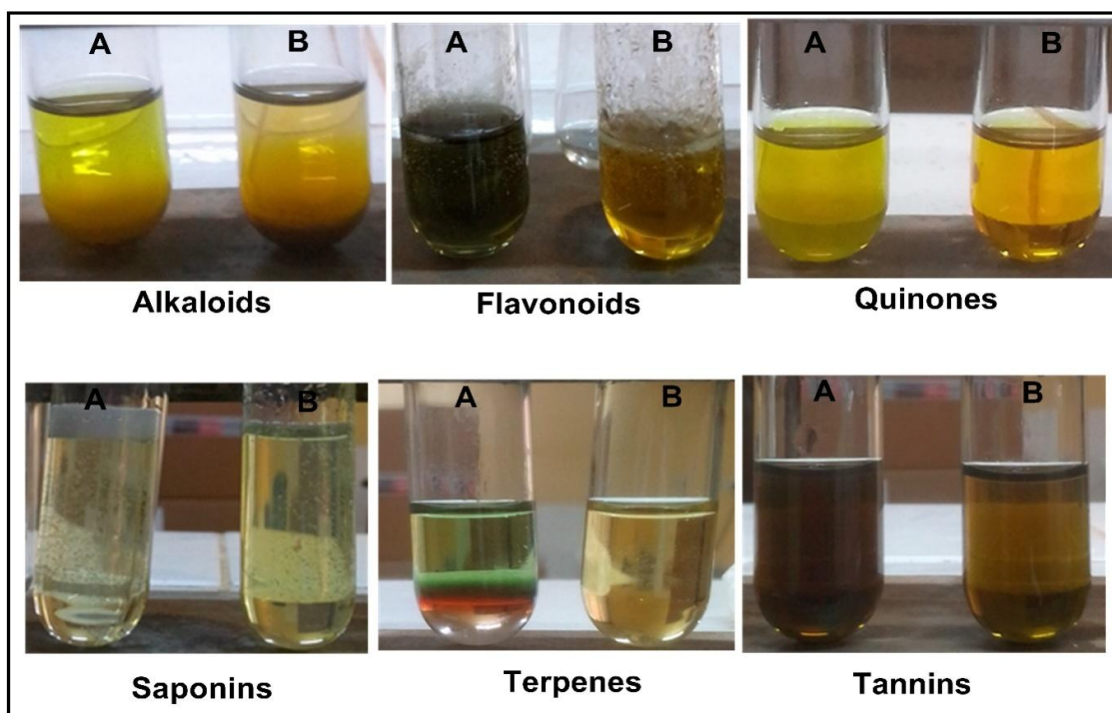


Figure 3 Photo of the different tubes for the secondary metabolites screening, (A) methanol extract, (B) dichloromethane extract

Table 3 Phenolic and flavonoid contents in the tested *L. multiflora* flower extracts

Extract	R (%)	Total phenolic (mg GAE/100 mg)	Total flavonoid (mg QE/100 mg)
Dichloromethane	2.07 ^b	25.71 ± 0.39 ^b	2.24 ± 0.02 ^b
Methanol	7.78 ^a	49.57 ± 2.74 ^a	2.87 ± 0.05 ^a

R: Rendement of extraction, GAE: Gallica cid equivalent, QE: Quercetin equivalent, values with different superscript letters in each column differ statistically ($P < 0.05$)

Table 4 Presence of the Secondary metabolites in prepared extracts of *L. multiflora*

Extract	Alkaloids	Flavonoids	Quinones	Saponins	terpenes	Tannins
MeOH	+	+	+	+	+	+
DCM	+	+	+	-	-	+

MeOH: methanol, DCM: dichloromethane, (+) presence, (-): absence

The analysis of Figure 3, which displays the colour of the tubes and the development of micelles, allowed us to identify various classes of secondary metabolites present in each extract. In tube A, the yellow precipitate, pink/orange colouration, yellow colouration, purple colour ring, brown colouration, and persistent moss indicated the presence of alkaloids, flavonoids, quinones, terpenes, tannins, and saponins, respectively, in the methanol extract. Conversely, tube B's absence of persistent moss and the purple colour signified that the dichloromethane extract does not contain terpenes or saponins. Table 4 summarizes the presence or absence of secondary metabolites in methanol and dichloromethane extracts. Alkaloids, flavonoids, quinones, and tannins were detected in both extracts, while saponins and terpenes were not found in the dichloromethane extract.

4 Discussion

Methanol and dichloromethane extracts of *L. multiflora* demonstrated significant bactericidal and antibiofilm activity against two bacteria, *S. aureus* and *S. mutans*, which are associated with dental and oral infections. Furthermore, these extracts exhibited strong antioxidant activities against DPPH and ABTS radicals and notable ferric-reducing power. The antibacterial and antioxidant properties of the extracts may be attributed to the presence of alkaloids, flavonoids, tannins, quinones, terpenes, and saponins. *S. mutans* is a commensal organism found in humans' and animals' oral cavities and respiratory tracts (Abranches et al. 2018). Under certain conditions, it can act as an opportunistic pathogen, leading to infections such as septicemia and endocarditis (Nomura et al. 2020). *S. mutans* produces lactic acid, dissolving hard tissues and extracellular polysaccharides, enhancing adhesion to dental surfaces and accelerating biofilm formation (Krzysciak et al. 2014). Similarly, *S. aureus* is an opportunistic pathogen in oral diseases, primarily causing suppurative cutaneous infections like whitlow and boils (Del-Giudice 2020). Both bacteria are significant contributors to oral infections, including dental caries. In biofilms, they exhibit increased resistance to conventional

antibiotic treatments. The oral biofilm comprises cariogenic bacteria, particularly *S. mutans* and *S. sobrinus*, which initiate caries disease. Other pathogens, such as *Lactobacillus*, *Actinomyces*, *S. aureus*, and *P. aeruginosa*, further contribute to biofilm progression (Zhu et al. 2023). The process of biofilm formation occurs in several stages: the establishment of an exogenous film, bacterial adhesion to surfaces, bacterial co-aggregation, maturation of the biofilm, and eventual detachment (Zubair et al. 2017).

In this study, the flowers of *L. multiflora*, particularly the dichloromethane extract, revealed very low minimal inhibitory and minimal bactericidal concentrations, indicating a robust bactericidal potential against *S. mutans* and *S. aureus*. This bactericidal potential of the extract could be advantageous for treating oral infections by effectively eliminating planktonic bacteria and preventing their growth and pathogenicity. The bactericidal effect of the extract may be attributed to various mechanisms, including disruption of the bacterial cell wall, inhibition of bacterial enzymes, blocking of bacterial DNA synthesis, or interference with bacterial efflux pumps. The presence of multiple phytochemical groups in the extract, especially tannins, alkaloids, quinones, and flavonoids, could play a role in these antibacterial mechanisms. Tannins and quinones are known for their bactericidal properties, as they inhibit the synthesis of peptidoglycans, a vital component of the bacterial cell wall. Additionally, alkaloids inhibit DNA and protein synthesis and ATP synthetase activity (Vaou et al. 2021). Flavonoids are bacterial enzyme inhibitors and efflux pump blockers (Waditzer and Bucar 2021).

Traditional anti-infective therapies (antibiotics) target bacteria during their planktonic phase; however, these methods face a significant limitation due to potential resistance development. Consequently, strategies aimed at different stages of biofilm formation present a promising alternative to combat antibiotic resistance. The dichloromethane extract exhibited the highest antibiofilm potential against *S. mutans* and *S. aureus*. The extract's

antibiofilm effect may be explained by inhibiting the synthesis of the biofilm's polysaccharide coating, disrupting biofilm adhesion by altering medium composition, or quelling biofilm maturation and detachment. Phenolic compounds, including flavonoids and phenolic acids, are recognized for inhibiting the synthesis of the protective biofilm envelope, which may elucidate the antibiofilm effects observed in this study (Nassima et al. 2019).

Additionally, *S. mutans* and *S. aureus* influence the cellular oxidative stress response during their pathogenic processes, which may exacerbate oral diseases (Wen et al. 2017). The malonyl dialdehyde (MDA) produced during oxidative stress is found in the superficial layers of cartilage and is associated with dental caries (de Sousa Né et al. 2023). In this study, methanolic and dichloromethane extracts exhibited vital antioxidant activities by inhibiting DPPH and ABTS radicals and demonstrating ferric (III) reduction capacity. These antioxidant properties of the extracts may help mitigate oxidative stress induced by bacteria involved in oral infections, thereby limiting the onset and progression of these infections.

Conclusion

The dichloromethane extract of *L. multiflora* flowers demonstrated significant inhibition of bacterial growth in both *S. mutans* and *S. aureus*. It also exhibited the most vigorous antibiofilm activity against these two bacteria, which are known to be responsible for oral infections. While previous studies have screened the extracts of *L. multiflora* leaves and flowers for their bactericidal properties, this is the first time that the antibiofilm potential of the flower extract has been evaluated specifically for *S. aureus* and *S. mutans*. This study indicates that *L. multiflora* flowers can potentially be a valuable source of therapeutic phytomolecules for addressing planktonic and biofilm-forming bacteria associated with oral infections.

Acknowledgments

Authors acknowledge the "Fonds National de la Recherche, de l'Innovation pour le Développement (FONRID)" for supporting the present study under the reference number *FONRID//AAP3/Malainfect/NCP/PC/2021*

Conflict of interest

All authors declared that no competing interest exists

References

Abranches, J., Zeng, L., Kajfasz, J. K., Palmer, S. R., Chakraborty, B., Wen, Z. T., Richards, V. P., Brady, L. J., & Lemos, J. A. (2018). Biology of Oral Streptococci. *Microbiology spectrum*, 6(5), 10.1128/microbiolspec.GPP3-0042-2018. <https://doi.org/10.1128/microbiolspec.GPP3-0042-2018>.

Bangou, J. M., Abarca, N. A., Meda, N. R., Yougbaré-ziébrou, M., Millogo-rasolodimby, J., & Nacoulma, G. O. (2012). *Lippia chevalieri* Moldenke: A brief review of traditional uses, phytochemistry and pharmacology. *International Journal of Drug Delivery*, 4, 289–296.

Clauss, A., Sie, A., Zabre, P., Schmoll, J., Sauerborn, R., & Listl, S. (2021). Population-Based Prevalence of Oral Conditions as a Basis for Planning Community-Based Interventions: An Epidemiological Study From Rural Burkina Faso. *Frontiers in public health*, 9, 697498. <https://doi.org/10.3389/fpubh.2021.697498>.

Compaoré, M., Meda, R. N.T., Bakasso, S., Vlase, L., & Kiendrebeogo, M. (2016). Antioxidative, anti-inflammatory potentials and phytochemical profile of *Commiphora africana* (A. Rich.) Engl. (Bursaceae) and *Loeseneriella africana* (Willd.) (Celastraceae) stem leaves extracts. *Asian Pacific Journal of Tropical Biomedicine*, 6(8), 665–670. DOI: <https://doi.org/10.1016/j.apjtb.2016.06.001>

de Sousa Né, Y. G., Lima, W. F., Mendes, P. F. S., Baia-da-Silva, D. C., Bittencourt, L. O., et al. (2023). Dental Caries and Salivary Oxidative Stress: Global Scientific Research Landscape. *Antioxidants (Basel, Switzerland)*, 12(2), 330. <https://doi.org/10.3390/antiox12020330>.

Del Giudice P. (2020). Skin Infections Caused by *Staphylococcus aureus*. *Acta dermato-venereologica*, 100(9), adv00110. <https://doi.org/10.2340/00015555-3466>.

Furuta, M., & Yamashita, Y. (2013). Oral Health and Swallowing Problems. *Current physical medicine and rehabilitation reports*, 1(4), 216–222. <https://doi.org/10.1007/s40141-013-0026-x>

Hilma, R., Hilma, A., & Almurdati, M. (2018). Determination of total phenolic, flavonoid content and free radical scavenging activity of ethanol extract Sawo stem bark (*Manilkara Zapota* (L.)). *Conference Proceeding CelSci Tech-UMRI*, 3, 62–68.

Hung, M., Moffat, R., Gill, G., Lauren, E., Ruiz-Negrón, B., Rosales, M. N., Richey, J., & Licari, F. W. (2019). Oral health as a gateway to overall health and well-being: Surveillance of the geriatric population in the United States. *Special care in dentistry: official publication of the American Association of Hospital Dentists, the Academy of Dentistry for the Handicapped, and the American Society for Geriatric Dentistry*, 39(4), 354–361. <https://doi.org/10.1111/scd.12385>.

Kalia, V. C., Patel, S. K. S., & Lee, J. K. (2023). Bacterial biofilm inhibitors: An overview. *Ecotoxicology and environmental safety*, 264, 115389. <https://doi.org/10.1016/j.ecoenv.2023.115389>.

Kamimura, R., Kanematsu, H., Ogawa, A., Kogo, T., Miura, H., et al. (2022). Quantitative Analyses of Biofilm by Using Crystal

- Violet Staining and Optical Reflection. *Materials (Basel, Switzerland)*, 15(19), 6727. <https://doi.org/10.3390/ma15196727>.
- Kilinc, F., Gessler, F., Kessel, J., Dubinski, D., Won, S. Y., et al. (2024). From the Oral Cavity to the Spine: Prevalence of Oral Cavity Infections in Patients with Pyogenic Spinal Infection. *Journal of clinical medicine*, 13(4), 1040. <https://doi.org/10.3390/jcm13041040>.
- Krzyściak, W., Jurczak, A., Kościelniak, D., Bystrowska, B., & Skalniak, A. (2014). The virulence of *Streptococcus mutans* and the ability to form biofilms. *European journal of clinical microbiology & infectious diseases : official publication of the European Society of Clinical Microbiology*, 33(4), 499–515. <https://doi.org/10.1007/s10096-013-1993-7>.
- Lucas, B. N., Nora, D. M. F., Boeira, C. P., Verruck, S., & Rosa, S. C. (2022). Determination of total phenolic compounds in plant extracts via Folin-Ciocalteu's method adapted to the usage of digital images. *Food Science and Technology*, 42, 1–6.
- Nadar, S., Khan, T., Patching, S. G., & Omri, A. (2022). Development of Antibiofilm Therapeutics Strategies to Overcome Antimicrobial Drug Resistance. *Microorganisms*, 10(2), 303. <https://doi.org/10.3390/microorganisms10020303>.
- Nassima, B., Nassima, B., & Riadh, K. (2019). Antimicrobial and antibiofilm activities of phenolic compounds extracted from *Populus nigra* and *Populus alba* buds (Algeria). *Brazilian Journal of Pharmaceutical Sciences*, 55, 1–10.
- Nomura, R., Otsugu, M., Hamada, M., Matayoshi, S., Teramoto, N., et al. (2020). Potential involvement of *Streptococcus mutans* possessing collagen binding protein Cnm in infective endocarditis. *Scientific reports*, 10(1), 19118. <https://doi.org/10.1038/s41598-020-75933-6>.
- Rouamba, A., Badini, D., Compaoré, E., Ouédraogo, V., & Kiendrebeogo, M. (2024a). *Lippia multiflora* Leaves Extracts Enhance Cefotaxime Bactericidal Effects and Quench the Biofilm Formation in Methicillin-Resistant *Staphylococcus aureus* ATCC 43300. *Avicenna journal of medical biotechnology*, 16(3), 193–199. <https://doi.org/10.18502/ajmb.v16i3.15746>.
- Rouamba, A., Compaoré, E., Kontogom, M., Zoungrana, Y., Ouédraogo, V., & Kiendrebeogo, M. (2024b). Essential oil of *Lippia multiflora* Moldenke Flowers Quenches *Pseudomonas aeruginosa* PAO1 Biofilm Formation and Motilities. *Journal of Pure and Applied Microbiology*, 18(2), 1043–1050.
- Roy, R. D., & Gupta, S. D. (2022). A novel method for early detection of MIC value – Broth dilution using indicator solution versus agar dilution: an original article. *Journal of Research in Clinical Medicine*, 10(27), 1–5.
- Septya, E. N., Amelia, R., & Suharyani, I. (2023). Minimum Inhibitory Concentration (MIC) and Minimum Bactericidal Concentration (MBC) Extract of NADES Nail Henna Leaves Against *Bacillus Cereus* Bacteria. *Journal of Health Science and Policy*, 1(1), 1–8. <https://doi.org/10.56855/jhsp.v1i1.168>.
- Sharma, S., Mohler, J., Mahajan, S. D., Schwartz, S. A., Bruggemann, L., & Aalinkeel, R. (2023). Microbial Biofilm: A Review on Formation, Infection, Antibiotic Resistance, Control Measures, and Innovative Treatment. *Microorganisms*, 11(6), 1614. <https://doi.org/10.3390/microorganisms11061614>.
- Vaou, N., Stavropoulou, E., Voidarou, C., Tsigalou, C., & Bezirtzoglou, E. (2021). Towards Advances in Medicinal Plant Antimicrobial Activity: A Review Study on Challenges and Future Perspectives. *Microorganisms*, 9(10), 2041. <https://doi.org/10.3390/microorganisms9102041>.
- Waditzer, M., & Bucar, F. (2021). Flavonoids as Inhibitors of Bacterial Efflux Pumps. *Molecules (Basel, Switzerland)*, 26(22), 6904. <https://doi.org/10.3390/molecules26226904>.
- Wen, Z. T., Liao, S., Bitoun, J. P., De, A., Jorgensen, A., Feng, S., et al. (2017). *Streptococcus mutans* Displays Altered Stress Responses While Enhancing Biofilm Formation by *Lactobacillus casei* in Mixed-Species Consortium. *Frontiers in cellular and infection microbiology*, 7, 524. <https://doi.org/10.3389/fcimb.2017.00524>.
- Yamin, R., Mistriyani, S., Ihsan, S., Armadany, F. I., Sahumena, M. H., & Fatimah, W. O. N. (2021). Determination of total phenolic and flavonoid contents of jackfruit peel and in vitro antiradical test. *Food Research*, 5(1), 84–90.
- Youssefi, M. A., & Afroughi, S. (2020). Prevalence and Associated Factors of Dental Caries in Primary Schoolchildren: An Iranian Setting. *International journal of dentistry*, 2020, 8731486. <https://doi.org/10.1155/2020/8731486>.
- Zhu, Y., Wang, Y., Zhang, S., Li, J., Li, X., Ying, Y., Yuan, J., Chen, K., Deng, S., & Wang, Q. (2023). Association of polymicrobial interactions with dental caries development and prevention. *Frontiers in microbiology*, 14, 1162380. <https://doi.org/10.3389/fmicb.2023.1162380>.
- Zubair, M., Ashraf, M., Raza, M., Mustafa, B., & Ahsan, A. (2017). Formation and Significance of Bacterial Biofilms. *International Journal of Current Microbiology and Applied Sciences*, 3(12), 917–923.



Journal of Experimental Biology and Agricultural Sciences

<http://www.jebas.org>

ISSN No. 2320 – 8694

EVALUATION OF *ASPERGILLUS NIGER* CONTAMINATION AND OCCURRENCE OF CITRININ IN RED CHILLI (*CAPSICUM ANNUUM*) SAMPLES

Arpita Mishra¹, Sangeetha Menon^{2*}, Challaraj Emmanuel E.S³, Kushbu Ravichandran⁴

¹Assistant Professor, Department of Life Sciences, Kristu Jayanti College Autonomous, Bengaluru- 560077

²Assistant Professor, Department of Life Sciences, Kristu Jayanti College Autonomous, Bengaluru- 560077

³Associate Professor, Department of Life Sciences, Kristu Jayanti College Autonomous, Bengaluru- 560077

⁴Assistant Professor, Department of Life Sciences, Kristu Jayanti College Autonomous, Bengaluru- 560077

Received – August 26, 2024; Revision – November 12, 2024; Accepted – November 23, 2024

Available Online – November 29, 2024

DOI: [http://dx.doi.org/10.18006/2024.12\(5\).694.704](http://dx.doi.org/10.18006/2024.12(5).694.704)

KEYWORDS

Red chilli

Mycotoxin

Aspergillus

HPLC

FTIR

Citrinin

ABSTRACT

Numerous Ascomycete fungi produce toxic, low-molecular-weight secondary metabolites known as mycotoxins. Mycotoxin contamination poses a global challenge to food safety, and growing regulatory expectations regarding the presence of mycotoxins in various products have spurred increased research into detecting these toxins in food and animal feed. Mycotoxin contamination has been reported in many significant spices, including chillies. However, most research has focused on aflatoxins as primary contaminants, highlighting the need to investigate other lesser-studied mycotoxins, such as citrinin and patulin. Consequently, the current study aimed to screen for fungal contamination in locally available red chilli varieties and detect the presence of mycotoxins. Random samples of red chilli were collected to isolate and identify the fungi responsible for producing mycotoxins. High-performance liquid chromatography (HPLC) techniques and Fourier transform infrared (FTIR) spectroscopy were employed to analyze the extracted mycotoxins qualitatively. Morphological and molecular characterization through 18S rRNA sequencing of the isolated samples confirmed the presence of *Aspergillus niger* in red chilli. HPLC and FTIR analyses of the red chilli samples confirmed the occurrence of citrinin. Very few studies have reported the production of Citrinin by *A. niger* in red chilli. Further research is necessary to conduct quantitative analyses and assess the effects of citrinin on human health.

* Corresponding author

E-mail: sangeethamenon@kristujayanti.com (Sangeetha Menon)

Peer review under responsibility of Journal of Experimental Biology and Agricultural Sciences.

Production and Hosting by Horizon Publisher India [HPI]
(<http://www.horizonpublisherindia.in/>).
All rights reserved.

All the articles published by [Journal of Experimental Biology and Agricultural Sciences](#) are licensed under a [Creative Commons Attribution-NonCommercial 4.0 International License](#) Based on a work at www.jebas.org.



1 Introduction

Mycotoxins are low molecular weight secondary metabolites produced by various fungal genera, including *Aspergillus*, *Fusarium*, and *Penicillium* (Doughari 2015). These toxins develop when fungi grow on different substrates under suitable conditions (Richard 2007; Tola and Kebede 2016). Mycotoxins can contaminate various food and feed samples (Bennett and Klich 2003; Pickova et al. 2021; Dey et al. 2022). Research has identified the presence of over a hundred mycotoxins in various dietary samples, which affect cereals, vegetables, fruits (Pereira et al. 2014; Zhao et al. 2018; Li et al. 2020; Wokorach et al. 2021), herbs (Altyn and Twauzek 2020; Chen et al. 2020; Caldeirao et al. 2021), spices (Boonzaaijer et al. 2008), and beverages like wine and milk (Myresiotis et al. 2015; Omar 2016; Carballo et al. 2021; Rocha et al. 2023).

Feed contamination poses additional food safety risks, as mycotoxins can carry over into animal-derived products, potentially affecting human health (Marin et al. 2013; Omotayo et al. 2019). These toxins have been linked to various health concerns, including hepatotoxicity (Ruan et al. 2022), nephrotoxicity (Weidemann et al. 2016), genotoxicity (Theumer et al. 2018), neurotoxicity (Wang et al. 2024), and immunosuppression (Benkerroum 2020). The most commonly found mycotoxins include Fumonisin, Zearalenone (ZEA), Aflatoxins (AF), Ochratoxins (OT), Citrinin, Patulin, and Trichothecenes (Hove et al. 2016). The World Health Organization (WHO) has established the highest regulatory limits for mycotoxins at 10-30 µg/kg, highlighting the severe health risks they pose to humans and animals (Lee et al. 2017).

Various analytical techniques detect and measure mycotoxins in food samples, including rapid strip screening assays, immunoassay-based methodologies, and chromatographic techniques (Agriopoulou et al. 2020). Techniques such as Thin Layer Chromatography (TLC), High-Performance Liquid Chromatography (HPLC), Gas Chromatography-Tandem Mass Spectrometry (GC-MS), and Enzyme-Linked Immunosorbent Assay (ELISA) are also utilized for quick mycotoxin analysis due to their profound implications (Lee et al. 2013; Younis et al. 2020; Liew and Sabran 2022).

Control measures for mycotoxins primarily focus on effective agricultural practices and management approaches, including modifying antifungal genes, using biocontrol agents, and breeding plants for tolerance (Chatterjee et al. 2023). Additionally, government programs aim to remove contaminated commodities from the food chain as part of regulatory efforts (Chatterjee et al. 2023). With the growing demand for healthy meals and legislative expectations, defining mycotoxin contamination limits has become imperative (Chatterjee et al. 2023).

Red chillies (*Capsicum annuum* Linn.) are one of the most popular spices consumed globally and are the second-largest production spice (Samyal and Sumbali 2020). They are mainly produced in tropical and subtropical regions, with China, India, and Thailand accounting for nearly half of the world's production (FAOSTAT 2017; Eskola et al. 2020). In India alone, they are cultivated over 8,000 hectares, resulting in an annual production of 1,872,000 Metric Tons (MT) (DACFW 2018). However, red chillies are significant sources of microbial contamination, particularly high aflatoxin levels (Romagnoli et al. 2007).

The crop is susceptible to various fungal pathogens and can be attacked by mycotoxin-producing fungi during cropping, harvesting, and post-harvesting stages (Golge et al. 2013). Commercially sold red chillies often contain mycotoxin concentrations that exceed the maximum permissible limits. Citrinin (CIT) is the most frequently occurring mycotoxin produced by the genera *Penicillium*, *Aspergillus*, and *Monascus* (AjithKumar et al. 2023). CIT is a polyketide typically found in stored grains, vegetables, fruits, juices, herbs, spices, and spoiled dairy products (Doughari 2015). A literature review indicated that studies on citrinin contamination in red chillies are limited; therefore, the present study was conducted to screen for fungal contaminants in red chilli samples. Further qualitative analysis and identification of purified mycotoxin were performed using HPLC and Fourier Transform Infrared (FTIR) techniques.

2 Materials and Methods

2.1 Collection of red chilli samples

For this investigation, samples of mycotoxin-contaminated red chilli (*Capsicum annuum*) were identified and procured from local markets in Bangalore, Karnataka, India. Thirty-day-old red chilli samples were used in this study. All samples were collected and transported directly to the microbiological laboratory in an airtight container under aseptic conditions to prevent fungal contamination from external sources. The samples were surface sterilized using a 2.5% sodium hypochlorite solution for three minutes, rinsed multiple times in sterile double-distilled water, and dried (Rajarajan et al. 2013).

2.2 Isolation of mycoflora from the collected contaminated samples

Crushed red chilli samples (1 g) were suspended in 9 mL sterile distilled water. For each sample, an aliquot (0.1 mL) of the suspension was serially diluted in sterile water and then spread onto Potato Dextrose Agar (PDA) plates containing chloramphenicol. The plates were incubated at 25°C for 7 days. Rose Bengal agar medium supplemented with chloramphenicol was also used to isolate fungal colonies with distinctive physical

characteristics. After the incubation period, mold colonies on each plate were counted, and the colony-forming units (CFU) per gram were determined (Kutama et al. 2022).

2.3 Identification of fungal strains isolated from red chilli samples

Different morphologies of fungal colonies were selected based on their source, and pure cultures of each isolate were maintained on both PDA plates and slants. The colony characteristics, including colour and morphology, were recorded for the isolated strains. The phenotypic morphologies of the fungal colonies were examined using Lactophenol Cotton Blue (LPCB) staining. This method helped determine the size of the conidia and the characteristics of vesicles, conidiophores, and phialides, which are essential for identifying the genus and order of the parasitic organisms. Species-level identification was conducted through 18S rRNA sequencing at Barcode Biosciences in Bengaluru (Setlem and Ramlal 2022; Chen et al. 2020).

2.4 Screening of mycotoxin production by isolated fungal strains

2.4.1 Growth on different media

The fungal isolates were cultured on various media, including Coconut Cream Agar (CCA), Malt Extract Agar (MEA), Yeast Extract Sucrose Agar (YES), and Czapek Dox Agar (CZA). The resulting cultures were tested for fluorescence under UV light. The different colours emitted from the cultures indicate the presence or absence of various types of mycotoxins (Zhang et al. 2016).

2.4.2 Ammonia Vapour Test

The selected fungal isolates were cultured on YES medium and incubated at 28°C without light. After three days, the plates were exposed to ammonium hydroxide in a closed chamber (Sadhasivam et al. 2017). The change in colour of the culture medium indicated whether the isolates were toxic (Darab et al. 2010). After ten minutes, if the undersides of the agar plates turned pink-red, this indicated the presence of mycotoxin-producing isolates. In contrast, the isolates were considered non-toxic if no colour changed (Moradi et al. 2017).

2.5 Extraction of a mycotoxin from contaminated red chilli samples

Fifty grams of contaminated red chilli samples were taken and blended in a methanol and water solvent system in a 55:45 volume/volume ratio. The mixture was supplemented with 2 grams of sodium chloride and 50 milliliters of hexane (Agriopoulou et al. 2020). The samples were blended at high speed for 5 to 10 minutes and filtered through the Whatman No. 1 filter paper. After

filtration, an equal volume of chloroform was added to the filtrate, and the mixture was vigorously agitated for 2 minutes before allowing it to rest for separation. The lower phase was collected, evaporated almost to dryness at 65 °C, and then redissolved in 10 milliliters of a methanol-water solvent system in an 80:20 volume/volume ratio (Setlam and Ramlal 2022).

2.6 Qualitative and quantitative analysis of mycotoxin extract

2.6.1 UV Spectrophotometric Analysis

UV analysis of the extracted mycotoxin sample, suspended in 1 ml of methanol, was conducted using a Vis spectrophotometer across wavelengths of 200-900 nm (Kumar and Suresh 2019). The spectrum was analyzed to identify the type of mycotoxin in the sample.

2.6.2 Thin Layer Chromatography (TLC)

To identify the presence of mycotoxins, 5 µL of the extracted toxin was applied to a 0.5 mm thick silica gel plate previously coated with glycolic acid. Standard mycotoxin solutions were also spotted on the same plate. The plate was then developed using a mobile phase consisting of 6 parts toluene, 3 parts ethyl acetate, and 1 part formic acid. After the development process, the plate was air-dried and examined under a UV lamp. The fluorescence intensities of the sample spots were recorded, and mycotoxins were identified based on the color and Retention Factor (Rf) of the spots compared to those of the standard spots. Additionally, further development of the spots was achieved through vapor exposure or immersion in aluminum chloride reagent, followed by viewing at a wavelength of 365 nm (Hongyin et al. 2021).

2.6.3 High-Performance Liquid Chromatography (HPLC)

The mycotoxin levels in the extract were assessed and measured using High-Performance Liquid Chromatography (HPLC) at the ALS Laboratory in Bengaluru, Karnataka, India. For the analysis, 500 µl of methanol was introduced into the HPLC system, equipped with a fluorescence detector (ALSIN Equipment). The column temperature was maintained at 25°C. The excitation and emission wavelengths were set to 335 nm and 500 nm, respectively. A 50 µl sample of the mycotoxin was injected into the HPLC. To determine the optimal detection conditions for each toxin, the excitation and emission wavelengths were varied: Aflatoxin B1 was measured at 365 nm (excitation) and 440 nm (emission), Ochratoxin A at 335 nm and 465 nm, and citrinin at 331 nm and 500 nm. The mobile phase consisted of 0.25N phosphoric acid, acetonitrile, and propanol in a ratio of 550:350:10 (v/v/v). The instrument was operated under isocratic conditions with a 0.5 mL/min flow rate. The mycotoxins were identified by comparing the peak areas with standard mycotoxins' calibration curves, as Li et al. (2012) described.

2.6.4 Fourier Transform Infra Red (FTIR) analysis

FTIR analysis was conducted on a methanolic extract of contaminated red chilli samples at VIT, Vellore, Tamil Nadu, to determine the optimal detection conditions for each toxin. The analysis used an FT-IR spectrometer in Attenuated Total Reflectance (ATR) mode, covering a 400-4000 cm^{-1} range. The spectrum revealed various modes of vibration.

2.7 Statistical Analysis

The experiments were conducted in triplicate. Statistical analysis was performed using SPSS version 25.0. The results are expressed as the mean \pm standard deviation (SD), with a statistical significance level of $P < 0.05$.

3 Results and Discussion

3.1 Isolation and identification of the mycoflora from red chilli samples

The analysis of red chilli samples for fungal contaminants identified a single type of fungal colony across all samples. The morphological characteristics, including colony color, shape, and size, were documented and are presented in Table 1. Microscopic examination revealed that the isolate belongs to the genus *Aspergillus* (Watanabe 2018).

The isolated fungal strain underwent 18S rRNA sequencing for further identification confirmation. The sequencing results were entered into the nucleotide BLAST program via the NCBI database to identify the isolates. Based on these sequences, a phylogenetic tree was constructed using MEGA software (Figure 1).

Morphological and microscopic observations, along with the 18S rRNA sequencing, led to the identification of the isolated fungal strain as *Aspergillus niger*. The occurrence of *A. niger* in red chilli has been reported in only a few recent studies by Rajendran et al. (2021), Tsehaynesh et al. (2021), Enamullah et al. (2002), and Lasram et al. (2022). In contrast, many studies have cited the prevalence of other members of the *Aspergillus* genus, such as *A. flavus* and *A. parasiticus*, in red chilli (Hossain et al. 2018; Rajendran et al. 2021; Darsana and Chandrasehar 2021). Although mycotoxin contamination is a concern in countries that produce red chilli (Singh and Cotty 2017), it has not been extensively studied in previous research.

3.2 Screening tests for mycotoxin production by isolated fungal strains

When the isolated strains were cultured on various media, including CCA, MEA, YES, and CZA, and exposed to UV light, green fluorescence indicated the presence of mycotoxins (Table 2) (Agriopoulou et al. 2020). Similarly, Rajarajan et al. (2021) reported the production of fluorescent pigments in coconut milk agar (CMA) by aflatoxin-producing *A. flavus*. This fluorescence may be attributed to the influence of coconut on the production of the fluorescent pigment.

3.3 Ammonium Vapour Test

Isolates grown on Potato Dextrose Agar exhibited pink pigmentation when exposed to ammonium vapor. This color change indicates the presence of mycotoxins, as ammonium vapor interacts with these toxins to produce pink to red pigmentation (Shekhar et al. 2017; Rajarajan et al. 2021).

Table 1 Colony morphology and microscopic observation of mycoflora isolated from red chilli samples

Colony Characteristics	Microscopic Morphology	Identified genus	Reference
Colonies had a cottony appearance and were grey to black on the top with a whitish reverse side.	The conidial head is biseriate and radiate, with conidia arranged in chains or dispersed when detached.	<i>Aspergillus</i> spp.	Watanabe 2018

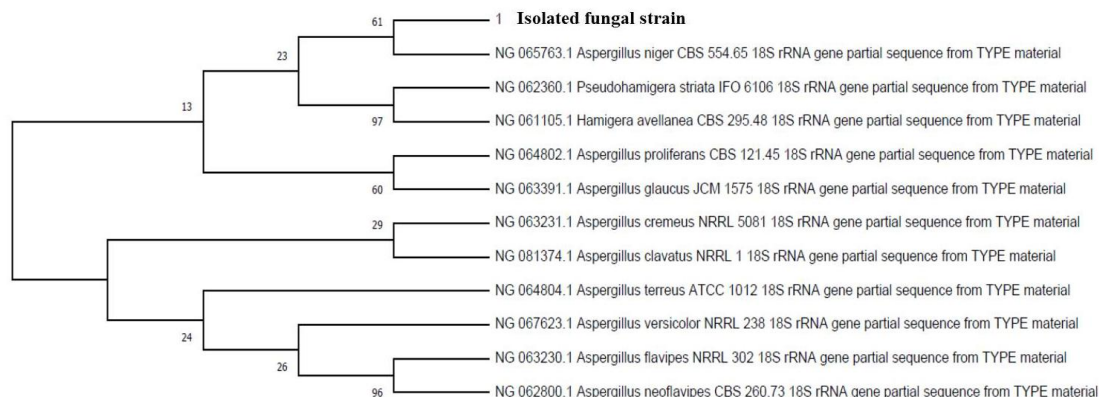


Figure 1 Phylogenetic tree of a fungal strain isolated from red chilli

Table 2 UV Fluorescence of Isolated Fungal Culture Cultivated in Different Media

Sample Source	Isolated Fungi	Media			
		CCA	MEA	CZA	YES
Red Chilli	<i>Aspergillus</i> spp.	+	+	-	+

CCA- Coconut Cream Agar, MEA- Malt Extract Agar, CZA-Czapek Dox Agar, YES – Yeast Extract Sucrose Agar

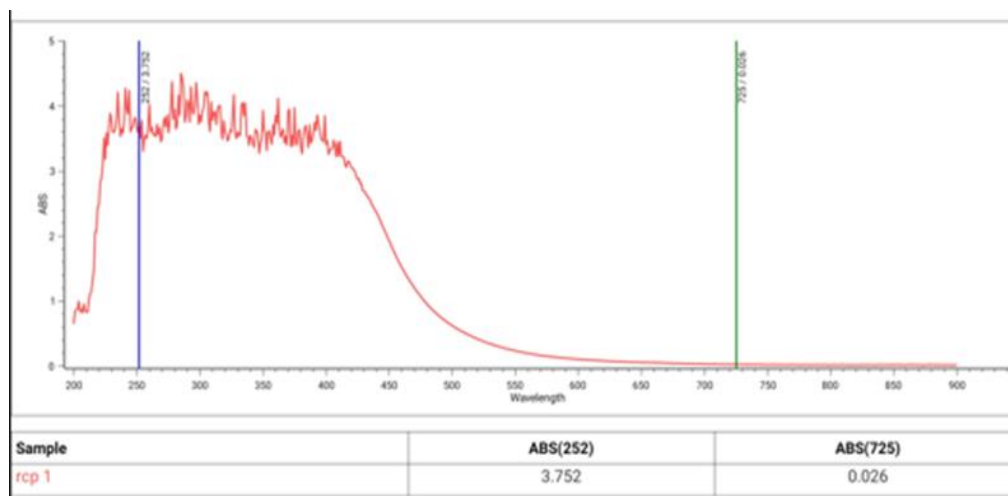


Figure 2 UV Spectrophotometric analysis of mycotoxin extracted from red chilli sample

3.4 Qualitative and quantitative analysis of mycotoxin extract

3.4.1 UV Spectrophotometric Analysis

The UV spectrum analysis of the mycotoxin extracts revealed a peak value of 252 nm, with an absorbance of 3.752 (Figure 2). Similar peaks at this wavelength were reported in mycotoxins from date palms by Kumar and Suresh (2019) and from animal feed by Rajarajan et al. (2021). Samyal and Sumbali (2021) and Akintola et al. (2024) have also documented the production of mycotoxins by various fungal species in red chilli.

3.4.2 Thin-layer chromatography (TLC) analysis

The thin-layer chromatography (TLC) plates observed under 365 nm light showed lemon yellow spots in the current investigation. The fluorescence of these spots was compared to standard mycotoxins, and the Rf value of the spot was determined to be 0.63. Based on this comparison, the mycotoxins produced by *Aspergillus niger* in this study were identified as Citrinin (Rasheva et al. 2003; Doughari 2015). Since the spots were faint and fragile, the TLC plate was sprayed with aluminum chloride, which caused the spots to change from yellow to blue. Additionally, incorporating glycolic acid into the silica gel enhanced the visibility of the spots with minimal diffusion, thus improving detectability. Mycotoxin detection using TLC is often semi-quantitative or quantitative, with a visual identification recovery limit of 0.01 ppm. Rasheva et al. (2003) reported that silica gel

treated with organic acid could detect various types of mycotoxins, including citrinin, aflatoxin, and fumonisin.

3.4.3 HPLC Analysis

HPLC is commonly used to detect mycotoxins. In the current study, a solvent composed of 0.25N phosphoric acid, acetonitrile, and 2-propanol in a ratio of 55:35:10 successfully eluted mycotoxins as a sharp peak within 3 minutes. This retention time confirmed the presence of the mycotoxin citrinin in the tested sample (Figure 3). Recently, citrinin was also reported in date palms infected with *A. niger* (Schmidt-Heydt et al. 2012; Sadhasivam et al. 2021). Among all *Aspergillus* species, *A. niger* is primarily responsible for the production of citrinin. While *A. niger* is the leading producer, other *Aspergillus* species such as *A. awamori*, *A. wentii*, *A. fumigatus*, *A. niveus*, *A. ostianus*, and *A. parasiticus* are also known to produce Citrinin (Doughari 2015). Similarly, Samyal and Sumbali (2020 & 2021) reported that some fungal pathogens, including *A. terreus*, *Penicillium expansum*, and *P. fellutanum*, produce citrinin in red chilli. Citrinin has a conjugated planar structure with natural fluorescence, making it detectable by reverse-phase HPLC using phosphoric acid as a mobile phase in food commodities (Wang et al. 2014). Li et al. (2012) reported that citrinin can be detected at concentrations as low as 2–5 ng, with a higher retention time and peak area. Mycotoxins are undesirable toxins produced by pathogenic fungi in poorly stored or processed spices, making their detection crucial. Therefore, HPLC combined with UV-VIS or MS/MS

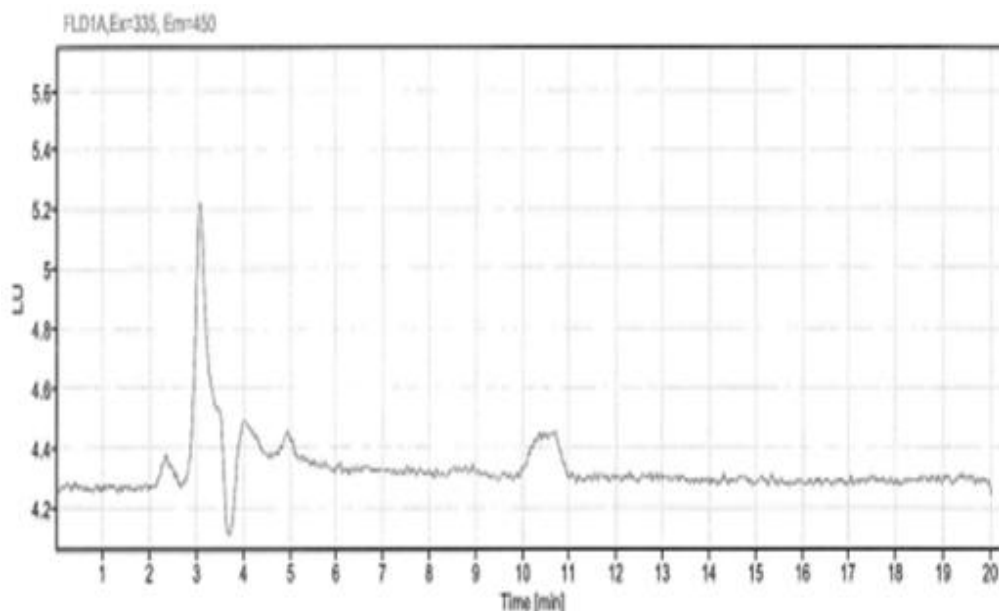


Figure 3 HPLC analysis for red chilli sample

Table 3 FTIR spectroscopic data of mycotoxin extracted from red chilli samples

S. N.	Obtained Peak (Wave number cm-1)	Frequency Range (Wave number cm-1)	Peak intensity	Absorption Band	Mode of vibration and Functional group	References
1.	3269	2500-4000	Weak	Broad	Hydrogen Bond	
2.	2924	2500-4000	Medium	Sharp and narrow	Aromatic -C-H and CH ₂	
3.	2852	2500-4000	Weak	Sharp and narrow	Aromatic -C-H and CH ₂	
4.	1739	1700-1800	Medium	Sharp	C=O stretching of carbonyl groups (ketones, esters, or acids)	
5.	1627	1485-1690	Weak	Broad	C=O, C-N stretching of amide, N-H, C-O bending and C-C, C-N stretching of amide	Kaya-Celiker et al. (2014); Dandashire and Almajir (2020)
6.	1371	1330-1410	Weak	Broad	Symmetric C-H bending of methyl group	
7.	1234	600-1500	Weak	Sharp	CH ₂ - Bending vibration	
8.	1155	1000-2000	Weak	Sharp	C-O, CH ₂ stretching, bending	
9.	1018	1000-2000	Strong	Broad	C-O, CH ₂ stretching, bending	

detectors has proven effective for determining mycotoxins in various species (Sahu et al. 2023).

3.4.4 FTIR Analysis

FTIR is a rapid, reliable, and sensitive technique for detecting mycotoxins in food samples. The FTIR results of the analyzed samples confirmed the presence of mycotoxins, as evidenced by the peaks and wave numbers specific to the functional groups of

mycotoxins found in their FTIR spectra. These peaks were documented, and the modes of vibration and the functional groups were analyzed, as outlined in Table 3. The FTIR analysis of a contaminated sample of dried red chilli revealed the presence of mycotoxins, indicated by peaks in the FTIR spectrum (Figure 4). These peaks correspond to the characteristic functional groups associated with mycotoxins, including ranges from 2500-4000 cm⁻¹, 1700-1800 cm⁻¹, 1485-1690 cm⁻¹, 1330-1410 cm⁻¹, 600-1500 cm⁻¹, and 1000-2000 cm⁻¹. Specifically, these involve

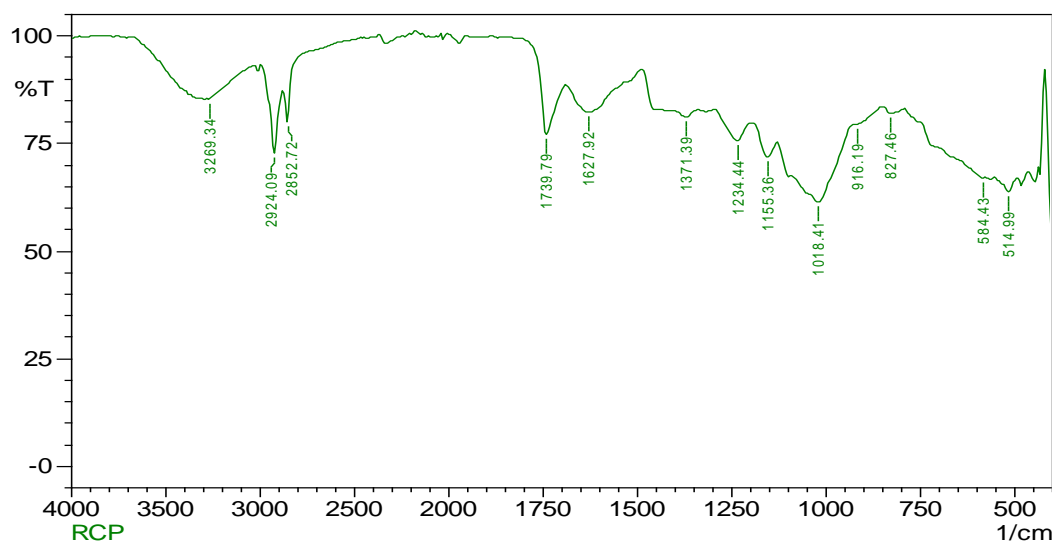


Figure 4 FTIR spectra of the mycotoxin extracted from red chilli samples

Aromatic C-H and CH₂ stretching, C=O stretching of carbonyl groups (such as ketones, esters, or acids), C-N stretching of amides, N-H bending, C-O bending, symmetric C-H bending of methyl groups, and CH₂-bending vibrations. FTIR spectroscopy is a nondestructive method for measuring the total amount of infrared energy absorbed by the sample under investigation. This user-friendly technique can evaluate sample depths ranging from 10 µm to 100 mm with minimal interference from surface light scattering (Lomont et al. 2022). The primary advantage of FTIR is its ability to perform depth profiling for the nondestructive evaluation of food items. Additionally, mycotoxins' wavelength and absorption patterns were similar in studies conducted by Kaya-Celiker et al. (2014) and Dandashire and Almajir (2020).

Recent reports indicate natural contamination of citrinin (CIT) in regional spices, with the highest concentrations found in dried ginger, black pepper, and red chilli, reaching up to 47.2%. Dried ginger exhibited the most significant average concentration of CIT at 85.1 µg/kg (Yogendrarajah 2015; Mair et al. 2021). A dietary exposure study conducted in Belgium by Meerpoel and Vidal (2021) revealed that 50% of the herbs and spices tested were contaminated with CIT, with the highest concentration recorded at 4.5 µg/kg. In 2019, the maximum regulatory limit for CIT was reduced from 2000 µg/kg to 100 µg/kg following an amendment to Section 2.8.1 of the Annex to Regulation (EC) 1881/2006. This change was related to EU regulations on red yeast rice food supplements. Recent European monitoring studies have detected CIT and its associated biomarkers. However, among the 72 recognized methods for mycotoxin analysis in food published by the International Organization for Standardization (ISO), the European Committee for Standardization (CEN), and the Association of Official Agricultural Chemists (AOAC), none have specifically targeted CIT (Ali and Degen 2019).

Conclusion

Mycotoxins are significant contaminants found in food and feed, threatening human and animal health, food safety and agriculture. This issue remains a concern despite global efforts to reduce or eliminate their presence. Public health authorities and governmental bodies are implementing strict regulations for the most commonly found classes of mycotoxins in food and feed. Various analytical techniques have been developed to minimize mycotoxin levels; however, the problem persists. This study investigates fungal contamination-producing mycotoxins in red chilli. Molecular characterization confirmed the presence of *A. niger*, and analytical methods such as Thin Layer Chromatography (TLC), High-Performance Liquid Chromatography (HPLC), and Fourier-Transform Infrared Spectroscopy (FTIR) identified the production of citrinin by the mycoflora in red chilli. This research reports the presence of citrinin produced by *A. niger* in red chilli. The combined detection approach provides better insights into recognizing the potential risks of mycotoxin contamination. It also paves the way for developing ultra-sensitive detection techniques, ensuring high-quality, safe, and contaminant-free food. Additionally, this paper emphasizes the importance of precautionary measures to be taken during the production, handling, and transportation of spices to reduce mycotoxin accumulation.

Acknowledgments

The authors thank Kristu Jayanti College Autonomous, Bangalore, for providing laboratory facilities.

Competing interests

The authors declare no competing interests.

References

- Agriopoulou, S., Stamatelopoulou, E., & Varzakas, T. (2020). Advances in analysis and detection of major mycotoxins in foods. *Foods*, 9(4), 518. <https://doi.org/10.3390/foods9040518>.
- Ajithkumar, K., Savitha, A.S., Renuka, M., Naik, M.K. (2023). Citrinin: A Potential Mycotoxin in Food and Feed with Possible Management Strategies to Combat Its Contamination. In D. Nagaraju, S. M. Yanjarappa, P. N. Achar, & A. M. Vaya (Eds.) *Anti-Mycotoxin Strategies for Food and Feed* (pp 133-154). John Wiley & Sons, Hoboken, NJ 07030, USA <https://doi.org/10.1002/9781394160839.ch6>.
- Akintola, A., Al-Dairi, M., Imtiaz, A., Al-Bulushi, I. M., Gibreel, T., Al-Sadi, A. M., & Velazhahan, R. (2024). The Extent of Aflatoxin B1 Contamination in Chilli (*Capsicum annuum* L.) and Consumer Awareness and Knowledge of Aflatoxins in Oman. *Agriculture*, 14(9), 1536-1549. <https://doi.org/10.3390/agriculture14091536>
- Ali, N., & Degen, G.N. (2019). Citrinin biomarkers: A review of recent data and application to human exposure assessment. *Archives of Toxicology*, 93, 3057–3066.
- Allyn, I., & Twarużek, M. (2020). Mycotoxin Contamination Concerns of Herbs and Medicinal Plants. *Toxins*, 12(3), 182-194.
- Benkerroum, N. (2020). Chronic and acute toxicities of aflatoxins mechanisms of action. *International Journal of Environmental Research and Public Health*, 17(2), 423-450.
- Bennett, J. W., & Klich, M. (2003). Mycotoxins. *Clinical Microbiology Review*, 16, 497-516.
- Boonzaaijer, G., van Osenbruggen, W., Kleinnijenhuis, A., & van Dongen, W. (2008). An exploratory investigation of several mycotoxins and their natural occurrence in flavor ingredients and spices, using a multi-mycotoxin LC-MS/MS method. *World Mycotoxin Journal*, 1(2), 167–174.
- Caldeirão, L., Sousa, J., Nunes, L.C., Godoy, H.T., Fernandes, J.O., & Cunha, S.C. (2021). Herbs and herbal infusions: Determination of natural contaminants (mycotoxins and trace elements) and evaluation of their exposure. *Food Research International*, 144, 110322.
- Carballo, D., Fernández-Franzón, M., Ferrer, E., Pallarés, N., & Berrada, H. (2021). Dietary exposure to mycotoxins through alcoholic and non-alcoholic beverages in Valencia, Spain. *Toxins*, 13 (7), 438.
- Chatterjee, S., Dhole, A., Krishnan, A.A., & Banerjee, K. (2023). Mycotoxin Monitoring, Regulation and Analysis in India: A Success Story. *Foods*, 12, 705. <https://doi.org/10.3390/foods12040705>
- Chen, L., Guo, W., Zheng, Y., Zhou, J., Liu, T., et al. (2020). Occurrence and Characterization of Fungi and Mycotoxins in Contaminated Medicinal Herbs. *Toxins*, 12(1), 30.
- Commission Regulation (EU) 2019/1901 of 7 November 2019 amending Regulation (EC) No 1881/2006 as regards maximum levels of citrinin in food supplements based on rice fermented with red yeast *Monascus purpureus* (Text with EEA relevance). Retrieved from <http://data.europa.eu/eli/reg/2019/1901/oj>
- Dandashire S.B., & Almajir, I.R. (2020). Aflatoxins and aflatoxigenic fungal contamination of common poultry feed products in Katsina State, Nigeria. *Novel Research in Microbiology Journal*, 4(1), 653-665.
- Darab, Y., Zainal Abidin. M.A., Tan Y.H., & Kamaruzaman S. (2010). Evaluation of the detection techniques of toxigenic *Aspergillus* isolates. *African Journal of Biotechnology*, 9 (45), 7654-7659. DOI: 10.5897/AJB10.1128.
- Darsana R., & Chandrasehar, G. (2021). Isolation and characterization of contaminant mycoflora from stored red peppers. *Journal of Pure and Applied Microbiology*, 15(3), 1187-1197. doi: 10.22207/JPAM.15.3.08
- Department of Agriculture, Cooperation and Farmers Welfare. (2018). Horticultural Statistics at a Glance 2018, Ministry of Agriculture & Farmers Welfare, Government of India, pp. 1-490
- Dey, D. K., Kang, J. I., Bajpai, V. K., Kim, K., Lee, H., Sonwal, S., & Shukla, S. (2022). Mycotoxins in food and feed: toxicity, preventive challenges, and advanced detection techniques for associated diseases. *Critical Reviews in Food Science and Nutrition*, 63(27), 8489–8510.
- Doughari, J. H. (2015) The Occurrence, Properties and Significance of Citrinin Mycotoxin. *Plant Pathology and Microbiology*, 6 (11), 321. doi:10.4172/21577471.1000321
- Enamullah, S.M., Rahman, A., Sahar, N. & Ehteshamul-Haque, S. (2022). Detection of aflatoxin contamination and incidence of fungi associated with red chilli available in local market of Karachi, Pakistan. *Pakistan Journal of Botany*, 54(6), 2335-2339. [http://dx.doi.org/10.30848/PJB2022-6\(14\)](http://dx.doi.org/10.30848/PJB2022-6(14))
- Eskola, M., Kos, G., Elliott, C.T., Hajlová, J., Mayar, S., & Krska, R. (2020). Worldwide contamination of food-crops with mycotoxins: Validity of the widely cited 'FAO estimate' of 25. *Critical Review in Food Science Nutrition*, 60, 2773–2789.
- FAOSTAT (2017). Agro-Statistics Database. Food and Agriculture Organization of the United Nations, Rome.

- Golge, O., Hepsag, F. & Kabak, B. (2013). Incidence and level of aflatoxin contamination in chilli commercialized in Turkey. *Food Control*, 33 (2), 514-520. <https://doi.org/10.1016/j.foodcont.2013.03.048>.
- Hongyin, Z., Joseph, A., Qiya, Y., Lina, Z., Xiaoyun, Z., & Xiangfeng, Z. (2021). A review on Citrinin: Its occurrence, risk implications, analytical techniques, biosynthesis, physiochemical properties and control. *Food Research International*, 141, 110075. <https://doi.org/10.1016/j.foodres.2020.110075>.
- Hossain, M.N., Talukder, A., Afroze, F., Rahim, M.M., Begum, S., Haque, M.Z., & Ahmed, M.M. (2018). Identification of aflatoxigenic fungi and detection of their aflatoxin in red chilli (*Capsicum annuum*) samples using direct cultural method and HPLC. *Advances in Microbiology*, 8(1), 42-53.
- Hove, M., De Boevre, M., Lachat, C., Jacxsens, L., Nyanga, L.K., & De Saeger, S. (2016). Occurrence and risk assessment of mycotoxins in subsistence farmed maize from Zimbabwe. *Food Control*, 69, 36-44.
- Kaya-Celiker, H., Mallikarjunan, P.K., Schmale III, D., & Christie, M.E. (2014). Discrimination of moldy peanuts with reference to aflatoxin using FTIR-ATR system. *Food Control*, 44, 64-71.
- Kumar, S., & Suresh, D. (2019). Isolation, identification and detection of aflatoxin from date palm (*Phoenix dactylifera* L.). *International Journal of Pharma and Bio Sciences*, 10(3), 158–164.
- Kutama, A.S., Muhammad A., Sani, M.D., & Mai –Abba, I. A. (2022). Isolation and identification of aflatoxin producing fungi from different foodstuffs at Shuwarin Market, Jigawa State, Nigeria. *Dutse Journal of Pure and Applied Sciences*, 8(1b), 9-15. <https://doi.org/10.4314/dujopas.v8i1b.2>
- Lasram, S., Hajri, H., & Hamdi, Z. (2022). Aflatoxins and Ochratoxin A in Red Chilli (*Capsicum*) Powder from Tunisia: Co-Occurrence and Fungal Associated Microbiota. *Journal of Food Quality and Hazards Control*, 9 (1), 32-42.
- Lee, H.S., Nguyen-Viet, H., Lindahl, J., Thanh, H.M., Khanh, T.N., Hien, L.T.T., & Grace, D. (2017). A survey of aflatoxin B1 in maize and awareness of aflatoxins in Vietnam. *World Mycotoxin Journal*, 10 (2), 195-202.
- Lee, S., Kim, G. & Moon, J. (2013). Performance improvement of the one-dot lateral flow immunoassay for aflatoxin B1 by using a smartphone-based reading system. *Sensors*, 13(4), 5109-5116.
- Li, Y., Zhang, X., Nie, J., Bacha, S.A.S., Yan, Z., & Gao, G. (2020). Occurrence and co-occurrence of mycotoxins in apple and apple products from China. *Food Control*, 118, 107354.
- Li, Y., Zhou, Y.C., Yang, M.H., & Ou-Yang, Z. (2012). Natural occurrence of citrinin in widely consumed traditional Chinese food red yeast rice, medicinal plants and their related products. *Food Chemistry*, 132 (2),1040-1045. <https://doi.org/10.1016/j.foodchem.2011.11.051>.
- Liew, W.P., & Sabran, M.R. (2022). Recent advances in immunoassay-based mycotoxin analysis and toxicogenomic technologies. *Journal of Food Drug Analysis*, 30(4), 23, 549-561.
- Lomont, J. P., Ralbovsky, N. M., Guza, C., Saha-Shah, A., Burzynski, J., Konietzko, J., Wang, S., McHugh, P. C., Mangion, I., & Smith, J. A. (2022). Process monitoring of polysaccharide deketalization for vaccine bioconjugation development using *in situ* analytical methodology. *Journal of Pharmaceutical and Biomedical Analysis*, 209, 114533. <https://doi.org/10.1016/j.jpba.2021.114533>
- Mair, C., Norris, M., Donnelly, C., Leeman, D., Brown, P., Marley, E., Milligan, C., & Mackay, N. (2021). Assessment of Citrinin in Spices and Infant Cereals Using Immunoaffinity Column Clean-Up with HPLC Fluorescence Detection. *Toxins*, 13, 715. <https://doi.org/10.3390/toxins13100715>
- Marin, S., Ramos, A.J., Cano-Sancho, G., & Sanchis, V. (2013). Mycotoxins: Occurrence, toxicology, and exposure assessment. *Food and Chemical Toxicology*, 60, 218–237.
- Meerpoel, C., & Vidal, A. (2021). Dietary exposure assessment and risk characterization of citrinin and ochratoxin A in Belgium. *Food and Chemical Toxicology*, 147, 111914.
- Moradi, M., Fani, S. R., Dargahi, R., Moghadam, M., & Sherafati, A. (2017). A simple procedure to evaluate competitiveness of toxigenic and atoxigenic isolates of *Aspergillus flavus* in solid and liquid media. *Journal of Chemical Health Risks*, 7, 105–112.
- Myresiotis, C.K., Testempasis, S., Vryzas, Z., Karaoglanidis, G.S., & Papadopoulou-Mourkidou, E. (2015). Determination of mycotoxins in pomegranate fruits and juices using a QuEChERS-based method. *Food Chemistry*, 182, 81–88.
- Omar, S. S (2016). Aflatoxin M1 levels in raw milk, pasteurized milk and infant formula. *Italian Journal of Food Safety*, 5(3), 5788.
- Omotayo, O.P., Omotayo, A.O., Mwanza, M., & Babalola, O.O. (2019). Prevalence of mycotoxins and their consequences on human health. *Toxicological Research*, 35(1),1-7.
- Pereira, V. L., Fernandes, J.O., & Cunha, S.C. (2014). Mycotoxins in cereals and related foodstuffs: A review on occurrence and recent methods of analysis. *Trends in Food Science and Technology*, 36(2), 96–136.

- Pickova, D., Ostry, V., Toman, J., & Malir, F. (2021). Aflatoxins: history, significant milestones, recent data on their toxicity and ways to mitigation. *Toxins*, *13*(6), 399.
- Rajarajan, P. N., Rajasekaran, K. M., & Devi, N. K. A. (2013). Isolation and quantification of aflatoxin from *Aspergillus flavus* infected stored peanuts. *Indian Journal of Pharmaceutical and Biological Research*, *1*(04), 76.
- Rajarajan, P., Sylvia, K., Periasamy, M.P., & Subramanian, M. (2021). Detection of aflatoxin producing *Aspergillus flavus* from animal feed in Karnataka, India. *Environmental Analysis Health and Toxicology*, *36*(3), e2021017. DOI: <https://doi.org/10.5620/eaht.2021017>
- Rajendran, S., Shunmugam, G., Vaikuntavasen, P., Palanisamy, J., & Subbiah, S. (2021). Isolation and Screening of Chilli Pepper for Fungal Contamination and Aflatoxin Production. *International Journal of Plant & Soil Science*, *33*(9), 20-25. <https://doi.org/10.9734/ijpss/2021/v33i930462>
- Rasheva, T.V., Nedeva, T.S., Hallet, J.N., & Kujumdzieva, A.V. (2003). Characterization of a non-pigment producing *Monascus purpureus* mutant strain. *Antonie van Leeuwenhoek*, *83*, 333–340.
- Richard, J.L. (2007). Some major mycotoxins and their mycotoxicoses- An overview. *International Journal of Food Microbiology*, *119*(1-2), 3-10.
- Rocha, A. R., Cardoso, M.S., Júnior, J.A.S., Júnior, E. A. G., Maciel, L. F., & Menezes-Filho, J.A. (2023). Occurrence of aflatoxins B1, B2, G1, and G2 in beers produced in Brazil and their carcinogenic risk evaluation. *Food Control*, *145*, 109348.
- Romagnoli, B., Menna, V., Gruppioni, N., & Bergamini, C. (2007). Aflatoxins in Spices, Aromatic Herbs, Herbs-Teas and Medicinal Plants Marketed in Italy. *Food Control*, *18*, 697-701. <https://doi.org/10.1016/j.foodcont.2006.02.020>
- Ruan, H., Lu, Q., Wu, J., Qin, J., Sui, M., et al. (2022). Hepatotoxicity of food-borne mycotoxins: molecular mechanism, anti-hepatotoxic medicines and target prediction. *Critical Reviews in Food Science and Nutrition*, *62*(9), 2281-2308.
- Sadhasivam, S., Barda, O., Zakin, V., Reifen, R., & Sionov, E. (2021). Rapid detection and quantification of patulin and citrinin contamination in fruits. *Molecules*, *26*, 4545. <https://doi.org/10.3390/molecules26154545>
- Sadhasivam, S., Britzi, M., Zakin, V., Kostyukovsky, M., Trostanetsky, A., Quinn, E., & Sionov, E. (2017). Rapid detection and identification of mycotoxigenic fungi and mycotoxins in stored wheat grain. *Toxins*, *9*(10): 10. <https://doi.org/10.3390/toxins9100302>
- Sahu, P.K., Purohit, S., Tripathy, S., Mishra, D. P., & Acharya, B. (2023). Current Trends in HPLC for Quality Control of Spices. In O. Núñez, S. Sentellas, M. Granados, & J. Saurina (Eds.) High Performance Liquid Chromatography - Recent Advances and Applications. Intech open publication. DOI: 10.5772/intechopen.110897.
- Samyal, S., & Sumbali, G. (2020). Mycological Society of India, Toxicogenic mycoflora and natural co-occurrence of toxins in red chillies from Jammu and Kashmir. *Kavaka*, *54*, 89–95. doi:10.36460/Kavaka/54/2020/89-95,
- Samyal, S., & Sumbali, G. (2021). Natural incidence of Aspergilli, Penicilli, Fusaria and their multiple toxins in the seeds of dried red chillies (*Capsicum annum* Linn.) from Jammu and Kashmir (UT). *Indian Phytopathology*, *74*, 95–102. DOI: <https://doi.org/10.1007/s42360-020-00291-2>
- Schmidt-Heydt, M., Cramer, B., Graf, I., Lerch, S., Humpf, H. U., & Geisen, R. (2012). Wavelength-dependent degradation of ochratoxin and citrinin by light *in vitro* and *in vivo* and its implications on *Penicillium*. *Toxins*, *4*(12), 1535–1551.
- Setlem, S.K., & Ramlal, S. (2022). Isolation, extraction and identification of aflatoxin producing *Aspergillus* fungi by HPLC analysis and its sequencing. *Clinical Case Reports International*, *6*, 1393.
- Shekhar, M., Singh, N., Dutta, R., Kumar, S., & Mahajan, V. (2017). Comparative study of qualitative and quantitative methods to determine toxicity level of *Aspergillus flavus* isolates in maize. *PLoS ONE*, *12*(12), e0189760. <https://doi.org/10.1371/journal.pone.0189760>
- Singh, P., & Cotty, P.J. (2017). Characterization of *Aspergilli* from dried red chillies (*Capsicum* spp.): Insights into the etiology of aflatoxin contamination. *International Journal of Food Microbiology*, *289*, 145-153. <https://doi.org/10.1016/j.ijfoodmicro.2018.08.025>.
- Theumer, M.G., Henneb, Y., Khoury, L., Snini, S.P., Tadriss, S., et al. (2018). Genotoxicity of aflatoxins and their precursors in human cells. *Toxicology Letters*, *287*, 100- 107.
- Tola, M., & Kebede, B. (2016). Occurrence, importance and control of mycotoxins: A review. *Cogent Food & Agriculture*, *2*(1), 1191103.
- Tsehaynesh, T., Abdi, M., Hassen, S., & Taye, W. (2021). *Aspergillus* species and aflatoxin contamination in pepper (*Capsicum annum*l.) in West Gojjam, Ethiopia. *African Journal of Food, Agriculture, Nutrition and Development*, *21*(1), 17178-17194. DOI: <https://doi.org/10.18697/ajfand.96.18815>

- Wang, W., Chen, Q., Zhang, X., Zhang, H., Huang, Q., Li, D., & Yao, J. (2014). Comparison of extraction methods for analysis of citrinin in red fermented rice. *Food Chemistry*, *157*, 408–412. <https://doi.org/10.1016/j.foodchem.2014.02.060>.
- Wang, Y., Wang, B., Wang, P., Hua, Z., Zhang S., Wang, X., Yang, X., & Zhang, C. (2024). Review of neurotoxicity of T-2 toxin. *Mycotoxin Research*, *40*(1), 85-95. doi: 10.1007/s12550-024-00518-5.
- Watanabe, T. (2018). Pictorial Atlas of Soilborne Fungal Plant Pathogens and Diseases. CRC Press.
- Weidemann, D.K., Weaver, V.M., & Fadrowski, J.J. (2016). Toxic environmental exposures and kidney health in children. *Pediatric Nephrology*, *31*, 2043–2054.
- Wokorach, G., Landschoot, S., Anena, J., Audenaert, K., Echodu, R., & Haesaert, G. (2021). Mycotoxin profile of staple grains in northern Uganda: Understanding the level of human exposure and potential risks. *Food Control*, *122*, 107813.
- Yogendrarajah, P. (2015). Risk assessment of mycotoxins and predictive mycology in Sri Lankan spices: Chilli and Pepper. PhD dissertation, Faculty of Bioscience Engineering, Ghent University, Belgium.
- Younis, M. R., Wang, C., Younis, M.A., & Xia, X.H. (2020). Use of biosensors for mycotoxins analysis in food stuff. In A. Wu, & W. S. Khan (Eds.) *Nanobiosensors: From design to applications* (pp. 171-201). Wiley-VCH Verlag GmbH & Co. KGaA, Boschstr. 12, 69469 Weinheim, Germany. <https://doi.org/10.1002/9783527345137.ch8>.
- Zhang, X., Li, Y., Wang, H., Gu, X., Zheng, X., et al. (2016). Screening and identification of novel Ochratoxin A producing fungi from grapes. *Toxins*, *8*, 333.
- Zhao, Z., Yang, X., Zhao, X., Chen, L., Bai, B., Zhou, C., & Wang, J. (2018). Method development and validation for the analysis of emerging and traditional *fusarium* mycotoxins in pepper, potato, tomato, and cucumber by UPLC-MS/MS. *Food Analytical Methods*, *11*, 1780–1788.



Journal of Experimental Biology and Agricultural Sciences

<http://www.jebas.org>

ISSN No. 2320 – 8694

Effect of salinity stress on antioxidant activity and secondary metabolites of *Piper betle*

Abhaya Kumar Sahu¹ , Preeti Priyadarshini¹ , Bishakha Dash¹ , Beda Saurav Behera¹ ,
Sunil Kumar Gochhi² , Dipransu Pradhan² , Punam Kumari^{1,3*} 

¹P.G. Department of Biosciences and Biotechnology, Fakir Mohan University, Vyasa Vihar, Balasore-756089, Odisha, India

²P.G. Department of Environmental Science, Fakir Mohan University, Vyasa Vihar, Balasore-756089, Odisha, India

³Centre of Excellence (CoE) for Bioresource Management and Energy Conservation Material Development, Fakir Mohan University, Vyasa Vihar, Balasore-756089, Odisha, India

Received – August 06, 2024; Revision – November 04, 2024; Accepted – November 21, 2024

Available Online – November 29, 2024

DOI: [http://dx.doi.org/10.18006/2024.12\(5\).705.729](http://dx.doi.org/10.18006/2024.12(5).705.729)

KEYWORDS

Betel vine

Salinity stress

Antioxidant activity

GC-MS

Secondary metabolites

ABSTRACT

Salt stress is the most devastating abiotic stress that drastically limits the productivity and quality of crops. This study assessed the impact of NaCl concentrations (100, 200, and 400 mM) on betel vine's antioxidant activities and secondary metabolites (*Piper betle* L.). Results of the study suggest that the activity of antioxidative enzymes was enhanced at 100 and 200 mM NaCl levels but reduced at 400 mM NaCl. Further, the GC-MS analysis revealed the increased production of secondary metabolites such as alkane, ester, fatty acid, phenolic, and terpene compounds during salt stress. These findings would be helpful for further investigations that could lead to enhanced production of secondary metabolites in betel vine for industrial and medicinal benefits.

* Corresponding author

E-mail: punam.lifescience@gmail.com (Punam Kumari)

Peer review under responsibility of Journal of Experimental Biology and Agricultural Sciences.

Production and Hosting by Horizon Publisher India [HPI]
(<http://www.horizonpublisherindia.in/>).
All rights reserved.

All the articles published by [Journal of Experimental Biology and Agricultural Sciences](#) are licensed under a [Creative Commons Attribution-NonCommercial 4.0 International License](#) Based on a work at www.jebas.org.



1 Introduction

Salinity affects the plant's phenotype, physiology, and metabolism. It can restrict plant development by disturbing photosynthesis, photorespiration, respiration, nutrient homeostasis, and energy generation, resulting in an imbalance of redox homeostasis, osmotic stress, and ion toxicity (Zhou et al. 2024). Additionally, salinity stress produces oxidative damage via increasing reactive oxygen species (ROS) and ROS levels above a toxicity threshold, resulting in cell death. Plants employ numerous defence strategies against salt-induced oxidative stress at morphological, physiological, and metabolic levels. For this, plants generate a diverse range of enzymatic (CAT, APX, SOD, and GPX) and non-enzymatic antioxidants (GSH, ASC, and carotenoids) to scavenge ROS (Hatami and Ghorbanpour 2024). Further, plants can synthesize key classes of volatile fatty acid derivatives, benzenoids, phenolics, terpenes, and phenylpropanoids to eliminate ROS under salinity stress.

The betel vine is a major perennial medicinal herb that encircles famous flavourings and is edible worldwide. There are over 2000 species in the genus *Piper*, and 21 of these are evergreen vines that may be recognized in India (Sen and Rengaiyan 2021). Betel vine contains secondary metabolites such as phenolics, alkanes, esters, essential oils (EO), fatty acids, and amino acid derivatives, which are involved in various pharmacological activities. For instance, phenolic metabolites have anti-inflammatory, anti-thrombotic, antimicrobial, antioxidant, and cardioprotective properties (Kumar et al. 2024). The constituents of betel vine EO (4-allyl-1, 2-diacetoxybenzene, chavicol, acetyleugenol, eugenol, bicycle (4.1.0), hept-3-en-camphene, germacrene B, 4-methyl-decanal, cis-cimene, germacrene, and cyclohexene) also have anti-inflammatory, antimicrobial, and antioxidant properties capacities (Biswas et al. 2022).

The secondary metabolites, such as phenolics, alkanes, EOs, esters, terpenoids, and fatty acids, are produced in plants during exposure to heavy metals, salt stress, light intensity, and drought stress (Ait Elallem et al. 2024). Flavonoids, coumarins, phenolics, and lignins accumulate in plants during salt stress. The EO compounds (menthol, cineole, and neomenthol) also exhibit antioxidant activity in *Mentha piperita* under drought stress (Lala 2021). Bistgani et al. (2019) suggested that salinity stress enhanced the level of EO (such as oxygenated monoterpenes like α -thujone and 1,8-cineole), carotenoids and flavonoids, and volatile compounds like γ -cadinene and α -cadinol synthesis in marigold (*Calendula officinalis*).

Although the detrimental impacts of salinity on various phenotypical traits, physiological processes, and biochemical processes of betel plants have been well documented, the current investigation was carried out to evaluate the effect of salt stress on antioxidant activity and biosynthesis of secondary metabolites in betel vine.

2 Materials and Methods

2.1 Analysis of leaf disc senescence and chlorophyll content

Healthy betel vine leaves were chopped into small discs with a diameter of 1 cm and incubated in distilled water (DW) containing NaCl (200, 400, and 600 mM), CdCl₂ (10, 20, and 40 mM), and mannitol (200, 400, and 600 mM) for 3–4 days, respectively. Leaf discs were subjected to cold stress for 5 days at 4°C and heat stress for 10 h at 42°C. Leaf discs kept in DW were used as the control. After an extraction of 80% acetone, the chlorophyll concentration was measured by spectrophotometry. The equation below was used for calculating the amount of chlorophyll (Sahu et al. 2024a):

$$\text{Chl } a \text{ (mg ml}^{-1}\text{)} = -1.93A_{646} + 11.93A_{663}$$

$$\text{Chl } b \text{ (mg ml}^{-1}\text{)} = 20.36A_{646} - 5.50A_{663}$$

$$\text{Total Chl (mg ml}^{-1}\text{)} = 6.43A_{663} + 18.43A_{646}$$

2.2 Testing of betel vine plants under salt stress

The 4-week-old plants were grown under a 16/8 h light-dark period at 36±2°C and 28±2°C temperature and relative humidity of 45±5% and 63±5%, respectively. These plants were irrigated with 100, 200, and 400 mM NaCl solutions, and control plants were irrigated with Hoagland nutrient solution only. Three plants from each salt-treated and control line were taken for physio-biochemical analysis.

2.3 Histochemical detection and estimation of O₂⁻, H₂O₂, and cell death

Daudi and O'Brien (2012) used the protocol for the histochemical localization of H₂O₂ in leaf tissues. Healthy leaves from each experimental setup were dipped in a DAB solution (1mg ml⁻¹, pH=4.0) in a sterilized glass beaker for 12 h under light at room temperature (RT). To bleach the leaves, they were boiled for 20 min after being immersed in 95% ethanol. After cooling, the localized H₂O₂ was observed as brown spots under a light microscope.

The O₂⁻ content was also determined by following the protocol of Kumari et al. (2015), which involved immersing leaf tissues for 1 h in 3 ml of a 10 mM phosphate buffer (pH=7.8) containing 10 mM sodium azide and 0.05% nitroblue tetrazolium chloride (NBT). The tissue extracts were boiled for 15 min at 85°C, and the optical density (OD) was measured at 580 nm by spectrophotometry and expressed in $\mu\text{mol g}^{-1}\text{f.w.}$

The protocol of Noreen et al. (2009) was utilized to estimate the H₂O₂ content. Each sample's leaf tissues weighed 0.1 g, then separately ground with 2 ml of 0.1% trichloroacetic acid. The homogenates were centrifuged for 15 min at 12,000 rpm. After that,

the reaction mixture, which consisted of 1 ml of 1 M KI, 0.5 ml of 10 mM phosphate buffer (pH=7.0), and 0.5 ml of the supernatant, was made and measured at 390 nm by spectrophotometer. The H₂O₂ content was expressed in $\mu\text{mol g}^{-1}\text{f.w.}$

Trypan blue was used to localize the dead cells following the Kerschbaum et al. (2021) protocol. For 1 min at RT, the leaves were merged in 40 ml of 0.01 g of trypan blue. In order to see the polymerized blue color as dead cells, the leaves were washed using a washing solution [ethanol and water (1:1)]. Gölge and Vardar (2020) method was used for the estimation of cell death content. Sterilized test tubes with 10 ml of 0.25 % Evans blue were used to dip the leaf tissues. The aliquot was measured at 600 nm and expressed in $\mu\text{g ml}^{-1}$ using spectrophotometry.

2.4 Assay of enzymatic antioxidants

The SOD activity of each sample was determined utilizing the NBT protocol of Kumari et al. (2015). 2 ml of 50 mM phosphate buffer (containing 2% PVP and 1 mM EDTA, pH=7.0) was used to homogenize 0.5 g of leaf tissue. The homogenate was centrifuged for 20 min at 4°C and 13,000 rpm. Next, 50 μl of the extracted enzyme was poured into sterile test tubes together with 50 mM phosphate buffer (0.3 ml of 750 μM NBT, 0.3 ml of 130 mM methionine, 0.3 ml of 20 μM riboflavin, 0.3 ml of 10 mM EDTA, and 0.25 ml of DW). For 10 min, the test tubes were kept beneath a mercury lamp. Using spectrophotometry, the OD was measured at 560 nm. The number of enzymes necessary to block the photoreduction activity of the NBT by 50% was denoted by one unit (U) of SOD activity. The SOD activity was denoted as $\text{U g}^{-1}\text{f.w.}$ and estimated by the given formula:

$\% \text{ of inhibition} = [1 - \text{Absorbance of each sample} / \text{Absorbance of the control}] \times 100$

The CAT activity was determined by the method of Zhang et al. (2021). 0.5 g of leaf tissue was homogenized with 2 ml of 50 mM phosphate buffer (pH=7.0) (containing 1 mM EDTA and 2% PVP). The extracts were centrifuged at 13,000 rpm for 20 min at 4°C. For the experiment, 2.9 ml of 50 mM enzyme extract and 50 μl of 30 mM H₂O₂ were mixed to prepare a reaction mixture in a cuvette. The decreased OD was estimated at 240 nm for 3 min by spectrophotometry and expressed in $\text{U g}^{-1}\text{f.w.}$

The APX activity was estimated by the protocol of Sahu et al. (2024b). 1 ml of the reaction mixture [contained 600 μl of 50 mM phosphate buffer solution (pH=7.0), 100 μl of 1 mM EDTA, 100 μl of 5 mM ascorbic acid, 100 μl of H₂O₂, and 100 μl of the enzyme extracts] were taken in a cuvette. The decreased OD was recorded at 290 nm by spectrophotometry and expressed in $\text{U g}^{-1}\text{f.w.}$ The enzyme is required to decrease 1 μmol of H₂O₂ min^{-1} under the same condition determined to be 1U of APX activity.

The GPX activity was estimated using the Techer et al. (2015) method. 0.5 g of leaf tissues was homogenized with a 50 mM PBS buffer solution (pH=7.4) that contained 2% PVP and 1 μM EDTA. The homogenates were centrifuged at 13,000 rpm for 20 min at 4°C, and the reaction mixture (contained enzyme extract, 30 mM guaiacol, 40 mM H₂O₂, and 50 mM PBS buffer) was kept for 30 min. Then, the OD was taken at 470 nm by spectrophotometry, and the enzyme activity was expressed in $\text{U g}^{-1}\text{f.w.}$

2.5 Analysis of stomata

The leaf specimens were taken and processed for scanning electron microscopy (SEM) to measure the stomatal density and length of the aperture of the stomata. Leaf materials were chopped into 5-10 mm long sections, dehydrated in various amounts of ethanol (50, 70, 90, and 100%) for 30 min each, then air dried for 12 h at RT. Then the leaf sections were attached to aluminium stubs with electron-conductive carbon cement. The length of the stomatal aperture was determined by Image J software. The stomatal density (SD) was calculated by counting the number of stomas per unit of leaf surface area using the following formula (Paul et al. 2017):

$$\text{SD} = \text{Number of stomata} \times 1 \text{mm}^2 / \text{Area of the field of view} (\pi r^2)$$

Leaves were chopped into discs (1 cm) and kept in DW for 1 d. The discs were dried for 4 h at 70°C. For every experiment, 6 discs were selected. The relative water content (RWC) was also determined by the given formula (Tahjib-Ul-Arif et al. 2018):

$$\text{RWC} (\%) = (\text{fresh weight} - \text{dry weight}) / (\text{turgid weight} - \text{dry weight}) \times 100.$$

2.6 Identification of volatile compounds by GC-MS

The betel vine leaf extraction for GC-MS analysis was performed following the procedure of Annegowda et al. (2013). Leaf tissue (1.0 g) was homogenized with 1ml of methanol and ethyl acetate, and the homogenates were purified, evaporated at RT, and mixed again with methanol and ethyl acetate solutions. The samples were analyzed using Shimadzu GC-MS QP 2020 NX GC-MS instrument (operating conditions: SH-Rxi-5ms capillary standard non-polar column, 30 m length, ID: 0.25 mm, film thickness: 0.25 μm). Helium was used as a carrier gas, and the mobile phase flow rate was set (1.0 ml/min). The injected quantity was 1 μl , and the heat setting range (Oven temperature) in the gas chromatography section was 35°C to 280°C at 5°C/min. The mass spectrometer was in EI/PCI/NCI mode, with a mass range of 35–650 m/z and a scan speed of 20,000 amu/s. The detector MS collected the data from FASST, AART, COAST, and LRI. Compared to the NIST20 library reference compounds, the non-polar compounds were identified, which used SH-Rxi-5ms capillary as a standard non-polar column.

2.7 Statistical analysis

Every assay was run separately and three times independently. All the biochemical data were statistically assessed by ANOVA, followed by a post hoc test with significance at $p \leq 0.05$ (*). Data was given as mean \pm standard deviation (SD). The graph was performed using the GraphPad Prism software.

3 Results and Discussion

Development and productivity are highly affected by salinity stress. The novelty of this work is to provide new information on how salt stress modulates physiological and biochemical processes with secondary metabolite production.

3.1 Effects of abiotic stress on chlorophyll content

The abiotic stress tolerance of betel vine plants was assessed using the leaf disc senescence assay. The betel vine leaf discs were exposed to various abiotic stresses such as NaCl, mannitol, CdCl₂, and temperature (4°C and 42°C). The chlorophyll content of leaf discs from each stress was measured. Abiotic stress triggered oxidative stress, which resulted in a reduction in chlorophyll content.

One important physiological-chemical process extremely vulnerable to stress is photosynthesis, especially in salinity stress. Salt stress significantly lowers pigment concentration, stomatal conductance, and photosystem II activity. The photosynthetic mechanism uses both Chl *a* and *b* as main pigments, but their biosynthesis is inhibited under salt stress, chlorophyll breakdown increases, or both occur. The contents of Chl *a*, Chl *b*, and total chlorophyll varied during salt stress (Figure 1a). The 200 mM NaCl treatment decreased the photosynthetic pigments (Chl *a* by 49.09%, Chl *b* by 10.00%, and total chlorophyll by 48.27%), whereas 400 and 600 mM NaCl treatments showed relatively high reduction in photosynthetic pigments (Chl *a* by 79.09%, Chl *b* by 50.00%, and total chlorophyll by 69.82%) and (Chl *a* by 86.36%, Chl *b* by 83.33%, total chlorophyll by 87.06%), respectively, as compared to control. This is reliable, as previous findings show lower photosynthetic pigment levels in *Capsicum annum* (Kusvuran et al. 2024).

Similar types of results were found in other abiotic stresses. Figure 1b shows a high reduction in content of Chl *a* by 73.31 to 91.66%, Chl *b* by 20.0 to 90.0%, and total chlorophyll by 60.00 to 90.00% during 10 to 40 mM CdCl₂ stress. There was a nearly complete loss of chlorophyll under 40 mM CdCl₂ stress. Similarly, the Cd stress reduced chlorophyll pigments in *Triticum aestivum* (Farhat et al. 2022) due to reduced size and number of chloroplasts, chlorophyll disintegration, and impaired photosystems. Figure 1c also showed high reductions in the content of Chl *a* by 26.66% to 55.83%, Chl *b* by 10.0% to 60.0%, and total chlorophyll by 25.20% to 56.91% after exposure to 200 to 600 mM mannitol stress as compared to control. In general, mannitol-induced

drought stress also reduces the chlorophyll content due to inhibition of photosynthetic enzymes, disruption of the thylakoid membrane, and inhibition of PS-I and PS-II in *Apocynum pictum* and *A. venetum* (Yang et al. 2021). Furthermore, exposure to cold (4°C) and heat (42°C) stress significantly reduced chlorophylls in the leaves of betel vine (Chl *a* by 73.77%, Chl *b* by 60.00%, and total chlorophyll by 68.55%) and (Chl *a* by 86.88%, Chl *b* by 75.07%, and total chlorophyll by 88.24%), respectively, as compared to control (Figure 1d, e). In the current findings, a negative relationship has been found between chlorophyll content and abiotic stress; this suggests that the abiotic stress causes the breakdown of photosynthetic pigments in betel vine. Similar reports have been found in tomato (Mesa et al. 2022) as well as in rice (Li et al. 2024) plants due to disruption of photosynthetic components, carbon reduction cycles, and impaired chlorophyll molecules under both cold and heat stress (Chaudhry and Sidhu 2022). It is concluded that reductions in chlorophyll content lead to a decline in plant development and the creation of dry materials.

3.2 Effect of salt stress on ROS scavenging enzymes and stomata

Plants hold different antioxidant molecules to endure both biotic and abiotic stresses. The salt stress interferes with the homeostasis between ROS scavenging and formation, leading to oxidative bursts in cellular organelles, including chloroplasts, mitochondria, and peroxisomes. ROS occurs in various biological signaling pathways at low or high levels in the cells.

The performance of plants under prolonged exposure to salt stress was also tested. The salt-treated plants showed curling and yellowing leaves, wilting, and dropping characteristics compared to control plants (Figure 2a). The salinity caused a significant formation of reddish-brown spots (an indicator of H₂O₂) in leaves (Figure 2b), which was followed by an increase in H₂O₂ content in the leaves; equivalent outcomes in rice have been found (Mostofa et al. 2015). Moreover, the salt-treated leaves exhibited more accumulation of blue-colored spots (an indicator of cell death) than the control (Figure 2c), which was also significant with the increment in cell death content. A rise in H₂O₂ content (27.72, 45.54, and 60.41 μ mol) and O₂⁻ content (23.80, 36.02, and 44.96 μ mol) in betel vine leaves exposed to 100 mM, 200 mM, and 400 mM NaCl stress, respectively than the control (Figure 2d, e). H₂O₂ and O₂⁻ are the prime signaling molecules, taking crucial functions in various metabolic pathways during salt stress; they induce stress-responsive pathways. In extreme conditions, salt stress leads to the overproduction of ROS because the mitochondria's and chloroplasts' electron transport chains (ETCs) are damaged (Hameed et al. 2021). The findings of the betel vine were consistent with rice and *Hibiscus cannabinus* (Hatami and Ghorbanpour 2024). The betel vine leaves exhibited cell death 0.55, 1.09, and 1.76 μ g in 100 mM, 200 mM, and 400 mM NaCl-induced salt stress compared to the control (Figure 2f).

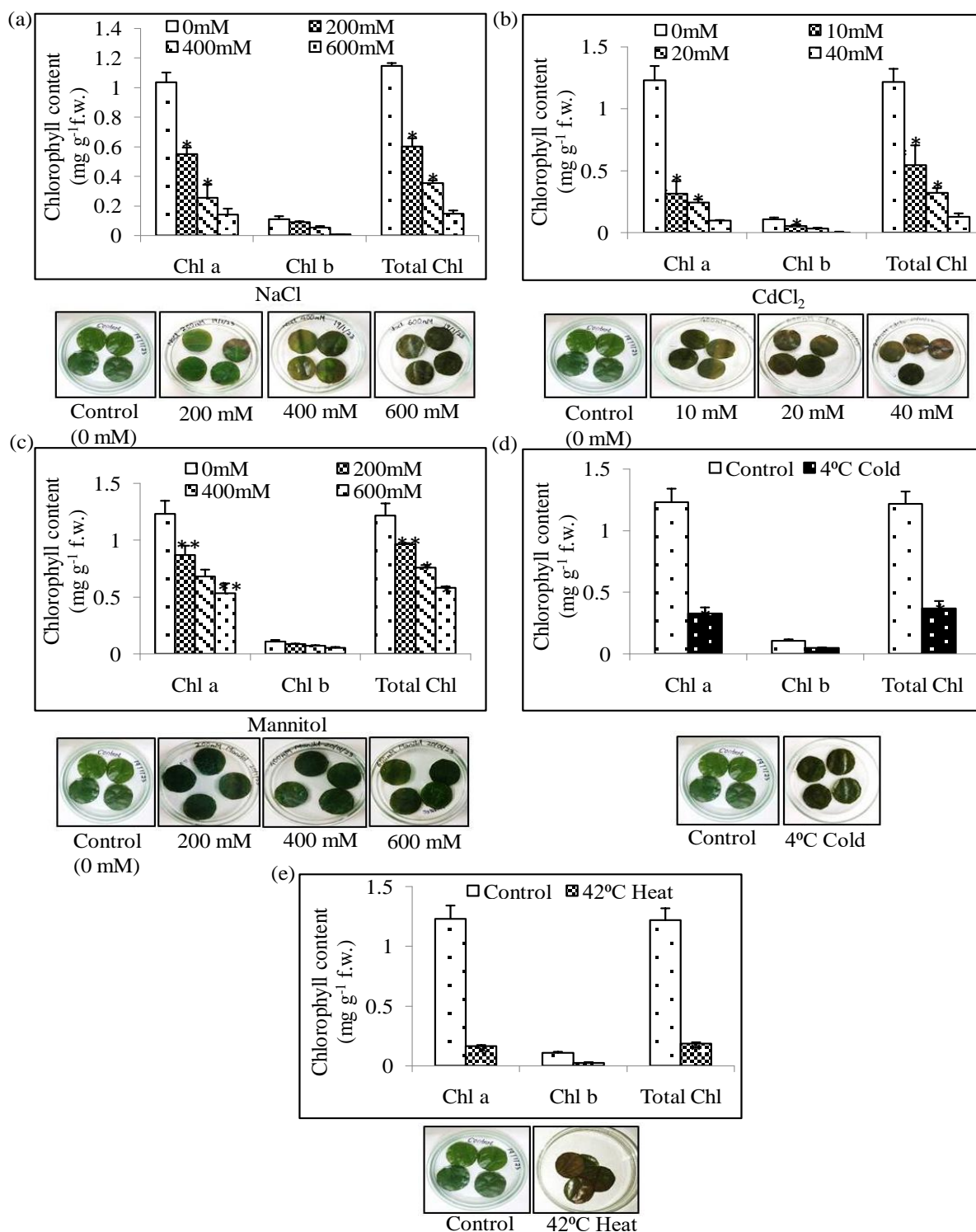


Figure 1 Assessment of betel vine plants for their tolerance towards various abiotic stresses. Leaf disc senescence assays for abiotic stress tolerance in betel vine plants. Leaf discs kept in Hoagland solution served as the experimental control. The chlorophyll content ($\text{mg g}^{-1}\text{f.w.}$) retained in corresponding leaf discs shown by histograms, (a) NaCl, (b) CdCl_2 (c) Mannitol, (d) 4°C Cold, and (e) 42°C Heat. The data represents mean \pm SD of three biological replicates. *, ** denote significance at $p \leq 0.05$ and $p \leq 0.001$, respectively.

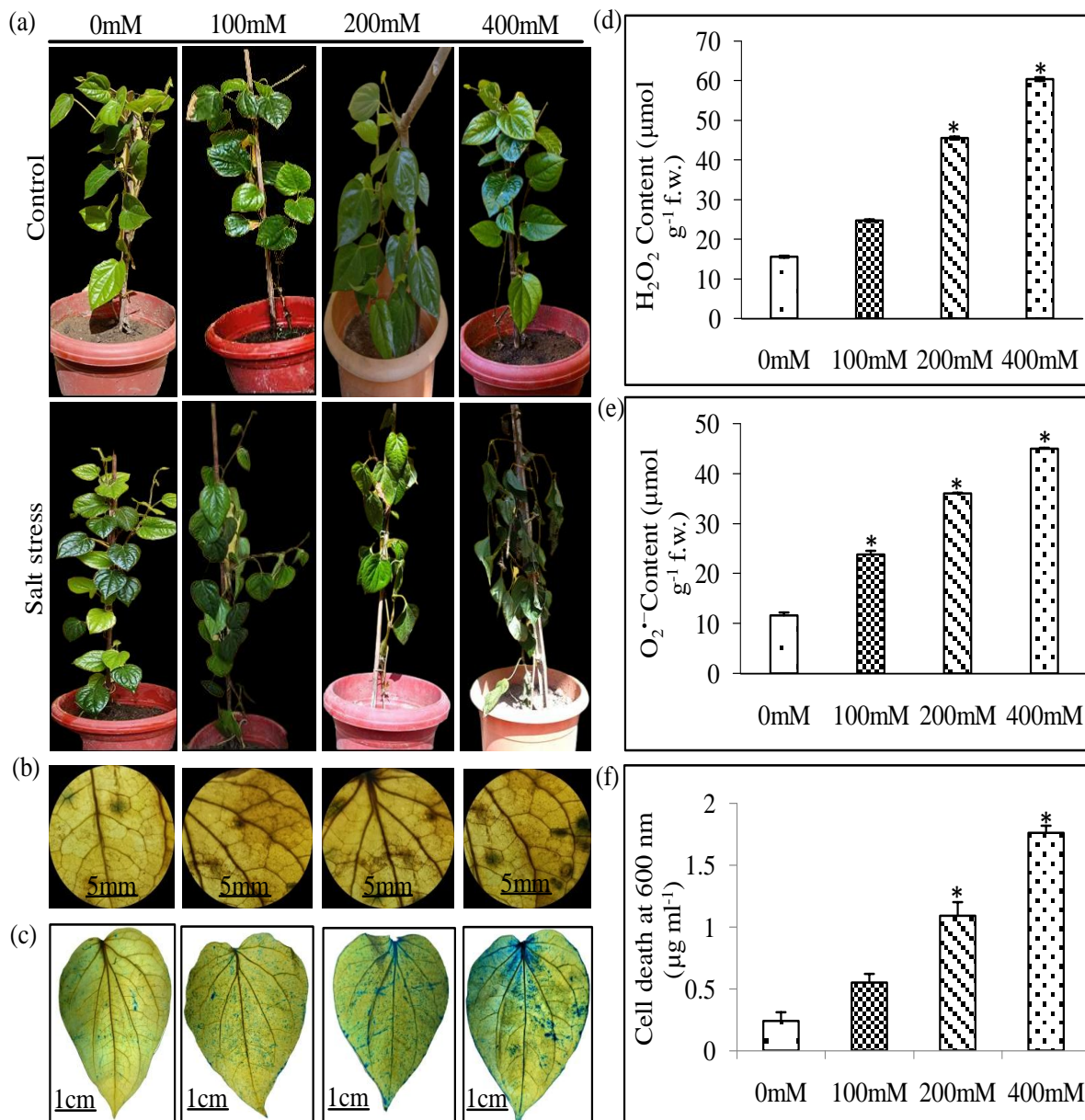


Figure 2 Effect of exposure of betel vine plants to salinity stress, (a) *Control panel* shows the phenotype of betel vine plants under non-stress condition. *Salt stress panel* shows the phenotypes of betel vine plants under salinity stress, (b) Histochemical localization of H₂O₂, (c) Histochemical localization of dead cells, (d) O₂⁻ content, (e) H₂O₂ content, (f) Cell death content. The data represents mean ± SD of three biological replicates. *denote significance at p ≤ 0.05, respectively.

To inhibit the generation of ROS, plants have a complex network that is systematically organized and comprises signalling components. Plants have dynamic enzymatic antioxidant machinery required to reduce ROS under stress. SOD is one of those enzymatic antioxidants that catalyses the transformation of O₂⁻ into H₂O₂. Then, H₂O₂ is detoxified by CAT, APX, and GPX. All of these enzymes' activities, i.e., SOD, CAT, APX, and GPX,

were increased by 7.49 to 16.39, 7.25 to 17.64, 0.08 to 0.15, and 1.8 to 2.68 U, respectively, in 0 mM to 200 mM of NaCl (Figure 3a, b, c, and d). These reports are concomitant with earlier reports that showed increased SOD in wheat seedlings (Esfandiari et al. 2007), *Solanum melongena* (Shumaila Ullah and Nafees 2023), CAT activity in *Cymbopogon nardus*, *Cynodon dactylon*, and *Pennisetum alopecuroides* (Mane et al. 2010), APX in sweet

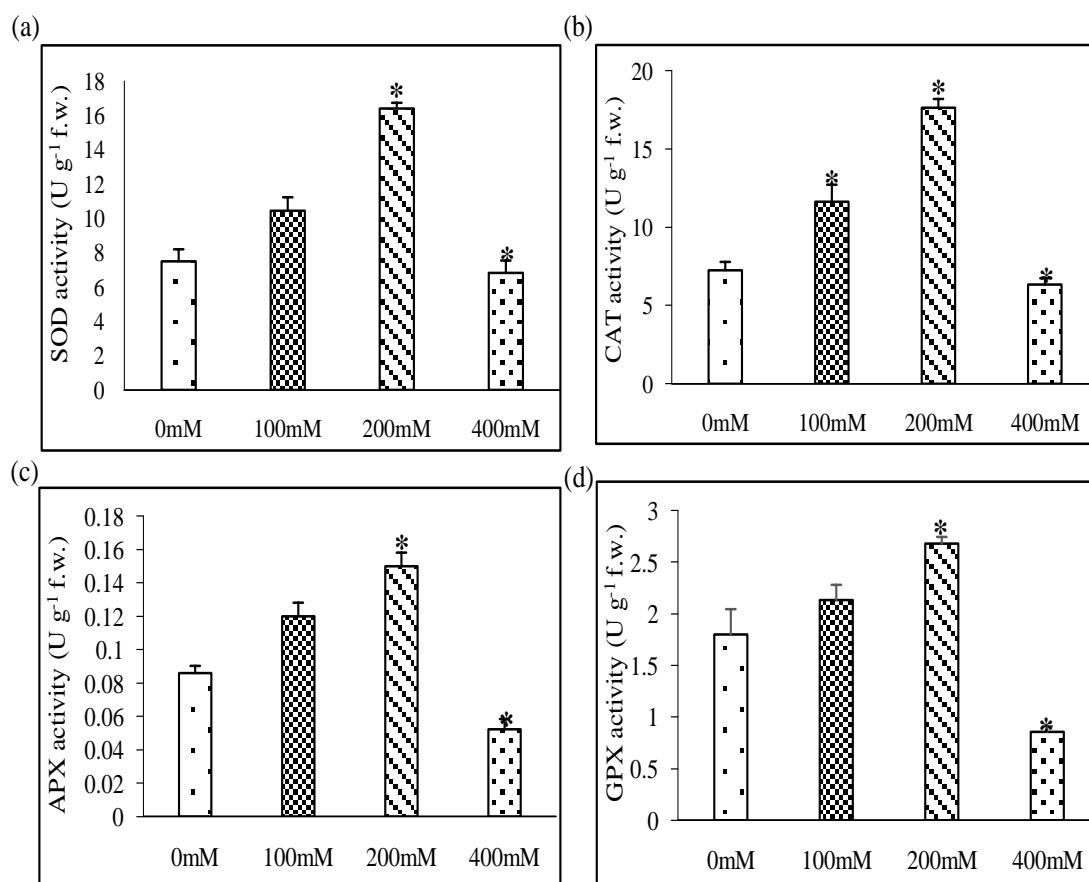


Figure 3 Antioxidant enzymes in the leaf of betel vine plant, (a) SOD activity, (b) CAT activity, (c) APX activity, and (d) GPX activity. The data represents mean \pm SD of three biological replicates. *denote significance at $p \leq 0.05$, respectively.

potato cultivars (Lin and Pu 2010), and GPX in foxtail millet under salt stress (Rathinapriya et al. 2020). The increased antioxidant enzymes might detoxify or prevent the detrimental effect of ROS in betel vine leaves under 100 and 200 mM NaCl. Moreover, these enzymes are prone to high oxidative stress, which affects their structural integrity and functions at the cellular level. In the current investigation, the betel vine leaves subjected to 400 mM NaCl stress showed decreased antioxidant enzyme activity. The *Sesuvium portulacastrum* (Kannan et al. 2013) and Tabarka variety *Cakile maritima* (Amor et al. 2006) showed decreased antioxidant enzyme activities. These findings suggest that under 100 and 200 mM NaCl stress, the betel vine plant preserved redox equilibrium by inhibiting enzyme denaturation and triggering the antioxidant machinery, but above that threshold, an imbalance occurred between the ROS-generating and scavenging systems.

The stomata are the primary structure in charge of gas and water exchange; variations in stomatal density and size can help control water consumption efficiency. Salt stress reduces leaf size, cell expansion, and transpiration flux in plants. The micrographs

revealed that stomatal density and the length of the stomatal aperture were drastically reduced with increasing salt concentrations (Figure 4a). The number of stomata was highly reduced in 400 mM NaCl-treated leaves. The stomatal numbers also decrease in *Populus alba* (Hasanuzzaman et al. 2009). The stomatal density was reduced by 32.3, 25, and 13.66 numbers in 100 mM, 200 mM, and 400 mM NaCl-treated betel vine leaves as compared to control, respectively (Figure 4b) and also in *Ocimum basilicum* plants (Barbieri et al. 2012). Moreover, a reduced length of stomatal aperture was also observed at 24.16, 21.66, and 13.38 μ m in betel vine leaves in comparison to the control condition when exposed to 100 mM, 200 mM, and 400 mM NaCl salt stress, respectively (Figure 4c). It occurs due to disruption in starch-sugar conversion, and lower water content reduces turgor pressure in leaf tissues. Under salt stress conditions, abscisic acid (ABA) also induces stomatal closure and a reduced transpiration rate to prevent excessive water loss. Some amorphous substances were found in the salt-treated leaves compared to the control and were also reported as salt particles in *Allium cepa* during salt stress (Burkhardt 2010). In addition, the perturbation of stomatal opening

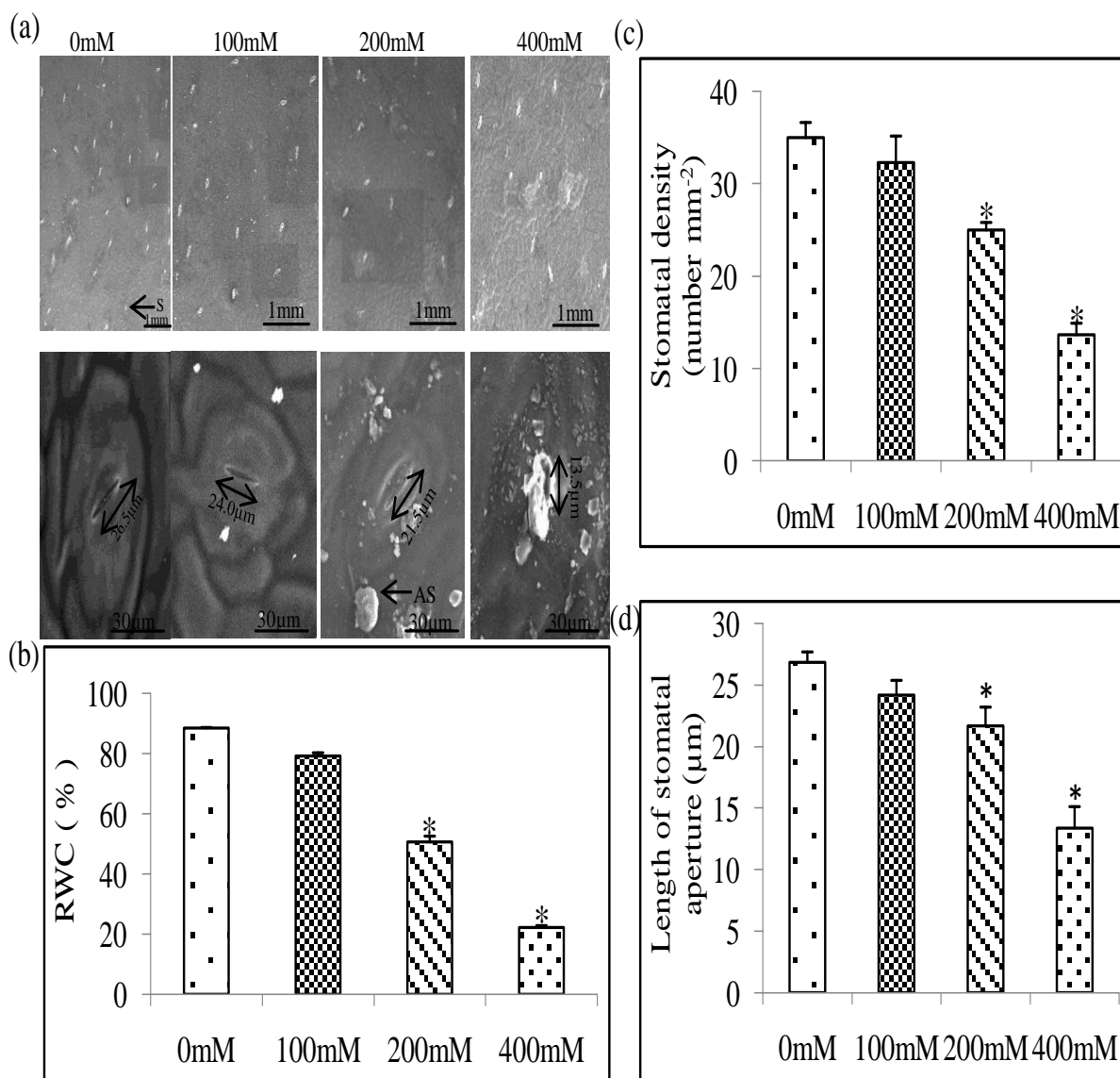


Figure 4 Effect of salt stress on stomatal anatomy, (a) Stomatal density and aperture in SEM analysis, (b) RWC, (c) Stomatal density, and (d) Length of stomatal aperture. The data represents mean \pm SD of three biological replicates.

*denote significance at $p \leq 0.05$, respectively. S-Stomata, AS-Amorphous Substances.

causes a decrease in the absorption of CO₂ and photosynthesis, ultimately altering the synthesis of metabolites. High salt concentrations cause cellular dehydration and lead to osmotic stress, which reduces RWC in plant leaves. RWC is a crucial plant water status marker because it distinguishes between transpiration and water supply in leaf tissues. The RWC content was reduced in 100 mM, 200 mM, and 400 mM NaCl-treated plants by 79.18, 50.63, and 22.2%, respectively, compared to control plants (Figure 4d). Therefore, the uptake of water and stomatal movement is perturbed, which causes deterioration of the plant's development and yield under saline conditions.

3.3 Salinity stress effect on biosynthesis of bioactive compounds

A total of seventy-five significant compounds of methanol and ethylacetate extracts, representing five classes like alkane, fatty acid, ester, phenolic, and terpene, were identified by GC-MS analysis. Figures 5 and 6 revealed the retention time of compounds of methanol and ethyl acetate extracts of betel vine, which are also mentioned in Tables 1 and 2. The findings of this study were in close agreement with the other reports of Madhumita et al. (2020). The GC-MS analysis identified methanolic compounds like eugenol

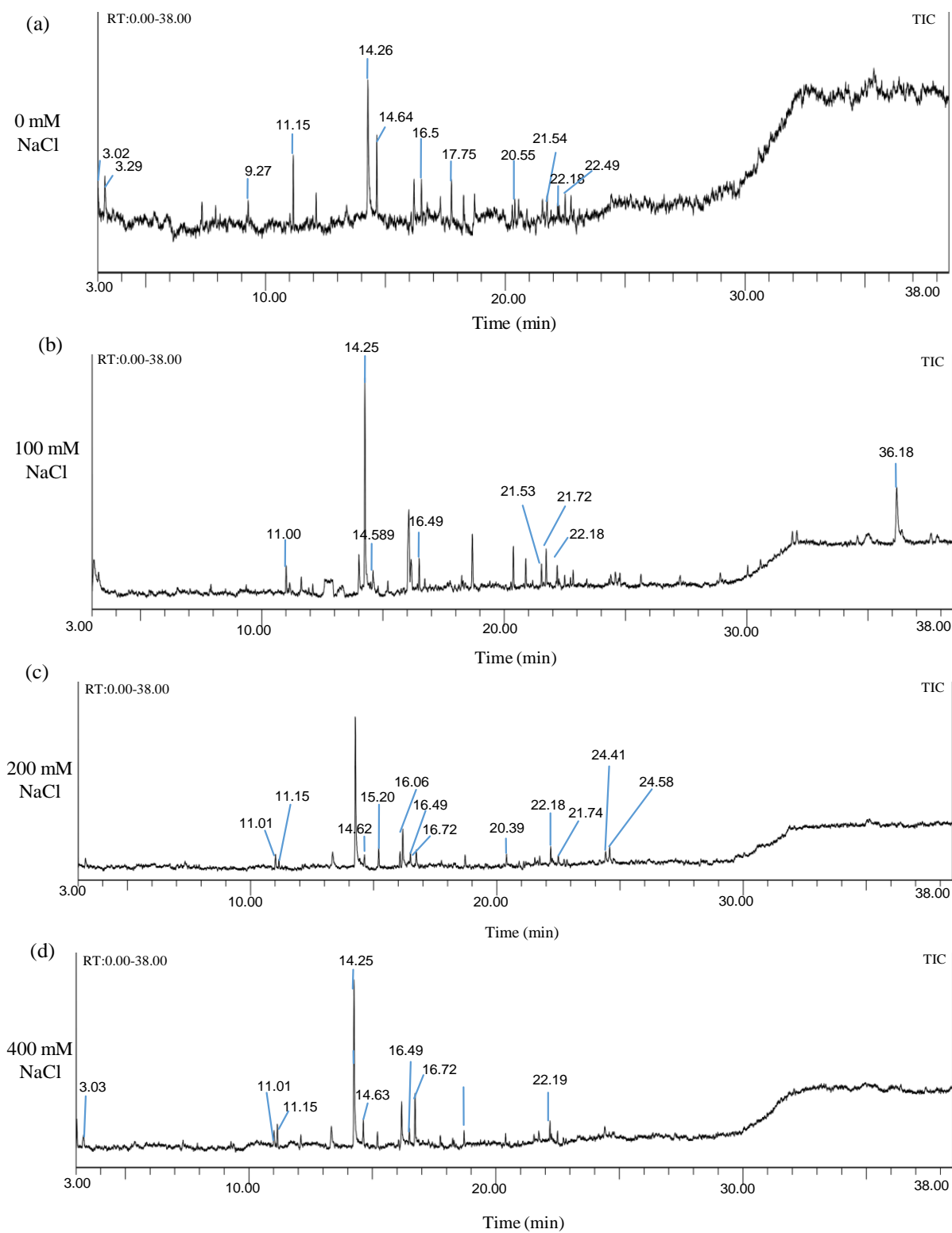


Figure 5 Chromatograph showing the retention time of volatile compounds of methanol extracts of betel vine leaves, (a) Control, (b) 100 mM NaCl, (c) 200 mM NaCl, and (d) 400 mM NaCl.

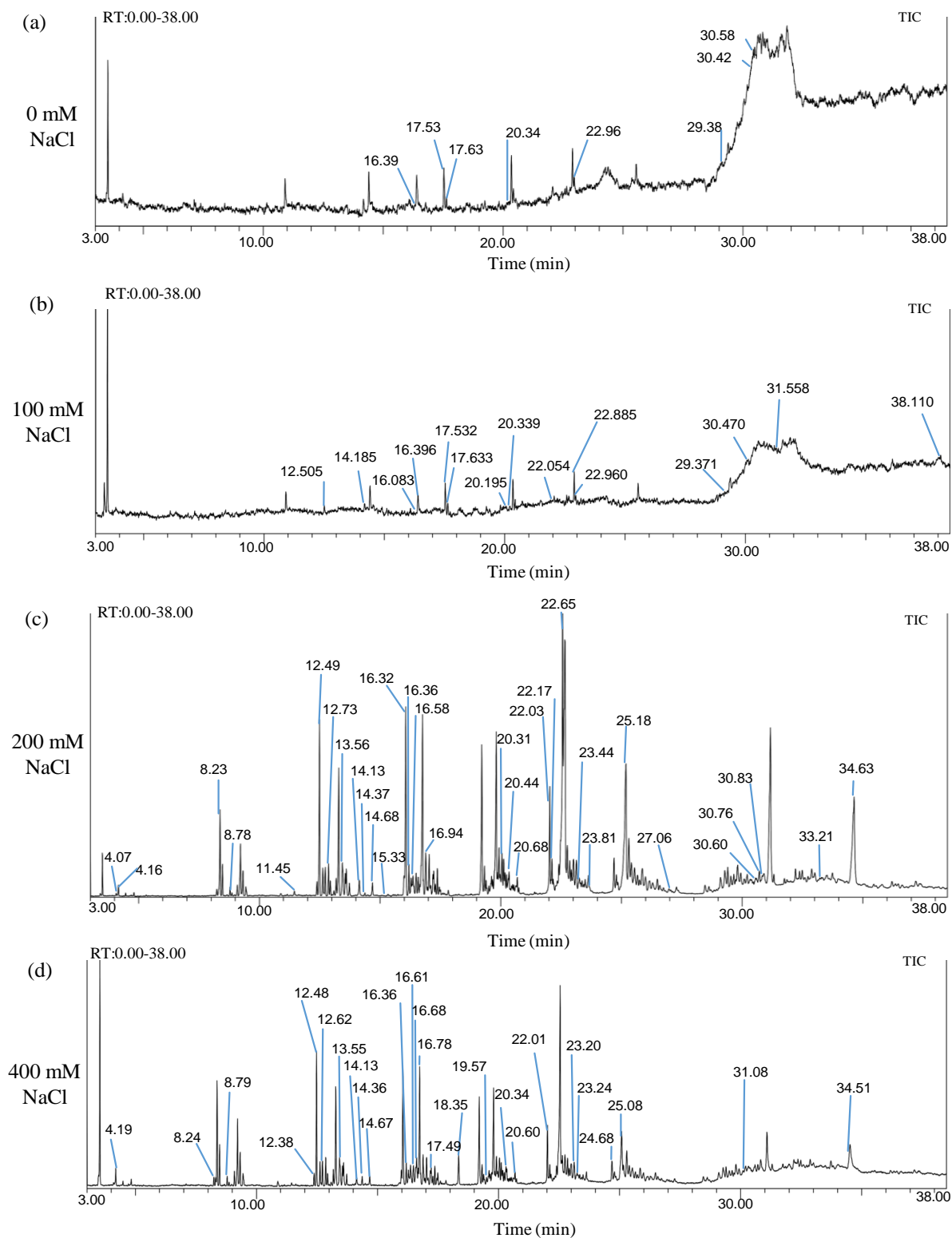


Figure 6 Chromatograph showing the retention time of volatile compounds of ethyl acetate extracts of betel vine leaves, (a) Control, (b) 100 mM NaCl, (c) 200 mM NaCl, and (d) 400 mM NaCl.

Table 1 Retention time of major volatile compounds in methanol extracts of betel vine leaves under salt stress.

Sl. No.	Components	Retention Time (min.)			
		NaCl concentrations (mM)			
		Control	100	200	400
1	Eugenol	14.26	14.25	-	-
2	2,2-Dimethoxybutane	3.29	-	-	-
3	Hexadecane	17.75	-	14.62	-
4	2,4-Di-tert-butylphenol	16.5	16.49	16.49	16.49
5	1,2-Benzenedicarboxylic acid	21.54	21.53	-	-
6	Hexadecanoic acid	22.18	22.18	22.18	22.19
7	Undecane	9.27	-	-	-
8	Glycerin	3.02	-	-	3.03
9	Dodecane	11.15	-	11.15	11.15
10	Tetradecane	14.6	-	-	14.63
11	Octadecane	20.55	-	-	-
12	Benzenepropanoic acid, 3,5-bis(1,1-dimethylethyl	22.49	-	-	-
13	13-Docosamide, (Z)-	-	36.18	-	-
14	2,4,6-Tris(trimethylsilyl)cyclohexane-1,3,5-trione	-	21.72	21.74	-
15	Naphthalene	-	11	11.01	11.01
16	Phytol	-	-	24.58	-
17	9,12,15-Octadecatrienoic acid, methyl ester	-	-	24.41	-
18	3,5-Diisopropoxy-1,1,1,7,7,7-hexamethyl-3,5	-	14.58	-	-
19	3-Allyl-6-methoxyphenol	-	-	-	14.25
20	Caryophyllene	-	-	15.2	-
21	3-Allyl-6-methoxyphenyl acetate	-	-	16.72	16.72
22	Gamma.-Muurolene	-	-	16.06	-
23	Phthalic acid, 3,5-dimethylphenyl 4-isopropyl	-	-	20.39	-

Table 2 Retention time of major volatile compounds in ethyl acetate extracts of betel vine leaves under salt stress.

Sl. No.	Components	Retention Time (min.)			
		NaCl concentrations (mM)			
		Control	100	200	400
1	1,2,3,4-Tetrahydronaphthalen-1-yl 2,2,3,3,3-pentafluoropropanoate	-	-	30.6	-
2	11-Methylnonacosane	-	20.19	-	-
3	11-Methyltricosane	-	-	23.81	23.2
4	1-Dodecanol, 3,7,11-trimethyl-	-	-	8.78	-
5	1-Hexacosene	-	29.37	-	-
6	1-Hexadecanol	-	-	-	17.49

Sl. No.	Components	Retention Time (min.)			
		NaCl concentrations (mM)			
		Control	100	200	400
7	1-Pentadecene	-	-	14.37	14.36
8	1-Tetracosene	-	22.88	-	-
9	2,4-Di-tert-butylphenol	-	16.39	16.36	16.36
10	2-Ethylbutyric acid, eicosyl ester	-	-	30.83	-
11	2-Undecanethiol, 2-methyl-	-	-	-	8.79
12	3,4-Dihydroxymandelic acid, 4TMS derivative	30.58	-	-	-
13	3-Allyl-6-methoxyphenol	-	-	14.13	14.13
14	3-Allyl-6-methoxyphenyl acetate	-	-	-	16.61
15	3-Ethyl-2,6,10-trimethylundecane	-	-	-	23.24
16	4-Allyl-1,2-diacetoxybenzene	-	-	-	18.35
17	5,5-Diethylpentadecane	-	-	30.76	-
18	5,5-Diethyltridecane	-	22.05	16.96	16.78
19	Benzaldehyde, 2,4-dimethyl-	-	-	11.45	-
20	Bis[di(trimethylsiloxy)phenylsiloxy]trimethylsiloxyphenylsioxane	-	38.11	-	-
21	Carbonic acid, eicosyl vinyl ester	-	-	15.33	-
22	Cyclononasiloxane, octadecamethyl-	30.42	31.55	-	-
23	Decane, 1-iodo-	-	-	27.06	20.6
24	Decane, 2,3,5,8-tetramethyl-	-	16.08	-	-
25	Dodecanal	-	-	14.68	14.67
26	Dodecane, 2,6,10-trimethyl-	-	12.5	-	-
27	Dodecane, 2,6,11-trimethyl-	-	-	12.49	12.62
28	Dodecane, 4-methyl-	-	-	13.56	13.55
29	Dotriacontane	-	-	22.03	22.01
30	E-14-Hexadecenal	17.53	17.53	-	-
31	E-15-Heptadecenal	20.34	20.33	20.31	-
32	Heneicosane	22.96	22.96	16.32	19.96
33	Heptadecane	-	-	16.58	12.38
34	Heptadecane, 2-methyl-	-	-	-	16.68
35	Heptane, 2,4-dimethyl-	-	-	4.16	4.19
36	Hexacontane	-	-	33.21	-
37	Hexacosylnonyl ether	-	-	23.44	-
38	Hexadecane	17.63	17.63	12.73	12.48
39	Hexadecane, 2,6,10,14-tetramethyl-	-	-	-	20.34
40	Hexadecane, 2-methyl-	-	-	-	19.57
41	Hexadecanoic acid, 2-hydroxy-1 (hydroxymethyl) ethyl	-	-	-	31.08

Sl. No.	Components	Retention Time (min.)			
		NaCl concentrations (mM)			
		Control	100	200	400
42	Hexane, 2,3,5-trimethyl-	-	-	4.07	-
43	1-(+)-Ascorbic acid 2,6-dihexadecanoate	-	-	22.65	-
44	Nonane, 5-butyl-	-	-	8.23	8.24
45	Octadecane, 1-iodo-	20.42	-	20.68	-
46	Octadecanoic acid	-	-	25.18	25.08
47	Octadecanoic acid, 2,3-dihydroxypropyl ester	-	-	34.63	34.51
48	Octadecyloctyl ether	-	-	20.44	-
49	Phenol, 2-methoxy-4-(2-propenyl)-, acetate	-	14.18	-	-
50	Phenol, 3,5-bis(1,1-dimethylethyl)-	16.39	-	-	-
51	Tetracosamethyl-cyclododecasiloxane	-	30.47	-	-
52	Tetrapentacontane	-	-	22.17	24.68

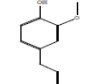
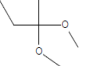

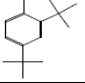
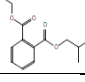


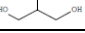
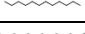
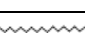
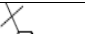
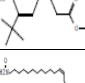

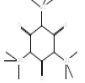
(20.85%), 2,2-Dimethoxybutane (5.51%), hexadecane (4.82%), 2,4-Di-tert-butylphenol (2,4-DTBP) (3.92%), 1,2-Benzenedicarboxylic acid (3.12%), hexadecanoic acid (1.63%), undecane (2.72%), dodecane (6.86%), tetradecane (7.87%), octadecane (1.77%), and benzenepropanoic acid, 3,5-bis(1,1-dimethylethyl)(2.57%) in control condition (Sulistiyorini 2020) (Table 3).

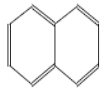


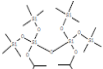
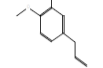
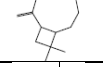
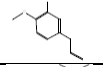
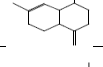
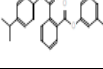
When exposed to salt stress, these compounds' proportional area (%) varied drastically. The different concentrations of salt treatment induced various types of metabolites such as phenolic (eugenol, 2,4-DTBP, 2,4,6-tris (trimethylsilyl) cyclohexane-1,3,5-trione, 3-Allyl-6-methoxyphenol, 3-Allyl-6-methoxyphenyl acetate), terpenes (naphthalene, phytol, caryophyllene), alkane (hexadecane, dodecane, tetradecane), and ester (1,2-Benzenedicarboxylic acid, 9,12,15-Octadecatrienoic acid, methyl ester, phthalic acid, 3,5-dimethylphenyl 4-isopropyl, hexadecanoic acid) (Table 3). Similarly, the salt stress also induces the formation of metabolites such as phenolics, carotenoids, 2,2'-azino-bis (3-ethylbenzothiazoline-6-sulfonic acid), flavonoids, anthocyanins, 2,2-diphenyl-1-picrylhydrazyl, as well as vitamin C in wheat microgreen extract under organic cultivation conditions (Islam et al. 2019). Moreover, salinity causes the modification of secondary metabolites in various plant species like *Coriander sativum*, peppermint, and *Origanum majoram* (Mahalakshmi et al. 2013). The 100 mM NaCl stimulated the eugenol compound by 15.97% compared to the control, but it was reduced under 200 and 400 mM NaCl stress. Eugenol is identified in betel vine at 0.32% concentration and is an antioxidant with anticancer, antibacterial, anti-inflammatory, analgesic, and neuroprotective properties (Chaudhary et al. 2023). The 2, 4-DTBP was reduced by 9.43 to 34.94% in 100 mM to 400 mM NaCl-treated plants compared to

control plants. In addition, 2,4-DTBP is also found in endophytic *Streptomyces* KCA-1, which promotes antioxidant activity at plant roots (Ayswarya et al. 2022). Another phenolic compound, like 3-Allyl-6-methoxyphenol synthesis, was higher in 200 and 400 mM NaCl and emerged as an abundant compound. The 3-Allyl-6-methoxyphenol showed antioxidant activity in the EO of *Cinnamomum verum* and antibacterial activity against two *Escherichia coli* strains (Al Ahadeb 2022). The 400 mM NaCl-treated plants also induced a phenolic compound such as 3-Allyl-6-methoxyphenyl acetate by 164.38% compared to 200 mM NaCl-treated plants. In addition, the naphthalene compound (as 4.05 and 3.17%) was obtained from plants exposed to 200 and 400 mM NaCl, which functioned as cytotoxicity and anti-tubulin activity in betel vine plants leading to senescence, along with biosurfactant and anti-inflammatory activity (Mohapatra and Phale, 2021). Caryophyllene (CP) is a natural sesquiterpene observed by 4.56% in 200 mM NaCl-treated plants, possessing numerous pharmaceutical activities such as antimicrobial, anticarcinogenic, anxiolytic, anti-inflammatory, antioxidant, and local anesthetic effects (Sharma et al. 2016).

Further, alkane compounds like hexadecane, a straight-chain 16-C compound, were reduced by 28.83% compared to the control in plants exposed to 200 mM NaCl. It is also a component of the EO of long pepper. This non-polar plant metabolite acts as a pheromone of the moth (*Acrolepiopsis assectella*) (Morris et al. 2005) and has antibacterial and antioxidant activities (Yogeswari et al. 2012). In addition, dodecane is a 12-C compound and shows a 71.72 and 32.65% reduction in plants exposed with 200 and 400 mM NaCl compared to the control. It is also isolated from *Zingiber officinale*, acts as a pheromone of *Glossina morsitans*, and attracts gravid females to its larvae (Adden et al. 2023).

Table 3 GC/MS analysis of volatile compounds in methanol extracts of betel vine leaves under salt stress.

Sl. No.	Compounds	KRI literature (Column)	Molecular formula	Structure of compounds	Types of compounds	Area (%)			
						Control	NaCl concentrations (mM)		
						100	200	400	
1.	Eugenol	1356 (DB-5)	C ₁₀ H ₁₂ O ₂		Phenolic	20.85±0.50	24.18±0.28*	Nd	Nd
2.	2,2-Dimethoxybutane	685	C ₆ H ₁₄ O ₂		Ether	5.51±0.34	Nd	Nd	Nd
3.	Hexadecane	1600(DB-5)	C ₁₆ H ₃₄		Alkane	4.82±0.15	Nd	3.43±0.16*	Nd
4.	2,4-Di-tert-butylphenol	1502(CP-Sil-5CB)	C ₁₄ H ₂₂ O		Phenolic	3.92±0.06	3.55±0.25*	2.19±0.22*	2.55±0.28*
5.	1,2-Benzenedicarboxylic acid	1917 (HP-Ultra-2)	C ₂₄ H ₃₈ O ₄		Ester	3.12±0.10	Nd	Nd	Nd
6.	Hexadecanoic acid	1984 (DB-5)	C ₇ H ₄ O ₂		Ester	1.63±0.11	Nd	3.48±0.13*	4.26±0.33*
7.	Undecane	1099 (DB-5)	C ₁₁ H ₂₄		Terpene	2.72±0.23	Nd	Nd	Nd
8.	Glycerin	940 (9DB-1)	C ₃ H ₈ O ₃		Triol	2.14±0.31	Nd	Nd	5.32±0.21*
9.	Dodecane	1199(DB-5)	C ₁₂ H ₂₆		Alkane	6.86±0.15	Nd	1.94±0.15*	4.62±0.16*
10.	Tetradecane	1399(DB-5)	C ₁₄ H ₃₀		Alkane	7.87±0.13	Nd	Nd	4.74±0.15*
11.	Octadecane	1800 (DB-500)	C ₁₈ H ₃₈		Alkene	1.77±0.18	Nd	Nd	Nd
12.	Benzenepropanoic acid, 3,5-bis(1,1-dimethylethyl)	3823	C ₁₈ H ₂₈ O		Ester	2.57±0.11	Nd	Nd	Nd
13.	13-Docosamide, (Z)-	2625 (HP-5MS)	C ₂₂ H ₄₃ NO		Fatty acid	Nd	12.48±0.37*	Nd	Nd
14.	2,4,6-Tris(trimethylsilyl)cyclohexane-1,3,5-trione	1904	C ₆ N ₆ O ₃		Phenolic	Nd	4.24±0.19*	1.21±0.09*	Nd

Sl. No.	Compounds	KRI literature (Column)	Molecular formula	Structure of compounds	Types of compounds	Area (%)				
						Control	NaCl concentrations (mM)			
							100	200	400	
15.	Naphthalene	266 (SE-52)	C ₁₀ H ₈		Terpene	Nd	2.71±0.18*	4.05±0.04*	3.17±0.16*	
16.	Phytol	1949 (DB-5)	C ₂₀ H ₄₀ O		Terpene	Nd	Nd	2.87±0.24	Nd	
17.	9,12,15-Octadecatrienoic acid, methyl ester	2058 (capillary)	C ₁₉ H ₃₂ O ₂		Ester	Nd	Nd	3.62±0.18	Nd	
18.	3,5-Diisopropoxy-1,1,1,7,7,7-hexamethyl-3,5	1648	C ₁₈ H ₅₀ O ₇ Si ₆		Hexamethylated cycloheptatriene	Nd	1.51±0.39*	Nd	Nd	
19.	3-Allyl-6-methoxyphenol	1322 (DB-5MS)	C ₁₀ H ₁₂ O		Phenolic	Nd	Nd	48.8±0.58*	51.36±0.80*	
20.	Caryophyllene	1428 (DB-5)	C ₁₅ H		EO	Nd	Nd	4.56±0.07*		
21.	3-Allyl-6-methoxyphenyl acetate	1513 (DB-5MS)	C ₁₂ H ₁₄ O ₃		Phenolic	Nd	Nd	4.24±0.07*	11.21±0.21*	
22.	Gamma.-Muurolene	1477(DB-5)	C ₁₅ H ₂₄		Elaidolinolenic acid	Nd	Nd	3.7±0.17*	Nd	
23.	Phthalic acid, 3,5-dimethylphenyl 4-isopropyl	Nm	C ₂₄ H ₂₂ O ₄		Ester	Nd	Nd	1.78±0.10*	Nd	
Most identified classes										
						Alkane	19.55±1.64	0	5.37±0.34	9.36±1.22
						Ester	7.32±0.78	0	8.88±0.63	4.26±0.67
						Phenolic	24.77±1.04	31.97±1.00*	56.44±1.02*	65.12±0.52*
						Terpene	2.72±0.12	2.71±0.32	6.92±0.78	3.17±0.92

Nd: not detected

* means of three replicates ± SD with significant differences at 5% (post hoc test).

KRI: Kovats retention index from literature

Nm: Not mentioned

The esteric component phthalic acid, 3,5-dimethylphenyl 4-isopropyl, was 1.78% in a 200 mM NaCl-treated plant. This compound is extracted from *Bacillus subtilis* SR22 and exhibited defence responses in tomatoes against *Rhizoctonia* root rot (Rashad et al. 2022). The hexadecanoic acid compound was synthesized by 113.49% and 161.34% in plants exposed to 200 and 400 mM NaCl, respectively, which acts as antioxidants to reduce DPPH, ABTS, and NO in the leaves of *Ipomoea eriocarpa*. It can also be antibacterial against *Klebsiella pneumonia*, *E. coli*, *Bacillus subtilis*, and *Staphylococcus aureus* (Ganesan et al. 2024). Plants have synthesized secondary metabolites, including phenolic, terpene, ester, and alkane compounds, to scavenge ROS during salt stress (Akbari et al. 2022), especially alkane compounds, which are utilized in industries and aligned with our present results. The two phenolic compounds 3-Allyl-6-methoxyphenol (51.36 ± 0.80) and 3-Allyl-6-methoxyphenyl acetate (11.21 ± 0.21) are found to exhibit antioxidant activity by reducing ROS or by stopping hydroperoxides from becoming free radicals (Alam et al. 2023).

The secondary metabolites of ethyl acetate extracts of control plants included 1-Hexacosene (4.9%), 3,4-Dihydroxymandelic acid, 4TMS derivative (5.59%), cyclononasiloxane, octadecamethyl (11.58%), E-14-Hexadecenal (5.39%), E-15-heptadecenal (6.08%), heneicosane (1.5%), hexadecane (1.5%), and phenol, 3,5-bis(1,1-dimethylethyl)-phenolic (4.97%) (Madhumita et al. 2019; Biswas et al. 2022) (Table 4). The different classes of metabolites such as phenolic (phenol, 2-methoxy-4-(2-propenyl)-, acetate, 3-Allyl-6-methoxyphenol, 2, 4-DTBP, 4-Allyl-1,2-diacetoxybenzene), alkane (11-Methyltricosane, 1-Pentadecene, 3-Ethyl-2,6,10-trimethylundecane, 5,5-Diethyltridecane, decane, 1-iodo-, decane, 2,3,5,8-tetramethyl-, dodecane, 2,6,10-trimethyl-, dodecane, heneicosane, 4-methyl-, dotriacontane, 2,6,11-trimethyl-, dodecane, hexadecane), EO (1-Dodecanol, 3,7,11-trimethyl-), terpene (dodecane, 1-tetracosene, 2,6,10-trimethyl-), ester (1,2,3,4-Tetrahydronaphthalen-1-yl 2,2,3,3,3-pentafluoropropanoate, 2-Ethylbutyric acid, eicosyl ester, 3-Allyl-6-methoxyphenyl acetate, 2-hydroxy-1 (hydroxymethyl) ethyl, carbonic acid, eicosyl vinyl ester, hexadecanoic acid, tetrapentacontane) and fatty acid (Octadecanoic acid, 11-Methylnonacosane, 2,3-dihydroxypropyl ester) were identified in 100 mM to 400 mM NaCl-treated plants, that have pharmacological properties, such as anti-inflammatory, wound-healing, anthelmintic, antiparasitic, antifungal, antihemolytic, antibacterial, antiseptic, antioxidant, anticancer, and antidiabetic, activities (Mahalakshmi et al. 2013) (Table 4). Similarly, the other phenolic compounds also have various properties, including 4-Allyl-1,2-diacetoxybenzene, phenol, 2-methoxy-4-(2-propenyl)-, acetate (as antibacterial and anti-biofilm activity), and 2, 4-DTBP, a toxic phenol compound (exhibiting considerable antioxidant, antibacterial, and antitumor activity) found in NaCl-treated plants, which inhibits the plant immune system (Zhao et al. 2020). The high salinity reduced 2,4-

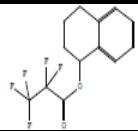
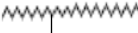
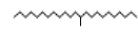




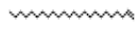
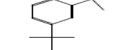
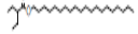
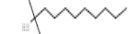
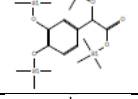
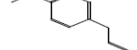
DTBP (88.8 to 78.57%) compared to plants exposed to 100 mM NaCl. In addition, a low amount of 3-Allyl-6-methoxyphenol was detected in plants exposed to 200 and 400 mM NaCl, which possess potent antioxidant, anti-inflammatory, antibacterial, nematocidal, antimicrobial, and pesticide properties (Sosa et al. 2016).

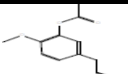
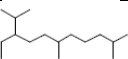
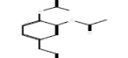
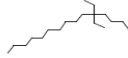
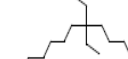
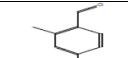
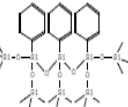

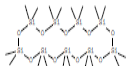

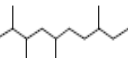

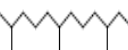
The alkylated phenol dodecane 2,6,10-trimethyl was 0.76% in 400 mM NaCl-treated plants. This compound also acts as an anti-proliferative and antioxidant agent in *Ficus pumila* (Torkornoo et al. 2019). 5,5-Diethyltridecane was induced as 0.55, 0.37, and 0.23% in 100, 200, and 400 mM NaCl-treated plants but absent in the control. This compound possesses the acaricidal activity of EO from *Satureja hortensis* (L.) and *Teucrium polium* (L.) against two-spotted spider mites (Ebadollahi et al. 2015). Another compound, heneicosane, was enhanced by 5.33% in 100 mM NaCl but reduced by 78 and 70% in plants exposed to 200 and 400 mM NaCl, respectively, compared to control. It is reported as a novel antimicrobial compound in *Plumbago zeylanica* leaf extracts, a reducing and stabilizing agent for preparing nanoparticles (ZnO, AgO), and utilized as a pheromone by the queen or king termites in the species *Reticulitermes flavipes* (Eyer et al. 2021).

1-Dodecanol, 3,7,11-trimethyl was observed at 0.17% in 200 mM NaCl-treated plants. This component possesses anti-inflammatory, antioxidant, and antimicrobial properties and also, in drug delivery and skin protection applications, acts as a surfactant in detergents, lubricants, and cosmetics (Nazarudin et al. 2022). 100 mM NaCl stimulated the 1-tetracosene terpene compound (by 4.9%) as compared to the control but not in 200 and 400 mM NaCl stress. This compound also exhibited cytotoxic and antioxidant activity in *Spiraea hypericifolia* (Kudaibergen et al. 2020).

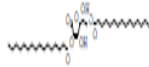
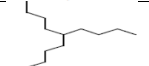
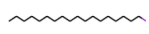
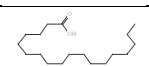
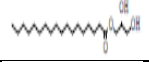
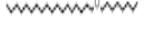
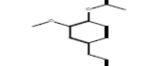
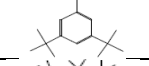


The ester compounds like hexadecanoic acid and 2-hydroxy-1 (hydroxymethyl) ethyl were 5.7% in 200 mM NaCl but decreased by 95.26% in plants exposed to 400 mM NaCl-treated plants. This compound also exhibits antifungal activity against the *Macrophomina phaseolina* pathogen and is found at 10.99% in *Chenopodium quinoa* plants (Khan and Javaid 2020). In addition, hexadecanoic acid, an ester component, possessed anticancer, antimicrobial, antioxidant, and antihemolytic activity (Dubey et al. 2014). Octadecanoic acid is a fatty acid molecule found at 2.95% in 400 mM NaCl-treated betel vine plants, which is utilized as softening plastics and in making candles, cosmetics, and hardening soaps. Compared to control, the antibiotic compound E-15-Heptadecenal was reduced by 16.61 and 95.88% in plants exposed to 100 and 200 mM NaCl. The E-15-Heptadecenal compound is also synthesized in *Jatropha curcas* under salt stress (Mahalakshmi et al. 2013). Similarly, a vitamin-type compound, l-(+)-Ascorbic acid 2,6-dihexadecanoate, was observed at 8.21% in plants exposed to

Table 4 GC/MS analysis of major volatile compounds in ethyl acetate extracts of betel vine leaves under salt stress.

Sl. No.	Compounds	KRI literature (Column)	Molecular formula	Structure of compounds	Types of compounds	Area (%)			
						Control	NaCl concentrations (mM)		
						100	200	400	
1	1,2,3,4-Tetrahydronaphthalen-1-yl 2,2,3,3,3-pentafluoropropanoate	Nm	C ₁₁ H ₁₆ C ₁ N		Ester	Nd	Nd	0.3±0.2	Nd
2	11-Methylnonacosane	2933(DB-5MS)	C ₃₀ H		Fatty acid	Nd	1.59±0.6*	Nd	Nd
3	11-Methyltricosane	2335 (DB-1)	C ₂₄ H ₅₀		Alkane	Nd	Nd	0.06±0.1*	0.06±0.12*
4	1-Dodecanol, 3,7,11-trimethyl-	1563	C ₁₅ H ₃₂ O		EO	Nd	Nd	0.17±0.08	Nd
5	1-Hexacosene	2593 (CP-Sil-8CB)	C ₂₆ H ₅₂		Aliphatic hydrocarbon	4.9±0.08	Nd	Nd	Nd
6	1-Hexadecanol	1854	C ₁₆ H ₃₄ O		Fatty alcohol	Nd	Nd	Nd	0.35±0.02
7	1-Pentadecene	1502	C ₁₅ H ₃₀		Alkane	Nd	Nd	Nd	0.24±0.01*
8	1-Tetracosene	2395	C ₂₄ H		Terpene	Nd	4.9±0.04*	Nd	Nd
9	2,4-Di-tert-butylphenol	1502 (CP-Sil-5CB)	C ₁₄ H ₂₂ O		Phenolic	Nd	4.2±0.4	0.47±0.01	0.9±0.01
10	2-Ethylbutyric acid, eicosyl ester	2709	C ₂₇ H ₅₄ O ₂		Ester	Nd	0.5±0.02	Nd	Nd
11	2-Undecanethiol, 2-methyl-	1433	C ₁₂ H ₂₆ S		Thiol	Nd	Nd	Nd	0.16±0.09
12	3,4-Dihydroxymandelic acid, 4TMS derivative	1936 (DB-1)	C ₂₀ H ₄₀ O ₅ Si		Catechol	5.59±0.08	Nd	Nd	Nd
13	3-Allyl-6-methoxyphenol	1322 (DB-5MS)	C ₁₀ H ₁₂ O		Phenolic	Nd	Nd	0.36±0.03	0.23±0.01

Sl. No.	Compounds	KRI literature (Column)	Molecular formula	Structure of compounds	Types of compounds	Area (%)			
						NaCl concentrations (mM)			
						Control	100	200	400
14	3-Allyl-6-methoxyphenyl acetate	1513 (DB-5MS)	C ₁₂ H ₁₄ O ₃		Ester	Nd	Nd	Nd	0.98±0.01
15	3-Ethyl-2,6,10-trimethylundecane	Nm	C ₁₆ H ₃₄		Alkane	Nd	Nd	Nd	2.94±0.004*
16	4-Allyl-1,2-diacetoxybenzene	1647 (ZB-5)	C ₁₃ H ₁₄ O ₄		Phenol and benzoate ester	Nd	Nd	Nd	0.96±0.004
17	5,5-Diethylpentadecane	1825	C ₁₅ H ₃₂		Hydrocarbon	Nd	Nd	0.16±0.04	Nd
18	5,5-Diethyltridecane	1205	C ₁₅ H ₃₂		Alkane	Nd	0.55±0.009	0.37±0.02	0.23±0.01
19	Benzaldehyde, 2,4-dimethyl-	1208	C ₉ H ₁₀ O		Benzaldehyde	Nd	Nd	0.22±0.1	Nd
20	Bis[di(trimethylsiloxy)phenylsiloxy]trimethylsiloxyphenylsiloxy siloxane	3343	C ₃₃ H ₆₀ O ₇ Si ₈		Siloxane	Nd	0.74±0.01	Nd	Nd
21	Carbonic acid, eicosyl vinyl ester	2497	C ₂₈ H ₅₄ O ₂		Ester	Nd	Nd	0.14±0.11	Nd
22	Cyclononasiloxane, octadecamethyl-	1860	C ₁₈ H ₅₄ O ₉ Si ₉		Siloxane	11.58±0.06	1.73±0.02*	Nd	Nd
23	Decane, 1-iodo-	1430	C ₁₀ H ₂₁ I		Alkane	Nd	Nd	0.06±0.02	0.33±0.12
24	Decane, 2,3,5,8-tetramethyl-	4714	C ₁₄ H ₃₀		Alkane	Nd	0.56±0.01	Nd	Nd
25	Dodecanal	1407 (DB-5)	C ₁₂ H ₂₄ O		Lauraldehyde	Nd	Nd	0.26±0.04	0.05±0.01
26	Dodecane, 2,6,10-trimethyl-	1320	C ₁₅ H ₃₂		Alkane	Nd	0.76±0.01	Nd	Nd

Sl. No.	Compounds	KRI literature (Column)	Molecular formula	Structure of compounds	Types of compounds	Area (%)			
						NaCl concentrations (mM)			
						Control	100	200	400
27	Dodecane, 2,6,11-trimethyl-	1320	C ₁₅ H ₃₂		Alkane	Nd	Nd	2.77±0.2	2.87±0.02
28	Dodecane, 4-methyl-	1249	C ₁₃ H ₂₈		Alkane	Nd	Nd	0.37±0.02	0.54±0.002
29	Dotriacontane	1600 (DB-5)	C ₃₂ H ₆₆		Alkane	Nd	Nd	7.41±0.14	1.64±0.1
30	E-14-Hexadecenal	1824 (DB-50)	C ₁₆ H ₃₀ O		Palmitol aldehyde	5.39±0.08	5.07±0.08*	Nd	Nd
31	E-15-Heptadecenal	2083 (HP-5MS)	C ₁₇ H ₃₂ O		Antibiotic	6.08±0.08	5.07±0.08	0.25±0.02*	Nd
32	Heneicosane	2100(DB-5)	C ₂₁ H		Alkane	1.5±0.05	1.58±0.05*	0.33±0.02*	0.45±0.01
33	Heptadecane	1700 (DB-5)	C ₁₇ H ₃₆		Alkane	Nd	Nd	0.27±0.05	Nd
34	Heptadecane, 2-methyl-	1746	C ₁₉ H ₄₀		Alkane	Nd	Nd	Nd	0.46±0.01
35	Heptane, 2,4-dimethyl-	788	C ₇ H ₁₆		Alkane	Nd	Nd	0.16±0.02	0.32±0.02
36	Hexacontane	1600 (DB-5)	C ₆₀ H ₁₂₂		Alkane	Nd	Nd	0.17±0.01	Nd
37	Hexacosyl nonyl ether	3550	C ₃₆ H ₇₄ O		Fatty alcohol	Nd	Nd	0.63±0.12	Nd
38	Hexadecane	1600(DB-5)	C ₁₆ H ₃₄		Alkane	1.56±0.09	0.24±0.04	0.45±0.03*	3.45±0.01*
39	Hexadecane, 2,6,10,14-tetramethyl-	1753	C ₂₀ H ₄₂		Alkane	Nd	Nd	Nd	0.38±0.008
40	Hexadecane, 2-methyl-	1647	C ₁₇ H ₃₆		Alkane	Nd	Nd	Nd	0.28±0.01
41	Hexadecanoic acid, 2-hydroxy-1 (hydroxymethyl) ethyl	2498	C ₂₀ H ₄₀ O ₃		Ester	Nd	Nd	5.7±0.21	0.27±0.01
42	Hexane, 2,3,5-trimethyl-	724	C ₉ H ₂₀		Alkane	Nd	Nd	0.04±0.04	Nd

Sl. No.	Compounds	KRI literature (Column)	Molecular formula	Structure of compounds	Types of compounds	Area (%)			
						Control	NaCl concentrations (mM)		
							100	200	400
43	l-(+)-Ascorbic acid 2,6-dihexadecanoate	Nm	C ₃₈ H ₆₈ O ₈		Vitamin C	Nd	Nd	8.21±0.06	Nd
44	Nonane, 5-butyl-	1204	C ₁₄ H ₃₀		Alkane	Nd	Nd	0.22±0.1	Nd
45	Octadecane, 1-iodo-	2272 (DB-1)	C ₁₈ H ₃₇ I		Alkyl halide	Nd	Nd	0.25±0.03	Nd
46	Octadecanoic acid	2124 (DB-5)	C ₁₈ H ₃₆ O ₂		Fatty acid	Nd	Nd	Nd	2.95±0.01
47	Octadecanoic acid, 2,3-dihydroxypropyl ester	2992	C ₂₁ H ₄₂ O		Fatty acid	Nd	Nd	4.45±0.12	1.98±0.02
48	Octadecyl octyl ether	1862	C ₂₆ H ₅₄ O		Ether	Nd	Nd	0.17±0.02	Nd
49	Phenol, 2-methoxy-4-(2-propenyl)-, acetate	1451(HP-5)	C ₁₂ H ₁₄ O		Phenolic	Nd	1.57±0.06	Nd	Nd
50	Phenol, 3,5-bis(1,1-dimethylethyl)-	1555	C ₂₇ H ₅₀ OP ₂		Phenolic	4.97±0.08	Nd	Nd	Nd
51	Tetracosamethyl-cyclododecasiloxane	2480	C ₂₄ H ₇₂ O ₁₂ Si		Siloxane	Nd	1.4±0.04	Nd	Nd
52	Tetrapentacontane	5389	C ₅₄ H ₁₁₀		Ester	Nd	Nd	5.63±0.12	1.47±0.01
Most identified classes									
Alkane						3.06±0.05	3.69±0.12	12.37±0.4*	14.19±0.35*
Fatty acid						0	1.59±0.23	4.45±0.52	4.93±0.65
Ester						0	0.5±0.04	11.94±0.8*	2.72±0.14*
Phenolic						4.97±0.12	5.77±0.24	0.83±0.32*	1.13±0.16

Nd: not detected

* means of three replicates ± SD with significant differences at 5% (post hoc test).

KRI: Kovats retention index from literature

Nm: Not mentioned

200 mM NaCl but was absent in other NaCl treatments. This compound also exhibits antimicrobial, antioxidant, anticancer, and antiulcerogenic properties in *Sesuvium portulacastrum* (Kumar et al. 2014). Due to oxidation, total phenolic compounds were observed at 5.77% in 100 mM but decreased to 0.83, and 1.13% in 200 and 400 mM NaCl-treated plants. The total alkane compounds were induced by 3.69, 12.37, and 14.19% in plants exposed to 100, 200, and 400 mM NaCl, respectively, and ultimately emerged as the most prevalent chemical group in ethyl acetate extracts of salt-treated plants. In addition, the fatty acid and ester compounds were also stimulated more in the saline condition. These alkanes, benzoate esters, and fatty acid methyl esters were polymerized to develop a cuticle layer in the epidermal tissues of wheat and barley leaves to check water loss under saline stress conditions (Hasanuzzaman et al. 2017). Our results indicate that the biosynthesis of phenolic, alkane, fatty acids, ester compounds, and activation of antioxidants are simultaneously stimulated to safeguard the general health of the betel vine when subjected to salinity stress. Moreover, these findings support our presumption that salt-stress-tolerant plants could provide good systems for the biosynthesis of secondary metabolites needed by the manufacturing and pharmaceutical sectors.

Conclusion

Many companies are looking for more natural, eco-friendly, and alternative sources of antioxidants, antibiotics, crop protection agents, and antimicrobials. There are no published data regarding manufacturing secondary metabolites like phenolic, alkane, and ester components in betel vines under various salinity stresses. This study showed that the photosynthetic pigments, RWC, stomatal density, and length of the stomatal aperture were reduced while H_2O_2 , $O_2^{\bullet-}$, and cell death contents were increased with increasing NaCl levels. Furthermore, the NaCl treatment enhanced the SOD, CAT, APX, and GPX activities at 100 and 200 mM NaCl to maintain cellular homeostasis, but the activities were declined in 400 mM NaCl. The production of bioactive compounds was also triggered by the salt stress, including eugenol, 3-Allyl-6-methoxyphenol, caryophyllene, hexadecane, 4-Allyl-1,2-diacetoxybenzene, 11-Methyltricosane, 1-Dodecano etc. Thus, the synthesis of these molecules at different salt concentrations could be a benefit of salinity stress for some plants, encouraging the production of chemicals of commercial and medicinal value.

List of abbreviations

NaCl: Sodium chloride; RWC: Relative water content; ROS: Reactive oxygen species; H_2O_2 : Hydrogen peroxidase; $O_2^{\bullet-}$: Superoxide anion; SOD: Superoxide dismutase; CAT: Catalase; APX: Ascorbate peroxidase; GPX: Guaiacol peroxidase; ASC: Ascorbate; GSH: Glutathione; GC-MS: Gas chromatography-mass spectrometry; EO: Essential oils; SEM: Scanning electron microscopy;

Author contributions

A. K. Sahu: Writing, Reviewing and Editing, Investigation. P. Priyadarshini: Data curation, Methodology, and Investigation. B. Dash: Data curation, Methodology, and Investigation. B. S. Behera: Data curation, Methodology, and Investigation. S. K. Gochhi: Data curation. D. Pradhan: Data curation. P. Kumari: Supervision, Conceptualization, Writing, Reviewing and Editing, Investigation, Validation.

Acknowledgments

The grants from OHEPEE, COE for Bioresource Management and Energy Conservation Material Development, F.M. University and Science & Engineering Research Board (SERB), Department of Science & Technology, Government of India, to Dr. Punam Kumari are gratefully acknowledged. The laboratory facilities provided by the P.G. Department of Biosciences and Biotechnology, F.M. University, are also gratefully acknowledged.

Funding

This work was financial assisted by OHEPEE, COE for Bioresource Management and Energy Conservation Material Development, F.M. University, and partial funds from the Science & Engineering Research Board (SERB), Department of Science & Technology, Government of India (No. EEQ/2022/000273).

Conflict of interest

The authors affirm that they have no competing interests.

Ethical clearance statement

This certifies that no animal or human models were involved in the study; therefore, ethical clearance is not required.

References

- Adden, A.K., Haines Acosta-Serrano, Á.L.R., & Prieto-Godino, L.L. (2023). Tsetse flies (*Glossina morsitansmorsitans*) choose birthing sites guided by substrate cues with no evidence for a role of pheromones. *Proceedings of the Royal Society B: Biological Sciences*, 290, 1-8. <https://doi.org/10.1098/rspb.2023.0030>
- Ait Elallem, K., Ben Bakrim, W., Yasri, A., & Boularbah, A. (2024). Growth, biochemical traits, antioxidant enzymes, and essential oils of four aromatic and medicinal plants cultivated in phosphate-mine residues. *Plants*, 13(18), 2656.
- Akbari, B., Baghaei Yazdi, N., Bahmaie, M., & Mahdavi Abhari, F. (2022). The role of plant-derived natural antioxidants in reduction of oxidative stress. *Biofactors*, 48(3), 611-633. <https://doi.org/10.1002/biof.1831>

- Al Ahadeb, J.I. (2022). Impact of *Cinnamomum verum* against different *Escherichia coli* strains isolated from drinking water sources of rural areas in Riyadh. *Saudi Arabia Journal of King Saudi University Science*, 34(2), 1-5. <https://doi.org/10.1016/j.jksus.2021.101742>
- Alam, M.B., Park, N. H., Song, B. R., & Lee, S.H. (2023). Antioxidant potential-rich betel leaves (*Piper betle* L.) exert depigmenting action by triggering autophagy and downregulating MITF/Tyrosinase *In Vitro* and *In Vivo*. *Antioxidants*, 12(2), 374. <https://doi.org/10.3390/antiox12020374>
- Amor, N. B., Jiménez, A., Megdiche, W., Lundqvist, M., Sevilla, F., & Abdelly, C. (2006). Response of antioxidant systems to NaCl stress in the halophyte *Cakile maritima*. *Physiologia Plantarum*, 126(3), 446-457.
- Annegowda, H.V., Tan, P.Y., Mordi, M.N., Ramanathan, S., Hamdan, M.R., Sulaiman, M.H., & Mansor, S.M. (2013). TLC–bioautography-guided isolation, HPTLC and GC–MS-assisted analysis of bioactives of *Piper betle* leaf extract obtained from various extraction techniques: *In vitro* evaluation of phenolic content, antioxidant and antimicrobial activities. *Food Analytical Methods*, 6, 715-726. <http://dx.doi.org/10.1007%2F12161-012-9470-y>
- Ayswarya, S., Radhakrishnan, S., Manigundan, K., Gopikrishnan, V., & Soyong, K. (2022). Antioxidant activity of 2, 4-di-tert-butylphenol isolated from plant growth promoting endophytic *Streptomyces* KCA-1. *International Journal of Agriculture Technology*, 18 (6), 2343.
- Barbieri, G., Vallone, S., Orsini, F., Paradiso, R., De Pascale, S., Negre-Zakharov, F., & Maggio, A. (2012). Stomatal density and metabolic determinants mediate salt stress adaptation and water use efficiency in basil (*Ocimum basilicum* L.). *Journal of Plant Physiology* 169 (17), 1737-1746. <https://doi.org/10.1016/j.jplph.2012.07.001>
- Bistgani, Z.E., Hashemi, M., DaCosta, M., Craker, L., Maggi, F., & Morshedloo, M.R. (2019). Effect of salinity stress on the physiological characteristics, phenolic compounds and antioxidant activity of *Thymus vulgaris* L. and *Thymus daenensis* Celak. *Industrial Crops and Products*, 135, 311-320. <https://doi.org/10.1016/j.indcrop.2019.04.055>
- Biswas, P., Anand, U., Saha, S.C., Kant, N., Mishra, T., Masih, H., & Dey, A. (2022). Betel vine (*Piper betle* L.): A comprehensive insight into its ethnopharmacology, phytochemistry, and pharmacological, biomedical and therapeutic attributes. *Journal of Cell and Molecular Medicine*, 26(11), 3083-3119. <https://doi.org/10.1111%2Fjcmm.17323>
- Burkhardt, J. (2010). Hygroscopic particles on leaves: nutrients or desiccants? *Ecological Monographs*, 80(3), 369-399. <https://doi.org/10.1890/09-1988.1>
- Chaudhary, P., Janmeda, P., Docea, A.O., Yeskaliyeva, B., Razis, A.F.A., Modu, B., & Sharifi-Rad, J. (2023). Oxidative stress, free radicals and antioxidants: potential crosstalk in the pathophysiology of human diseases. *Frontier in Chemistry*, 11, 1158198. <https://doi.org/10.3389/fchem.2023.1158198>
- Chaudhry, S., & Sidhu, G.P.S. (2022). Climate change regulated abiotic stress mechanisms in plants: A comprehensive review. *Plant Cell Reports*, 41(1), 1-31. <https://doi.org/10.1007/s00299-021-02759-5>
- Daudi, A., & O'brien, J. A. (2012). Detection of hydrogen peroxide by DAB staining in *Arabidopsis* leaves. *Bio-protocol*, 2(18), e263-e263.
- Dubey, D., Patnaik, R., Ghosh, G., & Padhy, R.N. (2014). *In vitro* antibacterial activity, gas chromatography–mass spectrometry analysis of *Woodfordia fruticosa* Kurz. leaf extract and host toxicity testing with *in vitro* cultured lymphocytes from human umbilical cord blood. *Osong Public Health and Research Perspectives*, 5(5), 298-312. <https://doi.org/10.1016/j.phrp.2014.08.001>
- Ebadollahi, A., Sendi, J.J., Aliakbar, A. J., & Razmjou, J.(2015). Acaricidal activities of essential oils from *Satureja hortensis* (L.) and *Teucrium polium* (L.) against the two spotted spider mite, *Tetranychus urticae* Koch (Acari: Tetranychidae). *Egyptian Journal of Biological Pest Control*, 25(1),171-176.
- Esfandiari, E., Shekari, F., Shekari, F., & Esfandiari, M. (2007). The effect of salt stress on antioxidant enzymes'activity and lipid peroxidation on the wheat seedling. *Notulae Botanicae Horti Agrobotanici Cluj-Napoca*, 35(1), 48.
- Eyer, P.A., Salin, J., Helms, A.M., & Vargo, E.L. (2021). Distinct chemical blends produced by different reproductive castes in the subterranean termite *Reticulitermes flavipes*. *Scientific Reports*, 11(1), 4471. <https://doi.org/10.1038/s41598-021-83976-6>
- Farhat, F., Arfan, M., Wang, X., Tariq, A., Kamran, M., Tabassum, H.N., & Elansary, H.O. (2022). The impact of bio-stimulants on Cd-stressed wheat (*Triticum aestivum* L.): Insights into growth, chlorophyll fluorescence, Cd accumulation, and osmolyte regulation. *Frontiers in Plant Science*, 13, 850567. <https://doi.org/10.3389/fpls.2022.850567>
- Ganesan, T., Subban, M., Christopher Leslee, D. B., Kuppannan, S. B., & Seedeivi, P. (2024). Structural characterization of n-hexadecanoic acid from the leaves of *Ipomoea eriocarpa* and its antioxidant and antibacterial activities. *Biomass Conversion and Biorefinery*, 14(13), 14547-14558.

- Gölge, B.H., & Vardar, F. (2020). Temporal analysis of Al-induced programmed cell death in barley (*Hordeum vulgare* L.) roots. *Caryologia*, 73(1), 45-55. <https://doi.org/10.13128/caryologia-185>
- Hameed, A., Ahmed, M. Z., Hussain, T., Aziz, I., Ahmad, N., Gul, B., & Nielsen, B. L. (2021). Effects of salinity stress on chloroplast structure and function. *Cells*, 10(8), 2023.
- Hasanuzzaman Abbruzzese, G., Beritognolo, I., Muleo, R., Piazzai, M., Sabatti, M., Mugnozza, G.S., & Kuzminsky, E. (2009). Leaf morphological plasticity and stomatal conductance in three *Populus alba* L. genotypes subjected to salt stress. *Environmental and Experimental Botany*, 66(3), 381-388. <http://dx.doi.org/10.1016/j.envexpbot.2009.04.008>
- Hasanuzzaman, M.D., Davies, N.W., Shabala, L., Zhou, M., Brodribb, T.J., & Shabala, S. (2017). Residual transpiration as a component of salinity stress tolerance mechanism: a case study for barley. *BMC Plant Biology*, 17, 1-12. <http://dx.doi.org/10.1186/s12870-017-1054-y>
- Hatami, M., & Ghorbanpour, M. (2024). Metal and metal oxide nanoparticles-induced reactive oxygen species: Phytotoxicity and detoxification mechanisms in plant cell. *Plant Physiology and Biochemistry*, 213, 108847. <https://doi.org/10.1016/j.plaphy.2024.108847>
- Islam, M. Z., Park, B. J., & Lee, Y. T. (2019). Effect of salinity stress on bioactive compounds and antioxidant activity of wheat microgreen extract under organic cultivation conditions. *International journal of biological macromolecules*, 140, 631-636. <https://doi.org/10.1016/j.ijbiomac.2019.08.090>
- Kannan, P. R., Deepa, S., Kanth, S. V., & Rengasamy, R. (2013). Growth, osmolyte concentration and antioxidant enzymes in the leaves of *Sesuvium portulacastrum* L. under salinity stress. *Applied biochemistry and biotechnology*, 171, 1925-1932. <https://doi.org/10.1007/s12010-013-0475-9>
- Kerschbaum, H.H., Tasa, B.A., Schürz, M., Oberascher, K., & Bresgen, N. (2021). Trypan blue-adapting a dye used for labelling dead cells to visualize pinocytosis in viable cells. *Cell Physiology and Biochemistry*, 55, 171-184. <https://doi.org/10.33594/000000380>
- Khan, I.H., & Javaid, A. (2020). Comparative antifungal potential of stem extracts of four quinoa varieties against *Macrophomina phaseolina*. *International Journal of Agriculture and Biology*, 24(3), 441-446. <http://dx.doi.org/10.17957/IJAB/15.1457>
- Kudaibergen, A.A., Nurlybekova, A.K., Kemelbek, M., Feng, Y., & Zhenis, J. (2020). GC-MS analysis of liposoluble components from *Spiraea hypericifolia* L. bulletin of the Eurasian National University named after L.N.GUMILYOV, series. *Chemistry Geography Ecology*, 133 (4), 44. <https://doi.org/10.3390/plants11101384>
- Kumar, A., Kumari, P.S., & Somasundaram, T. (2014). Gas chromatography-mass spectrum (GC-MS) analysis of bioactive components of the methanol extract of halophyte, *Sesuviumportulacastrum* L. *International Journal of Advances in Pharmacy Biology and Chemistry*, 3(3), 766-772.
- Kumar, R., Sharma, S., Kumar, S., Kumar, D., Lagarkha, R., Kumar, S., & Pandey, M. (2024). *In vitro* investigation of phytoconstituents, GC-MS, TLC, antioxidant activity, total phenolic & flavonoid contents from *Aegle marmelos* L. (Bael) leaves extract. *European Journal of Medicinal Plants*, 35(6), 187-199.
- Kumari, P., Mahapatro, G.K., Banerjee, N., & Sarin, N.B. (2015). Ectopic expression of GroEL from *Xenorhabdus nematophila* in tomato enhances resistance against *Helicoverpa armigera* and salt and thermal stress. *Translational Research*, 24, 859-873. <https://doi.org/10.1007/s11248-015-9881-9>
- Kusvuran, S., Cengil, B., & Mutlu, F. (2024). Effect of nano-silicon application on salt tolerance of pepper (*Capsicum annuum* L.). *Proceedings of the Bulgarian Academy of Sciences*, 77(3), 467-474.
- Lala, S. (2021). Nanoparticles as elicitors and harvesters of economically important secondary metabolites in higher plants: a review. *IET Nanobiotechnology*, 15, 28-57. <https://doi.org/10.1049/nbt2.12005>
- Li, X., Zhang, W., Niu, D., & Liu, X. (2024). Effects of abiotic stress on chlorophyll metabolism. *Plant Science*, 342, 112030. <https://doi.org/10.1016/j.plantsci.2024.112030>
- Lin, K. H., & Pu, S. F. (2010). Tissue-and genotype-specific ascorbate peroxidase expression in sweet potato in response to salt stress. *Biologia plantarum*, 54, 664-670. <https://doi.org/10.1007/s10535-010-0118-8>
- Madhumita, M., Guha, P., & Nag, A. (2019). Optimization of the exhaustive hydrodistillation method in the recovery of essential oil from fresh and cured betel leaves (*Piper betle* L.) using the Box- Behnken design. *Journal of Food Processing and Preservation*, 43(11), 14196. <http://dx.doi.org/10.1111/jfpp.14196>
- Madhumita, M., Guha, P., & Nag, A. (2020). Bio-actives of betel leaf (*Piper betle* L.): A comprehensive review on extraction, isolation, characterization, and biological activity. *Phytotherapy Research*, 34(10), 2609-2627. <https://doi.org/10.1002/ptr.6715>
- Mahalakshmi, R., Eganathan, P., & Ajay, P. (2013). Changes in secondary metabolite production in *Jatropha curcas* calluses treated with NaCl. *Analytical Chemistry Letters*, 3(5-6), 359-369. <http://dx.doi.org/10.1080/22297928.2013.873225>

- Mane, A. V., Karadge, B. A., & Samant, J. S. (2010). Salinity induced changes in catalase, peroxidase and acid phosphatase in four grass species. *Nature, Environment and Pollution Technology*, 9(4), 781-786.
- Mesa, T., Polo, J., Arabia, A., Caselles, V., & Munné-Bosch, S. (2022). Differential physiological response to heat and cold stress of tomato plants and its implication on fruit quality. *Journal of Plant Physiology*, 268, 153581. <http://dx.doi.org/10.1016/j.jplph.2021.153581>
- Mohapatra, B., & Phale, P.S. (2021). Microbial degradation of naphthalene and substituted naphthalenes: metabolic diversity and genomic insight for bioremediation. *Frontiers in Bioengineering and Biotechnology*, 9, 602445. <https://doi.org/10.3389/fbioe.2021.602445>
- Morris, B.D., Smyth, R.R., Foster, S.P., Hoffmann, M.P., Roelofs, W.L., Franke, S., & Francke, W. (2005). Vittatalactone, a β -lactone from the striped cucumber beetle, *Acalymma vittatum*. *Journal of Natural Products*, 68(1), 26-30. <https://doi.org/10.1021/np049751v>
- Mostofa, M.G., Fujita, M., & Tran, L.S.P. (2015). Nitric oxide mediates hydrogen peroxide-and salicylic acid-induced salt tolerance in rice (*Oryza sativa* L.) seedlings. *Plant Growth Regulation*, 77, 265-277. <http://dx.doi.org/10.1007/s10725-015-0061-y>
- Nazarudin, M.F., Yasin, I.S.M., Mazli, N.A.I.N., Saadi, A.R., Azizee, M.H.S., Nooraini, M.A., & Fakhruddin, I.M. (2022). Preliminary screening of antioxidant and cytotoxic potential of green seaweed, *Halimeda opuntia* (Linnaeus) Lamouroux. *Saudi Journal of Biological Sciences*, 29(4), 2698-2705. <https://doi.org/10.1016/j.sjbs.2021.12.066>
- Noreen, S., Ashraf, M., Hussain, M., & Jamil, A. (2009). Exogenous application of salicylic acid enhances antioxidative capacity in salt stressed sunflower (*Helianthus annuus* L.) plants. *Pakistan Journal of Botany*, 41(1), 473-479.
- Paul, V., Sharma, L., Pandey, R., & Meena, R. C. (2017). Measurements of stomatal density and stomatal index on leaf/plant surfaces. *Manual of ICAR Sponsored Training Programme for Technical Staff of ICAR Institutes on—Physiological Techniques to Analyze the Impact of Climate Change on Crop Plants*, 27.
- Rashad, Y.M., Abdalla, S.A., & Sleem, M.M. (2022). Endophytic *Bacillus subtilis* SR22 triggers defense responses in tomato against rhizoctonia root rot. *Plants*, 11(15), 2051. <https://doi.org/10.3390/plants11152051>
- Rathinapriya, P., Pandian, S., Rakkammal, K., Balasangeetha, M., Alexpandi, R., Satish, L., & Ramesh, M. (2020). The protective effects of polyamines on salinity stress tolerance in foxtail millet (*Setaria italica* L.), an important C4 model crop. *Physiology and Molecular Biology of Plants*, 26, 1815-1829. <https://doi.org/10.1007/s12298-020-00869-0>
- Sahu, A. K., Kumari, P., & Mittra, B. (2024a). *Fusarium* induced anatomical and biochemical alterations in wild type and dpa-treated wheat seedlings. *Journal of Pure & Applied Microbiology*, 18(1), 229-242. <https://doi.org/10.22207/JPAM.18.1.06>
- Sahu, A. K., Kumari, P., & Mittra, B. (2024b). Immunocompromisation of wheat host by L-BSO and 2, 4-DPA induces susceptibility to the fungal pathogen *Fusarium oxysporum*. *Stress Biology*, 4(1), 1-18. <https://doi.org/10.1007/s44154-023-00137-7>
- Sen, S., & Rengaiyan, G. (2021). A review on the ecology, evolution and conservation of *Piper* (Piperaceae) in India: future directions and opportunities. *The Botanical Review*, 88(3), 333-358. <http://dx.doi.org/10.1007/s12229-021-09269-9>
- Sharma, C., Al Kaabi, J. M., Nurulain, S. M., Goyal, S. N., Kamal, M. A., & Ojha, S. (2016). Polypharmacological Properties and Therapeutic Potential of β -Caryophyllene: A Dietary Phytocannabinoid of Pharmaceutical Promise. *Current pharmaceutical design*, 22(21), 3237-3264. <https://doi.org/10.2174/1381612822666160311115226>
- Shumaila Ullah, S., & Nafees, M. (2023). Biochar application to soil and seed pre-soaking on growth, yield and physiological response of *Solanum melongena* L. under induced abiotic stresses. *Journal of Plant Growth and Regulation*, 42(11), 1-24. <http://dx.doi.org/10.1007/s00344-023-10990-5>
- Sosa, A.A., Bagi, S.H., & Hameed, I.H. (2016). Analysis of bioactive chemical compounds of *Euphorbia lathyris* using gas chromatography-mass spectrometry and fourier-transform infrared spectroscopy. *Journal of Pharmacognosy and Phytotherapy*, 8(5), 109-126. <http://dx.doi.org/10.5897/JPP2015.0371>
- Sulistyorini, L. (2020). Induction and identification of bioactive compounds from callus extract of *Piper betle* L. Var. nigra. *Malaysian Journal of Analytical Sciences*, 24(6), 1024-1034.
- Tahjib-Ul-Arif, M., Sayed, M.A., Islam, M.M., Siddiqui, M.N., Begum, S.N., & Hossain, M.A. (2018). Screening of rice landraces (*Oryza sativa* L.) for seedling stage salinity tolerance using morpho-physiological and molecular markers. *Acta Physiologia Plantarum*, 40(4), 70. <https://doi.org/10.1007/s12298-014-0250-6>
- Techer, D., Milla, S., Fontaine, P., Viot, S., & Thomas, M. (2015). Acute toxicity and sublethal effects of gallic and pelargonic acids on the zebrafish *Danio rerio*. *Environmental Science and Pollution Research*, 22, 5020-5029.

- Torkornoo, D. C., Larbie, S., Agbenyegah, J. N. N., Dowuona, R., Appiah-Opong et al. (2019). Evaluation of the anti-proliferative effect, antioxidant and phytochemical constituents of *Ficus pumila* Linn. *International Journal of Pharmaceutical Sciences and Research*, 10(5), 2605-2618. [http://dx.doi.org/10.13040/IJPSR.0975-8232.10\(5\).2605-18](http://dx.doi.org/10.13040/IJPSR.0975-8232.10(5).2605-18)
- Yang, J., Zhang, L., Jiang, L., Zhan, Y.G., & Fan, G.Z. (2021). Quercetin alleviates seed germination and growth inhibition in *Apocynum venetum* and *Apocynum pictum* under mannitol-induced osmotic stress. *Plant Physiology and Biochemistry*, 159, 268-276. <https://doi.org/10.1016/j.plaphy.2020.12.025>
- Yogeswari, S., Ramalakshmi, S., Neelavathy, R., & Muthumary, J.Y. (2012). Identification and comparative studies of different volatile fractions from *Monochaetia kansensis* by GCMS. *Global Journal of Pharmacology*, 6(2),65-71.
- Zhang, Y., Zhou, X., Dong, Y., Zhang, F., He, Q., Chen, J., & Zhao, T. (2021). Seed priming with melatonin improves salt tolerance in cotton through regulating photosynthesis, scavenging reactive oxygen species and coordinating with phytohormone signal pathways. *Industrial Crops and Products*, 169, 113671.
- Zhao, F., Wang, P., Lucardi, R.D., Su, Z., & Li, S.(2020). Natural sources and bioactivities of 2, 4-di-tert-butylphenol and its analogs. *Toxins*, 12(1), 35. <https://doi.org/10.3390/toxins12010035>
- Zhou, H., Shi, H., Yang, Y., Feng, X., Chen, X., Xiao, F., & Guo, Y. (2024). Insights into plant salt stress signalling and tolerance. *Journal of Genetics and Genomics*, 51(1), 16-34.



Journal of Experimental Biology and Agricultural Sciences

<http://www.jebas.org>

ISSN No. 2320 – 8694

Real-time and *in silico*-based characterization of the heat stress-responsive gene *TaGASRI* from Indian bread wheat

Satish Kumar^{1,2} , Jasdeep C. Padaria² , Hardeep Singh Tuli¹ , Pawan Kumar³ ,
 Ritu Chauhan⁴ , Damandeep Kaur⁵ , Sachin Kumar Mandotra¹ , Diwakar Aggarwal^{1*} 

¹Department of Bio-Sciences and Technology, Maharishi Markandeshwar Engineering College, Maharishi Markandeshwar (Deemed to be University), Mullana, Ambala 133207, Haryana India

²National Institute for Plant Biotechnology, Pusa Campus, New Delhi-110012, India

³Institute of Plant Sciences, Agricultural Research Organization (ARO), The Volcani Center, Rishon LeZion, 7505101, Israel

⁴Department of Biotechnology, Graphic Era Deemed to be University, Dehradun 248002, Uttarakhand, India

⁵University Center for Research & Development (UCRD), Chandigarh University, Gharuan, Mohali, Punjab, India

Received – August 14, 2024; Revision – November 05, 2024; Accepted – November 17, 2024

Available Online – November 29, 2024

DOI: [http://dx.doi.org/10.18006/2024.12\(5\).730.741](http://dx.doi.org/10.18006/2024.12(5).730.741)

KEYWORDS

High-temperature

Real-time PCR

in silico studies

Gibberellin-stimulated transcript

Genetic resource

ABSTRACT

Wheat is a staple food for 80% of the global population, offering essential protein, calories, and nutrients. Earlier wheat heat interaction studies revealed that increasing temperatures can severely hinder plant growth and development, increasing overall productivity and sensitivity to extreme temperatures during seed emergence and anthesis. In this study, *TaGASRI* (*gibberellic acid-stimulated regulator 1*), a potential candidate for heat stress resistance, was isolated, and its expression was found to be significantly greater in HD3086 wheat than in HD2894 wheat at both the seedling and anthesis stages after exposure to 42 °C heat stress (HS). Furthermore, *in silico* studies validated the molecular findings, revealing a CDS region of 297 nucleotides with 2 ORFs, with ~93% sequence similarity to the *TaGASRI* gene from the TAM107 wheat variety. A 3D model of the target protein was designed using the C8C4P9.1 template, showing 95.92% sequence similarity and 100% query coverage with the gibberellin-stimulated transcript. Furthermore, studies of the conserved motifs and protein-protein interactions of the *TaGASRI* protein have identified three major functional partners: cold acclimation proteins, ABA-inducible proteins, and protein phosphatase 2C, emphasizing its role in abiotic stress responses. Hence, the *TaGASRI* gene is a promising candidate for further studies, as it positively responds under HS conditions. Therefore, future research should focus on its role across different species to cultivate heat-tolerant varieties, supporting sustainable development amid climate change. This would

* Corresponding author

E-mail: diwakaraggarwal@yahoo.co.in (Diwakar Aggarwal)

Peer review under responsibility of Journal of Experimental Biology and Agricultural Sciences.

Production and Hosting by Horizon Publisher India [HPI]
 (<http://www.horizonpublisherindia.in/>).
 All rights reserved.

All the articles published by [Journal of Experimental Biology and Agricultural Sciences](#) are licensed under a [Creative Commons Attribution-NonCommercial 4.0 International License](#) Based on a work at www.jebas.org.



encourage breeders and researchers to use this gene to advance wheat crop development, considering current and anticipated environmental conditions.

1 Introduction

The increase in urbanization and population has resulted in a shortage of cultivated land, which ultimately has been a great issue for agriculturists. Environmental change has also worsened the current scenario, making it difficult for plants to survive; ultimately, food security is a great warning for plant biologists. A comprehensive understanding of how environmental stress enhances yield under challenging conditions is essential to navigate this scenario. Expedient climate modifications and global warming lead to a decrease in the productivity of crops and hinder their growth, which is a major challenge in the cultivation period. The deprivation of crop production is caused by various environmental conditions, including abiotic factors such as salinity, drought and heat stress (HS). The maximum temperature is often expected in major wheat growing zones, sometimes above 5°C above the standard temperature (Hatfield and John 2015; Grosse-Heilmann et al. 2024).

Wheat (*Triticum aestivum* L.) is adapted for cultivation in a wide range of climatic conditions, making it the most important crop in the world, with an approximate production of 784.91 million metric tons in 2023-2024 (<https://www.statista.com/statistics/267268/production-of-wheat-worldwide-since-1990/>). It is estimated that by 2050, food production will need to increase by 60-70% to meet rising demands. However, continuously increasing the temperature may also induce osmotic stress, resulting in high salt concentrations and a decrease in yield per unit to approximately 2.8 tonnes ha⁻¹ (Masarmi et al. 2023). Therefore, combined stresses often impact wheat plants, highlighting the need for research on the adverse effects of heat stress. Future efforts should focus on developing genotypes that can withstand varying environmental conditions. Therefore, quality and production rates are affected worldwide by these types of environmental stresses, including heat and drought, during the growing season.

For food safety, the advancement of heat-tolerant varieties and enhanced pre-breeding materials is vital for any breeding program because of the increase in climatic temperature, which ultimately affects productivity (Ortiz et al. 2008; Tripathi et al. 2016; Sarkar et al. 2021). Proteins and genes related to the environment can be determined via transcriptomic and proteomic data, but further research is needed to develop various methods for adjusting to high temperature and climate variation (Altenbach 2012; Jiang et al. 2020). In wheat, embryonic cells are affected at 45 °C, which subsequently harms seed germination (Essemine et al. 2010; Khaeim et al. 2022). Heat stress promotes abscission, and leaf senescence causes a reduction in growth and photosynthesis (Kosova et al. 2011; Farhad et al. 2023). However, if a genotype

develops with agronomic rehearses, such effects can be achieved (Asseng et al. 2011; Chapman et al. 2012; Gawdiya et al. 2023).

Genetic modification is the only way to increase the stress resistance level of complex genome crops, such as wheat crop systems, in response to various environmental stresses (Chapman et al. 2012; Villalobos-López et al. 2022). Therefore, it is necessary to study the complexity of each crop genome and characterize heat stress-responsive TFs (transcription factors) from this large Hsfs family of crops involved in genetic improvement to increase heat tolerance, which could provide insight into wheat-heat interactions (Clavijo et al. 2017). Genetic engineering techniques such as transgenic approaches would more effectively alter the plant response to different stresses, which require the desired gene of interest (Zheng et al. 2012; Parmar et al. 2017). In recent studies, the complete genomes of many crop species have been sequenced, which proves their complexity level and the presence of genes, TFs and Hsps, as reported for genetic improvement to overcome high-temperature conditions (Wang et al. 2016; Clavijo et al. 2017). Therefore, several genes reported from different crop systems, including 21 from tomato, 97 from Rice and 82 from wheat, are involved in heat stress tolerance (Gua et al. 2015; Duan et al. 2019; Liu et al. 2023).

Similarly, the *gibberellic acid-stimulated regulator gene* (*GASR*) is a well-known heat stress-responsive gene involved in several biological processes belonging to the *GA-stimulated transcript* (*GAST*) family of genes, whose expression can be altered according to environmental conditions (Cheng et al. 2019). Earlier studies identified 15 *AtGASR*, 11 *OsGASR* and 37 *TaGASR* genes in various plant systems, such as *Arabidopsis thaliana*, Rice and wheat, respectively. Two homologues of *GASR*, namely, *OsGASR1* and *OsGASR2*, were identified in Rice and play a role in the division and differentiation of panicles. Furthermore, both were highly expressed in the florets and branches, as confirmed through transient expression experiments (Furukawa et al. 2006). The wheat *TaGASR1* gene has been reported in the heat-tolerant wheat variety TAM107, which shares 51.52% similarity with the rice *OsGASR1* gene (Zhang et al. 2017). The results revealed the existence of HS elements and several cis-elements involved in various HS-related pathways. Furthermore, their over-expression in *A. thaliana* and wheat heat-susceptible varieties enhances their tolerance to heat stress and decreases ROS accumulation (Zhang et al. 2017). Furthermore, 37 *TaGASR* genes were identified in common wheat (*Triticum aestivum* L.), designated TaGASR1-37.

In the present study, the *TaGASR1* gene was isolated from the heat-tolerant Indian bread wheat variety HD3086 known as 'Pusa Gautami'. The expression pattern of the *TaGASR1* gene was

analyzed through real-time PCR and subsequently cloned and inserted into the pJET1.2 blunt-end sequencing vector for further confirmation via Sanger sequencing. The obtained sequence data for the *TaGASRI* gene were submitted to the online NCBI database. *In-silico* analysis was carried out to validate the molecular work by performing multiple sequence alignments with orthologous species, phylogenetic tree analysis, secondary and 3D protein structure prediction, location in plant cells and conserved domain analysis, which demonstrated its importance in providing heat stress (HS) resistance in host plant species. Characterizing this gene through expression analysis and *in silico*-based studies could improve understanding of its structure and functions under HS conditions.

2 Materials and methods

2.1 Plant material and stress treatment

Seeds of high-temperature resistant and susceptible varieties of Indian bread wheat cv. HD3086, commonly called 'Pusa Gautami' and cv. HD2894 were obtained from National Seed Corporation, IARI, New Delhi, India, and grown in 6-inch pots at MMDU (Mullana, India) in growth chambers with 60 to 70% relative humidity. The photoperiod was 16/8 h light and dark at 25 ± 2 °C, with the optimum light intensity applied to the plants ($100 \mu\text{mol}/\text{m}^2/\text{s}$). Plants of both cultivars were exposed to extreme temperature treatments of 37 °C and 42 °C in a BOD incubator at the seedling stage (15 days old) and anthesis phase for 4 h by continuously increasing the temperature (1 °C per 10 min) (Vishwakarma et al. 2018). For subsequent experimentation, control plants were also maintained under normal growth conditions (25 ± 2 °C). The leaf tissues were harvested from stressed and unstressed plants, immediately frozen in liquid N₂ and placed at -80 °C (ultra-deep freezer) for further RNA extraction.

2.2 RNA isolation, cDNA synthesis, and semiq and real-time PCR analysis

Using a Plant Total RNA Kit (Sigma, USA), total RNA was isolated from heat-stressed and unstressed frozen leaves of HD3086 and HD2894 and passed through an on-column DNase I Kit (Sigma, USA) to remove unwanted gDNA contamination. To check purity and integrity, all the eluted RNA products were analyzed via a nanodrop (Thermo Scientific, USA), and their concentration was checked by the naked eye on a 1.2% TBE gel. Approximately 1 µg of RNA template from both heat-stressed and normal-grown plants was used for cDNA synthesis via a SMART PCR cDNA synthesis kit (Clontech Laboratories, USA) according to the instructions provided by the manufacturers.

Semiquantitative PCR was performed to analyze the expression of the *TaGASRI* gene at the seedling and grain-filling stages via gene-specific primers with ~100 ng of template (cDNA). To

compare the intensity of the *TaGASRI* bands, *TaActin* was detected and analyzed on 1.2% agarose after PCR. qRT-PCR was performed for expression analysis of the *TaGASRI* gene (Bio-Rad, USA), and the housekeeping gene (*TaActin*) was used as an endogenous control to normalize the target gene transcripts via the following reaction program: 3 min at 94 °C (initial denaturation), 35 cycles of target amplification followed by 94 °C for 15 sec, 60 °C for 15 sec, and 72 °C for 15 sec. The generated melting curves describe the interaction of the templates with the gene-specific primers, and each reaction was performed in three biological replicates. Furthermore, the Ct value was recorded for all samples separately, and the fold change in the *TaGASRI* gene was calculated according to the $2^{-\Delta\Delta\text{Ct}}$ equation (Livak and Schmittgen 2001; Rao et al. 2013).

2.3 Full-length gene isolation

The coding DNA sequence of the *TaGASRI* gene was amplified from the HD3086 (heat stress-tolerant) wheat variety via gene-specific primers. The forward (F) and reverse (R) primers already contained *Bam*HI and *Sac*I restriction sites (Table 1). PCR was carried out to amplify specific sequences of the gene via the proofreading polymerase enzyme and *TaGASRI* primers via the following program: 3 min at 94 °C (initial denaturation), followed by 29 cycles of target amplification (94 °C - 30 sec, 60 °C - 30 sec, 72 °C - 30 sec) with extension for 10 min at 72 °C.

Table 1 List of primers used in the study

Primer name	Sequence (5'-3')
<i>TaGASRI</i>	F- GGATCCTGCTCCTCGTCTTGCTCGT
	R- GAGCTCAGAAGCCGTTGGTGC GTT
β-actin	F- GAAGCTGCAGGTATCCATGAGACC
	R- AGGCAGTGATCTCCTTGCTCATC

The band intensity of the PCR target product was observed (1.5% agarose) and eluted via a gel extraction kit (Qiagen, USA). The extracted product was cloned and inserted into the pJET1.2 blunt-end easy vector (Thermo Scientific, USA) *via* transformation into *E. coli* cells. Vector backbone-specific flanking primers were used for screening colonies; positive clones were inoculated in 10 mL of Luria broth supplemented with ampicillin (100 µg/mL) and incubated on a shaker at 200 rpm and 37 °C overnight. To check the presence of the insert, the recombinant plasmid was isolated via a miniprep kit (Qiagen, USA) and digested with the *Eco*RI enzyme. The accession number was received after the CDS was submitted to the NCBI database.

2.4 *In silico*-based studies

Computer-assisted protein sequence studies are needed to confirm the results and reference several biological observations.

ProtParam software tools were used to calculate the amino acids present in the *TaGASR1* protein (<http://web.expasy.org/protparam/>) (Gasteiger et al. 2005; Roy et al. 2011). The location of the *GASR1* gene in plant cells was studied via the CELLO v.2.5 online tool (<http://cello.life.nctu.edu.tw/cgi/main.cgi>) (Yu et al. 2006; Yu et al. 2014). Total reading frames were predicted through the NCBI ORF tool (<http://www.ncbi.nlm.nih.gov/orffinder/>). The UK/Phyre2tool (Phyre2 (<http://www.sbg.bio.ic.ac>)) was used to analyze the secondary structure of the protein, whereas Swiss model software (<https://swissmodel.expasy.org>) was applied to the 3D structure of the *TaGASR1* protein. Furthermore, the generated models were checked through Ramachandran plot analysis via the Vadar 1.8 version tool (<http://vadar.wishartlab.com/>) (Schwede et al. 2003; Park et al. 2023). To predict the interaction of the *TaGASR1* protein with the homologous protein, STRING (<https://string-db.org/>) software tools were utilized (Szklarczyk et al. 2019). The MEME software tool was applied to predict the conserved domain motifs in *TaGASR1* (<http://meme-suite.org/>) (Bailey et al. 2009; Bailey et al. 2015). MEGA11 software performed sequence alignment and constructed a phylogenetic tree for the *TaGASR1* protein and its orthologous species (www.megasoftware.net/) (Tamura et al. 2021).

2.5 Statistical analysis

Student's t-test was performed for data analysis, and the significant results are marked with an asterisk (*) if the p-value was ≤ 0.05 .

3 Results and Discussion

3.1 RNA isolation, semiq PCR and real-time PCR

The RNA isolated from the HD3086 and HD2894 wheat genotypes was shown with intact 28S and 18S ribosomal RNA bands at their

respective locations. A good-quality isolated RNA-synthesized smear of cDNA was obtained. Under thermal stress conditions, *TaGASR1* transcripts were more abundant in the HD3086 wheat variety than in the HD2894 variety, according to the semi-Q-PCR results. Furthermore, this transcript was highly upregulated in the HD3086 variety at both the seedling and heading stages compared with the HD2894 variety, indicating that the transcripts provide additional thermal stress tolerance to the HD3086 variety (Figure 1).

qRT-PCR of the *TaGASR1* gene revealed various expression patterns with increased heat stress (HS) exposure. The *TaGASR1* gene was upregulated 2.4 and 3.8 fold during the seedling and anthesis stages in the HD3086 wheat variety under high-temperature stress conditions (42 °C) (Figure 1). In the case of the HD2894 variety, the expression of this gene increased from 1.2 - 1.44 fold after exposure to 42 °C HS (heat stress). Similarly, semiquantitative studies revealed the same pattern by analyzing the band intensity of the *TaGASR1* gene compared with that of the internal control *TaActin*. However, based on the semiq- and qRT-PCR results, this gene can be isolated from the HD3086 wheat variety. The qRT-PCR study validated the gene expression differences, with specificity confirmed through melting curve analysis of the amplified products, which revealed single peaks across varying temperatures, as reported by Padaria et al. (2013; 2014).

3.2 Full-length gene isolation and cloning

An intact CDS band (encoding the DNA sequence) of the *TaGASR1* gene appeared at ~300 bp and was cloned and inserted into the empty pJET1.2 vector, as confirmed through colony PCR and restriction endonuclease examination. Furthermore, sequencing analysis of the *TaGASR1* gene revealed its exact size of 297 bp, and the obtained sequence was submitted to the NCBI

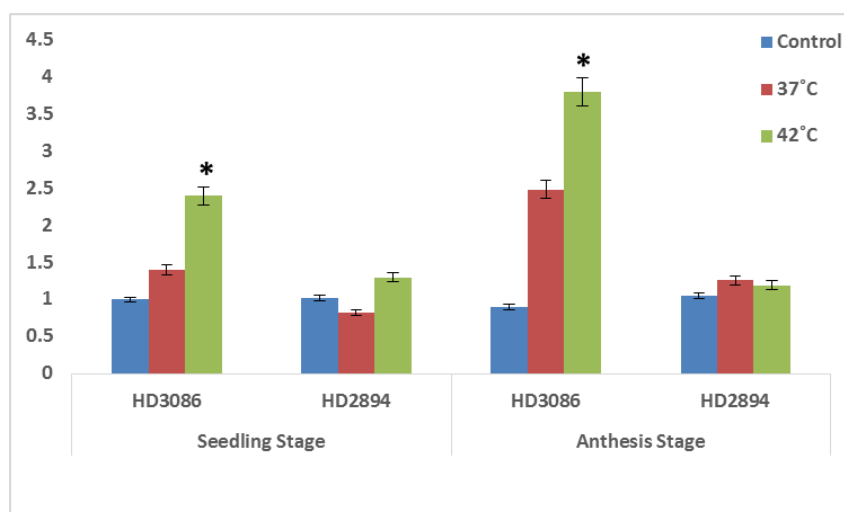


Figure 1 Expression analysis of wheat genotypes, cv. HD3086 and HD2894, before and after the exposure to 37 °C and 42 °C heat stress.

database (accession number: PQ582396). Linearized vector backbone and insert (transgene) bands were observed at ~3 kb and ~297 bp when successfully digested with the *Bam*HI and *Sac*I enzymes. However, these results confirmed that the gene *TaGASR1* (CDS) isolated from the wheat variety HD3086 was successfully cloned and inserted into a pJET sequencing vector. The pipeline used from gene isolation to cloning and sequence confirmation was similar to that used in earlier studies (Vishwakarma et al. 2018; Panzade et al. 2021; Kumar et al. 2023).

3.3 *In silico*-based studies of the *TaGASR1* gene

An *in silico*-based study was carried out using available online software tools to validate the results obtained from the molecular analysis. The physicochemical properties of the target protein, such

as the theoretical pI of *TaGASR1*, molecular formula, chemical formula, and aliphatic index, were computed, and the instability index, amino acid composition, hydropathicity index and total number of positive and negative residues were also described (Table 2). The protein *GASR1* has a molecular weight of 10360.36 and a theoretical pI value of 9.30, revealing its basic nature. This analysis also revealed the presence of 17 positively and 6 negatively charged amino acid residues in the *GASR1* protein complex, revealing its stability in alkaline environments because these amino acid residues can form ionic bonds in the protein exterior with oppositely charged amino acid residues. The predicted protein was characterized through the ExPASy tool ProtParam, developed by Gasteiger et al. (2005), and the present study showed uniformity with earlier analyses using the same tool (Vishwakarma et al. 2018; Panzade et al. 2021; Kumar et al. 2023).

Table 2 Physicochemical properties of the *TaGASR1* protein

Parameters	<i>TaGASR1</i>
Theoretical pI	9.30
Molecular weight	10360.36
Positive charged amino acids (Arg + Lys)	17
Negative charged amino acids (Asp + Glu)	6
Total no. of Atoms	1442
Molecular formula	C ₄₃₁ H ₇₃₂ N ₁₃₈ O ₁₂₅ S ₁₆
Ext. coefficient	2980
Absorbance at 0.1% (=1 g/L)	0.288
Instability index (unstable)	76.16
Aliphatic index	70.92
Hydropathicity	0.042
localization	Extracellular matrix

Table 3 Amino acid composition of the *TaGASR1* protein

Amino acid composition:					
Ala (A)	15	15.3%	Lys (K)	6	6.1%
Arg (R)	11	11.2%	Met (M)	3	3.1%
Asn (N)	0	0.0%	Phe (F)	1	1.0%
Asp (D)	3	3.1%	Pro (P)	7	7.1%
Cys (C)	13	13.3%	Ser (S)	8	8.2%
Gln (Q)	1	1.0%	Thr (T)	3	3.1%
Glu (E)	3	3.1%	Trp (W)	0	0.0%
Gly (G)	7	7.1%	Tyr (Y)	2	2.0%
His (H)	0	0.0%	Val (V)	4	4.1%
Ile (I)	0	0.0%	Pyl (O)	0	0.0%
Leu (L)	11	11.2%	Sec (U)	0	0.0%

Table 4 Atomic composition of the TaGASR1 protein

Atomic composition:		
Carbon	C	431
Hydrogen	H	732
Nitrogen	N	138
Oxygen	O	125
Sulphur	S	16

Further details of the amino acids and atomic composition of the TaGASR1 protein sequence are given in Tables 3 and 4. A total of 16 amino acids were formed in the complete structure of the protein, of which Ala, Arg, Cys, and Leu presented relatively high Mole percentages (Table 3). The most prevalent atoms involved in the consensus protein atomic composition, such as 431 carbon atoms, 732 hydrogen atoms, 125 oxygen atoms, 138 nitrogen atoms and only 16 sulphur atoms, are given in Table 4. CELLO v.2.0 revealed the subcellular location of the *TaGASR1* gene in the extracellular matrix with 3.432% reliability, whereas the nuclear region was less reliable at 0.546 (Figure 2A).

Only two open reading frames were detected through the NCBI ORF finder tool in the TaGASR1 protein sequence, one on the positive strand and the second on the negative strand (Figure 2B). A total of 41% alpha helices, zero beta sheets and 16% TM helices were detected during the secondary structure prediction of the consensus protein sequence of TaGASR1 with 20% disorder (Figure 3A). C8C4P9.1 was the template selected to predict the 3D structure of the TaGASR1 protein sequence. This C8C4P9.1 gene encodes a gibberellin-stimulated transcript, the alpha-fold DB model of the wheat (*Triticum aestivum*) *GAST1* gene, and no ligand binding site is detected. The consensus protein sequence showed 95.92% sequence similarity and 100% query coverage with the predicted model C8C4P9.1 sequence (Figure 3D). All the predicted models were further confirmed by plotting a Ramachandran plot through the Vadar tool, which revealed the presence of glycine, proline and preproline amino acid residues,

including 78 in the core region, which was the most favoured region; 6 in the allowed region, 3 in the generous region and 1 in the disallowed region (Figure 3B).

Our consensus protein sequence showed the most favourable protein-protein interactions with the GAST1 protein sequence of *Triticum aestivum*, which encodes gibberellin-stimulated transcript fragments. The consensus protein sequence showed 95.9% identity, a 191.4-bit score value and a lower e value ($1e-48$) with the GAST1 sequence. Furthermore, out of the 10 predicted functional partners, Wcor615, Wrab18 and PP2C also interacted with the cold acclimation protein WCOR615, ABA inducible protein and protein phosphatase 2C (Figure 3C).

Only 12 orthologous species of the *TAGASR1* gene were processed for the analysis of motif domains, and only four conserved motifs were identified in all the sequences, such as PTGRSGSRDEPCPYRDMMLTAGPRKRKPCP, GDAASGFCAG KCAVRCGRSRARGA, CMKYCGLCCEECACV, and AALLLVLLAAASLLQ (Figure 4). Similarly, 20 motifs were observed in TaGASR1 to 37 in an earlier study. Of these, 5 represent the GASA domain, 2 represent the variable region, and 3 represent the peptide signal putative region (Cheng et al. 2019). All the sequences were aligned for pair-wise multiple sequence alignment to interpret SNPs, which are highly similar and less similar in amino acid residues (Figure 5).

All the aligned protein sequences were further processed via the MEGA v.11 software tool. Using the neighbour-joining method, the phylogenetic tree was predicted with a bootstrap value of 1000. Our consensus protein sequence was highly similar to that of only the grass family species, meaning it is highly conserved in Poaceae family crop systems. This study was consistent with earlier studies related to wheat *GASR1* genes and other heat stress (HS)-related genes, and the identified TaGASR1 protein sequence also showed 93% identity with TaGASR1 isolated from the TAM107 wheat variety (Cheng et al. 2019; Kumar et al. 2023).

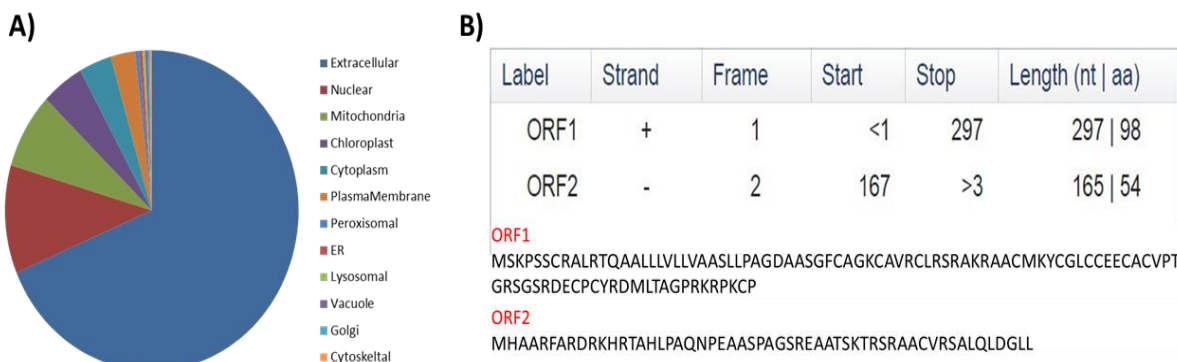


Figure 2 In silico analysis of protein sequences. A) Subcellular location of the TaGASR1 gene; B) presence of open reading frames

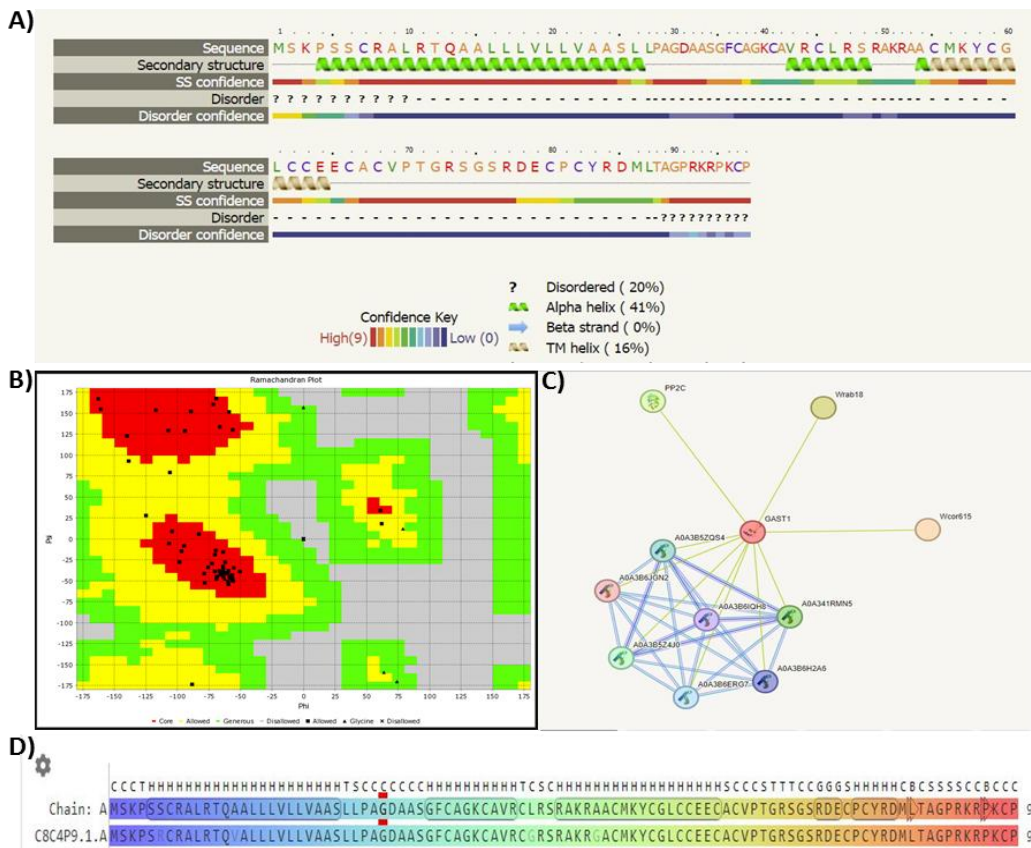


Figure 3 Characterization of the TaGASR1 protein sequence through online tools: A) secondary structure; B) Ramachandran plot; C) protein-protein interaction study via STRING software; D) predicted model template alignment with the consensus protein sequence

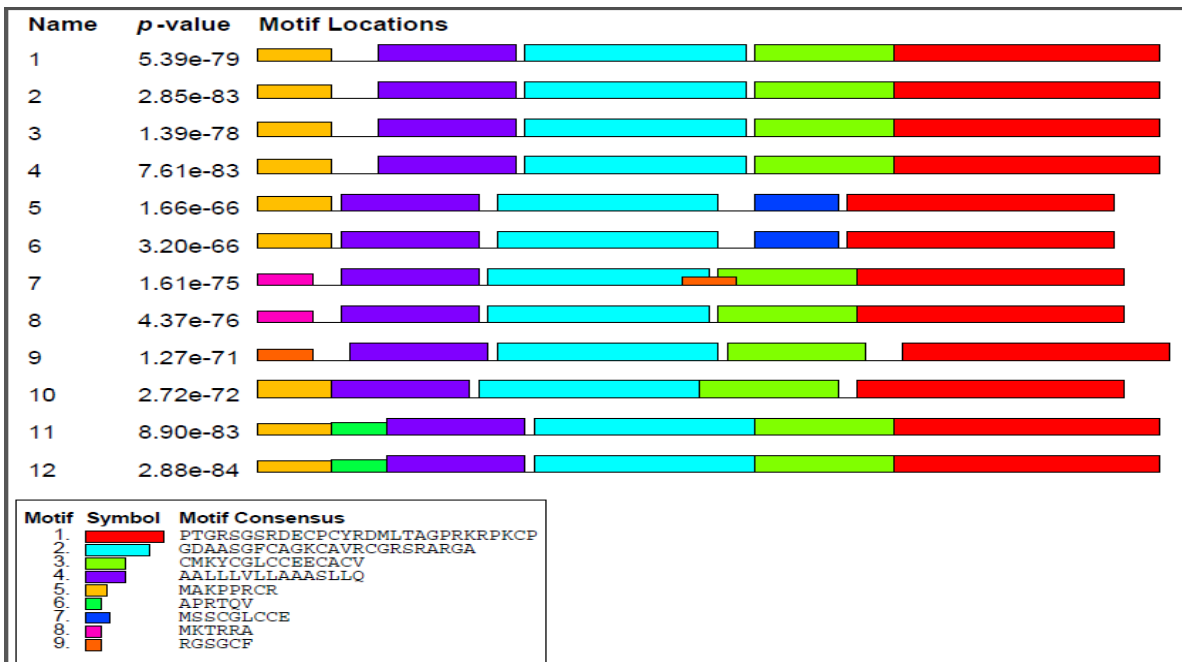
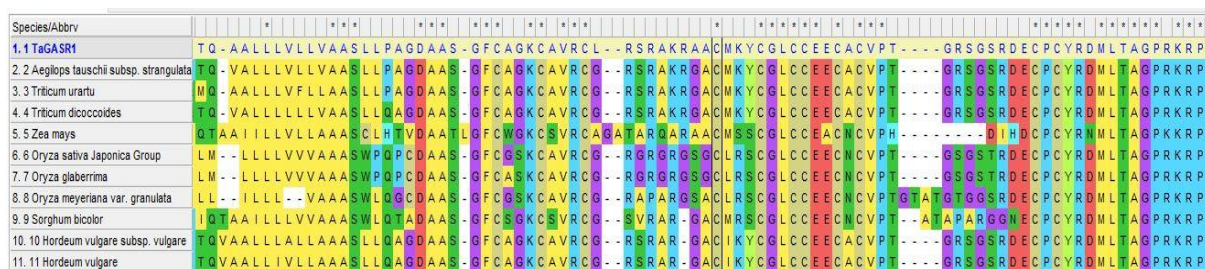
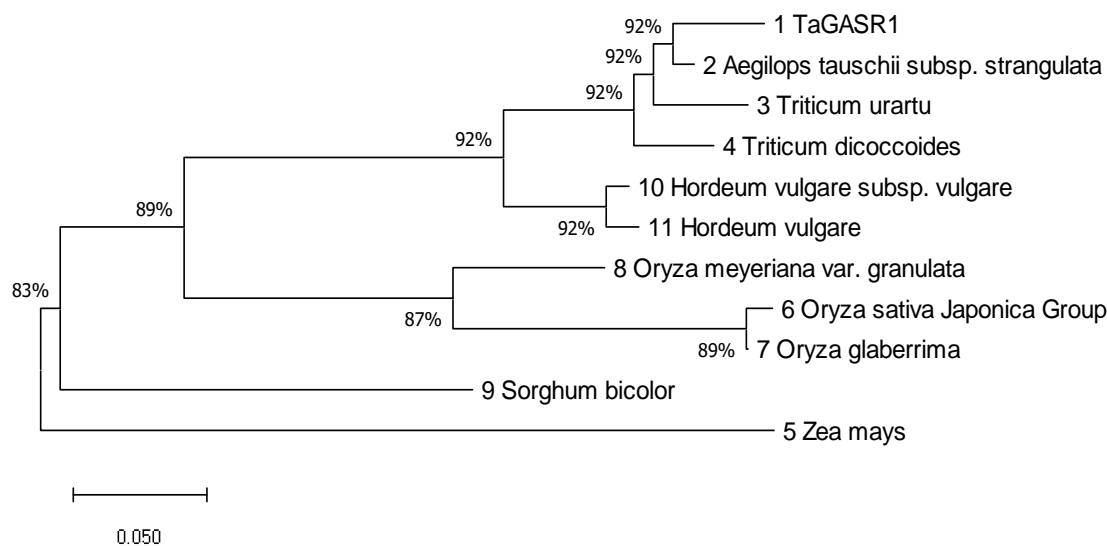


Figure 4 Conserved motif identification in the TaGASR1 protein and its orthologous species

Figure 5 MSA (multiple sequence alignment) of the *TaGASR1* gene with its orthologue speciesFigure 6 Phylogenetic tree prediction of the *TaGASR1* protein with orthologous species via the neighbor-joining method

The protein sequence is closely associated with *Aegilops tauschii* subsp. *Strangulata*, which means that they have higher sequence similarity and query coverage than others. Other species, such as *Triticum urartu*, *Triticum dicoccoides*, *Hordeum vulgare* and *Hordeum vulgare* subsp. *vulgare* were clustered in the same group and presented 92% query coverage. The coverage of the remaining species ranged from 83-89%, indicating a distant evolutionary relationship with the consensus sequence (Figure 6). Similarly, the identified *TaGASR1* protein sequence shares 87-89% identity with the Rice and *Arabidopsis thaliana* GASR proteins, revealing its involvement in abiotic stress tolerance (Cheng et al. 2019; Yang et al. 2023).

Wheat is considered a primary staple food crop compared with other cereal crops because of its high nutritional value and good source of protein, which is 15.1% per 100 g, 364 kcal of calories, 71g of carbohydrates, 20% of vitamins B-6 and minerals (19% of iron, 36% of magnesium and 3% of calcium), etc., per 100 g, which completes the daily diet of the total population of the world (Shewry and Hey 2015; Khalid et al. 2023). All these valuable parameters can be reduced due to extreme temperature exposure, especially during the flowering and grain-filling phases, which

ultimately causes considerable damage to the wheat reproductive stage and leads to a reduction in grain number, quality and weight (Farooq et al. 2011; Jamil et al. 2019; Matsunaga et al. 2021; Ullah et al. 2022). For the identification and isolation of genes responsible for HS, RNA sequencing and *in silico*-based studies are key methods in plant systems (Wang et al. 2009).

In the present study, the *TaGASR1* gene was isolated from the Indian bread wheat variety, known as a heat-tolerant variety; similarly, the same variety, HD3086, was used in an earlier study (Kumar et al. 2023). Gene expression was analyzed through semiquantitative and real-time PCR, and molecular work was subsequently validated via *in-silico* analysis, similar to the pipeline used in earlier studies (Vishwakarma and Sharma 2018; Panzade et al. 2021; Kumar et al. 2023). To the best of our knowledge, this is the first report of *TaGASR1* gene identification from the Indian bread wheat variety HD3086. The expression patterns of the *TaGASR1* gene during the seedling and grain-filling stages under heat stress conditions were investigated for the first time, and the results were consistent with previous studies (Vishwakarma et al. 2018; Kumar et al. 2023). The single peaks formed during the melting curve analysis of the *TaGASR1* gene amplification

products through qRT-PCR confirmed the specificity of the qRT-PCR amplification compared with the use of β -actin as an endogenous control (Padaria et al. 2013; 2014). Several studies have suggested that the genes belonging to the *GASTI* family are always involved in plant development and response to various environmental stresses, including the transition to flowering (Zhang et al. 2009), flower and fruit development (Moyano-Canete et al. 2013), hormonal signal transduction pathways (Rubinovich et al. 2014), and biotic and abiotic stress (Sun et al. 2013; Mao et al. 2011). The consensus protein sequence showed 95.92% sequence similarity and 100% query coverage with the generated template for 3D model prediction through the SWISS-MODEL tool, and the generated template C8C4P9.1 encoded a gibberellin-stimulated transcript, which belongs to the *GASTI* family of genes. Furthermore, our consensus protein sequence also showed higher sequence identity (95.9%) with *GASTI* family proteins analyzed through STRING software, where out of ten functional partners, three showed protein-protein interactions with cold acclimation protein, ABA inducible protein and protein phosphatase 2C, which indicated their involvement in abiotic stress tolerance (Bhaskara et al. 2012; Sah et al. 2016).

Zhang et al. (2017) reported that the overexpression of the *TaGASRI* gene in an *A. thaliana* model plant system provides heat stress tolerance and reduces the accumulation of ROS after heat stress induction. However, the consensus CDS of *TaGASRI* has 93% sequence similarity with the *TaGASRI* previously reported by Zhang et al. (2017). Only hypothetical pathways of *TaGASRI* are known to date, so more studies related to molecular analysis and *in silico* work, which may provide information about its role in the response to thermotolerance or tolerance to other abiotic stresses, are needed. Furthermore, the *TaGASRI* gene can generate transgenic plants with enhanced thermal stability. *In silico* studies related to *TaGASRI* could help researchers identify specific sites to change to improve their functionality at the gene level. BLAST of the consensus protein sequence revealed hits with mostly Poaceae family member species, indicating that this gene was highly conserved in the grass family, and the phylogenetic tree revealed its close evolutionary relationship, with 92% query coverage clustered in the same group. Therefore, *in silico* and real-time PCR-based studies of the *TaGASRI* gene could enhance the understanding of wheat-heat interactions. By introducing this type of GA-stimulated transcript into major cereal staple food crops, climate-smart traits can be developed through transgenic approaches.

Conclusion

In conclusion, the *TaGASRI* gene from the Indian bread wheat variety HD3086 was characterized for heat stress tolerance via real-time PCR and *in silico*-based studies. Multiple sequence alignment and phylogenetic clustering might be helpful to researchers for further studies because of their conserved nature,

especially in the Poaceae family species. Furthermore, the *TaGASRI* gene can generate various climate-adapted crops via transgenic technologies to overcome the adverse impacts of HS.

Acknowledgements

The authors would like to thank the National Institute for Plant Biotechnology, Pusa Campus, New Delhi and Maharishi Markandeshwar (Deemed to be University), and Mullana-Ambala for providing the necessary facilities and encouragement to carry out the work.

Funding declarations

Not applicable.

Conflict of interest

The authors declare no conflicts of interest.

Ethical approval

Not applicable

References

- Altenbach, S. B. (2012). New insights into the effects of high temperature, drought and postanthesis fertilizer on wheat grain development. *Journal of Cereal Science*, *56*, 39–50. <https://doi.org/10.1016/j.jcs.2011.12.012>
- Asseng, S., Foster, I., & Turner, N. C. (2011). The impact of temperature variability on wheat yields. *Global Change Biology*, *17*, 997–1012. <https://doi.org/10.1111/j.1365-2486.2010.02262.x>
- Bailey, T. L., Boden, M., Buske, F. A., Frith, M., Grant, C. E., Clementi, L., & Noble, W. S. (2009). MEME SUITE: tools for motif discovery and searching. *Nucleic acids research*, *37*, W202–W208.
- Bailey, T. L., Johnson, J., Grant, C. E., & Noble, W. S. (2015). The MEME suite. *Nucleic acids research*, *43*(W1), W39–W49. <https://doi.org/10.1093/nar/gkv416>
- Bhaskara, G. B., Nguyen, T. T., & Verslues, P. E. (2012). Unique drought resistance functions of the highly ABA-induced clade A protein phosphatase 2Cs. *Plant Physiology*, *160*, 379–395. <https://doi.org/10.1104/pp.112.202408>
- Chapman, S. C., Chakraborty, S., Dreccer, M. F., & Howden, S. C. (2012). Plant adaptation to climate change-opportunities and priorities in breeding. *Crop and Pasture Science*, *63*, 251–268. <http://dx.doi.org/10.1071/CP11303>
- Cheng, X., Wang, S., Xu, D., Liu, X., Li, X., et al. (2019). Identification and Analysis of the *GASR* Gene Family in Common

- Wheat (*Triticum aestivum* L.) and Characterization of *TaGASR34*, a Gene Associated With Seed Dormancy and Germination. *Frontiers in Genetics*, *10*, 980. <https://doi.org/10.3389/fgene.2019.00980>
- Clavijo, B. J., Venturini, L., Schudoma, C., Accinelli, G. G., Kaithakottil, G., et al. (2017). An improved assembly and annotation of the allohexaploid wheat genome identifies complete families of agronomic genes and provides genomic evidence for chromosomal translocations. *Genome Research*, *27*(5), 885–896. <https://doi.org/10.1101%2Fgr.217117.116>
- Duan, S., Liu, B., Zhang, Y., Li, G., & Guo, X. (2019). Genome-wide identification and abiotic stress-responsive pattern of heat shock transcription factor family in *Triticum aestivum* L. *BMC in Genomics*, *20*, 257. <https://doi.org/10.1186/s12864-019-5617-1>
- Essemine, J., Ammar, S., & Bouzid, S. (2010). Impact of heat stress on germination and growth in higher plants: physiological, biochemical and molecular repercussions and mechanisms of defence. *Journal of Biological Sciences*, *10*, 565–572. <http://dx.doi.org/10.3923/jbs.2010.565.572>
- Farhad, M., Kumar, U., Tomar, V., Bhati, P. K., Krishnan J, N., Berek, V., Brestic, M., & Hossain, A. (2023). Heat stress in wheat: a global challenge to feed billions in the current era of the changing climate. *Frontiers in Sustainable Food Systems*, *7*, 1203721. <https://doi.org/10.3389/fsufs.2023.1203721>
- Farooq, M., Bramley, H., Palta, J. A., & Siddique, K. H. M. (2011). Heat stress in wheat during reproductive and grain filling phases. *Critical Reviews in Plant Science*, *30*, 491–507. <https://doi.org/10.1080/07352689.2011.615687>
- Furukawa, T., Sakaguchi, N., & Shimada, H. (2006). Two *OsGASR* genes, rice GAST homologue genes that are abundant in proliferating tissues, show different expression patterns in developing panicles. *Genes and Genetic System*, *81*, 171–180. <https://doi.org/10.1266/ggs.81.171>
- Gasteiger, E., Hoogland, C., Gattiker, A., Duvaud, S., Wilkins, M. R., Appel, R. D., & Bairoch, A. (2005). Protein identification and analysis tools on the ExPASy server. In: J.M Walker (Eds). *The Proteomics Protocols Handbook* (112, pp. 571–607). Springer Protocols Handbooks, Humana Press, New Jersey, USA. <https://doi.org/10.1385/1-59259-890-0:571>
- Gawdiya, S., Kumar, D., Shivay, Y. S., Radheshyam, Nayak, S., Ahmed, B., & Mattar, M. A. (2023). Nitrogen-Driven Genotypic Diversity of Wheat (*Triticum aestivum* L.) Genotypes. *Agronomy*, *13*(10), 2447. <https://doi.org/10.3390/agronomy13102447>
- Grosse-Heilmann, M., Cristiano, E., Deidda, R., & Viola, F. (2024). Durum wheat productivity today and tomorrow: A review of influencing factors and climate change effects. *Resources, Environment and Sustainability*, *17*, 100170. <https://doi.org/10.1016/j.resenv.2024.100170>
- Guo, M., Lu, J. P., Zhai, Y. F., Chai, W. G., Gong, Z. H., & Lu, M. H. (2015). Genome-wide analysis, expression profile of heat shock factor gene family (*CaHsfs*) and characterization of *CaHsfA2* in pepper (*Capsicum annuum* L.). *BMC Plant Biology*, *15*, 1–20. <https://doi.org/10.1186/s12870-015-0512-7>
- Hatfield, J. L., & John, H. P. (2015). Temperature extremes: Effect on plant growth and development. *Weather and Climate Extremes*, *10*, 4–10. <https://doi.org/10.1016/j.wace.2015.08.001>
- Jamil, M., Ali, A., Gul, A., Ghafoor, A., Napar, A.A., Ibrahim, A. M., Naveed, N. H., Yasin, N. A., & Mujeeb-Kazi, A. (2019). Genome-wide association studies of seven agronomic traits under two sowing conditions in bread wheat. *BMC in Plant Biology*, *19*, 1–18. <https://doi.org/10.1186/s12870-019-1754-6>
- Jiang, C., Bi, Y., Mo, J., Zhang, R., Qu, M., Feng, S., & Essemine, J. (2020). Proteome and transcriptome reveal the involvement of heat shock proteins and antioxidant system in thermotolerance of *Clematis florida*. *Scientific reports*, *10*(1), 8883. <https://doi.org/10.1038/s41598-020-65699-2>
- Khaeim, H., Kende, Z., Balla, I., Gyuricza, C., Eser, A., & Tarnawa, Á. (2022). The effect of temperature and water stresses on seed germination and seedling growth of wheat (*Triticum aestivum* L.). *Sustainability*, *14*(7), 3887. <https://doi.org/10.3390/su14073887>
- Khalid, A., Hameed, A., & Tahir, M. F. (2023). Wheat quality: A review on chemical composition, nutritional attributes, grain anatomy, types, classification, and function of seed storage proteins in bread making quality. *Frontiers in Nutrition*, *10*, 1053196. <https://doi.org/10.3389/fnut.2023.1053196>
- Kosova, K., Vitamvas, P., Prasil, I. T., & Renaut, J. (2011). Plant proteome changes under abiotic stress-contribution of proteomics studies to understanding plant stress response. *Journal of Proteomics*, *74*, 1301–1322. <https://doi.org/10.1016/j.jprot.2011.02.006>
- Kumar, S., Vishwakarma, H., Loitongbam, A., & Aggarwal, D. (2023). Multiprotein-bridging factor 1c from *Triticum aestivum* L. confers tolerance to high-temperature stress in transgenic *Nicotiana tabacum*. *Plant Cell Tissue and Organ Culture*, *154*, 443–456. <https://doi.org/10.1007/s11240-023-02548-w>
- Liu, H., Zeng, B., Zhao, J., Yan, S., Wan, J., & Cao, Z. (2023). Genetic Research Progress: Heat tolerance in Rice. *International Journal of Molecular Science*, *24*(8), 7140. <https://doi.org/10.3390/ijms24087140>

- Livak, K. J., & Schmittgen, T. D. (2001). Analysis of relative gene expression data using real-time quantitative PCR and the $2^{-\Delta\Delta CT}$ method. *Methods*, 25(4), 402-408. <https://doi.org/10.1006/meth.2001.1262>
- Mao, Z. C., Zheng, J. Y., Wang, Y. S., Chen, G. H., Yang, Y. H., Feng, D. X., & Xie, B. Y. (2011). The new CaSn gene belonging to the snakain family induces resistance against root-knot nematode infection in pepper. *Phytoparasitica*, 39, 151-164. <http://dx.doi.org/10.1007/s12600-011-0149-5>
- Masarmi, A. G., Solouki, M., Fakheri, B., Kalaji, H. M., Mahdgingad, N., Golkari, S., & Yousef, A. F. (2023). Comparing the salinity tolerance of twenty different wheat genotypes on the basis of their physiological and biochemical parameters under NaCl stress. *Plos One*, 18(3), e0282606. <https://doi.org/10.1371/journal.pone.0282606>
- Matsunaga, S., Yamasaki, Y., Toda, Y., Mega, R., Akashi, K., & Hjjjoms, T. (2021). Stage-specific characterization of physiological response to heat stress in the wheat cultivar Norin 61. *International Journal of Molecular Science*, 22, 6942. <https://doi.org/10.3390/ijms22136942>
- Moyano-Canete, E., Bellido, M. L., Garcia-Caparrós, N., Medina-Puche, L., Amil-Ruiz, F., Gonzalez-Reyes, J. A., Caballero, J. L., Munoz-Blanco, J., & Blanco-Portales, R. (2013). *FaGAST2*, a strawberry ripening-related gene, acts together with *FaGAST1* to determine cell size of the fruit receptacle. *Plant and Cell Physiology*, 54, 218-236. <https://doi.org/10.1093/pcp/pcs167>
- Ortiz, R., Sayre, K. D., Govaerts, B., Gupta, R., Subbarao, G. V., Ban, T., Hodson, D., Dixon, J. M., Ortiz-Monasterio, J. I., & Reynolds, M. (2008). Climate change: can wheat beat the heat? *Agriculture, Ecosystems and Environment*, 126, 46-58. <https://doi.org/10.1016/j.agee.2008.01.019>
- Padaria, J. C., Bhatt, D., Biswas, K., Singh, G., & Raipuria, R. (2013). In-silico prediction of an uncharacterized protein generated from heat stress responsive SSH library in wheat (*Triticum aestivum* L.). *Plant Omics Journal*, 6, 150-156.
- Padaria, J. C., Vishwakarma, H., Biswas, K., Jasrotia, R. S., & Singh, G. P. (2014). Molecular cloning and in-silico characterization of high temperature stress responsive *pAPX* gene isolated from heat tolerant Indian wheat cv. Raj 3765. *BMC in Research Notes*, 7, 713. <https://doi.org/10.1186/1756-0500-7-713>
- Panzade, K. P., Vishwakarma, H., Awasthi, O. P., & Padaria, J. C. (2021). Molecular cloning and *in silico* analysis of heat stress responsive gene *ClpB1* from *Ziziphus nummularia* genotypes. *Indian Journal of Experimental Biology*, 59, 316-327. <http://nopr.niscpr.res.in/handle/123456789/57223>
- Park, S. W., Lee, B. H., Song, S. H., & Kim, M. K. (2023). Revisiting the Ramachandran plot based on a statistical analysis of static and dynamic characteristics of protein structures. *Journal of Structural Biology*, 215, 107939. <https://doi.org/10.1016/j.jsb.2023.107939>
- Parmar, N., Singh, K. H., Sharma, D., Singh, L., Kumar, P., Nanjundan, J., & Thakur, A. K. (2017). Genetic engineering strategies for biotic and abiotic stress tolerance and quality enhancement in horticultural crops: a comprehensive review. *Biotech*, 7, 1-35. <https://doi.org/10.1007/s13205-017-0870-y>
- Rao, X., Huang, X., Zhou, Z., & Lin, X. (2013). An improvement of the $2^{-\Delta\Delta CT}$ method for quantitative real-time polymerase chain reaction data analysis. *Biostatistics, bioinformatics and biomathematics*, 3(3), 71.
- Roy, S., Maheshwari, N., Chauhan, R., Sen, N. K., & Sharma, A. (2011). Structure prediction and functional characterization of secondary metabolite proteins of *Ocimum*. *Bioinformation*, 6(8), 315. <https://doi.org/10.6026/97320630006315>
- Rubinovich, L., Ruthstein, S., & Weiss, D. (2014). The Arabidopsis Cysteine-Rich GASA5 Is a Redox-Active Metalloprotein that Suppresses Gibberellin Responses. *Molecular Plant*, 7, 244-247. <https://doi.org/10.1093/mp/sst141>
- Sah, S. K., Reddy, K. R., & Li, J. (2016). Abscisic Acid and Abiotic Stress Tolerance in Crop Plants. *Frontiers in Plant Science*, 7, 571. <https://doi.org/10.3389/fpls.2016.00571>
- Schwede, T., Kopp, J., Guex, N., & Peitsch, M. C. (2003). SWISS-MODEL: an automated protein homology -modelling server. *Nucleic Acids Research*, 31(13), 3381-3385.
- Sarkar, S., Islam, A. A., Barma, N. C. D., & Ahmed, J. U. (2021). Tolerance mechanisms for breeding wheat against heat stress: A review. *South African Journal of Botany*, 138, 262-277. <https://doi.org/10.1016/j.sajb.2021.01.003>
- Shewry, P. R., & Hey, S. J. (2015). The contribution of wheat to human diet and health. *Food and energy security*, 4(3), 178-202. <https://doi.org/10.1002/fes3.64>
- Sun, S., Wang, H., Yu, H., Zhong, C., Zhang, X., Peng, J., & Wang, X. (2013). GASA14 regulates leaf expansion and abiotic stress resistance by modulating reactive oxygen species accumulation. *Journal of Experimental Botany*, 64, 1637-1647. <https://doi.org/10.1093/jxb/ert021>
- Szklarczyk, D., Gable, A. L., Lyon, D., Junge, A., Wyder, S., & Huerta-Cepas, J. (2019). STRING v11: protein-protein association networks with increased coverage, supporting functional discovery

- in genome-wide experimental datasets. *Nucleic Acids Research*, 47(D1), D607–D613. <https://doi.org/10.1093/nar/gky1131>
- Tamura, K., Stecher, G., & Kumar, S. (2021). MEGA11: Molecular Evolutionary Genetics Analysis Version 11. *Molecular Biology and Evolution*, 38(7) 3022–3027. <https://doi.org/10.1093/molbev/msab120>
- Tripathi, A., Tripathi, D. K., Chauhan, D. K., Kumar, N., & Singh, G. S. (2016). Paradigms of climate change impacts on some major food sources of the world: a review on current knowledge and future prospect. *Agriculture Ecosystems and Environment*, 216, 356–373. <https://doi.org/10.1016/j.agee.2015.09.034>
- Ullah, A., Nadeem, F., Nawaz, A., Siddique, K. H. M., & Farooq, M. (2022). Heat Stress effects on the reproductive physiology and yield of wheat. *Journal of Agronomy and Crop Science*, 208, 1–17. <https://doi.org/10.1111/jac.12572>
- Villalobos-López, M. A., Arroyo-Becerra, A., Quintero-Jiménez, A., & Iturriaga, G. (2022). Biotechnological advances to improve abiotic stress tolerance in crops. *International Journal of Molecular Sciences*, 23(19), 12053. <https://doi.org/10.3390/ijms231912053>
- Vishwakarma, H., & Sharma, J. (2018). Real time and in-silico based analysis of heat stress responsive transcription factor *MBF1c* from wheat. *International Journal of Advanced Scientific Research and Management*, 3(11), 2455–6378.
- Vishwakarma, H., Junaid, A., Manjhi, J., Singh, G. P., Gaikwad, K., & Padaria, J. C. (2018). Heat stress transcripts, differential expression, and profiling of heat stress tolerant gene *TaHsp90* in Indian wheat (*Triticum aestivum* L.) cv. C306. *PLoS One*, 13(6):e0198293. <https://doi.org/10.1371/journal.pone.0198293>
- Wang, X., Yan, B., Shi, M., Zhou, W., Zekria, D., Wang, H., & Kai, G. (2016). Over expression of a *Brassica campestris* HSP70 in tobacco confers enhanced tolerance to heat stress. *Protoplasma*, 253(3), 637–645. <https://doi.org/10.1007/s00709-015-0867-5>
- Wang, Z., Gerstein, M., & Snyder, M. (2009). RNA-Seq: a revolutionary tool for transcriptomics. *Nature reviews genetics*, 10(1), 57–63. <https://doi.org/10.1038/nrg2484>
- Yang, M., Liu, C., Zhang, W., Wu, J., Zhong, Z., Yi, W., & He, Y. (2023). Genome-Wide Identification and Characterization of Gibberellic Acid-Stimulated Arabidopsis Gene Family in Pineapple (*Ananascomosus*). *International Journal of Molecular Sciences*, 24(23), 17063. <https://doi.org/10.3390/ijms242317063>
- Yu, C. S., Chen, Y. C., Lu, C. H., & Hwang, J. K. (2006). Prediction of protein subcellular localization. *Proteins: Structure, Function and Bioinformatics*, 64, 643–651. <https://doi.org/10.1002/prot.21018>
- Yu, C. S., Cheng, C. W., Su, W. C., Chang, K. C., Huang, S. W., Hwang, J. K., & Lu, C. H. (2014). CELLO2GO: a web server for protein subCELlularLOCALization prediction with functional gene ontology annotation. *PloS one*, 9(6), e99368. <https://doi.org/10.1371/journal.pone.0099368>
- Zhang, L., Geng, X., Zhang, H., Zhou, C., Zhao, A., Wang, F., & Peng, H. (2017). Isolation and characterization of heat-responsive gene *TaGASRI* from wheat (*Triticum aestivum* L.). *Journal of Plant Biology*, 60, 57–65. <https://doi.org/10.1007/s12374-016-0484-7>
- Zhang, S., Yang, C., Peng, J., Sun, S., & Wang, X. (2009). *GASA5*, a regulator of flowering time and stem growth in *Arabidopsis thaliana*. *Plant Molecular Biology*, 69, 745–759. <https://doi.org/10.1007/s11103-009-9452-7>
- Zheng, B., Chenu, K., Dreccer, M. F., & Chapman, S. C. (2012). Breeding for the future: what are the potential impacts of future frost and heat events on sowing and flowering time requirements for Australian bread wheat (*Triticum aestivum*) varieties? *Global Change Biology*, 18, 2899–2914. <https://doi.org/10.1111/j.1365-2486.2012.02724.x>



Journal of Experimental Biology and Agricultural Sciences

<http://www.jebas.org>

ISSN No. 2320 – 8694

Exploring the Phosphate Solubilising Rhizobacteria isolated from Wild *Musa* Rhizosphere and their Efficacy on Growth Promotion of *Phaseolus vulgaris*

Mum Tatung , Chitta Ranjan Deb* 

Department of Botany, Nagaland University, Lumami 7098627, Nagaland, India

Received – July 04, 2024; Revision – September 08, 2024; Accepted – October 28, 2024

Available Online – November 29, 2024

DOI: [http://dx.doi.org/10.18006/2024.12\(5\).742.755](http://dx.doi.org/10.18006/2024.12(5).742.755)

KEYWORDS

Biofertilizer

IAA production

PGPR

Phosphate solubilisation

Siderophore production

Wild *Musa* rhizosphere

ABSTRACT

Plant growth-promoting rhizobacteria (PGPR) are recognized for enhancing plant growth, protecting against pathogens, and boosting productivity. The present study focused on isolating PGPR from the rhizosphere of wild *Musa*, screening for growth-promoting traits, and assessing their effects on the growth of *Phaseolus vulgaris* L. A total of 20 strains were isolated and evaluated for their capacity to solubilize phosphate, produce indole-3-acetic acid (IAA), synthesize siderophores, and their tolerance to salt and heavy metals. Among 20 isolates, four most effective isolates were selected and based on 16S rRNA sequencing these isolates were identified as: *Burkholderia cepacia* (RZ27), *Agrobacterium larrymoorei* (RZ23), *Pseudomonas taiwanensis* (RZ5), and *Pseudomonas orientalis* (RZ3). *P. orientalis* exhibited the highest phosphate solubilization ability (222.17 µg/ml), followed closely by *B. cepacia* (222.80 µg/ml), *A. larrymoorei* (71.57 µg/ml), and *P. taiwanensis* (19.20 µg/ml). Isolate RZ27 demonstrated the greatest salt tolerance at 14%, followed by RZ5 and RZ23 (10% each) and RZ3 (6%). Notably, only isolate RZ23 produced IAA, while all isolates except RZ27 could produce siderophores. The highest siderophore production was recorded with RZ23 (33.34% siderophore production unit, SPU), followed by RZ3 (29.07 SPU) and RZ5 (27.20 SPU). *A. larrymoorei* and *P. orientalis* showed the highest chromium tolerance (1840 µg/ml), followed by *B. cepacia* (1810 µg/ml) and *P. taiwanensis* (1300 µg/ml). There was a noticeable enhancement in plant growth when *P. vulgaris* was inoculated with the PGPR strains. Among the four isolates, RZ3 significantly increased both shoot and root lengths and biomass compared to the control; meanwhile, isolate RZ23 improved shoot fresh weight. These findings suggest that these isolates have the potential to be used as bioinoculants to improve plant development.

* Corresponding author

E-mail: debchitta@rediffmail.com, debchitta@gmail.com (Chitta Ranjan Deb)

Peer review under responsibility of Journal of Experimental Biology and Agricultural Sciences.

Production and Hosting by Horizon Publisher India [HPI]
 (<http://www.horizonpublisherindia.in/>).
 All rights reserved.

All the articles published by [Journal of Experimental Biology and Agricultural Sciences](#) are licensed under a [Creative Commons Attribution-NonCommercial 4.0 International License](#) Based on a work at www.jebas.org.



1 Introduction

Rhizobacteria found in the plant rhizosphere have the potential to improve plant growth. These beneficial microorganisms are plant growth-promoting rhizobacteria (PGPR) (Tatung and Deb 2024a; Deb and Tatung 2024; Megu et al. 2024a). PGPR interacts with plant roots and enhances growth through various mechanisms, including improved nutrient uptake (Qingwei et al. 2023), hormone production (Deb and Tatung 2024), siderophore production, and suppression of soil-borne diseases (Tatung and Deb 2023; 2024a, b; Qingwei et al. 2023; Deb and Tatung 2024; Megu et al. 2024a, b; Pongener et al. 2024).

Modern farming practices rely heavily on synthetic fertilizers and pesticides for higher yields. However, excessive chemical fertilizers can lead to soil degradation and environmental pollution (Aktar et al. 2021; Deb and Tatung 2024). Numerous studies have indicated that PGPR can mitigate the adverse effects of chemical fertilizers and serve as a viable alternative for sustainable agriculture (Tatung and Deb 2023; 2024a, b; Qingwei et al. 2023; Deb and Tatung 2024). For instance, Oo et al. (2020) reported that *Acromobacter insolitus* enhanced the seed germination of *Vigna radiata* and *Zea mays*, while *Pseudomonas plecoglossicida* increased the fresh weight of both crops. *Acromobacter insolitus* and *Enterobacter hormaechei* also improved maize and green gram root formation. Yamini et al. (2021) found that PGPR-derived phytohormones were more effective than crude hormones in promoting plant growth. Moreover, PGPR isolates such as *Staphylococcus* sp. and *Bacillus* sp. effectively ameliorated plant stress responses and enhanced the height of *Vallisneria natans* when subjected to sediment organic matter stress (Wang et al. 2021). In terms of stress adaptation, *Helianthus annuus*, and *Brassica juncea*, when grown under heavy metal contamination (Cd/Cu) and inoculated with PGPR consortia, showed improved growth characterized by enhanced shoot and root length, as well as increased fresh and dry weights (Tatung and Deb 2024a). In another study, Khanna et al. (2019) demonstrated that *Pseudomonas aeruginosa* and *Burkholderia gladioli* improved the seedling growth of *Lycopersicon lycopersicum* under Cd stress (0.4 mM). Additionally, *Bacillus aryabhatai* and *B. tequilensis*, both high salt-tolerant PGPR strains, boosted photosynthesis, transpiration, and stomatal conductance in rice plants, leading to increased yields (Shultana et al. 2020). Tatung and Deb (2023) noted that inoculating *Cicer arietinum* with *Kosakonia arachidis*, *Pseudomonas putida*, and *P. monteilii* increased growth compared to the control treatment. Lastly, *Cupriavidus necator*, either alone or in combination with *P. fluorescens*, improved shoot biomass, and enhanced phosphorus (P) and nitrogen (N) use efficiency in maize under water stress conditions (Pereira et al. 2020).

Cultivated *Musa* varieties are susceptible to various diseases, necessitating regular replacement of stock plants. In contrast, wild

bananas tend to thrive year after year with minimal infection. This resilience may be attributed to plant growth-promoting rhizobacteria (PGPR) associated with the rhizosphere of wild *Musa*, which helps mitigate different pathogens affecting these plants (Tatung and Deb 2023, 2024a).

Phaseolus vulgaris, commonly known as common beans, is an important food legume globally, with an annual production value of \$5.717 billion and a yield exceeding 12 million tons (FAO). However, the cultivation of common beans faces significant challenges, including high temperatures, drought, and various phytopathogens (Uebersax et al. 2023). Shockingly, approximately 143.88 million tons of chemical fertilizers are used worldwide to enhance crop production (Rana et al. 2011). Unfortunately, prolonged use of these fertilizers degrades soil quality and has adverse effects (Khurana and Kumar 2022). In light of these concerns, this study aimed to isolate PGPR from the rhizosphere of wild *Musa*, screen the isolates for beneficial traits, and conduct cross-inoculation of the selected isolates in *P. vulgaris* to investigate their potential for promoting plant growth.

2 Materials and Methods

2.1 Isolation of rhizobacteria

Rhizospheric soil was collected from the rhizosphere of *Musa balbisiana* at a depth of 15-20 cm from plants growing on the Nagaland University campus in Lumami, Nagaland, India. Care was taken to ensure the roots remained intact during the collection process. After gently shaking the soil from the roots, the collected soil was placed in sterile polythene bags to isolate rhizospheric bacteria further. A serial dilution technique was employed to isolate the rhizospheric bacteria. One gram of the soil sample was mixed with 10 ml of distilled water, and serial dilutions were carried out until a dilution of 10^{-5} was achieved. Forty milliliters of nutrient agar medium (composed of 20 g/L agar, 5 g/L sodium chloride, 10 g/L yeast extract, and 10 g/L peptide) was poured into Petri dishes. The medium was streaked with the diluted soil samples and incubated for three days at $28 \pm 2^\circ\text{C}$. Bacterial isolates were selected based on their physical characteristics and subcultured until pure cultures were obtained. A portion of these pure cultures was stored at -60°C in an 80% glycerol stock solution for future use.

2.2 Morphological studies and biochemical test of the bacterial isolates

Isolated bacterial strains were examined for their colony morphology characteristics, including elevation, shape, transparency, and colour. Twenty bacterial isolates from the mixed culture were subjected to a third-generation pure culture and used for biochemical tests. These tests included motility, Gram staining, methyl red testing, citrate

utilization, starch hydrolysis, catalase production, and sugar fermentation ability, as described by Tatung and Deb (2023).

2.3 Evaluation for plant growth promoting characteristics of isolates

To evaluate the isolated rhizobacteria as potential plant growth-promoting rhizobacteria (PGPR), they were subjected to tests for heavy metal (chromium) tolerance, salinity tolerance, IAA production, siderophore production, and phosphate solubilization capability.

2.3.1 Qualitative estimation of phosphate solubilization

The phosphate (NBRIP) growth medium developed by the National Botanical Research Institute was utilized to evaluate the phosphate solubilization capability of certain isolates. The culture medium consisted of the following components: 10 g/L glucose, 5 g/L $\text{Ca}_3(\text{PO}_4)_2$, 5 g/L $\text{MgCl}_2 \cdot 6\text{H}_2\text{O}$, 0.25 g/L $\text{MgSO}_4 \cdot 7\text{H}_2\text{O}$, 0.2 g/L KCl, 0.2 g/L $(\text{NH}_4)_2\text{SO}_4$, and 15 g/L water (You et al. 2020). The isolates were cultured on NBRIP agar plates for 7 days at $28 \pm 2^\circ\text{C}$. Phosphate-solubilizing isolates were identified by a distinct halo zone surrounding their colonies.

2.3.2 Quantitative assay of phosphate solubilization

Quantitative analysis of phosphate solubilization was conducted in a liquid NBRIP medium, following the method outlined by Pande et al. (2017). Phosphate solubilization was measured using 10 ml of NBRIP broth, which had the following composition (in g/L): 10 g of glucose, 5 g of $\text{Ca}_3(\text{PO}_4)_2$, 5 g of $\text{MgCl}_2 \cdot 6\text{H}_2\text{O}$, 0.25 g of $\text{MgSO}_4 \cdot 7\text{H}_2\text{O}$, 0.2 g of KCl, 0.1 g of $(\text{NH}_4)_2\text{SO}_4$, with the pH adjusted to 7.0. A control was prepared using NBRIP broth alone. Freshly cultured bacterial colonies were incubated in the NBRIP broth for 12 days at $28 \pm 2^\circ\text{C}$ to test the strains.

After incubation, 1 ml of supernatant was collected on the 2nd, 4th, 6th, 8th, 10th, and 12th days. The suspension cultures were centrifuged at 10000 rpm for 5 minutes, and the supernatants were collected and filtered for quantification. Approximately 600 μL of the filtered supernatant was mixed with 1500 μL of Barton's reagent, and the volume was adjusted to 5 ml with double-distilled water. This mixture was allowed to rest for 10 minutes. After the resting period, the intensity of the yellow colour was measured using a spectrophotometer (Thermo Scientific Multiskan Go) at a wavelength of 430 nm. The amount of phosphate solubilized was determined from a standard curve. The experiments were conducted in triplicate, and the results were expressed as mean values.

2.3.3 Qualitative analysis of siderophore production

For qualitative analysis of siderophore production, isolates were cultured on CAS agar medium for seven days (Tatung and Deb

2023). The presence of an orange ring surrounding the bacterial colonies indicated siderophore production.

2.3.4 Quantitative analysis of siderophore production

Each isolate was cultured in CAS nutrient broth for 10 days at $28 \pm 2^\circ\text{C}$. After the culture period, 2 μL samples from each isolate were collected every two days and centrifuged at 1000 rpm for 10 minutes. The supernatant was then collected, and its absorbance was measured at 630 nm using a microplate reader. The production of siderophores by the strains was calculated using the formula provided by Payne (1993):

$$\text{Percent Siderophore Unit (PSU)} = \frac{(A_r - A_s) \times 100}{A_r}$$

Where A_r - Reference Absorbance (Uninoculated broth +CAS reagent), A_s - Sample Absorbance (Sample's Cell-free supernatant +CAS solution).

2.3.5 IAA production

For the qualitative assessment of indole-3-acetic acid (IAA) production, 10 ml of nutrient broth supplemented with 0.1% w/v tryptophan was inoculated with freshly grown bacterial cultures and incubated at a temperature of $28 \pm 2^\circ\text{C}$ for 7 days. A control was set up using 10 ml of nutrient broth with 0.1% tryptophan but without bacterial inoculation. On the 7th day, 1 ml of the culture was taken and centrifuged for 5 minutes at 10000 rpm. The supernatant was then transferred to a vial containing 2 ml of Salkowski reagent. After incubating for 25 minutes, cultures that produced a pink colour were identified as positive for IAA production, while those that did not show any colour change were considered negative (Tatung and Deb 2023).

2.3.6 Salinity tolerance

The salinity tolerance level of the isolates was tested following Sharma et al. (2021a). Bacterial isolates were cultured on a nutrient agar medium fortified with different concentrations of sodium chloride (NaCl) (2-14%) with an increment of 2% and cultured for 72 h at $28 \pm 2^\circ\text{C}$. Isolates continued to grow on the NaCl-enriched medium, indicating their tolerance level.

2.3.7 Heavy metal tolerance (Chromium)

Bacterial isolates were evaluated for heavy metal tolerance using the minimum inhibitory concentration (MIC) method (Yadav et al. 2022). Nutrient agar plates were supplemented with various chromium concentrations, ranging from 30 to 2000 $\mu\text{g/ml}$ in increments of 30 μg . The plates were streaked with the bacterial isolates and incubated at $28 \pm 2^\circ\text{C}$ for 72 hours. A negative control plate without chromium was also inoculated and incubated for comparative purposes.

2.4 Molecular characterization of the isolates

Colony PCR targeted the 16S rRNA gene for partial sequencing to identify bacterial isolates. Freshly streaked bacterial cultures were grown on nutrient agar media for 24 hours. Colonies were picked using disinfected toothpicks and then suspended in 60 µL of Triton X-100 buffer in PCR tubes. This suspension was boiled for 10 to 15 minutes, followed by freezing for 2 to 3 minutes. After freezing, the samples were centrifuged for 3 to 4 minutes at 10000 rpm. PCR amplification of the target sequence was conducted using specific primers: the 1492R reverse primer and the 18F forward primer, as described by Tatum and Deb (2024a). The PCR mixture included 0.6 µL of dNTPs, 3 µL of buffer, 21.7 µL of sterile deionized water, 3 µL of the template, and 1 µL of Taq DNA polymerase. The PCR reaction was carried out using a Bio-Rad thermal cycler, starting with an initial denaturation at 95°C, followed by 30 cycles consisting of denaturation at 94°C for 50 seconds, annealing at 55°C for 90 seconds, and extension at 72°C for 1 minute, concluding with a final extension at 72°C for 3 minutes. The PCR products were analyzed using a 1% (w/v) agarose gel and subsequently sequenced. The resulting gene sequences were compared with those in the GenBank database using NCBI BLAST. The sequences were then submitted to the NCBI GenBank database for accession numbers. A phylogenetic tree was created using MEGA11 software.

2.5 Pot experiment

The growth-promoting abilities of four bacterial isolates were evaluated using *Phaseolus vulgaris* as a model plant. The isolates included strain RZ3 (*Pseudomonas orientalis*), strain RZ5 (*Pseudomonas taiwanensis*), strain RZ23 (*Aureobasidium larrymoorei*), and strain RZ27 (*Burkholderia cepacia*). A fully randomized design was implemented, featuring a control group and four treatment groups: C (control with no PGPR), RZ3, RZ5, RZ23, and RZ27. The potting mixture was prepared using a 1:1 ratio of soil and sand. This soil-sand mixture was then disinfected by autoclaving for 30 minutes at 121 psi before being placed in plastic pots. In each pot, 10 sterilized seeds were inoculated with different rhizobacterial isolates and allowed to germinate. After germination, the seedlings were thinned to three plants per pot. The control pots contained non-inoculated seeds. The plants were watered regularly with sterilized tap water. After 30 days, the

effects of the rhizobacteria on seedling growth were assessed. The plants were uprooted, and growth parameters, including root and shoot lengths and the fresh and dry weights of both shoots and roots, were compared.

2.6 Statistical analysis

Statistical analysis of the data was conducted using IBM SPSS Statistics software. The results are presented as the mean of three replicates ± standard error of the mean (SEM). The data were further analyzed with a one-way ANOVA. For significant F values, post hoc comparisons were carried out using the Least Significant Difference (LSD) test at a significance level of $P \leq 0.05$. Graphs were created using Microsoft Excel software.

3 Results

3.1 Isolation of the PGPR

From the mixed culture plates, 20 bacterial isolates were selected based on the morphological characteristics of bacterial colonies for raising pure cultures (Table 1). Third-generation pure cultures of the rhizobacterial isolates were considered for biochemical analysis (Table 2). Growth-promoting traits such as phosphate solubilization, IAA and siderophore production, chromium, and salt tolerance were tested for all isolated isolates. Subsequently, four best-performing bacterial isolates (R27, RZ23, RZ5, and RZ3) were chosen for inoculation onto *P. vulgaris* to evaluate their effects on various growth parameters.

3.2 Morphological and biochemical analysis of the bacterial isolates

Colony morphology characteristics, such as size, shape, colour, and growth pattern, were evaluated after 24 hours of growth on nutrient agar plates. There was significant variation in the colour and transparency of the bacterial colonies. All isolates, except for RZ23, which had a yellow colony, appeared off-white and opaque. Isolate RZ27 formed a raised colony, while the other three isolates produced flat colonies. The margins of the colonies also varied among the isolates; RZ27 had a regular margin, RZ23 had an entire margin, RZ5 had an undulate margin, and RZ3 exhibited a serrated margin. All isolates had round colonies except for RZ3, which had an irregular shape.

Table 1 Colony morphology of the bacterial isolates

Bacterial Isolates	Margin	Elevation	Shape	Colour	Transparency	Identification	Gen Bank Accession No.
RZ27	Regular	Raised	Round	Off-white	Opaque	<i>B. cepacia</i>	OL662932
RZ23	Entire	Flat	Round	Yellowish	Opaque	<i>A. larrymoorei</i>	OL662933
RZ5	Undulate	Flat	Round	Off-white	Opaque	<i>P. taiwanensis</i>	OL662931
RZ3	Serrated	Flat	Irregular	Off-white	Opaque	<i>P. orientalis</i>	OL662936

Table 2 Biochemical analysis of the isolated bacterial isolates

Bacterial isolates	Gram staining	Motility	Starch hydrolysis	Catalase test	Methyl red	Citrate utilization
RZ27	-	+	+	+	-	-
RZ23	-	+	-	+	-	-
RZ5	-	+	-	+	-	+
RZ3	-	+	+	+	-	+

'+' indicates positive, '-' indicates negative

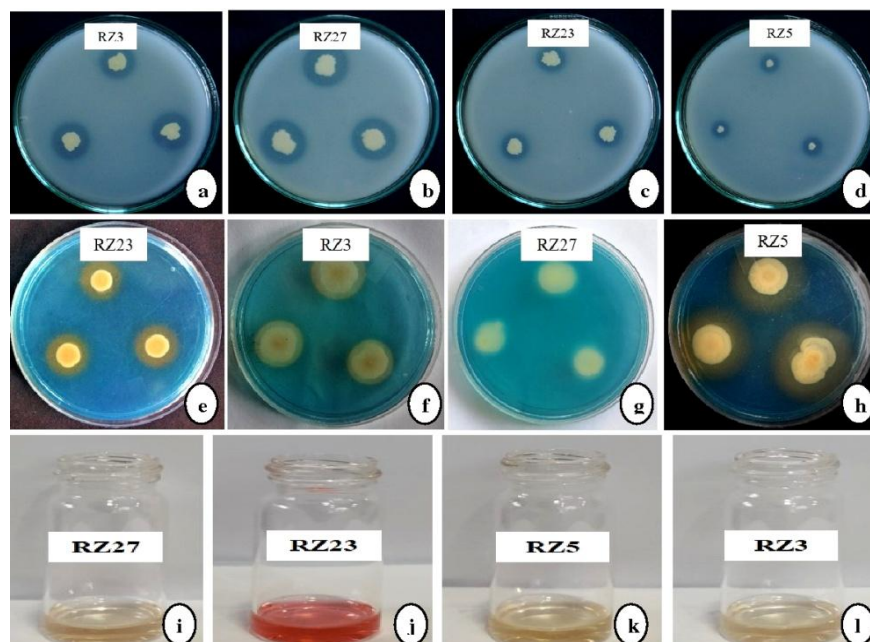


Figure 1 (a-d) Phosphate solubilization by the bacterial isolates a. RZ3, b. RZ27, c. RZ23, and d. RZ5 on NBRIP agar media indicated the development of a clear halo zone around the bacterial colony. e-h: Siderophore production test by the bacterial isolates on CAS-agar media e. RZ23, f. RZ3, g. RZ27, and h. RZ5. i-l: IAA production test by the bacterial isolates in Nutrient broth supplemented with 0.1% of L-tryptophan by the bacterial isolates i. RZ27, j. RZ23, k. RZ5, and l. RZ3.

Biochemical analysis indicated that all four isolates were gram-negative. They showed negative results in the methyl red test but tested positive in the catalase test and were found to be motile. Isolates RZ27 and RZ3 tested positive for starch hydrolysis, while RZ23 and RZ5 tested negative. Furthermore, isolates RZ27 and RZ23 were negative for citrate utilization, whereas RZ5 and RZ3 were positive (Tables 1 and 2).

3.3 Plant growth promoting screening

3.3.1 Phosphate solubilization

After incubating for 7 days on NBRIP agar plates containing tricalcium phosphate [$\text{Ca}_3(\text{PO}_4)_2$] as the sole phosphate source, 12 bacterial isolates demonstrated phosphate solubilizing activity. Four isolates with the highest phosphate solubilizing ability were taken for further analysis (Figure 1 a-d). Quantitative analysis revealed that isolate RZ3 exhibited the highest phosphate

solubilization ($337.11 \pm 0.58 \mu\text{g/ml}$), followed by RZ27 ($222.80 \pm 0.30 \mu\text{g/ml}$), RZ23 ($71.57 \pm 0.56 \mu\text{g/ml}$), and RZ5 ($19.20 \pm 0.33 \mu\text{g/ml}$). It was observed that with the increase of phosphate in the medium, the pH decreased, and among the tested isolates, culture with isolate RZ3 was found to have the lowest pH (4.23 ± 0.03), followed by RZ27 (4.45 ± 0.03), RZ23 (5.53 ± 0.02), and RZ5 (6.23 ± 0.01) (Tables 3 and 4).

3.3.2 Siderophore production

When tested for siderophore production on CAS agar plates, all isolates except RZ27 registered positive results (Figure 1 e-h). The development of an orange halo zone surrounding the colonies indicated siderophore production ability and served as a marker for positive isolates. Quantitative analysis revealed that RZ23 had the maximum production of siderophore ($33.34 \pm 0.03 \mu\text{g/ml}$) among the three positive isolates, followed by RZ3 ($29.07 \pm 0.09 \mu\text{g/ml}$) and RZ5 ($27.20 \pm 0.02 \mu\text{g/ml}$) on the 10th day of incubation.

Table 3 Growth-promoting traits of the bacterial isolates

Bacterial Isolates	Identification	IAA Production	Phosphate Solubilization	Siderophore Production	NaCl Tolerance (%)	Chromium Tolerance ($\mu\text{g/ml}$)
RZ27	<i>B. cepacian</i>	-	+	-	14	1810
RZ23	<i>A. larrymoorei</i>	+	+	+	10	1840
RZ5	<i>P. taiwanensis</i>	-	+	+	10	1300
RZ3	<i>P. orientalis</i>	-	+	+	6	1840

Note: '+' : Indicates positive, '-' : Indicates negative.

Table 4 Quantification of phosphate solubilization characteristics of the selected bacterial isolates under culture condition

Bacterial Isolates	Concentration of PO_4 ($\mu\text{g/ml}$)						pH of the medium					
	2 nd day	4 th day	6 th day	8 th day	10 th day	12 th day	2 nd day	4 th day	6 th day	8 th day	10 th day	12 th day
RZ27	43.18 \pm 0.25	88.41 \pm 0.09	109.79 \pm 0.77	165.27 \pm 1.07	222.80 \pm 0.32	108.09 \pm 0.13	4.95 \pm 0.03	4.71 \pm 0.01	4.54 \pm 0.02	4.47 \pm 0.04	4.45 \pm 0.03	4.24 \pm 0.01
RZ5	18.83 \pm 0.09	19.20 \pm 0.33	18.46 \pm 0.17	17.66 \pm 0.34	15.24 \pm 0.04	14.32 \pm 0.04	6.32 \pm 0.01	6.23 \pm 0.01	6.41 \pm 0.03	6.49 \pm 0.01	6.51 \pm 0.04	6.51 \pm 0.02
RZ23	19.28 \pm 0.31	29.24 \pm 0.43	46.86 \pm 0.28	57.47 \pm 0.41	64.85 \pm 0.70	71.57 \pm 0.56	5.93 \pm 0.02	5.85 \pm 0.01	5.34 \pm 0.01	5.31 \pm 0.02	5.25 \pm 0.01	4.23 \pm 0.03
RZ3	78.54 \pm 0.60	129.09 \pm 0.43	187.55 \pm 1.66	199.92 \pm 0.95	337.11 \pm 0.58	324.88 \pm 2.63	6.16 \pm 0.02	5.93 \pm 0.01	5.76 \pm 0.01	5.64 \pm 0.03	5.53 \pm 0.02	5.47 \pm 0.02

* Data was expressed as mean values of the three replicates with standard error.

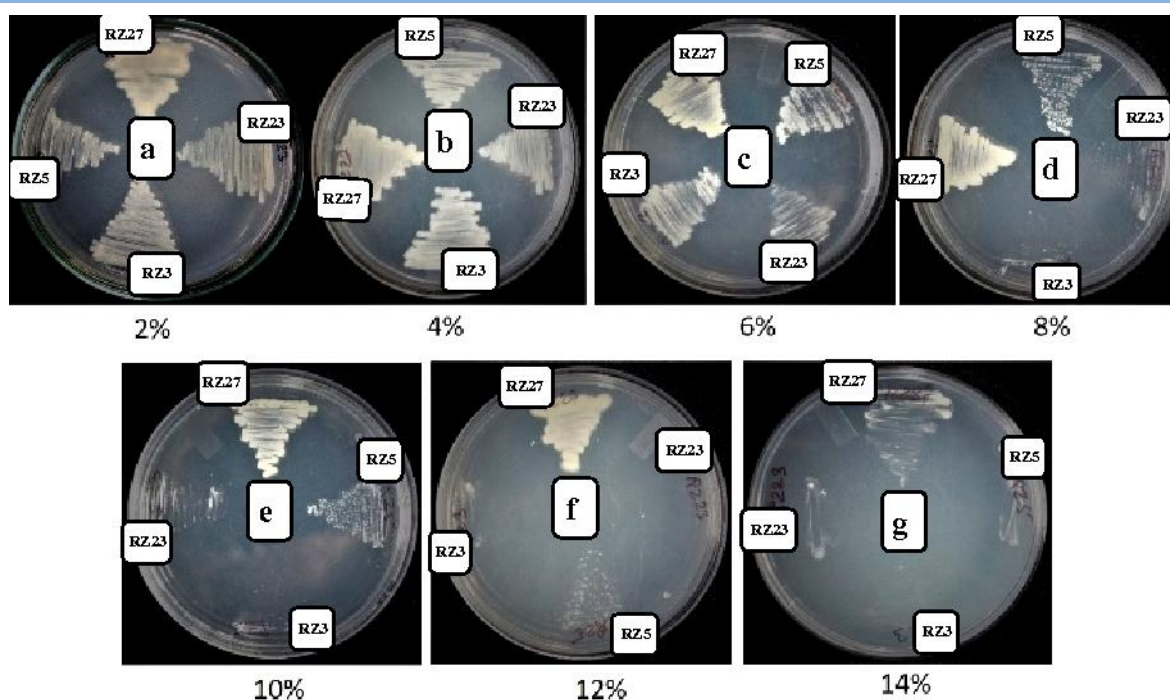


Figure 2 Salinity tolerance test of the bacterial isolates RZ27, RZ23, RZ5, and RZ3 on nutrient agar medium supplemented with different concentrations of NaCl (a. 2%, b. 4%, c. 6%, d. 8%, e. 10%, f. 12% and g. 14%, w/v).

3.3.3 Production of indole-3-acetic acid

Bacterial isolates underwent qualitative testing for IAA production, revealing that isolate RZ23 only produced IAA, and the remaining three isolates did not register any production (Figure 1 i-l and Table 3).

3.3.4 Bacterial growth under different concentrations of NaCl

When tested for salt tolerance level, all four strains were tolerant of NaCl at various levels. Amongst the four isolates, isolate RZ27 exhibited the highest tolerance, thriving up to 14% NaCl, followed by isolates RZ23 and RZ5 (each up to 10%) and RZ3 (6%) (Figure 2 and Table 3).

3.3.5 Heavy metal tolerance (chromium)

Various studies have extensively used plant growth-promoting rhizobacteria in the phytoremediation of heavy metal-contaminated soils. Heavy metals like chromium (Cr) are essential micronutrients for microbes, plants, and animals at lower concentrations. However, these metals become major toxins for all life forms at higher levels. In the present study, the chromium tolerance ability of the four selected isolates was tested, and the result revealed that different isolates had different tolerance levels of chromium. Amongst the four isolates, isolates RZ23 and RZ23 registered tolerance up to 1840 μ g/ml, followed by isolate RZ27 (1810 μ g/ml) and RZ5 (1300 μ g/ml). Heavy

metal concentrations on nutrient agar plates were gradually increased until the strains failed to grow. Cultures that grew at the highest concentration were subsequently transferred to plates with even higher concentrations. The MIC was determined when the isolates failed to grow (Table 3).

3.4 Molecular characterization of bacterial isolates

From the mixed culture plates, 20 rhizobacterial isolates were selected for pure cultures. Based on biochemical analysis, the best performing four isolates were subjected to molecular characterization based on *16S rRNA* sequence. Based on the targeted sequence, the isolates were confirmed RZ23 as *Agrobacterium larrymoorei* (GenBank accession No. OL662933), RZ5 as *Pseudomonas taiwanensis* (OL662931), RZ3 as *Pseudomonas orientalis* (OL662936), and RZ27 as *Burkholderia cepacia* (OL662932) (Table 1). Using Mega11 Software, a phylogenetic tree was built based on BLAST analysis to identify these bacterial species' closest relatives and homology (Figure 3).

3.5 Effect of bacterial inoculation on the growth of *Phaseolus vulgaris* L.

After 30 days of planting, the seedlings were uprooted, and their growth parameters were assessed. It was observed that all four rhizobacterial strains significantly enhanced various growth parameters of *Phaseolus vulgaris* seedlings in comparison to the control group (Figures 4 and 5). Each bacterial isolate positively

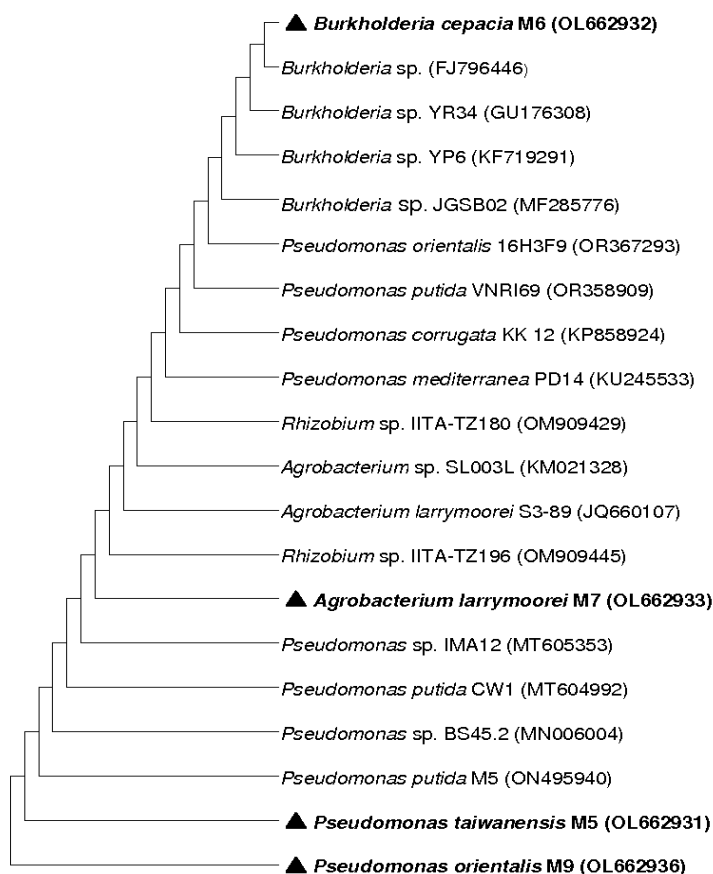


Figure 3 Neighbor-Joining method was used to infer the evolutionary history. The evolutionary distances were calculated using the Maximum Composite Likelihood method and are in the units of the number of base substitutions per site.

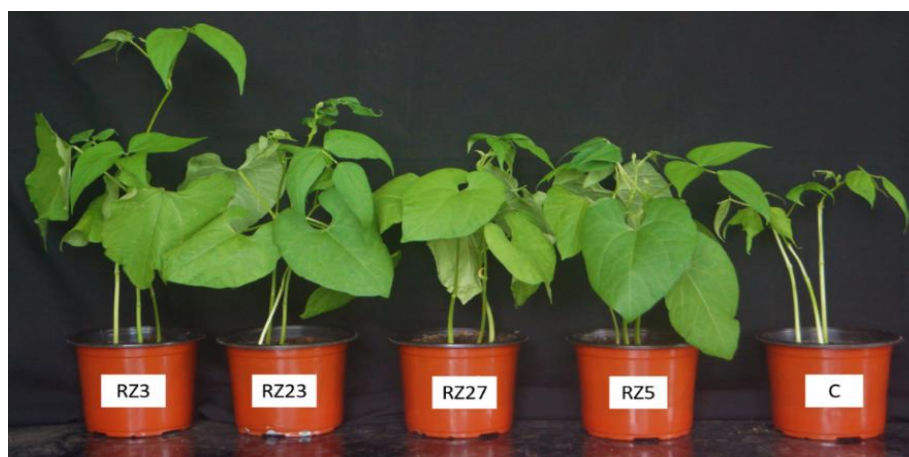


Figure 4 Plant growth promotion assay of common bean plant (*Phaseolus vulgaris* L.) by bacterial isolates (after 30 days post inoculation with strains a. RZ3, b. RZ23, c. RZ27, d. RZ5 and e. CONTROL (C)).

influenced one or more growth parameters of the experimental plants. Among the tested isolates, isolate RZ3 emerged as the best performer under the experimental conditions for all studied parameters, including shoot length (65.33 cm), root length (40.67 cm), shoot fresh weight (9.70 g), root fresh weight (6.48 g), shoot

dry weight (1.93 g), and root dry weight (0.78 g). These values were considerably higher than those of the control treatment, which recorded a shoot length of 14.00 cm, root length of 12.67 cm, shoot fresh weight of 1.46 g, root fresh weight of 0.85 g, shoot dry weight of 0.36 g, and root dry weight of 0.37 g.

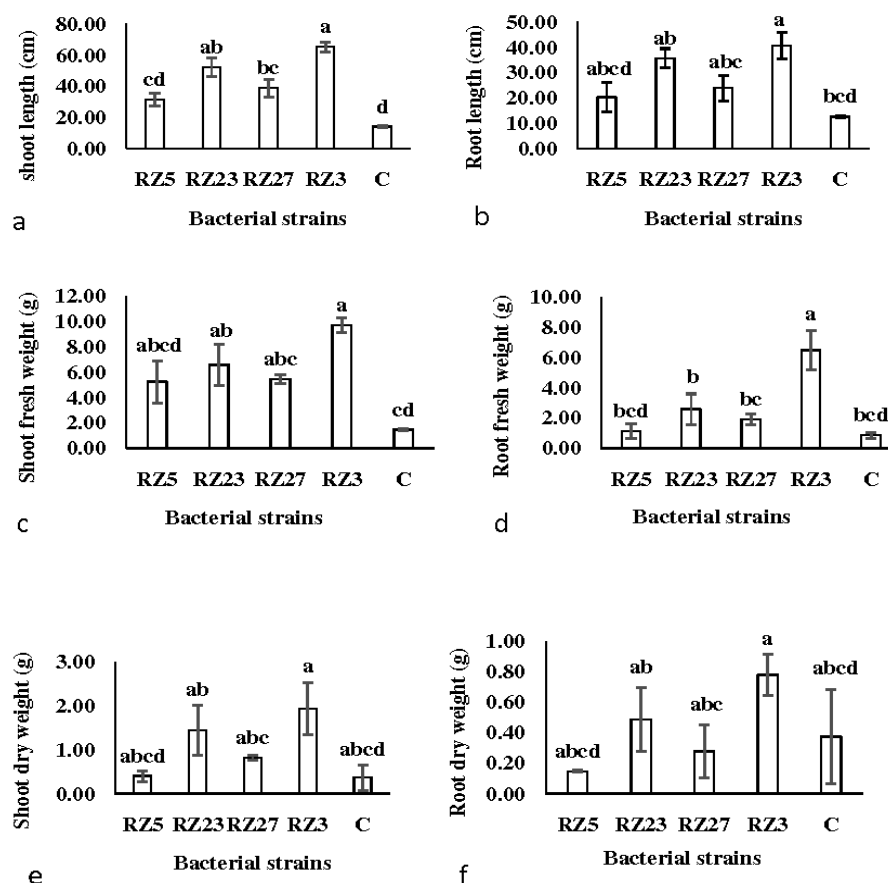


Figure 5 Effect of different bacterial isolates on shoot and root growth of *P. vulgaris* after 30 days of growth. a. Shoot length, b. Root length, c. Shoot fresh weight, d. Root fresh weight, e. Shoot dry weight and f. Root dry weight. Note: The PGPR isolates were RZ5, RZ23, RZ27, RZ3 and C (Control treatment). Mean averages (n=3). Different letters on bars indicate statistical differences between treatments according to the LSD Test ($p \leq 0.05$).

Isolate RZ23 significantly improved shoot length (52.33 cm) and shoot fresh weight (6.57 g). Increases in root length (35.67 cm), root fresh weight (2.59 g), shoot dry weight (1.44 g), and root dry weight (0.49 g) were also observed with RZ23, although these increases were not statistically significant ($p \geq 0.05$). Isolate RZ27 showed a significant increase only in shoot length (39.00 cm), with no significant changes in the other parameters. Similarly, isolate RZ5 did not exhibit any significant improvements in any of the growth parameters.

4 Discussion

In modern agriculture, a significant concern is the reliance on chemical fertilizers, which emphasizes the need for sustainable practices that reduce their use. This underscores the importance of exploring alternative methods to maintain agroecosystems while protecting the environment (Tatung and Deb 2021; 2023; 2024a, b; Deb and Tatung 2024; Yaghoubi et al. 2024). One promising solution lies in biofertilizers, biopesticides, and bioinsecticides,

which are eco-friendly, renewable, and do not lead to resistance in target organisms.

In the present study, plant growth-promoting rhizobacteria (PGPR) strains were isolated from the rhizosphere of *Musa balbisiana* growing in the forests of Nagaland. Their plant growth-promoting traits characterized these strains. Four promising isolates were identified among the experimental parameters evaluated: *A. larrymoorei*, *B. cepacian*, *P. taiwanensis*, and *P. orientalis*. These isolates were then tested on a model crop plant to assess their effect on plant growth.

After nitrogen, phosphate is the second most important macronutrient for plant growth and development. Although soils often contain abundant phosphate, only a small fraction (approximately 0.1%) is soluble and available for plant uptake (Hadjouti et al. 2022; Tatung and Deb 2023). Phosphate-solubilizing bacteria (PSB) are vital in converting insoluble inorganic phosphorus into soluble orthophosphates (Sanchez-Gonzalez et al. 2022).

In this study, all four selected bacterial strains demonstrated the ability to solubilize phosphate. Among them, *P. orientalis* exhibited the highest phosphate solubilization capability (337.11 µg/ml) after 10 days of culture, followed by *B. cepacian* (222.80 µg/ml after 10 days), *A. larrymoorei* (71.57 µg/ml after 12 days), and *P. taiwanensis* (19.20 µg/ml after 4 days). The quantification of available soluble phosphate in the culture medium was conducted using a standard curve prepared with various concentrations of KH_2PO_4 (0-600 µg/ml). The results showed that as the quantity of soluble phosphate in the medium increased, the pH decreased proportionately due to the accumulation of organic acids. This is a key mechanism for quantifying microbial phosphate solubilization (Sanchez-Gonzalez et al. 2022).

According to Chen et al. (2006), the solubilization of insoluble tricalcium phosphate largely relies on PSB and the reduction of pH in the NBRIP medium. In our findings, the lowest pH was observed with isolate RZ23 (*A. larrymoorei*) at 4.23 on the 12th day, closely followed by RZ27 (*B. cepacian*) at 4.24 on the 12th day, RZ3 (*P. orientalis*) at 5.47 on the 12th day, and RZ5 (*P. taiwanensis*) at 6.23 on the 4th day. Pande et al. (2017) reported that increased medium acidification accelerates mineral solubilization.

Phytohormones are essential chemical messengers that, although present in low concentrations, play a significant role in the growth and development of plants. They influence seed germination, flowering time, gender determination, leaf senescence, and fruit development (Tatung and Deb 2021). Among the four isolates tested, only *A. larrymoorei* could produce indole-3-acetic acid (IAA) in vitro, while the other three isolates did not show any colour change in the IAA production test.

Isolate *A. larrymoorei*, a relatively new species within the genus *Agrobacterium*, was first reported to induce tumours in the branches of *Ficus benjamina* (Bouzar and Jones 2001). It can be distinguished biochemically and genetically from other *Agrobacterium* species (Molinario et al. 2003). An alternative name, *Rhizobium larrymoorei*, was proposed based on Rule 34a of the International Code of Nomenclature of Bacteria (Prokaryotes) (Young 2004). Despite being known for over 20 years, there has been limited research on *A. larrymoorei*, particularly regarding its potential for promoting plant growth. This study has established that this species can be considered a Plant Growth-Promoting Rhizobacterium (PGPR).

Although the Earth's crust contains a significant amount of iron, its bioavailability in aerobic environments is limited due to the low solubility of iron (III) (Hider and Kong 2010; Deb and Tatung 2024). Siderophores are small extracellular organic compounds with low molecular weight, secreted by microorganisms and some

grass species under iron-deficient conditions. These compounds facilitate iron acquisition from the environment by solubilizing and transporting it (Ferreira et al. 2019).

In the current investigation, among the four isolates studied, only *B. cepacia* did not produce siderophores, while the other three isolates demonstrated siderophore production. This indicates that the positive isolates are effective in plant nutrient acquisition and have potential as biocontrol agents (Tatung and Deb 2021; 2023). The isolates that produced siderophores formed orange halo zones around their colonies on CAS-agar plates. This colour change occurs because the siderophores remove iron from the Fe-CAS complex, which is initially blue (Alexander and Zubber 1991).

Quantitative analysis revealed that *P. orientalis* showed the highest siderophore production on the 4th day, with a concentration of 29.07 µg/ml. This was followed by lower productions of 6.17 µg/ml on the 2nd day and 13.30 µg/ml on the 6th day, and no siderophore was detected on the 8th and 10th days. For *A. larrymoorei*, peak siderophore production also occurred on the 4th day at 33.34 µg/ml, with levels of 24.44 µg/ml on the 2nd day, 31.39 µg/ml on the 6th day, 25.75 µg/ml on the 8th day, and the lowest concentration of 18.00 µg/ml on the 10th day. *Pseudomonas taiwanensis* exhibited its highest siderophore production on the 4th day at 27.20 µg/ml, with lower levels of 14.70 µg/ml on the 2nd day, 20.96 µg/ml on the 6th day, and 17.08 µg/ml on the 8th day, and no siderophores detected on the 10th day.

Salinity stress significantly affects plant growth by impairing nitrogen metabolism, carbon acclimatization, and crop yield. It leads to osmotic imbalance and ionic toxicity, which hinders nutrient absorption (Li et al. 2020). Additionally, salinity stress generates reactive oxygen species (ROS), such as hydrogen peroxide (H_2O_2), superoxide ions, and singlet oxygen. These reactive species reduce the activity of plant defence enzymes, disrupt sodium balance, impair iron uptake, and alter the levels of phenols and trace elements (Sharma et al. 2021a).

In this investigation, *Burkholderia cepacia* exhibited the highest salt tolerance at 14% NaCl, followed by *Azospirillum larrymoorei* and *Pseudomonas taiwanensis*, which tolerated up to 10% NaCl. In contrast, *Pseudomonas orientalis* could withstand only up to 6% NaCl. The ability of rhizobacteria to adapt to salt stress is essential for their survival and growth in saline environments (Bakhshandeh et al. 2014; Tatung and Deb 2023). During salinity stress, plant growth-promoting rhizobacteria (PGPR) either activate or modulate plant response systems or produce anti-stress compounds (Giannelli et al. 2023). For instance, *Burkholderia* species have been reported to enhance several biochemical and morphological characteristics of rice seedlings under salinity stress compared to control treatments (Sarkar et al. 2018). Utilizing salt-tolerant PGPR can mitigate the harmful effects of salt stress on plants,

helping to improve physiological functions such as growth, yield, and disease resistance (Sharma et al. 2021a).

Chromium is one of the most toxic heavy metals, commonly found in nature and extensively used in industrial processes (Prasad et al. 2021). The Environmental Protection Agency sets the soil concentration limit for chromium between 95 and 1180 ppm (Mazhar et al. 2020). Chromium adversely affects plant growth by disrupting essential metabolic processes, primarily by producing reactive oxygen species (ROS), which induce oxidative stress in plants (Sharma et al. 2021b).

In the present study, rhizobacterial isolates showed varying levels of chromium tolerance: *A. larrymoorei* and *P. orientalis* tolerated up to 1840 µg/ml, followed by *B. cepacia* (1810 µg/ml) and *P. taiwanensis* (1300 µg/ml). According to Janaki et al. (2024), *B. cepacia* has demonstrated resistance to heavy metals like cadmium and lead, improving seed germination, plant height, plant biomass, and various enzyme activities, including peroxidase (PO), polyphenol oxidase (PPO), β-1,3-glucanase, and phenols. Furthermore, Kang et al. (2017) showed that inoculating *Brassica rapa* with *B. cepacia* enhanced plant growth, reduced zinc uptake, altered amino acid regulation, and increased flavonoid and phenolic levels. This inoculation significantly decreased levels of superoxide dismutase, endogenous abscisic acid, and salicylic acid, highlighting its bioremediation potential. These findings underline the plant growth-promoting and bioremediation capabilities of *B. cepacia*.

Molecular characterization based on the 16S rRNA sequence confirmed the identity of the four investigated isolates: *B. cepacia* (RZ27), *A. larrymoorei* (RZ3), *P. taiwanensis* (RZ5), and *P. orientalis* (RZ3), with homologies of 98.74%, 98.69%, 99.78%, and 100.00%, respectively, as determined using MEGA X software for phylogenetic analysis.

In this study, the selected PGPR strains were tested for their ability to promote the growth of *P. vulgaris*, a well-known bean crop plant exhibiting significant growth enhancements. Among the five treatments, *P. orientalis* resulted in the greatest improvements in both shoot and root length and in shoot and root fresh weight. This was followed by *A. larrymoorei*, *B. cepacia*, and *P. taiwanensis*, all of which performed better than the control treatment. These findings align with those reported by Mishra et al. (2023), who noted that *P. taiwanensis* improved wheatgrass's antioxidant and nutritional properties (*Triticum aestivum*) when used with reduced mineral fertilizers in saline soil. Additionally, *A. larrymoorei* exhibited significant plant growth-promoting traits, including phosphate solubilization, siderophore, and IAA production, indicating its potential to enhance plant growth alongside the other three isolates.

The growth-promoting traits of *B. cepacia* were also investigated by Wang et al. (2021), who observed its positive effects on maize

growth. You et al. (2020) reported that *B. cepacia* could effectively solubilize inorganic tricalcium phosphate under greenhouse conditions and contribute to crop yield. Furthermore, *B. cepacia* has been shown to promote rice growth by increasing grain yield and biomass under nitrogen-limited conditions (Li et al. 2022). Rhizobacteria such as *P. orientalis* and *Chaetomium cupreum*, when inoculated on *Eucalyptus globulus*, enhanced plant growth and alleviated copper toxicity (Ortiz et al. 2019). Collectively, these findings highlight the potential of these PGPR strains, isolated from the *Musa* rhizosphere, as promising bioinoculants for sustainable agriculture.

Conclusions

The findings of this study highlight that the wild *Musa* rhizosphere harbors a diverse range of PGPR with the ability to thrive under adverse conditions, thus boosting the growth and productivity of plants. The investigated isolates *P. orientalis* (OL662936), *A. larrymoorei* (OL662933), *B. cepacia* (OL662932), and *P. taiwanensis* (OL662931) demonstrated various beneficial traits, including salinity tolerance, IAA production, siderophore production, and phosphate solubilization. Inoculation of *P. vulgaris* with *P. orientalis* resulted in significant growth improvements, underscoring its potential as a biofertilizer. Further, rhizobacteria *A. larrymoorei* and *P. orientalis*, showing high chromium tolerance (1840µg/ml), could be a valuable resource for soil bioremediation. *B. cepacia*, with its high salt tolerance (14%), shows promise for improving plant growth under saline conditions. Understanding the mechanisms through which these strains promote growth and development could lead to establishing effective microbial consortia, offering future strategies for advancing sustainable agricultural practices.

Author's Contributions

CRD: Conceptualization, designing the work, Supervision, fund arrangement, correction of the manuscript; MT: Experiments, data analysis, original draft of the manuscript.

Declaration

There are no conflicts of interest among the authors

Acknowledgments

MT expresses deep gratitude to the Council of Scientific and Industrial Research (CSIR), Government of India, New Delhi, for providing financial support through the Junior Research Fellowship (JRF) and Senior Research Fellowship (SRF) programs. Appreciation is also extended to the DBT-sponsored Institutional Biotech Hub (File No. BT/22/NE/2011), UGC-SAP(DRS-III), and DST-FIST programs for the facilities used in this research.

References

- Akhtar, N., Ilyas, N., Yasmin, H., Sayyed, R.Z., Hasnain, Z., AElsayed, E., & El Enshasy, H. A. (2021). Role of *Bacillus cereus* in improving the growth and phytoextractability of *Brassica nigra* (L.) K. Koch in chromium contaminated soil. *Molecules*, 26(6), 1569. <https://doi.org/10.3390/molecules26061569>
- Alexander, D.B., & Zuberer, D.A. (1991) Use of chrome azurol S reagents to evaluate siderophore production by rhizosphere bacteria. *Biology and Fertility of Soils*, 12, 39-45. <https://doi.org/10.1007/BF00369386>
- Bakhshandeh, E., Rahimian, H., Pirdashti, H., & Nematzadeh, G.A. (2014). Phosphate solubilization potential and modeling of stress tolerance of rhizobacteria from rice paddy soil in northern Iran. *World Journal of Microbiology & Biotechnology*, 30(9), 2437–2447. <https://doi.org/10.1007/s11274-014-1669-1>
- Bouzar, H., & Jones, J.B. (2001). *Agrobacterium larrymoorei* sp. nov., a pathogen isolated from aerial tumours of *Ficus benjamina*. *International Journal of Systematic and Evolutionary Microbiology*, 51(3), 1023–1026. <https://doi.org/10.1099/00207713-51-3-1023>
- Chen, Y.P., Rekha, P.D., Arun, A.B., Shen, F.T., Lai, W.A., & Young, C.C. (2006). Phosphate solubilizing bacteria from subtropical soil and their tricalcium phosphate solubilizing abilities. *Applied Soil Ecology*, 34(1), 33-41. <https://doi.org/10.1016/j.apsoil.2005.12.002>
- Deb, C.R., & Tatung, M. (2024). Siderophore producing bacteria as biocontrol agent against phytopathogens for a better environment: a review. *South African Journal of Botany*, 165, 153-162. <https://doi.org/10.1016/j.sajb.2023.12.031>
- Ferreira, M.J., Silva, H., & Cunha, A. (2019). Siderophore-producing rhizobacteria as a promising tool for empowering plants to cope with iron limitation in saline soils: a review. *Pedosphere*, 29(4), 409-420. [https://doi.org/10.1016/S1002-0160\(19\)60810-6](https://doi.org/10.1016/S1002-0160(19)60810-6)
- Giannelli, G., Potestio, S., & Visioli, G. (2023). The contribution of PGPR in salt stress tolerance in crops: unravelling the molecular mechanisms of cross-talk between plant and bacteria. *Plants*, 12(11), 2197. <https://doi.org/10.3390/plants12112197>
- Hadjouti, R., Oulebsir-Mohandkaci, H., Farida, B., & Furze, J. (2022). Enhancing agriculture recovery of *Phaseolus vulgaris* L. and *Cucurbita pepo* L. with *Olea europaea* L. plant growth promoting rhizobacteria. *Soil Research*, 60, 850-863. <https://doi.org/10.1071/SR21320>
- Hider, R.C., & Kong, X. (2010). Chemistry and biology of siderophores. *Nature Product Reports*, 27(5), 637-57. <https://doi.org/10.1039/b906679a>
- Janaki, M., Kirupanantha-Rajan, P., Senthil-Nathan, S., Stanley-Raja, V., Al Farraj, D.A., Aljeidi, R.A., & Arokiyaraj, S. (2024). Beneficial role of *Burkholderia cepacia* in heavy metal bioremediation in metal-polluted soils and enhance the tomato plant growth. *Biocatalysis and Agricultural Biotechnology*, 57, 103032. <https://doi.org/10.1016/j.bcab.2024.103032>
- Kang, S.M., Shahzad, R., Bilal, S., Khan, A.L., You, Y.H., Lee, W.H., Ryu, H.L., Lee, K.E., & Lee, I.J. (2017). Metabolism-mediated induction of zinc tolerance in *Brassica rapa* by *Burkholderia cepacia* CS2-1. *Journal of Microbiology*, 55(12), 955–965. <https://doi.org/10.1007/s12275-017-7305-7>
- Khanna, K., Jamwal, V.L., Gandhi, S.G., Ohri, P., & Bhardwaj, R. (2019). Metal resistant PGPR lowered Cd uptake and expression of metal transporter genes with improved growth and photosynthetic pigments in *Lycopersicon esculentum* under metal toxicity. *Scientific Reports*, 9(1), 5855. <https://doi.org/10.1038/s41598-019-41899-3>
- Khurana, A., & Kumar, V. (2022). State of Biofertilizers and Organic Fertilizers in India, Centre for Science and Environment, New Delhi, India.
- Li, X., Sun, P., Zhang, Y., Jin, C., & Guan, C. (2020). A novel PGPR strain *Kocuria rhizophila*Y1 enhances salt stress tolerance in maize by regulating phytohormone levels, nutrient acquisition, redox potential, ion homeostasis, photosynthetic capacity and stress-responsive genes expression. *Environmental and Experimental Botany*, 174(3), 104023. <https://doi.org/10.1016/j.envexpbot.2020.104023>
- Li, Z., Henawy, A.R., Halema, A.A., Fan, Q., Duanmu, D., & Huang, R. (2022). A wild rice rhizobacterium *Burkholderia cepacia* BRDJ enhances nitrogen use efficiency in rice. *International Journal of Molecular Sciences*, 23(18), 10769. <https://doi.org/10.3390/ijms231810769>
- Mazhar, R., Ilyas, N., Arshad, M., Khalid, A., & Hussain, M. (2020). Isolation of heavy metal-tolerant PGPR strains and amelioration of chromium effect in wheat in combination with biochar. *Iranian Journal of Science and Technology, Transactions A: Science*, 44, 1-12. <https://doi.org/10.1007/s40995-019-00800-7>
- Megu, M., Paul, A. & Deb, C.R. (2024a). Isolation and screening of stress tolerant and plant growth promoting root nodulating rhizobial bacteria from some wild legumes of Nagaland, India. *South African Journal of Botany*, 168, 260-269. <https://doi.org/10.1016/j.sajb.2024.03.021>
- Megu, M., Paul, A. & Deb, C.R. (2024b). Potential nitrogen fixing rhizobia isolated from some wild legumes of Nagaland based on RAPD with *nif*-directed primer and their biochemical activities.

- Journal of Experimental Biology and Experimental Science*, 12(4), 388-605. [http://dx.doi.org/10.18006/2024.12\(4\).588.605](http://dx.doi.org/10.18006/2024.12(4).588.605)
- Mishra, P., Mishra, J., & Arora, N.K. (2023). Salt tolerant *Pseudomonas taiwanensis* PWR-1 in combination with a reduced dose of mineral fertilizers improves the nutritional and antioxidant properties of wheatgrass grown in saline soil. *World Journal of Microbiology & Biotechnology*, 40(1), 11. <https://doi.org/10.1007/s11274-023-03806-x>
- Molinaro, A., De Castro, C., Lanzetta, R., Parrilli, M., Raio, A., & Zoina, A. (2003). Structural elucidation of a novel core oligosaccharide backbone of the lipopolysaccharide from the new bacterial species *Agrobacterium larrymoorei*. *Carbohydrate Research*, 338(23), 2721–2730. [https://doi.org/10.1016/s0008-6215\(03\)00316-1](https://doi.org/10.1016/s0008-6215(03)00316-1)
- Oo, K., Win, T., Khai, A., & Fu, P. (2020). Isolation, screening and molecular characterization of multifunctional plant growth promoting rhizobacteria for a sustainable agriculture. *American Journal of Plant Sciences*, 11, 773-792. <https://doi.org/10.4236/ajps.2020.116055>
- Ortiz, J., Soto, J., Almonacid, L., Fuentes, A., Campos-Vargas, R., & Arriagada, C. (2019). Alleviation of metal stress by *Pseudomonas orientalis* and *Chaetomium cupreum* strains and their effects on *Eucalyptus globulus* growth promotion. *Plant and Soil*, 436(1-2), 449-461. <https://doi.org/10.1007/s11104-019-03946-w>
- Pande, A., Pandey, P., Mehra, S., Singh, M., & Kaushik, S. (2017). Phenotypic and genotypic characterization of phosphate solubilizing bacteria and their efficiency on the growth of maize. *Journal of Genetic Engineering & Biotechnology*, 15(2), 379–391. <https://doi.org/10.1016/j.jgeb.2017.06.005>
- Payne, S.M. (1993). Iron acquisition in microbial pathogenesis. *Trends in Microbiology*, 1(2), 66–69. [https://doi.org/10.1016/0966-842x\(93\)90036-q](https://doi.org/10.1016/0966-842x(93)90036-q)
- Pereira, S.I.A., Abreu, D., Moreira, H., Vega, A., & Castro, P.M.L. (2020). Plant growth-promoting rhizobacteria (PGPR) improve the growth and nutrient use efficiency in maize (*Zea mays* L.) under water deficit conditions. *Heliyon*, 6(10), e05106. <https://doi.org/10.1016/j.heliyon.2020.e05106>
- Pongener, B., Deb, C.R. & Paul, A. (2024). Prospecting beneficial microsymbiont associated with root nodules of crop legumes of North-Eastern India, Nagaland. *Proceedings of National Academy of Sciences, India Section B: Plant Science*, 94(4), 835-843. <https://doi.org/10.1007/s40011-024-01601-8>
- Prasad, S., Yadav, K.K., Kumar, S., Gupta, N., Cabral-Pinto, M.M.S., Rezaia, S., Radwan, N., & Alam, J. (2021). Chromium contamination and effect on environmental health and its remediation: a sustainable approaches. *Journal of Environmental Management*, 285, 112174. <https://doi.org/10.1016/j.jenvman.2021.112174>
- Qingwei, Z., Lushi, T., Yu, Z., Yu, S., Wanting, W., Jiangchuan, W., Xiaolei, D., Xuejiao, H., & Bilal, M. (2023). Isolation and characterization of phosphate-solubilizing bacteria from rhizosphere of poplar on road verge and their antagonistic potential against various phytopathogens. *BMC Microbiology*, 23(1), 221. <https://doi.org/10.1186/s12866-023-02953-3>
- Rana, A., Saharan, B., Joshi, M., Prasanna, R., Kumar, K., & Nain, L. (2011). Identification of multi-trait PGPR isolates and evaluating their potential as inoculants for wheat. *Annals of Microbiology*, 61(4), 893–900. <https://doi.org/10.1007/s13213-011-0211-z>
- Sarkar, A., Pramanik, K., Mitra, S., Soren, T., & Maiti, T.K. (2018). Enhancement of growth and salt tolerance of rice seedlings by ACC deaminase-producing *Burkholderia* sp. MTCC12259. *Journal of Plant Physiology*, 231, 434-442. <https://doi.org/10.1016/j.jplph.2018.10.010>
- Sanchez-Gonzalez, M.E., Mora-Herrera, M.E., Wong-Villarreal, A., De La Portilla-López, N., Sanchez-Paz, L., Lugo, J., Vaca-Paulín, R., Del Aguila, P., & Yañez-Ocampo, G. (2022). Effect of pH and carbon source on phosphate solubilization by bacterial strains in Pikovskaya medium. *Microorganisms*, 11(1), 49. <https://doi.org/10.3390/microorganisms11010049>
- Sharma, A., Dev, K., Sourirajan, A., & Choudhary, M. (2021a). Isolation and characterization of salt-tolerant bacteria with plant growth-promoting activities from saline agricultural fields of Haryana, India. *Journal of Genetic Engineering & Biotechnology*, 19(1), 99. <https://doi.org/10.1186/s43141-021-00186-3>
- Sharma, S., Shah, R., Rathod, Z., Jain, R., Lucie, K., & Saraf, M. (2021b). Isolation of heavy metal tolerant rhizobacteria from Zawarminesarea, Udaipur, Rajasthan, India. *Bioscience Biotechnology Research Communications*, 13, 233-238. <https://doi.org/10.3390/plants9010100>
- Shultana, R., Kee Zuan, A. T., Yusop, M.R., & Saud, H.M. (2020). Characterization of salt-tolerant plant growth-promoting rhizobacteria and the effect on growth and yield of saline-affected rice. *PloSOne*, 15(9), e0238537. <https://doi.org/10.1371/journal.pone.0238537>
- Tatung, M., & Deb, C.R. (2021). Plant growth promotion by rhizobacteria: a potential tool for sustainable agriculture. In C.R. Deb & A. Paul (Eds.), *Bioresources and Sustainable Livelihood of Rural India* (pp 29-49). Mittal Publications, New Delhi, India.

- Tatung, M., & Deb, C.R. (2023). Isolation, characterization, and investigation on potential multi-trait plant growth promoting rhizobacteria from wild banana (*Musa itinerans*) rhizospheric soil. *Journal of Pure and Applied Microbiology*, 17(3), 1578-1590. <https://doi.org/10.22207/JPAM.17.3.19>
- Tatung, M., & Deb, C.R. (2024a). Screening and characterization of heavy metal tolerant rhizobacteria from wild *Musa* rhizosphere from coal mining area of Changki, Nagaland, India and assessment of their growth promoting potential under Cd/Cu contaminated conditions. *South African Journal of Botany*, 165, 217-227. <https://doi.org/10.1016/j.sajb.2023.12.039>.
- Tatung, M., & Deb, C. R. (2024b). Bacterial siderophores as potential biocontrol agent against phytopathogens. In C.R. Deb, Talijungla & N. Puro (Eds.), *Bioresources: Conservation and Sustainability*. (pp 423-436). Mittal Publications, New Delhi, India.
- Uebersax, M.A., Cichy, K.A., Gomez, F.E., Porch, T.G., Heitholt, J., Osorno, J.M., Kamfwa, K., Snapp, S.S., & Bales, S. (2023). Dry beans (*Phaseolus vulgaris* L.) as a vital component of sustainable agriculture and food security—a review. *Legume Science*, 5(1), e155. <https://doi.org/10.1002/leg3.155>
- Wang, C., Wang, H., Li, Y., Li, Q., Yan, W., Zhang, Y., Wu, Z., & Zhou, Q. (2021). Plant growth-promoting rhizobacteria isolation from rhizosphere of submerged macrophytes and their growth-promoting effect on *Vallisneria natans* under high sediment organic matter load. *Microbial Biotechnology*, 14(2), 726–736. <https://doi.org/10.1111/1751-7915.13756>
- Yadav, J.S., Sharma, R.K., Yadav, J., Tiwari, S., Kumar, U., Singh, P.K., & Kumar, I. (2022). Isolation, identification, and characterization of cadmium resistant rhizobacterial isolates from long-term waste water irrigated soils. *Journal of Scientific Research*, 66(1), 201-208. <https://doi.org/10.37398/JSR.2022.660122>
- Yaghoubi, K.M., Strafella, S., Filannino, P., Minervini, F., & Creccchio, C. (2024). Importance of lactic acid bacteria as an emerging group of plant growth-promoting rhizobacteria in sustainable agroecosystems. *Applied Sciences*, 14, 1798. <https://doi.org/10.3390/app14051798>
- Yamini, P., Gopalakrishnan, R., Prasad, S., Karkuvelraja, R., Commerce, C.T., & Biodiversity, M. (2021). Isolation and identification of indole acetic acid (IAA) producing bacteria from organic soil: investigating its efficacy on plant growth. *Journal of University of Shanghai for Science and Technology*, 23, 1294-1312. <https://doi.org/10.51201/jusst/21/06443>
- Young J. M. (2004). Renaming of *Agrobacterium larrymoorei* Bouzar and Jones 2001 as *Rhizobium larrymoorei* (Bouzar and Jones 2001) comb. nov. *International journal of systematic and evolutionary microbiology*, 54(Pt 1), 149. <https://doi.org/10.1099/ijs.0.02870-0>
- You, M., Fang, S., MacDonald, J., Xu, J., & Yuan, Z.C. (2020). Isolation and characterization of *Burkholderia cenocepacia* CR318, a phosphate solubilizing bacterium promoting corn growth. *Microbiological Research*, 233, 126395. <https://doi.org/10.1016/j.micres.2019.126395>



Journal of Experimental Biology and Agricultural Sciences

<http://www.jebas.org>

ISSN No. 2320 – 8694

 Introgressing photoperiod/thermo-sensitive genic
 male sterile gene into Basmati 370 rice

 Beatrice Nyarangi Nyankemba , Edith Esther Arunga , Paul Njiruh Nthakanio* 

Department of Water and Agricultural Resource Management, University of Embu, Embu P.O. Box 6-60100, Embu, Kenya

Received – July 17, 2024; Revision – October 14, 2024; Accepted – November 02, 2024

Available Online – November 29, 2024

DOI: [http://dx.doi.org/10.18006/2024.12\(5\).756.769](http://dx.doi.org/10.18006/2024.12(5).756.769)

KEYWORDS

Basmati rice

fgr gene

Gene introgression

Pollen sterility

P/TGMS rice lines

ABSTRACT

The emasculation of male gametes in pollen-recipient parents among self-pollinated crops (rice) is key to producing quality hybrid rice seeds. One of the emasculation tools in rice breeding is the photoperiod-thermo sensitive genic male sterility (P/TGMS) method, which ultimately requires long daylight length and high-temperature growth conditions to induce male gametes sterility. Using the P/TGMS method to produce hybrid *Basmati* rice seeds has been slow because no commercial line has been developed. Crossing the *Basmati* rice line with a non-aromatic rice line produces F_1 with non-*basmati* quality traits. This study aimed to introgress the *ptgms12-1* gene into *Basmati 370* by treating P/TGMS lines (IR-7327-2376-157S and IR-75589-31-27833S) with daytime temperatures ($>33^\circ\text{C}$) under a polythene greenhouse to emasculate pollen and cross-pollinating them with *Basmati 370*. Marker-assisted backcrossing was used to develop the BC_1F_2 *Basmati* breeding lines evaluated for pollen sterility and agro-morphological traits. Pollen sterility was tested by staining with 1% iodine potassium-iodide solution (I_2KI), in which fertile and sterile pollen grains were stained with blue-black and yellow-pink dyes, respectively. The acquisition of near-complete pollen sterility among female parents is a manifestation of the greenhouse temperatures effectively emasculating pollen in P/TGMS parents and BC_1F_2 . Analysis of variance on agro-morphological data showed significantly better agro-morphological traits in BC_1F_2 than the parents and significantly higher pollen sterility in P/TGMS lines than *Basmati 370* ($P \leq 0.05$). The presence of the *fgr* gene in BC_1F_2 lines was confirmed using SSR markers, and the hybrids had both homozygous aromatic and heterozygous non-aromatic traits, the successful development of BC_1F_2 with *ptgms12-1* and *fgr* genes. The results obtained from this study are a major milestone towards improving *Basmati* rice yields in Kenya using hybrid seeds.

* Corresponding author

E-mail: nthakanio.paul@embuni.ac.ke (Paul Njiruh Nthakanio)

Peer review under responsibility of Journal of Experimental Biology and Agricultural Sciences.

 Production and Hosting by Horizon Publisher India [HPI]
 (<http://www.horizonpublisherindia.in/>).
 All rights reserved.

 All the articles published by [Journal of Experimental Biology and Agricultural Sciences](#) are licensed under a [Creative Commons Attribution-NonCommercial 4.0 International License](#) Based on a work at www.jebas.org.


1 Introduction

Rice (*Oryza sativa* L.) is the world's second most-grown cereal crop after maize and is a staple food for more than half of the world population (Sreedhar and Reddy 2019). It is a strategic food crop in many African countries, where its demand has steadily increased in the past three decades in urban and rural populations (Uyeh et al. 2021). Most global rice is grown and consumed in Asia, constituting more than half of the world's population (Cordero-Lara 2020). Rice was first introduced by European settlers in the coastal region of Kenya from Asia as a cultivated crop in 1907 (Atera et al. 2018). In Kenya, consumer demand for rice has grown over the years and is estimated at 983,000 Mt, exceeding national rice production (181,000 Mt) (Yılmaz and Njora 2021). Kenya's main rice growing areas include Mwea, West Kano, Bunyala and Ahero irrigation schemes, with an average yield of 4.0 t/ha. Mwea Irrigation Scheme is the main rice growing area, accounting for 87% of national rice production (Atera et al. 2018). Potential 9 t/ha rice yields have been reported in Kenya (Atera et al. 2018), highlighting large rice yield gaps.

Basmati rice (locally known as *Pishori*) has good cooking and palatability qualities (Denis et al. 2022). Thus, Kenyan growers and consumers prefer the variety. One of its signature qualities is its characteristic aroma, which increases its demand and, thus, fetches high market prices. In Kenya, *Basmati* 217 and 370 are the key aromatic rice varieties grown, with *Basmati* 370 accounting for over 98% of the total rice grown by farmers at the Mwea Irrigation Scheme (Denis 2020). The main challenge with the commonly grown *Basmati* variety is low yield (about 4.0 t/ha) compared with other high-yielding local rice varieties such as *Komboka*, which yields about 7.0 t/ha (Ng'endo et al. 2022). Consumers' higher demand for *Basmati* rice is among the factors that have kept prices higher than expected in the Kenya market.

Hybrid rice technology exploits heterosis by pushing the breeding plateau above that of the inbred lines by over 25% (Prasanna et al. 2024). Efforts have been made to improve *Basmati* 370 yield by developing hybrid cultivars, but no significant yield increase has been realized (Akhter and Haider 2020). In hybrid rice technology, a female parent with male gametes completely emasculated is necessary to avoid self-pollination. Two major approaches used in hybrid rice production are cytoplasmic male sterility (CMS) and environment-sensitive genic male sterility (EGMS). In CMS, three lines (CMS, maintainer and restorer lines) are involved (Chang et al. 2016), while EGMS involves two lines, including the maternal parent (EGMS) and the paternal parent with fertile male gametes (restorer). Since rice is predominantly self-pollinated, male sterility systems (MSS) are the most effective methods in hybrid development (Ahmed et al. 2020).

The EGMS involves photoperiod-sensitive genic male sterility (PGMS), first discovered in the *Nongken* 58S rice variety (Zheng et al. 2024) and thermo-sensitive genic male sterility (TGMS) that was discovered in the *Annong* S-1 rice variety (Ali et al. 2021). Collectively referred to as EGMS, the PGMS and TGMS rice lines have sterility-inducing genes in male gametes under long-day light and high-temperature growth conditions. The gametes are, however, viable at the average daylight length of 12 hours and temperatures ranging between 19 and 30°C (Nthakanio and Kariuki 2019). The EGMS system is controlled by recessive nuclear genes, influenced by temperature in TGMS and photoperiod length in PGMS (Amist and Singh 2020). Simple sequence repeats (SSR) markers have been developed and utilized to select *p/tgms12-1* genes of chromosome 12 in the rice genome (Zhou et al. 2012). The use of EGMS rice lines in hybrid rice seed production involves two lines, making it cheaper than the CMS method, which uses three lines. Besides, in the EGMS system, the adverse effects of sterility-inducing cytoplasm are not encountered (Abebrese et al. 2018).

Hybrid rice seed technology has improved rice yield by 25-30% above the pure lines (Tongmark et al. 2021). Despite all the achievements, the use of technology is limited in *Basmati* rice because the quality traits such as aroma are under recessive gene control and are thus masked when crossed with non-aromatic rice varieties (Chukwu et al. 2019). Currently, there is a lack of a market-ready *Basmati* breeding line with male sterile genes possessing consumer-preferred quality traits, thus limiting the use of the EGMS method in *Basmati* rice hybrid seeds production. This study aimed to introduce the *p/tgms12-1* gene into *Basmati* 370 to produce breeding lines with consumer-preferred traits for crossing with ordinary *Basmati* 370 in a hybrid rice seed breeding program.

2 Materials and Methods

2.1 Study site

The following research was conducted at the Kenya Agricultural and Livestock Research Organization (KALRO), Mwea, in Kirinyaga County, Kenya. It is within Kenya's main rice growing area, where most *Basmati* rice is grown (Atera et al. 2018). The site coordinates are Latitude 00° 37'S and Longitude 37° 20'E and receives about 850 mm of rainfall annually. Mwea is approximately 1159 meters above sea level with a temperature range of 15.6°C to 28.6°C and a daily mean temperature of 22°C.

2.2 Plant materials and seeding

The plant materials used for the experiment were two P/TGMS lines (IR-73827-23-76-15-7S and IR-75589-31-27-8-33S) and *Basmati* 370, designated as V1 and V3, respectively. *Basmati* 370 certified seeds were provided by the Mwea Irrigation Agricultural

Development Centre (MIAD), while the Hybrid Rice Project provided the two P/TGMS lines at the University of Embu, Kenya. The seeds were soaked separately in germinating bags and treated by submerging them in 3% hydrogen peroxide (H₂O₂) for 24 hours to break seed dormancy and then incubated for 72 hours at 35°C in an incubator for post-nursery germination. Upon germination, the seedlings were sown in a containerized nursery filled with soil for 21 days in a greenhouse at KALRO, Mwea.

2.3 Evaluation of pollen sterility among rice parents

2.3.1 Experimental design

Two seedlings were transplanted into 10-litre polythene bags filled with farm soil at a spacing of 15 cm between plants. The experimental block comprised 10 bags with two seedlings (totalling 20) of each variety (V1, V3, and *Basmati* 370). The seedlings were placed inside a polyethylene greenhouse, and 10 bags of each variety were placed outside the greenhouse in a completely randomized design (CRD). All agronomic field practices were carried out as per the required standards practice for rice management. At the primordial growth stage (30 days to heading), the greenhouse temperature was maintained above 22°C at night and 33°C during the day. The polythene greenhouse was used to effectively realize this temperature because it is affordable for small-scale farmers at the Mwea Irrigation scheme. The greenhouse temperature was first calibrated by lowering the side walls to retain temperature and raising the side walls during the daytime to avoid overheating (Nthakanio and Kariuki 2019). The temperature treatment was maintained to induce male gamete sterility in female parents until the plants attained 50% heading when the treatment was withdrawn. Temperature readings were taken hourly using a maximum-minimum digital thermometer (ISOLAB® Laborgeräte GmbH 059.03.002). Greenhouse temperatures were routinely monitored to retain it below 38°C (to avoid physiological damage) by gradually opening up the greenhouse side walls cover between 9.30 am and 3.00 pm to allow air circulation and avoid overheating and thereafter lowering the walls cover to conserve the temperature till the next day (Nthakanio and Kariuki 2019). This was repeated in the 10 days of the critical fertility point (CSP).

2.3.2 Test for pollen sterility

Pollen sterility was determined using the iodine potassium iodide (I₂KI) staining method following the procedure of Chen et al. (2011). The average temperature in the greenhouse was a mean of 35.1°C. During the first 10 days of heading, 5 plants per line were sampled inside and outside the greenhouse every two days. Three undehisid spikelets from the panicle top, middle and base were randomly picked for pollen sterility testing. The samples were preserved in 70% ethanol inside an Eppendorf tube and transported

to the University of Embu Research Lab for testing and microscopic observation. Three anthers from each spikelet were stained with a drop of 1% I₂KI onto a glass slide. After staining, the anthers were macerated with forceps to release the pollen and other residues were removed. Pollen observation was done under ×10 objective of the ordinary compound light microscope and categorized into yellow/pink and dark blue stained pollen. The yellow/pink pollen grains were considered sterile, while the dark blue stained pollen was considered fertile as per Chen et al. (2011) procedure. Pollen sterility was expressed as a percentage (Hamad et al. 2022) as shown in the equation below;

$$\% \text{Pollen sterility} = \frac{\text{Total number of sterile pollen}}{\text{Total number of pollen grains}} \times 100$$

2.4 Introgression of P/TGMS in *Basmati* 370 rice line

2.4.1 Development of F₁, BC₁F₁ and BC₁F₂

The F₁ populations were developed by crossing V1 × *Basmati* 370 and V3 × *Basmati* 370 plant lines, as shown in Figure 1. Pollen from the male *Basmati* 370 that was planted outside the greenhouse was dusted on the female parent glumes of V1 and V3 plants that were treated with the sterility-inducing temperature inside the greenhouse, and thereafter, the panicles were bagged to avoid undesired cross-pollination and sterility-inducing temperature withdrawn. Successful hybrids were confirmed using anthocyanin pigmentation on the base of the stem of F₁ hybrid seedlings. The F₁ population data collected included plant height, panicle length, total number of tillers, productive tillers, days to heading, days to flowering, days to maturity, total number of glumes, and total filled and unfilled glumes of hybrid plants.

To recover the aroma trait, F₁ plants grown outside the greenhouse and manually male-gamete emasculated were backcrossed with *Basmati* 370 as the recurrent parent to obtain BC₁F₁. After that, the BC₁F₁ were grown in a soil-filled concrete trough measuring 16m X 3m in the greenhouse with optimum physiological growth conditions for effective self-pollination to produce BC₁F₂. The obtained BC₁F₂ population was treated with the greenhouse sterility-inducing temperature to segregate the EGMS and non-EGMS lines. Selection of lines with the *fgr* gene was made using simple sequence repeats (SSR) markers: External Sense Primer (ESP), Eternal Antisense Primer (EAP), Internal Fragrant Antisense Primer (IFAP) and Internal Non-Fragrant Sense Primer (INSP) while SSR marker RM12521 was used to select for *p/tgms12-1* gene.

2.4.2 Molecular Analysis

DNA extraction from 21-day-old leaves of parents and BC₁F₂ plants was done following the procedure of Mahuku (2004). Molecular markers (Table 1) were used to select the lines with aroma gene (*fgr*) and *p/tgms12-1*.

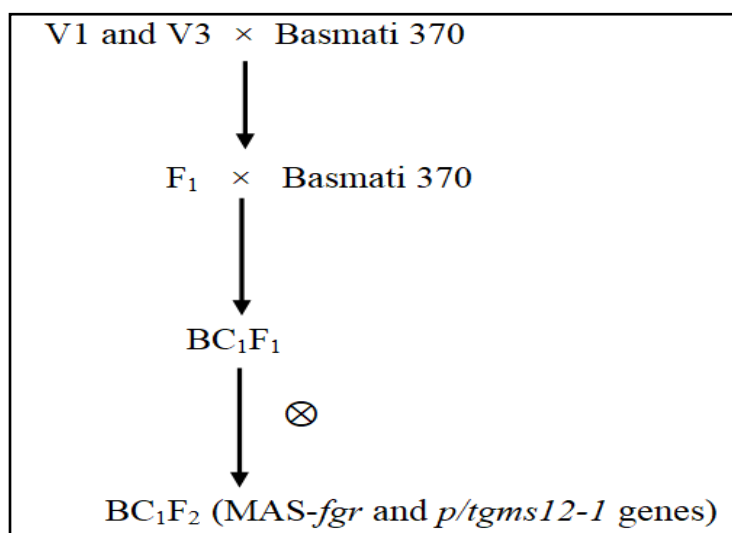


Figure 1 Marker-assisted backcross breeding scheme to introgress *p/tgms12-1* gene into Basmati 370 rice. V1 and V3 are used as female parents, while Basmati 370 is used as a recurrent parent

Table 1 Molecular markers used to screen for *fgr* and *p/tgms12-1* genes

SSR marker	Primer sequences	Tagged gene	References
ESP	TTGTTTGGAGCTTGCTGATG	<i>fgr</i>	Bradbury et al. 2005
EAP	AGTGCTTTACAAAGTCCCGC		
IFAP	CATAGGAGCAGCTGAAATATATAC		
INSP	CTGGTAAAAAGATTATGGCTCA		
RM12521	F:5'=CCCTTATCTGCTAGCCTCACACC-3' R:3'=CCACCGGATAATCCTTTAAGTGC-5'	<i>p/tgms12-1</i>	Zhou et al. 2012

Note- F is forward primer, and R is reverse primer.

A polymerase chain reaction (PCR) (9800 Fast Thermal Cycler®) was used to amplify the extracted DNA. The PCR reaction mixture of 20 μ l was prepared in 0.2 ml Biologix® strip tubes composed of 1.5 μ l-50 ng/ μ l of rice genomic DNA, 1 μ l-10 μ M of forward and reverse primers, 4 μ l Accuris™ *Taq*-buffer, 12 μ l molecular grade water, 1 μ l-5 mM dNTPS and 0.2 μ l of 5 units Accuris™ *Taq* polymerase. The PCR amplification profile of the aroma markers (ESP, EAP, IFAP and INSP) was initial denaturation at 95°C for 2 minutes, followed by 30 cycles at 95 °C for 30 seconds, 58 °C annealing for 30 seconds, 72°C elongation for 30 seconds and a final extension at 72 °C for 5 minutes, and storage at 4°C. While for the RM12521 primers, initial denaturation occurs at 94 °C for 2 minutes, followed by 30 cycles of 94°C for 30 seconds, 55°C annealing for 30 seconds, 72 °C elongation for 1 minute, a final extension at 72 °C for 5 minutes, and storage at 4 °C. After amplification, the PCR products were resolved in 1.2 % agarose gel electrophoresis, pre-stained with 10 μ l-10,000 \times SafeView™ Classic staining dye and ran in 1 \times sodium borate buffer at a voltage of 70 V and current of 250mA for 1 hour. Accuris™ Smart Check™ DNA (0.1mg/ml) ladder (3 μ l) was used to estimate the

amplicon sizes of the PCR product. The resolved DNA fragments were observed under a UVP® Benchtop Variable Transilluminator, and the images were captured using a Canon® camera. The individuals were selected based on the expected band sizes.

2.5 Evaluation of agro-morphological traits of BC₁F₂ population

2.5.1 Experimental design

Seeds of BC₁F₂ generation and the parents were prepared by soaking in hydrogen peroxide as described earlier and were sown in a containerized nursery filled with soil for 21 days. Four seedlings of each hybrid and parent line were row-transplanted into three soil-filled concrete troughs measuring 16m X 3m with three replications in a completely randomized block design in the greenhouse at a spacing of 15 cm between plants and 20 cm between rows. All the required agronomic practices were implemented, including watering, weeding and fertilization. High-

temperature treatment at the rice primordial growth stage to induce pollen sterility was also tested on the BC₁F₂ population to validate the successful introgression of the *p/gms12-1* gene. The average daytime temperatures in the greenhouse within the pollen sterility-inducing sensitive phase of the plant growth cycle were effectively sustained at 36.4°C.

2.5.2 Data collection for Agro-morphological traits

Data on the plant height, total number of tillers, and productive tillers was collected at physiological maturity. Evaluation for pollen sterility was conducted, as explained earlier.

2.6 Data Analysis

Data on pollen viability of the parents, plant height, total number of tillers, number of productive tillers, sterile pollen, number of sterile spikelets, days to heading, days to flowering, days to maturity and 1000-grain weight was subjected to analysis of variance (ANOVA) using SAS 9.4 computer software. Tukey's student's test at $P \leq 0.05$ was used for mean separation for all traits, and Pearson's correlation of coefficient analysis of the parameters was implemented.

3 Results

3.1 Effectiveness of greenhouse temperatures on inducing pollen sterility in BC₁F₂ and parental lines

Differences in pollen sterility were noted when the stained pollen was observed under 10× magnification under a light microscope. The pollen grains from the greenhouse stained yellow, while those obtained from outside the greenhouse stained dark blue (Figure 2). Plants grown outside the greenhouse conditions had fertile spikelets (Figure 2D), while spikelets of BC₁F₂ -EGMS under greenhouse growth conditions were completely sterile (Figure 2H).

The analysis of variance results showed significant differences at $p \leq 0.05$ in pollen sterility between the plants grown inside the greenhouse conditions and those grown outside the greenhouse conditions (Table 2). Under the GH conditions, the average percentage of pollen sterility for ten days of pollen collection was 97% (V3), 96% (V1) and 85% (*Basmati 370*). The lines carrying the *p/tgms12-1* gene showed higher sterility in the GH than *Basmati 370* despite being grown under similar conditions. The plants that were grown outside the greenhouse showed low pollen sterility of 3.6% (*Basmati 370*), followed by 5.2% (V1) and 6.2%

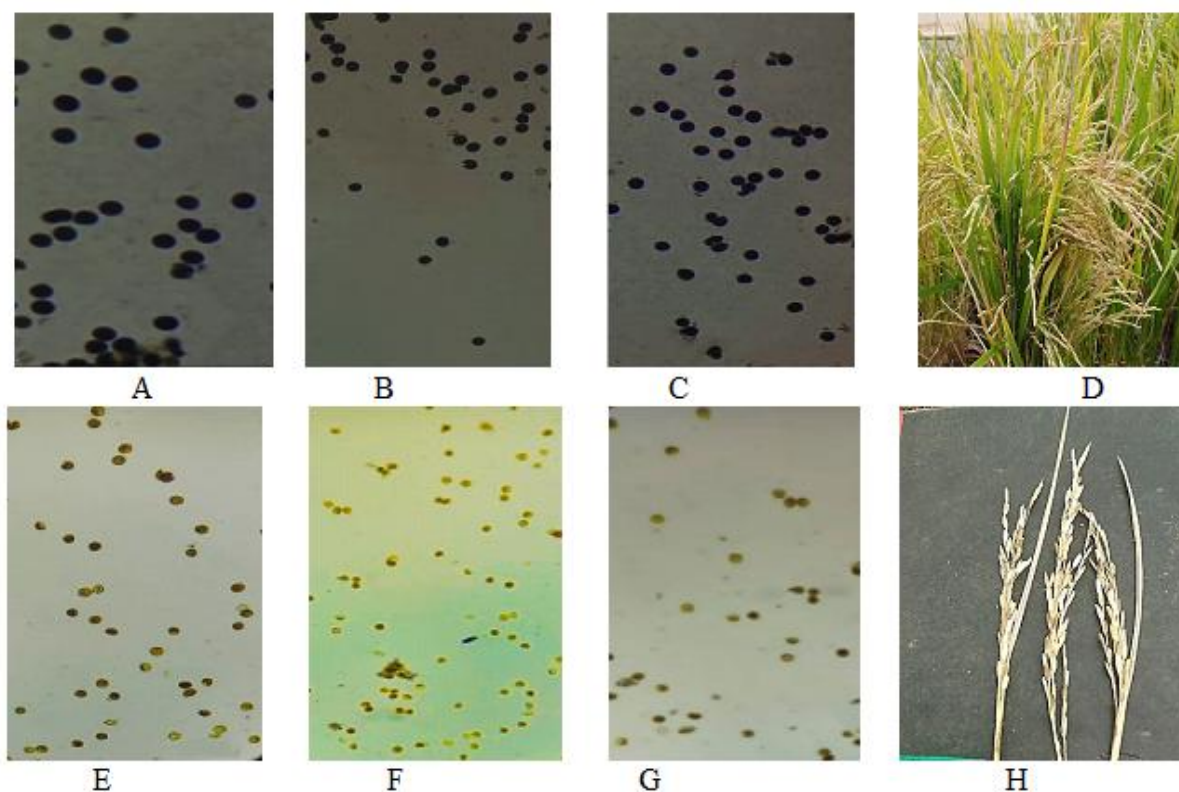
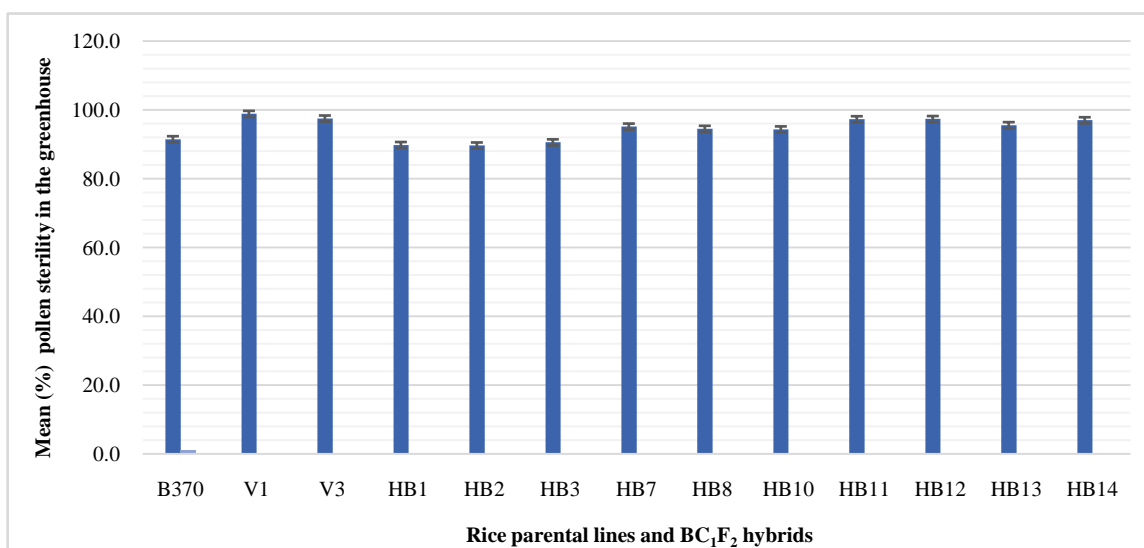


Figure 2 Effects of high temperature on BC₁F₂ pollen and spikelet sterility, figures A, B, and C show dark blue pollen from plants grown outside the greenhouse conditions, while figures E, F and G show yellow-stained pollen from plants grown inside the greenhouse conditions, figure D shows fertile spikelets from plants grown outside the greenhouse while figure H shows sterile spikelets from plants grown inside the greenhouse.

Table 2 Mean pollen sterility percentages of three rice varieties grown under greenhouse conditions (GH) and outside greenhouse (OGH)

Line	GH	OGH
V1	95.6±6.08 ^a	5.2±2.04 ^{ab}
V3	96.7±4.16 ^a	6.2±1.75 ^b
Basmati 370	85.2±3.16 ^b	3.6±0.97 ^a
Mean	92.5 ^a	5.0 ^b
CV%	5.0	33.0
P value	<.0001	0.0056

Figure 3 The BC₁F₂ lines sterility levels, SPGH - Sterile pollen in the greenhouse, HB1-HB8- V3 × Basmati 370, HB10 - HB14 =V1 × Basmati 370, B370= Basmati 370, V1 and V3 - EGMS.Table 3 Selection of BC₁F₂ EGMS plants

Crosses	Seeds obtained	F ₁ plants selected	BC ₁ F ₁ seeds obtained	Plants selected	BC ₁ F ₂ plants selected using SSR markers
V1× <i>Basmati</i> 370	232	96	72	23	5
V3× <i>Basmati</i> 370	468	173	66	30	5
Total	700	269	138	53	10

(V3) (Table 2). Although the environment by variety interaction was significant ($p < 0.05$), the ranking of the varieties based on pollen sterility did not change. The mean average temperature for the season outside the GH was 23.8°C, which is conducive for pollen fertility (Table 2).

V1 and V3 had the highest percentage of pollen sterility (98%) compared to the BC₁F₂ hybrids, but there was no significant difference between the parents and the hybrids (Figure 3).

3.2 Introgression of *p/tgms12-1* gene into *Basmati* 370

Successful hybridization between V1 × *Basmati* 370 and V3 × *Basmati* 370 produced F₁ hybrids that were distinguished from the

parents by the presence of anthocyanin pigmentation at the base of the stem and purple tips of the glume (Figure 4). Out of 700 F₁ seeds generated from V1 × *Basmati* 370 and V3 × *Basmati* 370, 269 plants were selected using anthocyanin pigmentation. These F₁ materials were backcrossed to form a population of 138 BC₁F₁ seeds, which were then selfed and selected to obtain 53 BC₁F₂ progenies (Table 3).

3.3 Agro-morphological analysis of the parents and F₁ hybrids grown outside the greenhouse

Analysis of variance carried out on the agro-morphological traits showed a significant difference ($p < 0.05$) concerning plant height, total tillers, days to heading, days to flowering and days to maturity.



Figure 4 Use of anthocyanin pigmentation as a morphological maker in the selection process of *Basmati 370* cross breeds, figure 4A, B and C shows rice parents V1, V3 and *Basmati 370* respectively, figure 4D shows F₁ hybrid (V3 × *Basmati 370*), figure 4E shows BC₁F₁ and 4F shows purple tips observed F₁ hybrids.

Table 4 Means of agronomic traits of rice parents and F₁ hybrids grown outside the greenhouse

Line	Plant height (cm)	Total number of tillers	Productive tillers	Sterile spikelets	50% Days to heading	50% Days to flowering	50% Days to maturity	1000-grain weight(g)
V1 × <i>Basmati 370</i>	112.13±8.02 ^b	20.06±1.20 ^b	16.0±1.70 ^b	89.19±13.75 ^a	98.50±0.65 ^b	100.25±0.63 ^{bc}	129.25±0.48 ^b	20.5±1.041 ^a
V3 × <i>Basmati 370</i>	104.44±2.14 ^c	19.25±1.11 ^b	15.94±0.83 ^b	61.75±7.87 ^b	91.50±6.54 ^b	93.75±6.59 ^c	129.25±1.25 ^b	22.75±0.95 ^a
<i>Basmati 370</i>	132.44±3.85 ^a	29.88±2.08 ^a	26.44±1.92 ^a	11.06±1.70 ^c	105.5±2.72 ^b	108.25±2.96 ^b	130.25±0.63 ^b	19.75±0.25 ^a
V1	85.063±0.78 ^d	20.75±1.92 ^b	17.94±2.04 ^b	47.19±11.58 ^c	123.75±0.48 ^a	126.0±0.71 ^a	139.5±0.65 ^a	21.0±1.23 ^a
V3	84.0±5.19 ^d	21.50±0.76 ^b	19.13±13.64 ^b	31.94±1.85 ^d	128.75±0.85 ^a	130.75±0.85 ^a	141.75±0.25 ^a	19.5±1.19 ^a
Mean	103.61	22.29	19.09	48.23	109.60	111.80	134.00	20.70
Value	<.0001	0.0010	0.0014	0.0002	<.0001	<.0001	<.0001	0.2061

Means with different superscript letters within a column are significantly different ($p \leq 0.05$) according to Tukey's test, the lines V1, V3 and *Basmati 370* are rice parent lines.

There was no significant difference with respect to productive tillers and 1000-grain weight. The number of spikelet sterility ranged from 11.06 for *Basmati 370* to 89.19 for V1 × *Basmati 370*. Among the hybrids, V1 × *Basmati 370* had a higher panicle sterility rate than V3 × *Basmati 370*. Spikelet sterility percentages were 11.06, 47.19 and 31.94 percent for *Basmati 370*, V1 and V3,

respectively. Hybrids had significantly higher spikelet sterility than the parents. Spikelet sterility of the V1 × *Basmati 370* hybrid was significantly higher than the parental controls. Although V3 × *Basmati 370* had higher spikelet sterility than the parent, it was only significant to *Basmati 370*, while this was not significant to V1 and V3 (Table 4).

3.4 Correlation coefficient analyses of parent and F₁ hybrids grown outside the greenhouse

A significant and negative correlation was observed between days to heading with plant height ($r=0.575^{**}$), days to flowering ($r=-0.558^{**}$) at $P<0.05$ and days to maturity ($r=-0.724^*$). Sterile spikelets negatively correlated with total tillers ($r=-0.439^{***}$) and days to flowering ($r=-0.442^{***}$). There was a positive correlation between heading days with flowering days ($r=0.999^{***}$) and days to maturity ($r=0.841^{***}$). Days to flowering was positively correlated with days to maturity ($r=0.834^{***}$) and negatively with sterile spikelets ($r=-0.442^{***}$), as shown in Table 5.

3.5 Marker-assisted selection for BC₁F₂ with *fgr* genes

Five BC₁F₂ lines developed had three bands similar to *Basmati* 370 parent when amplified using 257 bps, 355 bps and 580 bps markers, which identifies them as heterozygous non-aromatic. In contrast, the remaining three hybrids had positive bands for 257 bps and 355 bps markers, associated with heterozygous non-aromatic traits. Two hybrids had one band when amplified with

257 bps marker, a show of homozygous aromatic trait, while V1 and V3 had one band each associated with 355 bps marker, indicating that it is homozygous non-aromatic (Figure 5).

3.6 Selection BC₁F₂ with P/TGMS

The RM12521 marker is a recessive marker linked to a *p/tgms12-1* gene fragment of size 375 and amplified as a monomorphic band. Among 10 BC₁F₂, five had a clear banding pattern similar to V1 and V3, while five hybrids had faint bands inclining toward the *Basmati* 370 banding pattern (Figure 6).

3.7 Agro-morphological performance of the parents and BC₁F₂ lines under high-temperature treatment

Analysis of variance carried out on the agro-morphological traits showed a significant difference ($p<0.001$) with respect to plant height, total tillers and total number of effective tillers. There were significant differences ($p<0.001$) with respect to the total number of tillers, productive tillers and plant height. The plant height ranged from 55.03 cm for V1 to 102.47 cm for HB14 (V3 × *Basmati* 370). Most of the hybrids were significantly shorter than *Basmati* 370;

Table 5 Correlation coefficients (r) of agronomic traits of parents and F₁ plants

PH	PH							
TT	0.531		TT					
PT	0.123	0.395	PT					
HD	-0.575**	0.072	0.340	HD				
FD	-0.558**	0.073	0.337	0.999***	FD			
MD	-0.724*	-0.183	0.224	0.841***	0.834***	MD		
SS	-0.012	-0.439***	-0.271	-0.427	-0.442***	-0.265	SS	
GW	-0.060	-0.299	-0.265	-0.361	-0.360	-0.197	0.255	GW

Significance codes are *, ** and *** representing $p<0.05$, 0.01 and 0.001 respectively, PH - plant height, TT - total tillers, PT - productive tillers, HD - days to heading, FD - days to flowering, MD - days to maturity, SS - sterile spikelets and GW - 1000 grain weight.

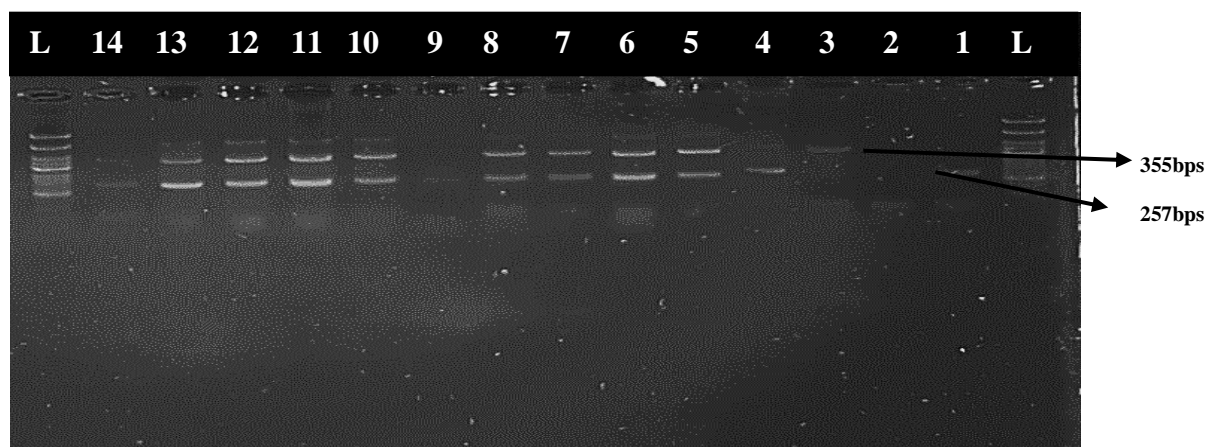


Figure 5 Agarose gel image showing BC₁F₂ breeding population amplified using molecular markers linked to *fgr* gene, L - 1000bps ladder, 2 - V1, 3- V3 while 12- *Basmati* 370 and 1, 4-11, 13 and 14 -BC₁F₂ hybrids.

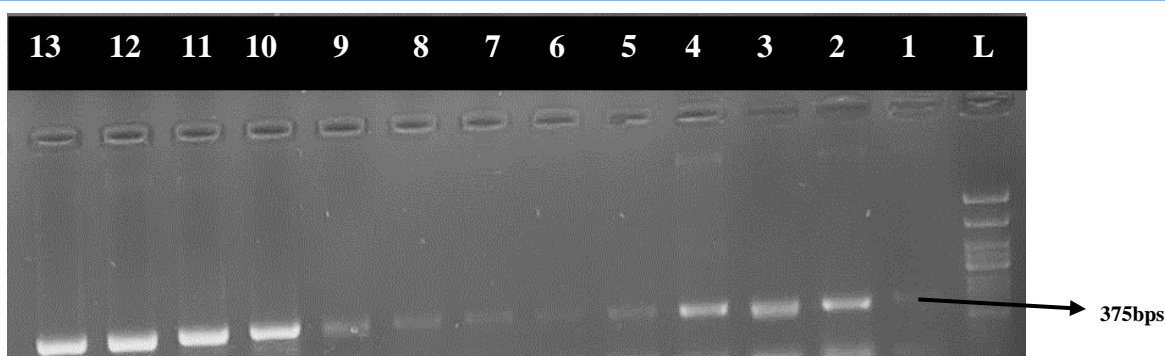


Figure 6 Agarose gel image of BC₁F₂ breeding lines showing RM12521 primer linked to *p/tgms12-1* gene, L - 1000bs ladder, 1 - Basmati 370, 2 - V1, 3 - V3 parents and 1-13 - BC₁F₂ hybrid lines.

Table 6 Means of agronomic traits of rice parents and BC₁F₂ hybrids under high-temperature treatment

Line	Total number of tillers (TT)	Number of productive tillers (PT)	Plant height (cm)
V1	11.33±1.07 ^{ab}	10.44±0.96 ^{ab}	55.03±0.63 ^d
V3	7.22±0.63 ^c	6.36±0.53 ^c	63.36±1.46 ^d
<i>Basmati 370</i>	12.06±0.8 ^{ab}	10.92±0.71 ^{ab}	100.81±2.66 ^a
V3 × <i>Basmati 370</i> (HB1)	15.11±1.05 ^a	13.25±0.91 ^a	90.06±4.10 ^{abc}
V3 × <i>Basmati 370</i> (HB2)	11.33±0.55 ^{ab}	10.17±0.49 ^{ab}	78.86±4.29 ^c
V3 × <i>Basmati 370</i> (HB3)	10.81±0.83 ^{bc}	9.28±0.56 ^{bc}	101.72±2.43 ^a
V3 × <i>Basmati 370</i> (HB7)	11.50±0.82 ^{ab}	10.39±0.75 ^{ab}	79.94±2.57 ^{bc}
V3 × <i>Basmati 370</i> (HB8)	12.44±0.82 ^{ab}	11.17±0.70 ^{ab}	96.19±1.61 ^a
V1 × <i>Basmati 370</i> (HB10)	11.69±0.89 ^{ab}	9.78±0.79 ^b	92.92±2.84 ^{ab}
V1 × <i>Basmati 370</i> (HB11)	10.94±0.71 ^{bc}	9.75±0.58 ^b	82.28±2.86 ^{bc}
V1 × <i>Basmati 370</i> (HB12)	11.08±0.81 ^b	9.39±0.65 ^{bc}	92.31±3.22 ^{ab}
V1 × <i>Basmati 370</i> (HB13)	11.33±0.94 ^{ab}	9.69±0.76 ^b	90.89±4.11 ^{abc}
V1 × <i>Basmati 370</i> (HB14)	13.00±0.62 ^{ab}	11.19±0.52 ^{ab}	102.47±1.34 ^a
Pooled Mean	11.53	10.14	86.68
P value	<.0001	<.0001	<.0001

The means with a different superscript letter within a column are significantly different ($P \leq 0.05$) according to Tukey's test, lines V1, V3 and *Basmati 370* are rice parent lines and HB1 to HB14 are BC₁F₂ lines.

Table 7 Correlation coefficients (r) of agronomic traits of parents and F₂ plants

Parameter	TT	PT	PH
Total no. of tillers	1.00000		
Productive tillers	0.93670***	1.00000	
Plant height	0.25252***	0.21831***	1.00000

***, significance at $p < 0.001$, Plant height (PH), total number of tillers (TT), and number of productive tillers (PT).

hence, plant height was significantly decreased. Hybrid 1, 14 and 8 had the highest total number of tillers (15.11, 13.00 and 12.44), respectively. Similarly, hybrids 1, 14 and 8 had the highest productive tillers, including 13.25, 11.19 and 11.17, respectively (Table 6).

3.8 Pearson's correlation coefficient analysis in the BC₁F₂ population

Significant positive correlations were observed between productive tillers, the total number of tillers ($r=0.9367$ ***), and plant height

($r = 0.25252^{***}$). In addition, productive tillers and plant height were significantly and positively correlated ($r = 0.21831^{***}$), as shown in Table 7.

4 Discussion

High greenhouse temperatures maintained in the simple greenhouse induced near complete sterility in P/TGMS rice lines that were in contrast to those plants grown under normal temperatures outside the greenhouse. The average temperatures at the study site, Kenya's main rice growing area, ranged from 15.6°C to 28.6°C, which is not conducive to induce complete sterility in P/TGMS rice. In this research, greenhouse intervention could sustain temperatures to above 22°C at night and above 33°C during the day, which is ideal for hybrid rice seed production using P/TGMS lines. This type of hybrid seed technology is essential to rice yield improvement since it can raise yield by 25% to 30% above purebred varieties (Tongmark et al. 2021).

The P/TGMS lines form an important component in a two-line hybrid rice seed production system (Li et al. 2024). Male sterility occurrence in P/TGMS is environmentally dependent on temperature and/or photoperiod (Ashraf et al. 2020). The pollen viability in P/TGMS is one of the most important parameters in ensuring hybrid seeds are not contaminated by self-bred seeds (Njau 2017). High temperature (24-32°C) is the key factor contributing to complete sterility in P/TGMS, while low temperatures (below 23°C) contribute to male fertility. Photoperiod also influences the P/TGMS rice lines, where longer photoperiods (>14 hours) enhance male sterility while shorter photoperiods (<12 hours) enhance male fertility (Ashraf et al. 2020). Photoperiod is effective between the critical fertility point (CFP) and critical sterility point (CSP), and this range of temperature is known as the temperature range of photo-sensitivity (Swaminathan 2021). High average temperatures in P/TGMS lines lower the critical photoperiod level required to induce sterility (Peng et al. 2023). When the temperatures are high, they compensate for the reduced photoperiod required to induce complete pollen sterility (Liu et al. 2023). Fertility alteration in P/TGMS lines usually starts from the formation stage of the pollen mother cell to the meiotic division stage. Therefore, the interaction of photoperiod and temperature has been used to realize better induction of pollen sterility, especially in P/TGMS rice lines (El-Mowafi et al. 2021).

In this research, the P/TGMS were treated under greenhouse growth conditions at the primordial stage up to the initiation of heading. This was adequate to induce sterility levels above 90%, comparable to the report of Vishvapriya et al. (2023) and Swaminathan (2021), who observed that complete sterility can be induced when the P/TGMS rice lines at the critical-sterility phase are grown under high-temperature conditions. Pollen sterility correlated positively with high temperature, confirming the ability

of greenhouse temperatures to induce sterility significantly in the EGMS lines. Temperatures above 35°C lasting more than one hour during anthesis lead to high sterility levels in rice plants (Hu et al. 2021). Therefore, the greenhouse growth conditions were adequate for complete male gamete sterility in EGMS and significantly reduced hybrid seed adulteration by self-bred seeds.

Breeding efforts using the P/TGMS rice lines have been made by scientists in the last three decades, leading to the release of new varieties using the EGMS breeding method (Swaminathan 2021). The P/TGMS lines have greatly improved the yield potential and grain quality of different rice varieties (Wang et al. 2022). The P/TGMS lines produce fertile hybrid seeds during the sterile phase by crossing them with a fertile male pollinator, thus utilizing heterosis to increase yield. When grown under optimum temperature during their fertile phase, the P/TGMS self-pollinate to propagate themselves for breeding continuity (Ashraf et al. 2020). A single recessive gene controls the P/TGMS traits in rice lines. Since it is a nuclear gene, it is easily transferable through backcrossing to desired varieties (Fang et al. 2023). This provides a broader genetic resource for rice breeding and has helped in the production of rice hybrids with strong hybrid vigour.

Visual scoring for the *ptgms12-1* gene using RM12521 SSR markers on agarose gel electrophoresis in the BC₁F₂ population was not specific to the target gene since the marker was monomorphic; hence, it was challenging to use markers-assisted selection to identify hybrid from parents in this research. This agreed with Njau (2017), who used the same marker and found that the bands were not polymorphic. The cross between V1 and *Basmati* 370 provided a BC₁F₂ with over 89% pollen sterility grown under male gametes emasculation temperature conditions. Attempts to use heterosis in *Basmati* rice improvement have been reported (Budhlakoti and Baskheti 2021). However, no commercial breeding varieties have been released to the market. The novel BC₁F₂ is a milestone towards producing commercial hybrid rice varieties of *Basmati* origin.

Flavour in rice, made up of taste and aroma, is one of the most important factors in evaluating rice quality (Hu et al. 2020). Scented rice with distinct aroma and good quality traits fetches a premium value in national and international markets (Roy et al. 2020). However, most of these aromatic rice varieties are limited by low yields, poor agronomic performance, and susceptibility to environmental conditions. In addition, they are produced in only a few countries (Dar et al. 2021). The new BC₁F₂ lines, once stabilized and released into the market, will improve *Basmati* yield through heterosis that has been used to break the purebred lines breeding plateau (Njau 2017).

Different volatile aromatic compounds in rice include aldehydes, ketones, organic acids, alcohols, esters, hydrocarbons, phenols,

pyrazines, and pyridine. The 2-acetyl-1-pyrroline (2-AP) is the key compound responsible for the aroma due to low sensory threshold and strong popcorn and sweet flavour (Verma and Srivastav 2022). The 2-AP is a vital characteristic of aromatic rice (Luo et al. 2020). Genetically, aroma in rice is thought to originate from spontaneous recessive mutations in *fgr* (also known as *OsBadh2/badh2/osbadh2/os2-AP* genes) (Dutta et al. 2022). These mutations inhibit the flow of γ -aminobutyraldehyde (GAB-ald) to γ -aminobutyric acid (GABA), which results in the conversion of accumulated GAB-ald to a fragrance component s2-AP through a non-enzymatic reaction process with methylglyoxal (Proadhan and Qingyao 2020).

In *Basmati* 370 rice, the aroma trait is under a recessive gene control (Varatharajan et al. 2021) and has elevated levels of the 2-acetyl-1-pyrroline(2AP) in the aerial parts of the rice plant (Bradbury et al. 2005). The betaine aldehyde dehydrogenase (BAD2) enzyme responsible for aroma is due to a deletion in the gene encoding BAD2 on chromosome 8, deactivating the normal BAD2 gene (Bradbury et al. 2005). Rice breeders use a single tube allele-specific PCR to determine the genotypic status of the rice plant if it is either homozygous aromatic, homozygous non-aromatic or heterozygous non-aromatic (Bradbury et al. 2005). Using this method, three heterozygous non-aromatic BC₁F₂ lines and two homozygous aromatic BC₁F₂ were confirmed in this study.

Breeding for recessive genes requires either selection at F₂ segregation or backcrossing F₁ with a recessive gene donor to get homozygous recessive offspring (Hussain et al. 2021). In this research, *Basmati* 370 was used as a donor to produce lines with the *p/tgms12-1* gene. The hybrids produced were not expected to have aroma since the *fgr* gene is a recessive trait. This breeding challenge needs to be solved by producing *Basmati* with *p/tgms12-1* genes, and if it is achieved, then both male and female parents in the hybrid rice programme will have the aroma and hence the F₁s. This research indicates that the *fgr* and *p/tgms12-1* genes were successfully introgressed into a *Basmati* 370 rice variety validated using molecular marker analysis. Carsono et al. (2023) found that crosses of aromatic and non-aromatic rice varieties resulted in non-aromatic hybrids, and since the *fgr* is a recessive gene, backcrossing with a recessive aromatic line is needed to enable the selection of homozygous with aroma trait.

Successful crosses of *Basmati* 370 with V1 and V3 to obtain BC₁F₂ were ascertained using morphological and SSR molecular markers. The SSR molecular markers are commonly used to confirm the hybrids in many plant species, including rice because they are highly polymorphic and codominant (Adiredjo and Ardiarini 2023). In BC₁F₂, the hybrids were isolated with both *fgr* and *p/tgms12-1*, demonstrating the ability to breed a fragrant rice line with *Basmati*-like traits.

Hybrids that involve *Basmati* 370 and the P/TGMS lines (V1 and V3) have conspicuous incidences of anthocyanin, making them distinct from their parents (Njiruh et al. 2013). Therefore, anthocyanin can be used as an ideal morphological marker in selecting F₁ hybrids of *Basmati* 370 and P/TGMS lines (V1 and V3). In this study, the F₁ hybrids were distinguished by the presence of anthocyanin pigmentation in their stem and spikelet tips. These results are similar to previous studies involving *Basmati* 370 hybrids (Njiruh et al. 2013; Nthakanio and Kariuki 2019). The hybrids in this study contained anthocyanin at the base of the stem, spikelet tips and the stigma. Therefore, anthocyanin is a promising and reliable morphological marker for selecting F₁ hybrids involving *Basmati* 370 and P/TGMS lines.

Agro-morphological traits such as plant height (cm), total number of tillers, days to heading, days to flowering and days to maturity showed a positive heterosis between the hybrids and the parents in the F₁ population. The F₁ population planted outside the greenhouse showed some levels of panicle sterility at maturity despite being planted in fertility-inducing conditions. Sterility in F₁ has been reported in hybrids lacking wide compatibility genes (Rao et al. 2021). *Basmati* 370 (cK) had the lowest percentage of panicle sterility because it lacks the *p/tgms12-1* gene present in the F₁ hybrids and their parents V1 and V3. Among the F₁ hybrids, V1 hybrids had a higher percentage of panicle sterility than V3 hybrids. In addition, the V1 parent has a higher panicle sterility than the V3 parent. This shows that the V1 has higher heritability than the V3 and is thus more useful in producing an EGMS breeding line. This agrees with Asante et al. (2006), who conducted a study on the inheritance of spikelet fertility from two rice crosses. An increased number of spikelets in the hybrids obtained are an indication of positive heterosis and a yield benefit of hybrid rice lines.

The BC₁F₂ population had more sterile spikelets than *Basmati* 370 under greater than 30 °C growth conditions. This indicates the presence of the *p/tgms12-1* gene in the hybrids and the absence of the same gene in *Basmati* 370 (cK). This indicates successful introgression of *p/tgms12-1* and *fgr* gene into BC₁F₂, indicating possible production of EGMS of *Basmati* origin. Days to heading, days to flowering and days to maturity were significantly different (shorter) in F₁ populations compared to V1 and V3. Shortening the days to maturity is a desirable trait to help in improving the rice breeding program since a shorter maturing period reduces pest and disease management costs (Heredia et al. 2022). Negative heterosis for traits such as days to heading and plant height is desirable for breeding semi-dwarf and early maturing lines (Gaballah et al. 2022). In the BC₁F₂ population, there was a positive correlation between the number of productive tillers and the total number of tillers. This is a clear indication of positive heterosis, which is a desired trait for breeders to increase yield. Plant height had a

positive correlation with the total number of tillers and the total number of productive tillers, which is agreed upon by Prajapati et al. (2022).

Conclusion

This study revealed that high temperatures above 30°C in the greenhouse during the day effectively induce the expression of the *p/tgms12-1* gene in the EGMS and BC₁F₂ lines, which can potentially expand the space for hybrid seed production. Using polythene greenhouses will accelerate the breeding of novel EGMS lines in medium altitude regions such as Mwea, Kenya, where the normal daylight length and temperature levels are not conducive to applying EGMS system in rice breeding. From this study, it is possible to introgress *p/tgms12-1* genes into *Basmati 370* rice to develop novel lines with *p/tgms12-1* and *fgr* gene, a breakthrough that will enable the advancement of heterosis in *Basmati* rice yield improvement. From this study, the BC₁F₂ breeding lines had better agronomical traits than the parents, which will benefit rice breeders more.

Acknowledgement

This project was funded by the National Research Fund (NRF-Kenya). I acknowledge the University of Embu and KALRO Mwea for providing research facilities.

References

- Abebrese, S. O., Dartey, P. K. A., Akromah, R., Gracen, V. E., Offei, S. K., & Danquah, E. Y. (2018). Genetics of anther indehiscence with exerted stigmas and its application in hybrid rice breeding. *Journal of Crop Improvement*, 32(4), 552-565.
- Adiredjo, A. L., & Ardiarini, N. R. (2023). Genetic Purity Analysis Using Polymorphic SSR Markers in Rice Genotypes (*Oryza sativa* L.) and Their Confirmation for the Parental Lines. *Plant breeding and biotechnology*, 11(3), 220-224.
- Ahmed, M. S., Siddique, F., Satti, A. M., Ullah, Z., & Hussain, I. (2020). Indigenization of hybrid rice development in Pakistan: Breeding prospects and approaches. *Journal of Pure and Applied Agriculture*, 5(4): 1 – 10.
- Akhter, M., & Haider, Z. (2020). Basmati rice production and research in Pakistan. *Sustainable Agriculture Reviews*, 39, 119 – 136.
- Ali, J., Paz, M. D., & Robiso, C. J. (2021). Advances in Two-Line Heterosis Breeding in Rice via the Temperature-Sensitive Genetic Male Sterility System. In Ali, J., Wani, S.H. (eds) *Rice Improvement* (pp. 99-145). Springer, Cham. https://doi.org/10.1007/978-3-030-66530-2_4.
- Amist, N., & Singh, N. B. (2020). Male sterility system for hybrid rice breeding and seed production. In A. Roychoudhury (eds) *Rice Research for Quality Improvement: Genomics and Genetic Engineering: Volume 2: Nutrient Biofortification and Herbicide and Biotic Stress Resistance in Rice* (pp. 269-289). Springer, Singapore. https://doi.org/10.1007/978-981-15-5337-0_13
- Asante, M. D., Akromah, R., Darty, P. K., & Ofori, J. (2006). Inheritance of spikelet fertility in two rice crosses. *Journal of Science and Technology (Ghana)*, 26(3), 40 – 45.
- Ashraf, M. F., Peng, G., Liu, Z., Noman, A., Alamri, S., et al. (2020). Molecular control and application of male fertility for two-line hybrid rice breeding. *International Journal of Molecular Sciences*, 21(21), 7868.
- Atera, E. A., Onyancha, F. N., & Majiwa, E. B. (2018). Production and marketing of rice in Kenya: Challenges and opportunities. *Journal of Development and Agricultural Economics*, 10(3), 64 – 70.
- Bradbury, L. M., Fitzgerald, T. L., Henry, R. J., Jin, Q., & Waters, D. L. (2005). The gene for fragrance in rice. *Plant Biotechnology Journal*, 3(3), 363 – 370.
- Budhlakoti, V., & Baskheti, D. C. (2021). Studies on heterosis for grain yield and yield component traits in basmati rice (*Oryza sativa* L.). *Journal of Pharmacognosy and Phytochemistry*, 10(1), 1920-1925.
- Carsono, N., Tambunan, R. R., Sari, S., & Wicaksana, N. (2023). Molecular and phenotypic markers for pyramiding multiple traits in rice. *Open Agriculture*, 8(1), 20220187.
- Chang, Z., Chen, Z., Wang, N., Xie, G., Lu, J., et al. (2016). Construction of a male sterility system for hybrid rice breeding and seed production using a nuclear male sterility gene. *Proceedings of the National Academy of Sciences*, 113(49), 14145 – 14150.
- Chen, L., Zhao, Z., Liu, X., Liu, L., Jiang, L., et al. (2011). Marker-assisted breeding of a photoperiod-sensitive male sterile japonica rice with high cross-compatibility with indica rice. *Molecular Breeding*, 27, 247 – 258.
- Chukwu, S. C., Rafii, M. Y., Ramlee, S. I., Ismail, S. I., Oladosu, Y., Okporie, E., & Jalloh, M. (2019). Marker-assisted selection and gene pyramiding for resistance to bacterial leaf blight disease of rice (*Oryza sativa* L.). *Biotechnology & Biotechnological Equipment*, 33(1), 440-455.
- Cordero-Lara, K. I. (2020). Temperate japonica rice (*Oryza sativa* L.) breeding: History, present and future challenges. *Chilean journal of agricultural research*, 80(2), 303-314.

- Dar, M. H., Bano, D. A., Waza, S. A., Zaidi, N. W., Majid, A., et al. (2021). Abiotic stress tolerance-progress and pathways of sustainable rice production. *Sustainability*, *13*(4), 2078.
- Denis, B. E. (2020). *Assessment of yield, grain quality and combining ability of selected rice cultivars in Kenya* (Doctoral dissertation, University of Nairobi, Kenya).
- Denis, B. E. J., Ngugi, K., & Kimani, J. M. (2022). Genotypic Performance of Kenyan Rice Cultivars for Grain Yield and Quality. *Journal of Agricultural Studies*, *10*(4), 201 – 217.
- Dutta, C., Nath, D. J., & Phyllei, D. (2022). Aromatic rice and factors affecting aroma in rice. *International Journal of Environment and Climate Change*, *12*(11), 1773-1779.
- El-Mowafi, H. F., AlKahtani, M. D., El-Hity, M. A., Reda, A. M., Al Husnain, L., El-Degwy, E. S., & Attia, K. A. (2021). Characterization of fertility alteration and marker validation for male sterility genes in novel PTGMS lines hybrid rice. *Saudi Journal of Biological Sciences*, *28*(8), 4109 – 411.
- Fang, X., Sun, Y., Li, J., Li, M., & Zhang, C. (2023). Male sterility and hybrid breeding in soybean. *Molecular Breeding*, *43*(6), 47.
- Gaballah, M. M., Attia, K. A., Ghoneim, A. M., Khan, N., El-Ezz, A. F., Yang, B., & Al-Doss, A. A. (2022). Assessment of genetic parameters and gene action associated with heterosis for enhancing yield characters in novel hybrid rice parental lines. *Plants*, *11*(3), 266.
- Hamad, H. S., Ghazy, M. I., Bleih, E. M., Gewaily, E. E., Gaballah, M. M., et al. (2022). Evaluation of advanced mutant restorer lines for enhancing outcrossing rate and hybrid seed production of diverse rice cytoplasmic male sterile lines. *Agronomy*, *12*(11), 2875.
- Heredia, M. C., Kant, J., Prophan, M. A., Dixit, S., & Wissuwa, M. (2022). Breeding rice for a changing climate by improving adaptations to water saving technologies. *Theoretical and Applied Genetics*, *135*(1), 17-33.
- Hu, Q., Wang, W., Lu, Q., Huang, J., Peng, S., & Cui, K. (2021). Abnormal anther development leads to lower spikelet fertility in rice (*Oryza sativa* L.) under high temperature during the panicle initiation stage. *BMC Plant Biology*, *21*, 1-17.
- Hu, X., Lu, L., Guo, Z., & Zhu, Z. (2020). Volatile compounds, affecting factors and evaluation methods for rice aroma: A review. *Trends in food science & technology*, *97*, 136-146.
- Hussain, A., Arshad, K., Abdullah, J., Aslam, A., Azam, A., et al. (2021). A Comprehensive Review on Breeding Technologies and Selection Methods of Self-pollinated and Cross-Pollinated Crops. *Asian Journal of Biotechnology and Genetic Engineering*, *4*(3), 35-47.
- Li, J., Luo, X., & Zhou, K. (2024). Research and development of hybrid rice in China. *Plant Breeding*, *143*(1), 96-104.
- Liu, D., Shi, J., Liang, W., & Zhang, D. (2023). Molecular mechanisms underlying plant environment-sensitive genic male sterility and fertility restoration. *Seed Biology*, *2*(1), 13 doi: 10.48130/SeedBio-2023-0013.
- Luo, H., Zhang, T., Zheng, A., He, L., Lai, R., et al. (2020). Exogenous pyrroline induces regulation in 2-acetyl-1-pyrroline (2-AP) biosynthesis and quality characters in fragrant rice (*Oryza sativa* L.). *Scientific Reports*, *10*(1), 13971.
- Mahuku, G. S. (2004). A simple extraction method suitable for PCR-based analysis of plant, fungal, and bacterial DNA. *Plant Molecular Biology Reporter*, *22*, 71 – 81.
- Ng'endo, M., Kinyua, M., Chebet, L., Mutiga, S., Ndung'u, J., et al. (2022). The importance of market signals in crop varietal development: lessons from *Komboka* rice variety. *CABI Agriculture and Bioscience*, *3*(1), 1 – 21.
- Njau, K. S. (2017). Production of hybrid rice using environment sensitive genic male sterile (EGMS) and basmati rice lines (Doctoral dissertation, Kenyatta University, Nairobi, Kenya).
- Njiruh, N. P., Kanya, J. I., Kimani, J. M., & Wajogu, R. (2013). Production of Hybrid Basmati Rice in Kenya: Progress and Challenges. *International Journal of Innovations in Bio-Sciences*, *3* (4), 115-124.
- Nthakanio, P. N., & Kariuki, S. N. (2019). Production of Hybrid Rice seeds using environment sensitive genic male sterile (EGMS) and basmati rice lines in Kenya. *BioRxiv*, 755306.
- Peng, G., Liu, Z., Zhuang, C., & Zhou, H. (2023). Environment-sensitive genic male sterility in rice and other plants. *Plant, Cell & Environment*, *46*(4), 1120-1142.
- Prajapati, M. R., Bala, M., Patel, V. P., Patel, R. K., Sushmitha, U. S., Kyada, A. D., & Patel, D. P. (2022). Analysis of genetic variability and correlation for yield and its attributing traits in F2 population of rice (*Oryza sativa* L.). *Electronic Journal of Plant Breeding*, *13*(3), 983-990.
- Prasanna, G. S., Parveen, S. S., Muraleedharan, A., & Joshi, J. L. (2024). Heterosis Analysis for Yield and Resistance to Yellow Stem Borer (*Scirpophaga incertulas* Wlk.) in F₁ Progenies Derived from Six Crosses of Rice (*Oryza sativa* L.). *Environment and Ecology*, *42*(3B), 1431-1439.

- Prodhan, Z. H., & Qingyao, S. H. U. (2020). Rice aroma: A natural gift comes with price and the way forward. *Rice Science*, 27(2), 86-100.
- Rao, J., Wang, X., Cai, Z., Fan, Y., & Yang, J. (2021). Genetic analysis of s5-interacting genes regulating hybrid sterility in rice. *Rice*, 14, 1-9.
- Roy, S., Banerjee, A., Basak, N., Kumar, J., & Mandal, N. P. (2020). Aromatic rice. *The future of rice demand: Quality beyond productivity*, 251-282. DOI: https://doi.org/10.1007/978-3-030-37510-2_11.
- Sreedhar, S., & Reddy, R. U. (2019). Association studies for yield and its traits in rice (*Oryza sativa* L.) genotypes. *International Journal of Current Microbiology and Applied Sciences*, 8(1), 2337 – 2342.
- Swaminathan, M. (2021). Progress and Prospects of Two Line Rice Breeding in India. In M. Huang (Ed.) *Integrative Advances in Rice Research*. Intechopen publication. DOI: 10.5772/intechopen.99545
- Tongmark, K., Chakhonkaen, S., Sangarwut, N., Wasinanon, T., Panyawut, N., Dithab, K., & Muangprom, A. (2021). Development of high yielding two-line hybrid rice in Thailand. *Science Asia*, 47(2), 153-161. doi: 10.2306/scienceasia1513-1874.2021.019.
- Uyeh, D. D., Asem-Hiablie, S., Park, T., Kim, K., Mikhaylov, A., Woo, S., & Ha, Y. (2021). Could Japonica Rice Be an Alternative Variety for Increased Global Food Security and Climate Change Mitigation? *Foods (Basel, Switzerland)*, 10(8), 1869 – 1869.
- Varatharajan, N., Sekaran, D. C., Murugan, K., & Chockalingam, V. (2021). Rice aroma: Biochemical, genetics and molecular aspects and its extraction and quantification methods. In M. Huang (Ed.) *Integrative Advances in Rice Research*, 33. DOI: 10.5772/intechopen.98913.
- Verma, D. K., & Srivastav, P. P. (2022). Extraction, identification and quantification methods of rice aroma compounds with emphasis on 2-acetyl-1-pyrroline (2-AP) and its relationship with rice quality: A comprehensive review. *Food Reviews International*, 38(2), 111-162.
- Vishvapriya, M., Binodh, A. K., Manonmani, S., Kumaresan, D., Senthil, A., & Kumar, G. S. (2023). Genetics of sterility behaviour in Thermo sensitive genic male sterility system in rice (*Oryza sativa* L.). *Electronic Journal of Plant Breeding*, 14(3), 1105 – 1110.
- Wang, H., Xiong, R., Zhou, Y., Tan, X., Pan, X., et al. (2022). Grain yield improvement in high-quality rice varieties released in southern China from 2007 to 2017. *Frontiers in Sustainable Food Systems*, 6, 986655.
- Yılmaz, H., & Njora, B. (2021). Analysis of the impact of agricultural policies on food security in Kenya. *Eurasian Journal of Agricultural Research*, 5(2), 66-83.
- Zheng, X., Wei, F., Cheng, C., & Qian, Q. (2024). A historical review of hybrid rice breeding. *Journal of Integrative Plant Biology*, 66(3), 532-545.
- Zhou, H., Liu, Q., Li, J., Jiang, D., Zhou, L., et al. (2012). Photoperiod-and thermo-sensitive genic male sterility in rice are caused by a point mutation in a novel noncoding RNA that produces a small RNA. *Cell research*, 22(4), 649 – 660.



Journal of Experimental Biology and Agricultural Sciences

<http://www.jebas.org>

ISSN No. 2320 – 8694

ASSESSMENT OF THE ECONOMIC BENEFIT OF CABBAGE PRODUCTION UNDER DIFFERENT IRRIGATION LEVELS AND SOIL AMENDMENTS IN A SEMI-ARID ENVIRONMENT

Kuume B. P. ENGUWA^{1,*} , Lydia N. HORN² , Simon K. AWALA¹ , Stefan Glaser³ 

¹Department of Crop Production and Agricultural Technologies, School of Agriculture and Fisheries Sciences, University of Namibia, Oshakati, Namibia

²Zero Emissions Research Initiative, Multi-disciplinary Research Centre, University of Namibia, Windhoek, Namibia 12007

³Gesellschaft für Internationale Zusammenarbeit (GIZ), Farming for Resilience (F4R), Namibia

Received – May 30, 2024; Revision – August 19, 2024; Accepted – November 05, 2024

Available Online – November 29, 2024

DOI: [http://dx.doi.org/10.18006/2024.12\(5\).770.783](http://dx.doi.org/10.18006/2024.12(5).770.783)

KEYWORDS

Economic benefit

Irrigation

Soil amendments

Cabbage production

ABSTRACT

Crop production in small-scale farming communities in semi-arid Central Namibia faces significant challenges due to the high costs associated with irrigation and fertilizers. This study evaluated the impact of different irrigation levels (full and reduced) and six types of soil amendments—biochar, compost, zeolite, NPK, Be-Grow Boost (L) hydrogel, hoof and horn combined with a bone meal (HHB meal), and control on the economic benefits of cabbage production and assessed their feasibility. In the first experiment, irrigation was implemented at 79.6 m³ (100% of the water requirement) for four days a week, classified as full irrigation, and at 39.6 m³ (50% of the water requirement) for two days a week, termed reduced irrigation. Among the fully irrigated treatments, Be-Grow Boost (L) hydrogel, zeolite, and NPK demonstrated the highest Benefit-Cost Ratios (BCRs) at 3.81, 3.67, and 3.65, respectively. In the second experiment, irrigation schedules were adjusted to five and four days per week, using a total of 136.0 m³ (170% of the water requirement) and 124.8 m³ (150% of the water requirement) of water. The compost, HHB meal, and NPK application rates were also modified. The fully irrigated Be-Grow Boost (L) hydrogel, NPK, and reduced irrigation with HHB meal achieved the highest and comparable yields of marketable cabbage heads per hectare, with BCRs of 3.43, 3.24, and 3.29, respectively. In conclusion, utilizing fully irrigated Be-Grow Boost (L) hydrogel, NPK, and reduced irrigation with HHB meal could be effective practices for sustainable crop production in the semi-arid, sandy soil conditions typical of Central Namibia. Moreover, local biochar production could enhance sustainability by reducing overall production costs.

* Corresponding author

E-mail: benenguwa@gmail.com (Kuume B. P. Enguwa)

Peer review under responsibility of Journal of Experimental Biology and Agricultural Sciences.

Production and Hosting by Horizon Publisher India [HPI]
(<http://www.horizonpublisherindia.in/>).
All rights reserved.

All the articles published by [Journal of Experimental Biology and Agricultural Sciences](#) are licensed under a [Creative Commons Attribution-NonCommercial 4.0 International License](#) Based on a work at www.jebas.org.



1 Introduction

With alarming global population growth, meeting the increasing food demand is becoming a significant challenge, mainly due to the impacts of climate change and inflated input prices affecting crop production. In sub-Saharan Africa (SSA), and specifically in the semi-arid region of Central Namibia, the challenges in crop production primarily stem from low fertilizer usage, the result of unfavourable input prices (Araya et al. 2024), poor sandy soils, and lack of irrigation (Chivenge et al. 2022), all of which lead to low yields. Furthermore, many farmers in this area are small-scale farmers most affected by these challenges due to their limited financial resources (Chivenge et al. 2022; Wanga et al. 2022).

The increasing rural-to-urban migration also hinders food security in Central Namibia, where Windhoek, the capital city, is a preferred destination for many migrants. Many Windhoek inhabitants are food-insecure women living in informal settlements (Kazembe et al. 2024). Additionally, according to the Namibia Statistics Agency (NSA) national census report (2013), the population of the Khomas region is projected to rise to 827,619 by 2041, up from 342,141 in 2010, constituting approximately 24% of the Namibian population. Alongside urban migration and population growth, Namibia's agricultural sector contributes a mere 5% to the GDP (Sichoongwe 2024), in contrast to 23% for SSA (Nyambo et al. 2022). The Namibian crop industry accounts for only 2% of the local sector, compared to 3% of the livestock industry. Furthermore, Namibia imports around 60% of its crop and vegetable needs (Neema and Kalitanyi 2023), primarily from neighbouring South Africa (World Integrated Trade Solution "WITS" 2021). Therefore, increasing crop production, particularly in Central Namibia, is crucial to ensure the region's food security amidst the rapidly growing population.

The abundant natural resources available, such as soil amendments and fertilizers, can be leveraged to address these challenges and enhance crop production. These resources hold the potential to bridge the gap between current crop production levels and the potential yields required to meet increasing food demand (Van Ittersum et al. 2016). However, these inputs must remain affordable to keep production costs low while achieving high yields, ensuring sustainable crop production.

Globally, researchers have studied the use of soil amendments to improve crop yields and economic benefits. Naik et al. (2020) evaluated the effects of hydrogel polymer on castor crops. They found that applying 5 kg ha⁻¹ of hydrogel polymer combined with synthetic NPK significantly improved overall seed yield by 43%, yielding a higher benefit-cost ratio than the control (no hydrogel polymer). In a separate study, Roy et al. (2022) examined the effects of combining organic and inorganic fertilizers on rice. Their findings indicated that combining 75% synthetic nitrogen with 25% organic

nitrogen (from either farmyard manure or Brassicaceous seed meal) improved rice yield and benefit-cost ratio compared to 100% synthetic nitrogen. Additionally, Roy et al. (2022) investigated the impact of irrigation levels and fertilization practices on tomato yield and economic benefits, finding that combining soluble chicken manure with soluble chemical fertilizer provided high net profit and significantly higher yield than the control.

Another advocated concept, particularly in areas with scarce water resources, is deficit or reduced irrigation. Reduced irrigation has been shown to improve water use efficiency in various crops, including cabbage (Sabah et al. 2023), cucumber (Piri et al. 2022), and tomato (Muroyiwa et al. 2023), although this often comes at the expense of overall yield compared to full irrigation. Sabah et al. (2023) reported that providing 50% of cabbage's water requirements resulted in higher water use efficiency than providing 75% or 100% of the required water, although yields were reduced at the 50% and 75% water levels. Similarly, Lubajo and Karuku (2022) found that irrigating at 25% of field capacity improved maize water use efficiency compared to 50%, 75%, and 100% of field capacity irrigation, though the yield decreased at lower field capacity levels. Nonetheless, the reduced yields from lower irrigation levels may be acceptable, considering the cost savings from water conservation in water-scarce areas (Lubajo and Karuku 2022).

Although studies assessing the economic benefits of various irrigation levels and soil amendment applications have been conducted in other regions, similar research is lacking in Namibia. Our previous study provided agronomic results on the effects of different irrigation levels and soil amendments on cabbage productivity in semi-arid Central Namibia (Enguwa et al. 2023). Against this backdrop, the current study aims to assess the economic benefits (total production cost, net returns, and benefit-cost ratio) of different amended soils under full and reduced irrigation levels to determine their feasibility.

2 Materials and Methods

2.1 Experimental site

Two field experiments were conducted in 2021 and 2022 at the Tsumis Arid Zone Agricultural Centre (TAZAC) in the Rehoboth Rural Constituency of the Hardap region in Central Namibia. The geographical coordinates are approximately 23.7308° S latitude and 17.1987° E longitude (Figure 1). This area is classified as semi-arid, with average annual rainfall ranging from 250 to 300 mm and average temperatures ranging from a minimum of 13.5 °C to a maximum of 28.1 °C (Grab and Zumthurm 2020; Shikangalah et al. 2022). The first experiment occurred from October 2021 to February 2022, while the second was conducted from June to November 2022. The topography of Tsumis is primarily flat, with some mountainous regions.

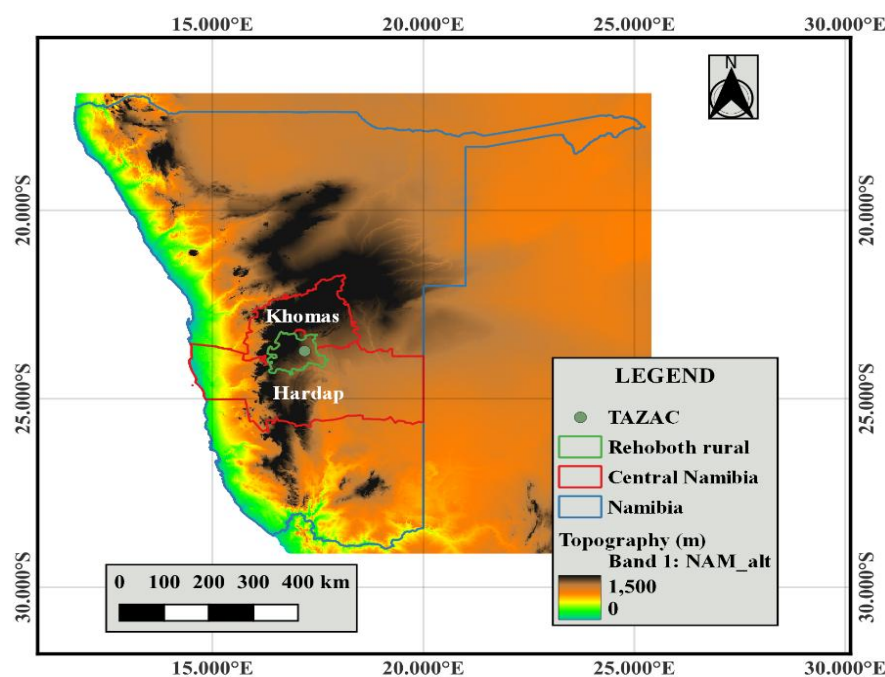


Figure 1 Map indicating Central Namibia and the Tsumis Arid Zone Agricultural Centre (TAZAC)

2.2 Treatments and plant materials

A split-plot design was utilized in both experiments, featuring two irrigation levels, full and reduced irrigation, as the main plots. In addition, six soil amendments were tested in the subplots: biochar, compost, zeolite, NPK, Be-Grow Boost (L) hydrogel, hoof, and horn + bone meal (HHB), and a control group with no soil amendment. Each treatment was replicated three times. The total experimental area measured $39.9 \text{ m} \times 22.5 \text{ m}$, with each subplot covering $4.8 \text{ m} \times 3 \text{ m}$. Each subplot consisted of 64 plants, spaced 0.75 m apart in the inter-rows and 0.30 m apart in the intra-rows. The cabbage hybrid variety Star 3301 F1 was grown in the first experiment. However, in the second experiment, a different variety, *Menzania*, was used due to the unavailability of the Star 3301 F1 hybrid in the market. Both varieties are hybrids known for their large head sizes, ranging from 4 to 6 kg, and they perform well in both cool and warm seasons (Seminis 2014; Starke Ayres 2020). Cabbage was chosen as the test crop because of its high nutritional requirements, responsiveness to various soil treatments, and strong local demand (Carla et al. 2016).

2.3 Irrigation management

The surface drip irrigation method was used in this study, utilizing flowmeters (Sensus Z15NRV02 XNP plastic meter from Xylem Inc., South Africa). During the three weeks following transplanting, all plots received equal water based on the crops' requirements. After this period, irrigation was automated using a controller (Hunter Node-400, Hunter Industries, South Africa).

The drip pipes had a discharge rate of 1 liter per hour per dripper, with a dripper spacing of 30 cm. Each schedule was set for one hour for both irrigation levels, supplying approximately 1 liter of water per plant daily, based on the cabbage's water requirement of 4 mm/day (Beshir 2017). The difference in irrigation was created by varying the irrigation frequency for full and reduced irrigation levels.

In sandy soils, it is recommended that cabbage be irrigated frequently, at least three times a week (Beshir 2017; Bute et al. 2021; Nyatuame et al. 2013; Rasanjalia et al. 2020). Therefore, in the first experiment, irrigation was scheduled for three days a week for the full irrigation level and two days a week for the reduced irrigation level. The two days of irrigation for the reduced treatment were intended to create a water-stressed condition for the plants. Consequently, 79.6 m^3 (100% water requirement) and 39.6 m^3 (50% water requirement) were applied for the full and reduced irrigation levels during the crop growing period.

In the second experiment, the irrigation frequency was increased in response to the slightly poor quality of the cabbage heads observed in the first experiment, which was believed to be due to insufficient watering. In this experiment, water was applied five times a week for the full irrigation treatment and four times a week for the reduced irrigation treatment, resulting in a total application of 136.0 m^3 (170% water requirement) and 124.8 m^3 (150% water requirement) under the full and reduced irrigation levels during the crop production period. The treatment details for the study are presented in Table 1.

Table 1 Treatments for experiments 1 and 2 comprising different soil amendments and irrigation regimes.

First experiment		Second experiment		Treatments
Irrigation (Factor 1)	Soil amendment (Factor 2)	Irrigation	Soil amendment	
Full-3 irrigation days week ⁻¹ (100% water requirement)	Ctr	Full-5 irrigation days week ⁻¹ (170% water requirement)	Ctr	Full-Ctr
	NPK (21:31:21 + 6 (S) kg ha ⁻¹ + Procote Zn)		NPK (88.:40:27 + 8 (S) kg ha ⁻¹ + Procote Zn)	Full-NPK
	Co (97 t ha ⁻¹)		Co (24 t ha ⁻¹)	Full-Co
	Bio (20 t ha ⁻¹) + NPK		Bio+ NPK	Full-Bio
	HHB (2 t ha ⁻¹)		HHB (2.8 t ha ⁻¹)	Full-HHB
	Ze (14 t ha ⁻¹) + NPK		Ze+ NPK	Full-Ze
Be (44 kg ha ⁻¹) + NPK	Be (88 kg ha ⁻¹) + NPK	Full-Be		
Reduced-2 irrigation days week ⁻¹ (50% water requirement)	Ctr	Reduced-4 irrigation days week ⁻¹ (150% water requirement)	Ctr	Reduced-Ctr
	NPK (21:31:21 + 6 (S) kg ha ⁻¹ + Procote Zn)		NPK (88.:40:27 + 8 (S) kg ha ⁻¹ + Procote Zn)	Reduced-NPK
	Co (122 kg ha ⁻¹)		Co (24 t ha ⁻¹)	Reduced-Co
	Bio (20 t ha ⁻¹) + NPK		Bio+ NPK	Reduced-Bio
	HHB (2 t ha ⁻¹)		HHB (2.8 t ha ⁻¹)	Reduced-HHB
	Ze (14 t ha ⁻¹) + NPK		Ze + NPK	Reduced-Ze
Be (44 kg ha ⁻¹) + NPK	Be (88 kg ha ⁻¹) + NPK	Reduced-Be		

2.4 Soil amendment management

In the first experiment, all plots were tilled with a broad fork and leveled with a rake before applying the amendments. Biochar and compost were broadcast and incorporated into the soil, while zeolite and Hoof and Horn + Bone (HHB) meal were spread along the rows and worked into the soil. The Be-Grow Boost (L) hydrogel and synthetic NPK fertilizer [2:3:2 (35) + 2.9% S + Procote Zn] were applied to the transplanting holes. A mixture of Hoof and Horn (HH) meal and Bone (B) meal was applied in a 1:1 proportion to create the HHB treatment. HH meal has a higher nitrogen (N) concentration (12%) but a lower phosphorus (P) concentration (2%), while B meal is a rich source of P (15%) but has only about 3% N (Möller and Schultheiß 2015; Njoshi 2015; Oluwafisayo and Olusegun 2023). Consequently, in this experiment, the HH meal served as the nitrogen source and the B meal as the phosphorus source in the HHB treatment.

Additionally, the application rates for biochar, zeolite, HHB meal, and compost were 20 t ha⁻¹ (Hossain et al. 2020; Toková et al. 2020), 14 t ha⁻¹ (Chen et al. 2017; Zheng et al. 2018), 2 t ha⁻¹ (Wang et al. 2017), and 97 t ha⁻¹ (Carla et al. 2016; Papafilippaki et al. 2015), respectively. The Be-Grow Boost (L) hydrogel was applied at 44 kg ha⁻¹ (1 g per planting hole) (Yang et al. 2019) at a depth of 20 cm during transplanting. Due to the limited nutrient content in biochar, zeolite, and Be-Grow Boost (L) hydrogel, they were complemented with synthetic fertilizers at the following application rates: 21 kg ha⁻¹ N, 31 kg ha⁻¹ P, 21 kg ha⁻¹ K, and 6

kg ha⁻¹ S. Of the total synthetic fertilizer application, 50% was applied at the transplanting stage, and the remaining half was applied as top dressing six weeks later. The same application rates were used for the NPK treatment plots based on laboratory soil analysis results. No synthetic or organic fertilizers (compost and HHB meal) were applied to the control plots. The chemical compositions of the soil amendments are presented in Enguwa et al. (2023).

In the second experiment, the experimental area was not tilled. The application rates of HHB meal and Be-Grow Boost (L) hydrogel were increased to 2.8 t ha⁻¹ and 88 kg ha⁻¹ (2 g per transplanting hole), respectively. Additionally, the synthetic NPKS fertilizer application rates were increased to a total of 88 kg ha⁻¹ N, 40 kg ha⁻¹ P, 27 kg ha⁻¹ K, and 8 kg ha⁻¹ S. For nitrogen, 15% was applied at transplanting, 70% as a top dressing six weeks later, and the remaining 15% eight weeks following transplanting. For phosphorus and potassium, 50% of each was applied at transplanting, with the remaining half applied as top dressing eight weeks later. The compost application rate was reduced to 24 t ha⁻¹ in the second experiment (down from 97 t ha⁻¹ in the first experiment) due to poor plant performance under the higher application rate in the first experiment. The application methods for the amendments were the same as in the first experiment. Biochar and zeolite were not reapplied in this experiment since these materials are reported to remain stable in the soil for many years (Maroušek et al. 2017; Soudejani et al. 2019). The treatment details for the study are shown in Table 1.

2.5 Quantitative agronomic data analysis

The data on the number of marketable heads were tested for normality to determine if it followed a normal distribution. An Analysis of Variance (ANOVA) was conducted to evaluate significant differences among the treatment means. This analysis was performed using General Statistics Software [GenStat 64-bit Release 20.1 (PC/Windows 8-10)]. The treatment means were

found to be statistically different at a significance level of 5% using the Least Significant Difference (LSD) method.

2.6 Economic analysis

Tables 2 and 3 present the costs incurred during the study. Budgets were created for all soil amendment systems to determine their Total Production Cost (TPC), estimate their Net

Table 2 Costs estimation of the initial investment for cabbage cultivation in the first experiment

Incurred Cost	COST (N\$ ha ⁻¹)						
	CTR	NPK	Co	Bio	HHB	Ze	Be
Full irrigation (79.6180 m ³)							
Permanent labour	15720.00	15720.00	15720.00	15720.00	15720.00	15720.00	15720.00
Casual labour	5000.00	5000.00	5000.00	5000.00	5000.00	5000.00	5000.00
Land preparation	3750.00	3750.00	3750.00	3750.00	3750.00	3750.00	3750.00
Seeds	11100.00	11100.00	11100.00	11100.00	11100.00	11100.00	11100.00
Seedling trays	15885.00	15885.00	15885.00	15885.00	15885.00	15885.00	15885.00
Nutrigrow substrate	1068.00	1068.00	1068.00	1068.00	1068.00	1068.00	1068.00
NPK	0.00	3250.00	0.00	3250.00	0.00	3250.00	3250.00
Amendment	0.00	0.00	451360.00	32240.00	15640.00	4260.56	6800.00
Urea	0.00	0.00	0.00	0.00	0.00	0.00	0.00
Irrigation	3538.60	3538.60	3538.60	3538.60	3538.60	3538.60	3538.60
Neem	30240.00	30240.00	30240.00	30240.00	30240.00	30240.00	30240.00
Cypermethrin	0.00	0.00	0.00	0.00	0.00	0.00	0.00
Metacystox	0.00	0.00	0.00	0.00	0.00	0.00	0.00
Total cost	86301.60	89551.60	537661.60	121791.60	101941.60	93812.16	96351.60
Reduced irrigation (39.6200 m ³)							
Permanent labour	15720.00	15720.00	15720.00	15720.00	15720.00	15720.00	15720.00
Casual labour	5000.00	5000.00	5000.00	5000.00	5000.00	5000.00	5000.00
Land preparation	3750.00	3750.00	3750.00	3750.00	3750.00	3750.00	3750.00
Seeds	11100.00	11100.00	11100.00	11100.00	11100.00	11100.00	11100.00
Seedling trays	15885.00	15885.00	15885.00	15885.00	15885.00	15885.00	15885.00
Nutrigrow substrate	1068.00	1068.00	1068.00	1068.00	1068.00	1068.00	1068.00
NPK	0.00	3250.00	0.00	3250.00	0.00	3250.00	3250.00
Amendment	0.00	0.00	451360.00	32240.00	15640.00	4260.56	6800.00
Urea	0.00	0.00	0.00	0.00	0.00	0.00	0.00
Irrigation	1760.80	1760.80	1760.80	1760.80	1760.80	1760.80	1760.80
Neem	30240.00	30240.00	30240.00	30240.00	30240.00	30240.00	30240.00
Cypermethrin	0.00	0.00	0.00	0.00	0.00	0.00	0.00
Metacystox	0.00	0.00	0.00	0.00	0.00	0.00	0.00
Total cost	84523.80	87773.80	535883.80	120013.80	100163.80	92034.36	94573.80

Values were extrapolated to 1 ha; Ctr, Control; Co, Compost; Bio, Biochar; HHB meal, Hoof and Horn + Bone meal; Ze, Zeolite; and Be, Be-Grow boost (L) hydrogel

Table 3 Costs estimation of the initial investment for cabbage cultivation in the second experiment

Incurred Costs	COST (N\$ ha ⁻¹)						
	Ctr	NPK	Co	Bio	HHB	Ze	Be
Full irrigation (136.0092 m ³)							
Permanent labour	18864.00	18864.00	18864.00	18864.00	18864.00	18864.00	18864.00
Casual labour	5000.00	5000.00	2500.00	5000.00	5000.00	5000.00	5000.00
Land preparation	3750.00	3750.00	3750.00	3750.00	3750.00	3750.00	3750.00
Seeds	11100.00	11100.00	11100.00	11100.00	11100.00	11100.00	11100.00
Seedling trays	15885.00	15885.00	15885.00	15885.00	15885.00	15885.00	15885.00
Nutrigrow substrate	1068.00	1068.00	1068.00	1068.00	1068.00	1068.00	1068.00
NPK	0.00	3250.00	0.00	3250.00	0.00	3250.00	3250.00
Amendment	0.00	0.00	90350.00	32240.00	15640.00	4260.56	6800.00
Urea	0.00	1950.00	0.00	390.00	0.00	1950.00	1950.00
Irrigation	6044.80	6044.80	6044.80	6044.80	6044.80	6044.80	6044.80
Neem	30240.00	30240.00	30240.00	30240.00	30240.00	30240.00	30240.00
Cypermethrin	900.00	900.00	900.00	900.00	900.00	900.00	900.00
Metacystox	900.00	900.00	900.00	900.00	900.00	900.00	900.00
Total cost	93751.80	98951.80	181601.80	129631.80	109391.80	103212.36	105751.80
Reduced irrigation (124.8040 m ³)							
Permanent labour	18864.00	18864.00	18864.00	18864.00	18864.00	18864.00	18864.00
Casual labour	5000.00	5000.00	5000.00	5000.00	5000.00	5000.00	5000.00
Land preparation	3750.00	3750.00	3750.00	3750.00	3750.00	3750.00	3750.00
Seeds	11100.00	11100.00	11100.00	11100.00	11100.00	11100.00	11100.00
Seedling trays	15885.00	15885.00	15885.00	15885.00	15885.00	15885.00	15885.00
Nutrigrow substrate	1068.00	1068.00	1068.00	1068.00	1068.00	1068.00	1068.00
NPK	0.00	3250.00	0.00	3250.00	0.00	3250.00	3250.00
Amendment	0.00	0.00	90350.00	32240.00	15640.00	4260.56	6800.00
Urea	0.00	1950.00	0.00	390.00	0.00	1950.00	1950.00
Irrigation	5546.80	5546.80	5546.80	5546.80	5546.80	5546.80	5546.80
Neem	30240.00	30240.00	30240.00	30240.00	30240.00	30240.00	30240.00
Cypermethrin	900.00	900.00	900.00	900.00	900.00	900.00	900.00
Metacystox	900.00	900.00	900.00	900.00	900.00	900.00	900.00
Total cost	93253.80	98453.80	183603.80	129133.80	108893.80	102714.36	105253.80

Values were extrapolated to 1ha; Ctr, Control; Co, Compost; Bio, Biochar; HHB meal, Hoof and Horn + Bone meal; Ze, Zeolite; and Be, Be-Grow boost (L) hydrogel

Economic Return (NER), and compute their Benefit-Cost Ratios (BCR). Data from both experiments and market prices were utilized for budgeting. The parameters used in constructing the budgets included the inputs and their prices (including soil amendments), the farm gate cabbage price, agronomic practices, and labor used (Kanton et al. 2017). The total cost of cabbage

production under each soil amendment system, from sowing to harvesting, was calculated for each irrigation level. Additionally, the TPC of each system was interpolated to a single cabbage head by dividing the TPC of each production system by the total marketable cabbage heads (TMH) produced by each system (EQN 1).

Borehole water was used in the study; therefore, the cost of irrigation was considered as the cost incurred for pumping the necessary water under each irrigation level, based on the pump specifications and the unit cost of electricity (10 m³/hr, 10 kW/hr, and N\$2.00/kW). The fixed labor cost was based on the minimum wage for entry-level agricultural employees in Namibia, which is N\$5.40/hr (Ministry of Labour, Industrial Relations and Employment Creation 2021), and casual labor at N\$100.00/day. Each system's Gross Return (GR) per hectare was calculated by multiplying the farm gate price of cabbage, N\$13.80/head (Namibian Agronomic Board 2023), by the TMH per hectare for each system. The TPC was then subtracted from the GR to obtain the NER, which was also interpolated to a single cabbage head (EQN 2). Furthermore, the BCR was calculated by dividing the GR by the TPC (EQN 3).

$$\text{Total Production Cost (head)} = \frac{\text{Total Production Cost (hectare)}}{\text{Total Marketable Heads}} \quad (\text{EQN 1})$$

$$\text{Net Economic Returns (head)} = \frac{\text{Net Economic Returns (hectare)}}{\text{Total Marketable Heads}} \quad (\text{EQN 2})$$

$$\text{Benefit - Cost Ratio} = \frac{\text{Gross Return}}{\text{Total Production Cost}} \quad (\text{EQN 3})$$

3 Results

3.1 Effect of irrigation levels on Cabbage Number of marketable heads and economic benefits

The effects of irrigation levels on the number of marketable cabbage heads and their associated economic benefits are summarized in Table 4. In the first experiment, the irrigation levels

did not significantly impact the number of marketable cabbage heads. However, the fully irrigated treatment yielded slightly more marketable heads, with a count of 21561, compared to 19345 under reduced irrigation. Additionally, full irrigation resulted in a lower total production cost (TPC) of N\$7.98, compared to N\$8.55 for reduced irrigation. Full irrigation also demonstrated a higher net economic return (NER) of N\$5.82, compared to N\$5.25 with reduced irrigation. Furthermore, full irrigation produced a higher benefit-cost ratio (BCR) of 2.70, compared to 2.36 under reduced irrigation.

In the second experiment, full irrigation again yielded slightly more marketable heads, producing 23,909 compared to 21,958 under reduced irrigation. The full irrigation level also had a lower TPC of N\$5.67, along with a higher NER per head at N\$ 8.13 and a BCR of 2.81, compared to N\$ 5.82, N\$ 7.98, and 2.66, respectively, under reduced irrigation. Moreover, full irrigation achieved a significantly higher NER per hectare of N\$ 201974.58, compared to N\$ 177927.98 under reduced irrigation.

3.2 Effect of soil amendments on cabbage marketable heads and economic benefits

The results presented in Table 5 highlight the effects of soil amendments on the number of marketable cabbage heads and their economic implications. In the first experiment, the application of biochar, Be-Grow boost (L) hydrogel, zeolite, and NPK resulted in a significantly higher number of marketable heads, yielding 24884, 23958, 22801, and 22454 heads per hectare, respectively. In contrast, the control group had the lowest number of marketable heads, with only 13079 heads per hectare recorded. Additionally, the NPK, Be-Grow boost (L) hydrogel, zeolite, and biochar

Table 4 Effect of irrigation levels on cabbage number of marketable heads and economic benefits in the first and second experiments

Irrigation levels	No. of Marketable heads	Total production cost/head (N\$)	Net economic return/head (N\$)	Net economic return/ha (N\$)	Benefit-cost ratio
First Experiment					
Full	21561	7.98	5.82	136482.98	2.70
Reduced	19345	8.55	5.25	99468.98	2.36
SEM±	2116	0.84	0.55	11389.62	0.25
LSD	NS	NS	NS	NS	NS
Second Experiment					
Full	23909	5.67	8.13	201974.58 ^a	2.81
Reduced	21958	5.82	7.98	177927.98 ^b	2.66
SEM±	2496	0.59	0.83	19347.97	0.28
LSD	NS	NS	NS	55452.75 [*]	NS

1 US\$ = 18.51; N\$ - Values with the same letters within a column are not statistically significant by Fisher's protected LSD at a 5% probability level; SEM - standard error mean; LSD - least significant difference; NS - not significant. *,** and *** denote significance at P ≤ 0.05, P ≤ 0.01 and P ≤ 0.001, respectively

Table 5 Effect of soil amendments on cabbage number of marketable heads and economic benefits, experiments 1 and 2.

Soil amendments	No. of Marketable heads	Total production cost/head (N\$)	Net economic return/head (N\$)	Net economic return/ha (N\$)	Benefit-cost ratio
First Experiment					
Ctr	13079 ^c	6.53 ^{bc}	7.27 ^b	95070.60 ^b	2.11 ^b
NPK	22454 ^a	3.96 ^d	9.84 ^a	221202.50 ^a	3.49 ^a
Co	19792 ^{ab}	27.12 ^a	-13.32 ^c	-263643.10 ^c	0.51 ^c
Bio	24884 ^a	4.90 ^{cd}	8.90 ^{ab}	222496.50 ^a	2.84 ^{ab}
HHB	16204 ^{ab}	7.20 ^b	6.60 ^{ab}	93810.20 ^b	1.93 ^{bc}
Ze	22801 ^a	4.15 ^d	9.65 ^{ab}	221730.54 ^a	3.38 ^a
Be	23958 ^a	4.00 ^d	9.80 ^a	235164.60 ^a	3.46 ^a
SEM±	2296	0.73	1.00	21845.67	0.30
LSD (0.05)	6366.93 ^{***}	2.09 ^{***}	2.49 ^{***}	56523.60 ^{***}	1.07 ^{***}
Second Experiment					
Ctr	14873 ^c	7.65 ^{ab}	6.15 ^b	99761.60 ^c	2.07 ^c
NPK	23553 ^{ab}	4.42 ^{bc}	9.38 ^a	222338.10 ^{ab}	3.25 ^a
Co	18461 ^{bc}	10.09 ^a	3.71 ^c	74551.00 ^d	1.41 ^d
Bio	27199 ^a	5.01 ^{bc}	8.79 ^a	228396.00 ^{ab}	2.76 ^{bc}
HHB	25752 ^{ab}	4.26 ^c	9.54 ^a	248633.70 ^a	3.28 ^a
Ze	23206 ^{ab}	4.74 ^{bc}	9.06 ^a	198913.94 ^b	2.93 ^{ab}
Be	27489 ^a	4.06 ^c	9.74 ^a	257066.90 ^a	3.44 ^a
SEM±	2442	0.74	0.88	19678.02	0.30
LSD (0.05)	6609.84 ^{***}	3.25 ^{**}	2.24 ^{**}	57449.11 ^{***}	0.80 ^{***}

1 U\$ - 18.51 N\$; Values with the same letters within a column are not statistically significant by Fisher's protected LSD at a 5% probability level; Ctr - Control; Co - Compost; Bio - Biochar; HHB meal, Hoof and Horn + Bone meal; Ze - Zeolite; and Be, Be- Grow boost (L) hydrogel; SEM - standard error mean; LSD - least significant difference; NS - not significant. *, ** and *** denote significance at $P \leq 0.05$, $P \leq 0.01$ and $P \leq 0.001$, respectively

treatments exhibited the lowest total production costs (TPC) per head, which were N\$ 3.96, N\$ 4.00, N\$ 4.15, and N\$ 4.90, respectively. Compost, however, had the highest TPC at N\$ 27.12. The same treatments also provided the highest net economic return (NER) per head, with values of N\$ 9.84, N\$ 9.80, N\$ 9.65, and N\$ 8.90, while compost produced the lowest, resulting in a negative NER of N\$ 13.32. Furthermore, NPK, Be-Grow boost (L) hydrogel, zeolite, and biochar systems achieved the highest benefit-cost ratios (BCRs) of 3.49, 3.46, 3.38, and 2.84, respectively, whereas compost showed an unprofitable BCR of 0.51.

In the second experiment, the Be-Grow boost (L) hydrogel and biochar treatments resulted in significantly higher marketable heads, yielding 27,489 and 27,199 heads per hectare, respectively. The control group again had the lowest, with only 14,873 heads per hectare. The Be-Grow boost (L) hydrogel, HHB meal, and NPK treatments also recorded the lowest total

production costs per head, at N\$ 4.06, N\$ 4.26, and N\$ 4.42, respectively, compared to N\$ 7.65 for the control group and the highest TPC of N\$ 10.09 for compost. Moreover, these treatments provided the highest NER per head, yielding N\$ 9.74, N\$ 9.54, and N\$ 9.38, respectively, while compost recorded a NER of only N\$ 3.71. Finally, Be-Grow boost (L) hydrogel, HHB meal, and NPK achieved the highest BCRs of 3.44, 3.28, and 3.25, while compost had the lowest BCR of 1.41.

3.3 Interactive effect of irrigation level with soil amendments on marketable heads of cabbage and economic benefits

Table 6 presents the interactive effects of irrigation levels and soil amendments on the number of marketable cabbage heads and the economic parameters associated with cabbage production. In the first experiment, no significant interaction was observed between irrigation and soil amendments concerning the number of marketable heads. However, full irrigation combined with biochar,

Table 6 Interactive effect of irrigation levels and soil amendments on cabbage number of marketable heads, total production costs, and economic benefits for experiments 1 and 2

Irrigation levels × Soil amendments	No. of Marketable heads	Total Production Cost (N\$)	Net Economic Return/head (N\$)	Net Economic Return/ha (N\$)	Benefit-Cost Ratio (N\$)	
First Experiment						
Full	Ctr	13194	6.54	7.26	95775.60	2.11 ^{bc}
	NPK	23843	3.76	10.04	239481.80	3.67 ^a
	Co	19908	27.01	-13.21	-262931.20	0.51 ^d
	Bio	27315	4.46	9.34	255155.40	3.10 ^{ab}
	HHB	15278	6.67	7.13	108894.80	2.07 ^{bc}
	Ze	25926	3.62	10.18	263966.64	3.81 ^a
	Be	25463	3.78	10.02	255037.80	3.65 ^a
Reduced	Ctr	12963	6.52	7.28	94365.60	2.12 ^{bc}
	NPK	21065	4.17	9.63	202923.20	3.31 ^a
	Co	19676	27.24	-13.44	-264355.00	0.51 ^c
	Bio	22453	5.35	8.45	189837.60	2.58 ^{bc}
	HHB	12963	7.73	6.07	78725.60	1.79 ^{bc}
	Ze	19676	4.68	9.12	179494.44	2.95 ^{ab}
	Be	22454	4.21	9.59	215291.40	3.28 ^a
SEM±	2858.262	0.96	1.27	26656.54	0.37	
LSD (0.05)	NS	NS	NS	NS	1.07 [*]	
Second Experiment						
Full	Ctr	9028 ^d	10.38	3.42 ^b	30830.00 ^d	1.33 ^c
	NPK	28009 ^a	3.53	10.27 ^a	287577.00 ^a	3.91 ^a
	Co	21759 ^{abc}	8.35	5.45 ^a	118677.00 ^c	1.65 ^c
	Bio	27546 ^a	4.71	9.09 ^a	250507.60 ^{ab}	2.93 ^{ab}
	HHB	23148 ^{ab}	4.73	9.07 ^a	210050.60 ^b	2.93 ^{ab}
	Zeo	23611 ^{ab}	4.37	9.43 ^a	222624.04 ^b	3.16 ^{ab}
	Be	28935 ^a	3.65	10.15 ^a	293555.80 ^a	3.78 ^a
Reduced	Ctr	18982 ^{bc}	4.91	8.89 ^a	168693.20 ^{bc}	2.81 ^b
	NPK	18518 ^{bc}	5.32	8.48 ^a	157099.20 ^c	2.60 ^b
	Co	15509 ^{cd}	11.84	1.96 ^b	30425.00 ^d	1.17 ^c
	Bio	24306 ^{ab}	5.31	8.49 ^a	206284.40 ^{bc}	2.60 ^b
	HHB	28703 ^a	3.79	10.01 ^a	287212.20 ^a	3.64 ^a
	Zeo	20139 ^{bc}	5.10	8.70 ^a	175203.84 ^{bc}	2.71 ^b
	Be	23611 ^{ab}	4.46	9.34 ^a	220578.00 ^b	3.10 ^{ab}
SEM±	3009.499	1.08	1.03	22742.47	0.36	
LSD (0.05)	9775.99 ^{**}	NS	2.43 ^{***}	59549.11 ^{***}	0.86 ^{**}	

1 US\$= 18.51 N\$; Values with the same letters within a column are not statistically significant by Fisher's protected LSD at a 5% probability level; Ctr - Control; Co - Compost; Bio - Biochar; HHB - Hoof and Horn + Bone meal; Ze - Zeolite; Be - Be-Grow boost (L) hydrogel; SEM - standard error mean; LSD - least significant difference; NS - not significant. *,** and *** denotes significance at P≤ 0.05, P≤ 0.01 and P≤ 0.001, respectively

zeolite, Be-Grow Boost (L) hydrogel, and NPK resulted in the highest number of marketable heads, specifically 27315, 25926, 25463, and 23843 heads per hectare, respectively. In contrast, reduced irrigation using the control and HHB meal produced the fewest marketable heads, with each yielding 12963 heads per hectare. Furthermore, total production cost (TPC) ranged from N\$ 3.62 to N\$27.24 in the first experiment. Under full irrigation, zeolite, NPK, and Be-Grow Boost (L) hydrogel had the lowest TPCs per head at N\$ 3.62, N\$ 3.76, and N\$ 3.78, respectively, while compost used under reduced irrigation had the highest TPC at N\$27.24. This means that for each cabbage head produced with zeolite, NPK, and Be-Grow Boost (L) hydrogel under full irrigation, a farmer spent N\$3.62, N\$3.76, and N\$3.78, respectively, compared to N\$27.24 for compost under reduced irrigation. Notably, zeolite, NPK, Be-Grow Boost (L) hydrogel, and biochar exhibited lower TPCs than the control in both irrigation levels. Additionally, except for the control, full irrigation and soil amendments combined resulted in relatively lower TPCs than reduced irrigation.

Under full irrigation, zeolite, NPK, and Be-Grow Boost (L) hydrogel yielded the highest net economic returns (NERs) per head at N\$10.18, N\$10.04, and N\$10.02, respectively. Conversely, compost under reduced irrigation led to a negative NER of N\$-13.44. Moreover, all soil amendments, except compost under both irrigation levels, demonstrated higher NERs compared to the control (Table 5). Similarly, under full irrigation, zeolite, NPK, and Be-Grow Boost (L) hydrogel exhibited the highest benefit-cost ratios (BCRs) of 3.81, 3.67, and 3.65, respectively. Importantly, all soil amendments, except for compost across all irrigation levels, had higher BCRs than the control, while compost consistently showed an unprofitable BCR of 0.51 across all irrigation regimes (Table 6).

In the second experiment, combining full irrigation with Be-Grow Boost (L) hydrogel, NPK, and biochar resulted in significantly more marketable heads, producing 28935, 28009, and 27546 heads per hectare. Reduced irrigation with HHB meal yielded a comparable number of marketable heads at 28703 per hectare. The economic analysis indicated that NPK and Be-Grow Boost (L) hydrogel under full irrigation, along with HHB meal under reduced irrigation, had the lowest TPCs of N\$3.53, N\$3.65, and N\$3.79, respectively, compared to N\$10.38 for the full irrigation control and a maximum TPC of N\$11.84 under reduced irrigation with compost. Additionally, NPK, Be-Grow Boost (L) hydrogel under full irrigation, and HHB meal under reduced irrigation generated relatively higher NERs per head, at N\$ 10.27, N\$ 10.15, and N\$ 10.01, compared to N\$ 3.42 for the control and the lowest NER of N\$ 1.96 for compost under reduced irrigation. Thus, for every cabbage head produced under full irrigation using NPK, a farmer could expect a net profit of N\$ 10.27, compared to N\$ 3.42 from the control under the same irrigation regime, suggesting a potential 66% improvement in NER (Table 6).

4 Discussion

The primary goal of commercial crop production is to maximize marketable yields while minimizing production inputs, such as irrigation water and fertilizers. With water scarcity affecting many regions worldwide, including Central Namibia, and the high cost of fertilizers, it is crucial to identify methods and systems that require fewer resources while maximizing output for more significant economic benefits. This study aimed to evaluate the economic advantages (including total production cost, net returns, and benefit-cost ratio) of various amended soils—such as biochar, compost, zeolite, hoof and horn with bone meal, Be-Grow Boost (L) hydrogel, and NPK under both full and reduced irrigation levels to assess their feasibility.

The first experiment indicated that full irrigation led to more marketable heads than reduced irrigation. This increase in marketable heads under full irrigation was associated with lower Total Production Costs (TPC) and higher Net Economic Returns (NER), resulting in a better Benefit-Cost Ratio (BCR) than what was observed under reduced irrigation (Table 4). Moreover, different soil amendments significantly enhanced the number of marketable heads and the associated economic benefits (Table 5). Specifically, amendments like Biochar, Be-Grow Boost (L) hydrogel, zeolite, and NPK resulted in a notably higher number of marketable heads. This improvement can be attributed to these amendments' positive effects on nutrient availability and water dynamics within the soil (Baiaomonte et al. 2020; Dorraji et al. 2010; Mondal et al. 2021). Theoretically, if we assume that the TPCs of the various amendments were equal, the amendments producing the most marketable heads would demonstrate better economic viability through lower TPC and increased NER and BCR. However, in reality, the interaction of both factors affects the viability of the amendments. For example, while biochar produced the highest number of marketable heads, its BCR was lower than that of NPK, Be-Grow Boost (L) hydrogel, and zeolite, which had lower TPCs and higher NERs than biochar due to the high cost associated with biochar (Table 5).

The control group, which did not use any soil amendments, did not yield the lowest total production costs (TPC) or the highest net economic return (NER) despite not incurring any amendment costs. This was mainly due to the few marketable heads produced (Table 5). Considering the potential for on-farm production of biochar, which could be more cost-effective than purchasing amendments, using biochar presents a viable economic alternative. The bush encroachment problem in Namibia, particularly in central regions (Shikangalah and Mapani 2020), offers farmers a chance to harvest biomass from encroaching bushes for biochar production. This practice could contribute to sustainable crop production in these areas. The economic unviability of compost stemmed from its low number of marketable heads, resulting in a much higher

TPC and a lower NER. In contrast, amendments applied under full irrigation resulted in slightly more marketable heads, leading to relatively lower TPC and higher NER and benefit-cost ratios (BCR) (Table 6).

The economic benefits of crop production are closely tied to marketable yield and selling price while inversely related to production costs (Lim et al. 2015). Therefore, since market conditions typically determine selling prices and production costs, farmers should maximize their yields and efficiently utilize inputs to achieve the greatest economic benefits. In the second experiment, different irrigation levels resulted in a similar number of marketable heads, with full irrigation leading to a slightly higher count of marketable heads and a greater Benefit-Cost Ratio (BCR) (Table 4). The Be-Grow Boost (L) hydrogel, followed by HHB meal and NPK, demonstrated the highest economic benefits due to their relatively high number of marketable heads, low Total Production Costs (TPC), and high Net Economic Return (NER) compared to other amendments. Additionally, compost proved economically viable when its application rate decreased from 192 kg to 35 kg, reducing TPC (Table 5). Combining full irrigation with various soil amendments led to significantly higher economic benefits than reduced irrigation due to increased marketable heads (Table 6). Therefore, full irrigation (4 mm/day, five days a week) of amended soils may be the most economically viable option in semi-arid Central Namibia.

Other than compost, all systems in the first experiment showed slightly better economic benefits than those in the second experiment (Tables 4, 5, and 6). This difference was primarily due to fewer applications of fertilizers and pesticides in the first experiment, resulting in lower overall costs. In the second experiment, two additional pesticides (cypermethrin and metasystox) were used (Tables 2 and 3), and the rates and frequencies of fertilizer applications were increased (Table 1). However, the cabbage heads produced in the second experiment were larger than those in the first, making them more likely to be preferred by consumers in the market (Enguwa et al. 2023). The positive economic benefits of full irrigation in crop production, as found in this study, align with findings from other researchers (Bairwa et al. 2023; Onkoba et al. 2021; Xiang et al. 2019). Bairwa et al. (2023) reported that irrigating Blond psyllium at 0.5 and 0.4 cumulative pan evapotranspiration (CPE) resulted in higher yields, net returns, and a better benefit-cost ratio compared to irrigation at 0.2 and 0.3 CPE. Similarly, Jat et al. (2018) found that growing Indian mustard at 0.8 CPE irrigation levels produced higher seed yields and benefit-cost ratios compared to the control (no irrigation) and other irrigation levels (0.4, 0.6, and 0.7 CPE). Soil moisture is crucial in crop production, significantly affecting economic yield and benefits (Xiang et al. 2019).

The positive economic benefits associated with hydrogel polymers have been consistently highlighted in the current study and acknowledged by numerous authors (Bairwa et al. 2023; Cornejo et al. 2022; Patra et al. 2022; Ram et al. 2018; Rathore et al. 2019). For instance, Ram et al. (2018) reported that applying hydrogel polymer to lentils resulted in higher net returns per kilogram of lentil grains and a better benefit-cost ratio compared to the control group. Similarly, Cornejo et al. (2022) found that using hydrogel polymer significantly improved the net economic return per tomato plant and benefit-cost ratio over the control. Additionally, Rathore et al. (2019) showed that hydrogel polymer treatments under various irrigation regimes in a semi-arid region yielded greater net returns per kilogram of mustard seeds than those without hydrogel. Their study also indicated that applying the hydrogel polymer with full irrigation (0.8 CPE) led to higher mustard yields and a better benefit-cost ratio than rain-fed treatments and other irrigation levels (0.4 and 0.6 CPE), consistent with the current study's findings. The high benefit-cost ratio of the HHB meal in the second experiment can be attributed to the long-term positive effects of the amendment on the number of marketable cabbage heads. This reduced total production costs (TPC) and increased net economic returns (NER). HHB meal acts as a slow-release fertilizer, meaning its effects may take longer to manifest than other amendments (Jain 2019; NJoshi 2015; Peter et al. 2019).

Conclusion

This study evaluated the economic feasibility of applying different irrigation levels and soil amendments to improve cabbage production in semi-arid Central Namibia. The results indicated that Be-Grow Boost (L) hydrogel, NPK fertilizer, and biochar consistently produced the highest number of marketable cabbage heads. Furthermore, apart from biochar, these same amendments also demonstrated the most significant economic benefits in both experiments. In the second experiment, HHB meal showed a relatively high number of marketable heads and economic benefits, surpassing NPK's, suggesting a long-term positive effect of this amendment. Full irrigation complemented by Be-Grow Boost (L) hydrogel, NPK, and reduced irrigation with HHB meal resulted in the highest number of marketable cabbage heads and benefit-cost ratios (BCRs). Therefore, the application of Be-Grow Boost (L) hydrogel (88 kg/ha) and NPK (88:40:27 + 8 [S] kg/ha + Procote Zn) with full irrigation (4 mm of daily irrigation for five days a week) can be a viable strategy for increasing marketable cabbage production and achieving higher BCRs in semi-arid regions like Central Namibia. Similarly, the consecutive seasonal application of HHB meal at 2.8 t/ha can also enhance the number of marketable heads and BCR. Finally, local production of biochar has the potential to reduce total production costs (TPC) while increasing BCR in its application.

Acknowledgment

The authors thank the Deutsche Gesellschaft für Internationale Zusammenarbeit (GIZ) Namibia for their financial support in conducting the research experiments. The Namibian Ministry of Agriculture also supported the study by providing a research plot on their Tsumis farm.

Conflict of interest

The authors declare no conflicts of interest.

Ethical Clearance

No animal model was utilized in this study; therefore, ethical clearance is not required.

References

- Araya, T., Ochsner, T. E., Mnkeni, P. N. S., Hounkpatin, K. O. L., & Amelung, W. (2024). Challenges and constraints of conservation agriculture adoption in smallholder farms in sub-Saharan Africa: A review. *International Soil and Water Conservation Research*, 1–16. <https://doi.org/10.1016/j.iswcr.2024.03.001>
- Baiamonte, G., Minacapilli, M., & Crescimanno, G. (2020). Effects of biochar on irrigation management and water use efficiency for three different crops in a desert sandy soil. *Sustainability*, 12(18), 1–19. <https://doi.org/10.3390/su12187678>
- Bairwa, D. D., Chaplot, P. ., Prajapat, B. S., Meena, S., & Jat, M. L. (2023). Effect of irrigation schedules and hydrogel levels on yield and economics of blond psyllium (*Plantago ovata*). *Indian Journal of Agronomy*, 68(March), 73–76.
- Beshir, S. (2017). Review on estimation of crop water requirement, irrigation frequency and water use efficiency of cabbage production. *Journal of Geoscience and Environment Protection*, 05, 59–69. <https://doi.org/10.4236/gep.2017.57007>
- Bute, A., Iosob, G. A., Antal-Trenuricl, A., Brezeanu, C., Brezeanu, P. M., Oana, C. T., & Ambarus, S. (2021). The most suitable irrigation methods in cabbage crops (*Brassica oleracea* L . Var . capitata): A review. *Horticulture*, LXV(1), 399–405.
- Carla, V. C., Aline, M. de S. G., Bruno, N. M. M., Ana, E. B. T., Natalia, de B. L. L., Antonio, I. I. C., & Regina, M. E. (2016). Response of broccoli to sulphur application at topdressing in the presence or absence of organic compost at planting. *African Journal of Agricultural Research*, 11(35), 3287–3292. <https://doi.org/10.5897/ajar2016.11398>
- Chen, T., Xia, G., Wu, Q., Zheng, J., Jin, Y., Sun, D., Wang, S., & Chi, D. (2017). The influence of zeolite amendment on yield performance, quality characteristics, and nitrogen use efficiency of paddy rice. *Crop Science*, 57(5), 2777–2787. <https://doi.org/10.2135/cropsci2016.04.0228>
- Chivenge, P., Zingore, S., Ezui, K. S., Njoroge, S., Bunquin, M. A., Dobermann, A., & Saito, K. (2022). Progress in research on site-specific nutrient management for smallholder farmers in sub-Saharan Africa. *Field Crops Research*, 281(2022), 1–11. <https://doi.org/10.1016/j.fcr.2022.108503>
- Cornejo, F., Mayorga, P., & Negoita, L. (2022). Effect of water-saving technologies on productivity and profitability of tomato cultivation in Galapagos, Ecuador. *Journal of Applied Horticulture*, 24(3), 1–7.
- Dorraj, S. S., Golchin, A., & Ahmadi, S. (2010). The effects of hydrophilic polymer and soil salinity on corn growth in sandy and loamy soils. *Clean - Soil, Air, Water*, 38(7), 584–591. <https://doi.org/10.1002/clen.201000017>
- Enguwa, K. B. P., Horn, L. N., & Awala, S. K. (2023). Comparative effect of different irrigation levels and soil amendments on cabbage productivity in semi-arid Central Namibia. *Irrigation and Drainage*, 73(2), 538–556. <https://doi.org/10.1002/ird.2906>
- Grab, S., & Zumthurn, T. (2020). "Everything is scorched by the burning sun": Missionary perspectives and experiences of 19th- and early 20th-century droughts in semi-arid Central Namibia. *Climate of the Past*, 16(2), 679–697. <https://doi.org/10.5194/cp-16-679-2020>
- Hossain, M. Z., Bahar, M. M., Sarkar, B., Donne, S. W., Ok, Y. S., et al. (2020). Biochar and its importance on nutrient dynamics in soil and plant. *Biochar*, 2(4), 379–420. <https://doi.org/10.1007/s42773-020-00065-z>
- Jain, G. (2019). Biofertilizers- a way to organic agriculture. *Journal of Pharmacognosy and Phytochemistry*, 7(4), 49–52.
- Jat, A. L., Rathore, B. S., Desai, A. G., & Shah, S. K. (2018). Production potential, water productivity and economic feasibility of Indian mustard (*Brassica juncea*) under deficit and adequate irrigation scheduling with hydrogel. *Indian Journal of Agricultural Sciences*, 88(2), 1–5. <https://doi.org/10.56093/ijas.v88i2.79170>
- Kanton, R. A. L., Buah, S. S. J., Larbi, A., Mohammed, A. M., Bidzakin, J. K., & Yakubu, E. A. (2017). Soil amendments and rotation effects on soybean and maize growths and soil chemical changes in Northern Ghana. *International Journal of Agronomy*, 2017, 1–9. <https://doi.org/10.1155/2017/4270284>
- Kazembe, L., Tawodzera, G., & Nickanor, N. (2024). *International migration and food insecurity in urban Namibia* (Issue 15).

- Retrieved from <https://mifood.org/wp-content/uploads/2024/08/MiFOOD15-International-Migration.pdf>.
- Lim, S. L., Wu, T. Y., Lim, P. N., & Shak, K. P. Y. (2015). The use of vermicompost in organic farming: Overview, effects on soil and economics. *Journal of the Science of Food and Agriculture*, 95(6), 1143–1156. <https://doi.org/10.1002/jsfa.6849>
- Lubajo, B. W., & Karuku, G. N. (2022). Effect of deficit irrigation regimes on growth, yield, and water use efficiency of maize (*Zea mays*) in the semi-arid area of Kiboko, Kenya. *Tropical and Subtropical Agroecosystems*, 25, 1–14.
- Maroušek, J., Vochozka, M., Plachý, J., & Žák, J. (2017). Glory and misery of biochar. *Clean Technologies and Environmental Policy*, 19(2), 311–317. <https://doi.org/10.1007/s10098-016-1284-y>
- Ministry of Labour Industrial Relations and Employment Creation. (2021). *Government gazette of the Republic of Namibia* (Vol. 2021, Issue December). Retrieved from <https://archive.gazettes.africa/archive/na/2021/na-government-gazette-dated-2021-12-21-no-7712.pdf>.
- Möller, K., & Schultheiß, U. (2015). Chemical characterization of commercial organic fertilizers. *Archives of Agronomy and Soil Science*, 61(7), 989–1012. <https://doi.org/10.1080/03650340.2014.978763>
- Mondal, M., Biswas, B., Garai, S., Sarkar, S., Banerjee, H., et al. (2021). Zeolites enhance soil health, crop productivity and environmental safety. *Agronomy*, 11(3), 1–29. <https://doi.org/10.3390/agronomy11030448>
- Muroyiwa, G., Mashonjowa, E., Mhizha, T., & Muchuweti, M. (2023). The effects of deficit irrigation on water use efficiency, yield and quality of drip-irrigated tomatoes grown under field conditions in Zimbabwe. *Water SA*, 49(4), 363–373. <https://doi.org/10.17159/wsa/2023.v49.i4.3935>
- Naik, K. A., Chaithra, G., Kiran, K. N., Madhu, G., Nataraja, M., Umesh, S., & Madhu, B. (2020). Effect of hydrogel on growth, yield and economics of rainfed castor. *The Pharma Innovation Journal*, 9(7), 36–39.
- Namibia Statistics Agency [NSA]. (2013). *Namibia 2011 Population & Housing Census - Main Report*. Namibia Statistics Agency. Retrieved from [http://www.nsa.org.na/files/downloads/Namibia 2011 Population and Housing Census Main Report.pdf](http://www.nsa.org.na/files/downloads/Namibia%2011%20Population%20and%20Housing%20Census%20Main%20Report.pdf)
- Namibian Agronomic Board. (2023). *Monthly average prices for selected vegetables month: 01-28 February 2023*.
- Neema, M., & Kalitanyi, V. (2023). Factors affecting farmers' entrepreneurial action at Etunda Green scheme project, Namibia. *International Journal of Research in Business and Social Science*, 12(1), 350–361. <https://doi.org/10.20525/ijrbs.v12i1.2252>
- NJoshi, N. (2015). Production and utilization strategies of organic fertilizers for organic farming: an eco-friendly approach. *IOSR Journal of Agriculture and Veterinary Science*, 8(8), 58-61.
- Nyambo, P., Nyambo, P., Mavunganidze, Z., & Nyambo, V. (2022). Sub-Saharan Africa Smallholder Farmers Agricultural Productivity: Risks and Challenges. In H.A. Mupambwa, A.D. Ncizah, P. Nyambo, B. Muchara, N.N. Gabriel (eds) *Food Security for African Smallholder Farmers* (pp. 47–58). Springer, Singapore. https://doi.org/10.1007/978-981-16-6771-8_3
- Nyatume, M., Ampaw, F., Owusu-Gyimah, V., & Mabinde Ibrahim, B. (2013). Irrigation scheduling and water use efficiency on cabbage yield. *International Journal of Agronomy and Agricultural Research*, 3(7), 29–35.
- Oluwafisayo, A. F., & Olusegun, O. S. (2023). Responses of leaf amaranth (*Amaranthus hybridus* L.) Amaranthaceae to composts enriched with organic nitrogen sources. *Journal of Agricultural, Food Science and Biotechnology*, 1(2), 74–82. <https://doi.org/10.58985/jafsb.2023.v01i02.09>
- Onkoba, S. O., Onyari, C. N., & Gichimu, B. M. (2021). Productivity of selected cabbage varieties under varying drip irrigation schedules in humic nitisols of Embu County, Kenya. *International Journal of Agronomy*, 2021, 1–7. <https://doi.org/10.1155/2021/9978974>
- Papafilippaki, A., Paranychianakis, N., & Nikolaidis, N. P. (2015). Effects of soil type and municipal solid waste compost as a soil amendment on *Cichorium spinosum* (spiny chicory) growth. *Scientia Horticulturae*, 195(2015), 195–205. <https://doi.org/10.1016/j.scienta.2015.09.030>
- Patra, S. K., Poddar, R., Brestic, M., Acharjee, P. U., Bhattacharya, P., et al. (2022). Prospects of hydrogels in agriculture for enhancing crop and water productivity under water deficit conditions. *International Journal of Polymer Science*, 2022, 1–15. <https://doi.org/10.1155/2022/4914836>
- Peter, E. A. C., Hudson, N., & Evans, C. (2019). An efficacious supplementary fertilizer formulation from agricultural farm biomass. *Chemical Science International Journal*, 28(4), 1–15. <https://doi.org/10.9734/csji/2019/v28i430145>
- Piri, H., Naserin, A., & Albalasmeh, A. A. (2022). Interactive effects of deficit irrigation and vermicompost on yield, quality, and irrigation water use efficiency of greenhouse cucumber. *Journal of Arid Land*, 14(11), 1274–1292. <https://doi.org/10.1007/s40333-022-0035-7>

- Ram, B., Punia, S. S., Tatarwal, J. P., Meena, D. S., & Chaudhary, H. R. (2018). Effect of hydrogel and foliar nutrition sprays on productivity and profitability of lentil under rainfed situation of South Eastern plain zone of Rajasthan. *International Journal of Advanced Scientific Research and Management*, 1, 67–70.
- Rasanjalia, K. G. A. ., De Silva, C. S., & Jayakody, L. K. R. R. (2020). Influence of super absorbent polymer (ZEBA) on growth, yield of cabbage (*Brassica oleracea*), and soil water retention under temperature and water stress condition. *Journal of Agriculture and Value Addition*, 3(2), 73–89. <https://doi.org/10.13140/RG.2.2.27178.08643>
- Rathore, S. S., Shekhawat, K., Dass, A., Premi, O. P., Rathore, B. S., & Singh, V. K. (2019). Deficit irrigation scheduling and superabsorbent polymer-hydrogel enhance seed yield, water productivity and economics of Indian mustard under semi-arid ecologies. *Irrigation and Drainage*, 68 (3), 531–541. <https://doi.org/10.1002/ird.2322>
- Roy, D., Das, A., Id, D. G., Brahmachari, K., & Skalicky, M. (2022). The combination of organic and inorganic fertilizers influences the weed growth, productivity and soil fertility of monsoon rice. *PLoS ONE*, 17(1), 1–18.
- Sabah, S. H., Karim, T. H., & Tahir, H. T. (2023). Interactive Effect of Deficit Irrigation and Water Quality on Yield and Water Use Efficiency of Red Cabbage (*Brassica oleracea* var. capitata L.) under Drip Irrigation. *IOP Conference Series: Earth and Environmental Science*, 1262(8), 1–10. <https://doi.org/10.1088/1755-1315/1262/8/082005>
- Seminis. (2014). *Cabbage- Menzania* (p. 2). Retrived from <https://agroconsult-buinov.com/en/produkt/cabbage-menzania/>.
- Shikangalah, R., Mapani, B., Mapaure, I., & Herzsuh, U. (2022). Responsiveness of *Dichrostachys cinerea* to seasonal variations in temperature and rainfall in Central Namibia. *Flora*, 286(2022), 1–7. <https://doi.org/10.1016/j.flora.2021.151974>
- Shikangalah, R. N., & Mapani, B. S. (2020). A review of bush encroachment in Namibia : from a Problem to an opportunity? *Journal of Rangeland Science*, 10(3), 1–16.
- Sichoongwe, K. (2024). Sectoral contribution to economic growth : The case of Namibia. *International Journal of Development and Sustainability*, 13(4), 251–263.
- Soudejani, H. T., Kazemian, H., Inglezakis, V. J., & Zorpas, A. A. (2019). Application of zeolites in organic waste composting: a review. *Biocatalysis and Agricultural Biotechnology*, 22, 1–28. <https://doi.org/10.1016/j.bcab.2019.101396>
- Starke Ayres. (2020). *Cabbage- Star 3301*. Retrived from <https://www.starkeyayres.com/uploads/files/STAR-3301-2020.pdf>.
- Toková, L., Igaz, D., Horák, J., & Aydin, E. (2020). Effect of biochar application and re-application on soil bulk density, porosity, saturated hydraulic conductivity, water content and soil water availability in a silty loam haplic luvisol. *Agronomy*, 10(7), 1–17. <https://doi.org/10.3390/agronomy10071005>
- Van Ittersum, M. K., Van Bussel, L. G. J., Wolf, J., Grassini, P., Van Wart, J., et al. (2016). Can sub-Saharan Africa feed itself? *Proceedings of the National Academy of Sciences of the United States of America*, 113(52), 14964–14969. <https://doi.org/10.1073/pnas.1610359113>
- Wang, Y., Magid, J., Thorup-Kristensen, K., & Jensen, L. S. (2017). Genotypic differences in growth, yield and nutrient accumulation of spring wheat cultivars in response to long-term soil fertility regimes. *Acta Agriculturae Scandinavica Section B: Soil and Plant Science*, 67(2), 126–133. <https://doi.org/10.1080/09064710.2016.1229018>
- Wanga, M. A., Shimelis, H., & Mengistu, G. (2022). Sorghum production in Northern Namibia : farmers' Perceived constraints and trait preferences. *Sustainability (Switzerland)*, 14(2022), 1–16. <https://doi.org/10.3390/su141610266>
- World Integrated Trade Solution (WITS). (2021). *Namibia Vegetable Imports by country*. WITS. Retrived from https://wits.worldbank.org/CountryProfile/en/Country/NAM/Year/LTS/T/TradeFlow/Import/Partner/by-country/Product/06-15_Vegetable
- Xiang, Y., Zou, H., Zhang, F., Qiang, S., Wu, Y., et al. (2019). Effect of irrigation level and irrigation frequency on the growth of mini Chinese cabbage and residual soil nitrate nitrogen. *Sustainability (Switzerland)*, 11(1), 1–20. <https://doi.org/10.3390/su11010111>
- Yang, W., Guo, S., Li, P., Song, R., & Yu, J. (2019). Foliar antitranspirant and soil superabsorbent hydrogel affect photosynthetic gas exchange and water use efficiency of maize grown under low rainfall conditions. *Journal of the Science of Food and Agriculture*, 99(1), 350–359. <https://doi.org/10.1002/jsfa.9195>
- Zheng, J., Chen, T., Xia, G., Chen, W., Liu, G., & Chi, D. (2018). Effects of zeolite application on grain yield, water use and nitrogen uptake of rice under alternate wetting and drying irrigation. *International Journal of Agricultural and Biological Engineering*, 11(1), 157–164. <https://doi.org/10.25165/j.ijabe.20181101.3064>